UNIVERSITY OF BATH

DOCTOR OF ENGINEERING (ENGD)

Design and validation of a thermal management 1D simulation model for a high efficiency high performance powertrain.

Di Blasio, Davide

Award date:
2024

Awarding institution:
University of Bath

Link to publication

Alternative formats

If you require this document in an alternative format, please contact:
openaccess@bath.ac.uk

Design and validation of a thermal management 1D simulation model for a high efficiency high performance powertrain.

Volume 1

Davide Di Blasio

A thesis submitted for the degree of Doctor of Philosophy

University of Bath

Department of Mechanical Engineering

July 2023

Copyright notice

Restrictions on use and Licensing

Declaration

The material presented here for examination for the award of a higher degree by research has / has not been incorporated into a submission for another degree.

(If applicable, provide the relevant details i.e., those parts of the work which have previously been submitted for a degree, the University to which they were submitted and the degree, if any, awarded).

Candidate's typed signature: Davide Di Blasio

Declaration of authorship

Declaration of any previous submission of the work

The material presented here for examination for the award of a higher degree by research has / has not been incorporated into a submission for another degree.

(If applicable, provide the relevant details i.e., those parts of the work which have previously been submitted for a degree, the University to which they were submitted and the degree, if any, awarded).

Candidate's typed signature: Declaration of authorship

I am the author of this thesis, and the work described therein was carried out by myself personally, with the exception of_____ academic paper / book chapter where _____ (detail the amount in percentage terms) of the work was carried out by other researchers (e.g., detail any collaborative works included in the thesis in terms of formulation of ideas, design of methodology, experimental work, and presentation of data in journal format).

Candidate's typed signature:

Table of Contents

List of Figures

List of Tables

Acknowledgments

I would like to express my sincerest thanks and appreciation to Prof Sam Akehurst, Dr Andrew Lewis and Prof Chris Brace for the guidance, supervision, support throughout this work. I would like to thank McLaren for the support received along the SPEEDV project.

I would like to thank all my colleagues in IAAPS and at the University of Bath past and present. Everyone helped me to complete this journey and I will be always more than grateful, and you will be always in my heart. *Thanks*.

Special mention goes to Dr. Stefan Tuechler, Dr. Eric Fong, Dr. Dom Parson, Dr. Karl Giles, Nick Evans and Brian Rutter that they are true friends before being awesome colleagues.

I would like to thank all my family for the incredible support. My parents Mariacristina and Vincenzo and my sisters Dr. Mariadele Di Blasio and Elisa for the incredible opportunities they give me in life and supporting me in all my adventures.

I would like to thank all my close friends from Castiglione Messer Raimondo, Bologna, and Bath, in particular the ones that shared with me this fantastic but a bit painful journey: Stefano, Luca, Daniele, Fabio, Mattia, Mirko, Dr. Lorenzo De Colli, Matteo, Francesco, Dr. Melissa Di Rocco, Simona, Alessandra, Dr Andrea De Bartolomeis, Dr. Fabrizio Bucciarelli, Dr. Francesco Flora, Dr. Marco Boccaccio, Dr. Giulia Coccia, Antonietta

My deepest thank go to my girlfriend *Elisa,* for being patient and supportive for all this time and putting so much though and care into everything we passed together. It makes me grateful that you are by my side.

Abstract

Over the past decades, a significant portion of powertrain research has been dedicated to exploring engine thermal management systems. The focus has been on enhancing system efficiency, reducing energy demand, and mitigating fluid-associated parasitic losses by controlling fluid temperatures and flow through a demand-oriented engine cooling system. The development of a robust 1D simulation model has been crucial for investigating and optimizing thermal management systems, with the goal of improving overall engine performance, reducing emissions, and extending engine life.

This work specifically delves into the creation of a 1D model for a V6 High-Performance Engine Cooling System, aiming to establish guidelines and methodologies for designing thermal management systems. The objective is to enhance engine performance, minimize fuel consumption, and optimize engine warm-up. The utilization of a mono-dimensional simulation model proves advantageous, significantly reducing simulation runtime compared to an "ideal" 3D CFD simulation model. From an engineering perspective, this approach facilitates early-stage project decision-making, providing a simpler simulation toolchain applicable for various purposes and resulting in time savings, reducing the costs of future engine development and helping to accelerate cleaner propulsion systems to market.

Furthermore, this research highlights its relevance to renewable fuels and diverse applications, encompassing emerging powertrain technologies such as hybrid electric vehicles (HEVs and PHEVs), electric vehicles (BEVs and FCEVs), hydrogen combustion engines, and mild hybrid systems. The developed thermal management system simulation tool is designed to accommodate these technologies, aiming to contribute to sustainable practices in both light and heavy-duty applications. The research underscores the versatility of these innovations, aligning with the broader objective of advancing eco-friendly solutions in powertrain engineering across a spectrum of automotive platforms.

In addressing the specific challenges posed by a power-dense V engine, the hydraulic modelling phase plays a pivotal role. The work introduces a revised

approach to hydraulic modelling, particularly in treating the water jackets for a V6 engine. A primary challenge addressed is the balanced distribution of water mass flow rate between the two engine banks, ensuring improved mass flow rate distribution along the engine. This hydraulic technique is developed to accommodate different V engine geometries, enhancing the versatility of the model.

Additionally, the research outlines a comparison between lumped mass and finite element thermal modelling approach and a novel thermal calibration strategy that considers the unique aspects of power-dense V engines such as high power output, compact design weight consideration and performance. It validates this strategy using experimental thermal data obtained from an engine thermal survey. The calibration process incorporates a innovative approach, utilizing experimental engine metal temperature combined with a dedicated heat transfer multiplier for the engine block and head. This calibrated simulation model is then optimized, and the heat transfer multiplier is calculated for various engine operating points, to validate an engine thermal model.

Abbreviations

BMEP – Brake Mean Effective Pressure

CAD – Computer Aided Design

CARB – California Air Resource Board

CFD – Computational Fluid Dynamic

CO_2 – Carbon dioxide

EGR – Exhaust Gas Recirculation

ECS – Engine cooling system

EOC – Engine Oil Cooler

EV – Electric Vehicle

FE – Finite Element

FTP-75 – Federal Test Procedure (light duty vehicles)

FRM – Fast running model

GDI – Gasoline direct ignition

HEV – Hybrid Electric Vehicle

HTC – Heat Transfer Coefficient

IMEP – Indicated Mean Effective Pressure

MA – Model A

MC –Model C

MD – Model D

ME – Model E

MF – Model F

MH – Model H

NEDC – New European Drive Cycle

NOx – Nitrogen oxide

NSGA-II – Non-dominated sorting genetic algorithm II

OEM – Original equipment manufacturer

PHEV – Plug In Hybrid Electric Vehicle

RDE – Real driving emissions

SI – Spark ignition

TDC – Top Dead Centre

TDI – Turbocharged Direct injection

TMS – Thermal management system

TOC – Transmission Oil Cooler

WHR – Waste heat recovery

WLTP – Worldwide Harmonised Light Vehicle Test Procedure

WOT – Wide Open Throttle

Chapter 1 - Introduction

In this chapter, the background and motivation for developing a modelling methodology for 1D engine simulation models are presented as well as the challenge that Vehicle Manufacturers (OEMs) face when developing these simulation models. This is followed by an introduction to the project, its objectives, scope, and the work carried out. From there, the research questions are presented along with the structure of the thesis, its aims and objectives.

1.1 Summary

The current chapter provides an overview of the structure of the work and the steps taken to achieve the results.

I.   Background and Motivation.

- The description of the thesis background and the motivation that motivated the current work.

II. Aim and objectives.

- The list of aims and objectives to follow to finalise the thesis work.

III. Thesis structure.

- The description of each chapter and their content.

IV. Chapter conclusion

- Final chapter conclusion with the description of the reason for the development of a 1D thermal engine simulation model.

1.2 Background and Motivation

"If one way is better than another, that you may be sure is nature's way"

Aristotle

"The Earth is a fine place and worth fighting for"

Ernest Hemingway

As a global community, we are facing one of the most challenging times in our history. The Earth's ecosystem is being hit by a perfect storm in terms of climate change. Over the past few decades, Nature has been showing us how the future can change, giving us a glimpse of what will come next if we do not take serious action to change the course of climate change caused by global warming.

A more environmentally conscious generation is growing up, demanding for more climate justice and a sustainable economy which means a better future for planet Earth.

Governments, OEMs and scientists are not only listening, but they are taking action to reduce global warming. In 2015 the Paris Agreement agreed upon at COP21 saw almost every country around the world enter in legally binding commitment to reduce emissions. Every country pledged to cut carbon emissions to limit global warming to well below 2 degrees and ideally 1.5 degrees above a pre-industrial level and it was bottom-up in that it left room for each country to decide how to get there. These were called Nationally Determined Contributions (NDCs)[1]

The COP26 conference between 31 October and 12 November 2021 announced that the target set in Paris would lead to warming well above 3 degrees by 2100 compared to the pre-industrial levels. If this is the trend, the temperature will continue to rise bringing even more catastrophic flood, wildfires, extreme weather and species loss. Progress has been made in recent years but not enough to uphold the previous agreement.

The following are made [1]:

- Around 70% of the global economy is now committed to achieving net zero-emission.

- More than 80 countries have formally updated their NDCs and all G7 countries have announced new NDC targets that put them on the path to net-zero emission by 2050.

- Solar and wind are now cheaper than new coal and gas power plants in two-thirds of the world's countries.

- Over 20 countries have joined the Adaption Action Coalition building on the 2019 Call for action on Adaption and Resilience, which was signed by more than 120 countries.

- The Organization for Economic Co-Operation and Development (OECD) estimated that $78.9bn of climate finance was mobilised in 2018.

- The Glasgow Financial Alliance for Net Zero represent over $70 trillion of asset committed to net-zero by 2050.

- This will have an impact on global greenhouse emissions but is not enough. Those emissions can be broken by economic activities as Figure 1 shows:
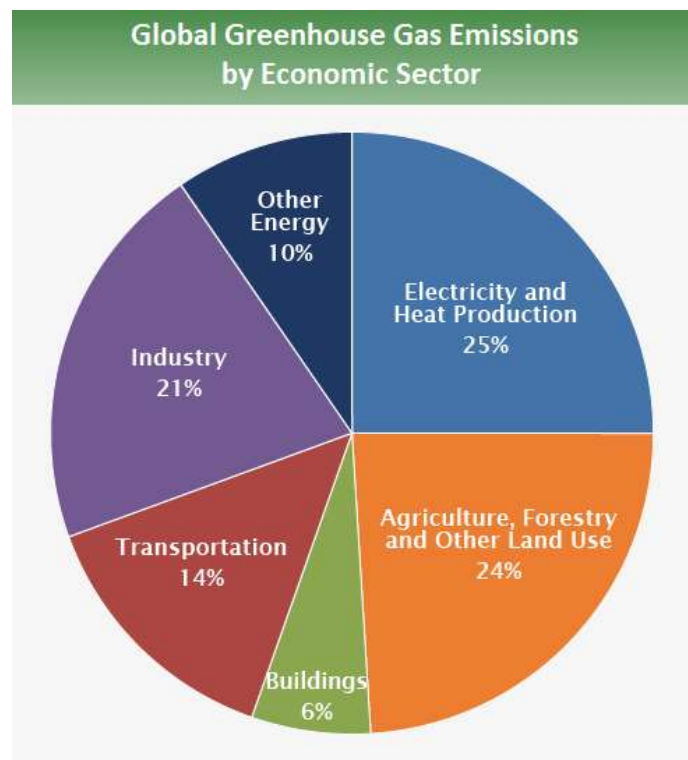
Figure 1: Global greenhouse gas emissions by economic sector [2].

The situation is quite complex and each of the factors play an important role in how global warming can be reduced. The transportation sector accounts for the 14% in terms of global emissions and will play a huge role in terms of technical know-how to help society to achieve the goal of reducing global warming [2].

An overview of the emissions from each of the world's continents will help us to understand the role of the transportation sector in global greenhouse emissions.

The International Council of Clean Transportation defines:

Europe [3] is one of the largest markets in the world, the historic home of automotive, aircraft manufacturing, shipbuilding industries, innovative engineering companies, an engine of global trade and the hub of the intricate transport infrastructure. . The European Union has been at the forefront of environmental policy in the transportation sector and has an indispensable and growing role to play in global efforts to respond to the threats of climate change.

China [4] is the largest market for new light-duty and heavy-duty vehicles. Seven of the world's ten largest container ports are in China and a significant portion of the world's freight moves through them. This industrial dynamism has also brought the country to well-publicized air-quality problems, making it the world's leading emitter of carbon (though not per capita). China's policymakers have responded creatively and forcefully.

India [5] has the world's larger increase in total vehicle sales, from about 10 million in 2007 to over 21 million in 2016 and the total number of vehicles on the road is expected to almost double to around 200 million by 2030. Air pollution, especially in terms of particulate matter, will be a serious challenge.

Latin America [6] can be overshadowed on the global transport policy stage by the United States, Europe, China and India, with their highly publicised urban air quality challenges and high-profile roles in global climate change. However, Brazil is the fourth largest vehicle market in the world and an important factor in the global biofuels industry. Mexico is also an important global market and the region as a whole plays a key role in the global energy economy. Countries in the region may offer, by the very fact that they do differ from those larger economies, valuable insights into effective policymaking for similar-sized countries in Africa and Asia;

Chile, with its innovative feebate programme to promote passenger-vehicle efficiency, is one example.

The United States [7] pioneered the regulation of vehicle air pollutant emissions and fuel economy in the 1960s and 1970s and has continued to implement far-sighted, well-designed and effective regulations and policies to control air pollution from light-duty and heavy-duty vehicles, to encourage manufacturers to design and build more efficient cars and trucks and promote renewable and low-carbon fuels and zero-emission vehicles. Over this half-century, policy ambition has also ebbed and flowed, as the initiative has passed from one set of stakeholders to another. With a dynamic economy driving innovation in engineering, design, manufacturing, and information technology, it remains an essential testing and proving ground clean vehicle and fuel policy.

The response of different countries is proven by the actions of their government with stricter regulations, but there is still no convergence towards a unified. This is because different regions of the world are growing faster than others and the energy demand varies from country to country.

The transportation sector is a clear example of this divide gap. Europe and the USA, are ready to act because of their economy and status while China India and South America are still in the development process. In terms of the transportation sector this means that vehicles will play an important role in terms of economic growth. These actions will result in a new generation of vehicle technologies such as:

- Hybrid

- Plug-in hybrid electric PHEVs

- Hybrid electric HEVs

- Hydrogen

- Fuel Cell electric vehicles FCEVs

- ICE vehicle

- Natural Gas

- Synthetic eFuel

These actions also push the research boundaries for ICE technologies giving them a new perspective and a new role in the fight against global warming. Pushing the research boundaries also boosts the research tools used to cope with the new level of complexity. Digitalisation is not only a concept but a reality to reach important milestones in the vehicle development process. Simulation tools now play a key role in the V model for engineering development. Digital modelling and optimisation algorithms have been and will continue to be used extensively to reduce cost and time and to improve certainty in the development process.

Simulation software are widely used in vehicle engines research to investigate fuel consumption, emissions and methods to make engines more efficient and increase their performance. The engine thermal management system plays a significant role in the overall performance, emissions and durability of an engine. However, as the internal combustion engine designs become more advanced and new technologies are implemented to meet the ever-increasing customer's demands for performance, reliability as well as emissions legislation, the design and development of an active and smart thermal management system is becoming even further a necessity.

The hydraulic and thermal approaches investigated and outlined in this work will play a significant role in the engine thermal management system, not only for V gasoline engines but also for hybrid vehicles (HEVs and PHEVs), electric vehicles (BEVs and FCEVs), hydrogen combustion engines, and, finally, mild hybrid systems. This will help push the boundaries in the 1D modelling phase during engine development, reducing simulation runtime foremost. This consideration also extends to the heavy-duty sector, where a new era of combustion engines is approaching, and these tools will aid in further investigation and pushing the boundaries. The clear understanding of informative decisions, such as when lamp mass thermal methodology is better than finite element thermal methodology for modelling the engine is crucial based on needs and result quality. Finally, and most importantly, the understanding how to model various complex powertrain systems, such as a V-type engine, and being able to study critical areas, including the exhaust side of the head, engine block interbore, exhaust valve bridge.

Considering the complexity of the hybridization due to the thermal management of the batteries, controllers and generator units, there is significant scope for further optimizing the integration of the thermal management system. The challenges

ahead are many and only a global view of the thermal management system will help to overcome these difficulties. Cooling systems are becoming increasingly complex and the ability to study only critical conditions is not sufficient. This is because regulations are becoming more stringent and more flexible strategies are required. These strategies must be able to understand the actual operating conditions of the engine and be representative of reality.

This research aims to implement a methodology to create a 1D simulation engine thermal model capable of improving all these aspects and most importantly will help to reduce costs of future engine and accelerate cleaner propulsion system to the market.

1.3 Aim and objectives

The primary aim of this thesis is to investigate and validate a renew modelling methodology to be adopted by the OEMs and the research field in the thermal management simulation environment. Creating a hydraulic and thermal calibration strategy that can be rapidly applied to different revisions of engine cooling geometries. This is driven by the need for a more efficient simulation tool to examine more complex problem in the engine development phase. As described, thermal management plays and will continue to play a significant role in engine and powertrain development.

To achieve the aim described the following objectives are presented:

- Research the state of art for 1D thermal engine modelling (using a 1D commercial software, GT-Suite).

- Evaluate a range of different modelling approaches and associated calibration methodologies.

- Detail a robust approach to the hydraulic and thermal calibration process.

- Compare and identify the most promising methodologies.

- Select the best methodology.

1.4 Thesis Structure

The contents of the chapters are summarized below:

- Chapter 1 - Introduction

A general introduction to the project, background, motivation and challenges in developing a thermal engine model. Finally, it summarizes the project objectives, aims and it poses the research questions.

- Chapter 2 – Literature Review

A review of the relevant literature on thermal management modelling. It provides the necessary background of 1D thermal modelling in GT-Suite its trade-offs and different simulation methodology options available for assessing engine performance. Next, it dives into the modelling procedures used in the literature, it compares them and finally it outlines the research gaps that will be evaluated in this thesis.

- Chapter 3 – Hydraulic Modelling Methodology

The hydraulic modelling methodology applied to two different engines is presented. The steps on how the 3D CAD will be discretised into a 1D model and the different options available are described.

- Chapter 4 – Thermal Modelling Methodology

Two different thermal modelling approaches based on the hydraulic methodologies discovered in the previous chapter are investigated. A "Lumped Mass" and "Finite Element" thermal model setting are exploited prior to the thermal calibration methodology. An analysis of the thermal calibration results is carried out and finally a heat transfer multiplier calculation is performed to proceed to the next stage of the work.

- Chapter 5 – Thermal Modelling Comparison - Results

A full comparison between the two thermal modelling methodologies is presented, analysed and discussed. The chapter begins by describing the direct comparison between the four simulations results and consequently the analysis continues with

the two best models. One for the Lumped mass model and one for the FE model. A deep engine thermal analysis is carried out finalising the benefit of the two models.

This section l presents the best methodology found to have the most suitable thermal simulation model.

- Chapter 6 – Conclusion and Outlook

Summary of the main findings and conclusions of the thesis, as well as identifying areas for further research.

- Chapter 7 – Future Work

Possible next steps of the current work are exploited focusing more on what can be implemented during the modelling phase and the calibration phase.

1.5 Chapter conclusions

The advancement of research boundaries is integral to enhancing tools designed to handle the increasing complexity in vehicle development. Digitalization has evolved from a conceptual idea to a tangible reality, playing a crucial role in achieving significant milestones. Simulation tools, embedded within the V model for engineering development, utilize digital modelling and optimization algorithms extensively. This application is instrumental in reducing costs, minimizing time, and enhancing certainty in the development process.

Simulation software is a cornerstone in vehicle engine research, used extensively to explore fuel consumption, emissions, and methods for enhancing engine efficiency and performance. The pivotal role of the engine thermal management system in overall engine performance, emissions, and durability cannot be overstated. As internal combustion engine designs progress and new technologies emerge to meet evolving customer demands and emissions regulations, the necessity for designing and developing an active and intelligent thermal management system becomes increasingly apparent.

The hydraulic and thermal approaches discussed in this work will significantly influence engine thermal management systems, catering not only to V gasoline engines but also to a wide array of vehicles, including hybrid vehicles, electric vehicles, hydrogen combustion engines, and mild hybrid systems. This exploration is particularly impactful in advancing the 1D modelling phase during engine development, resulting in a reduction of simulation runtime. This significance extends to the heavy-duty sector, anticipating a new era of combustion engines, where these tools facilitate further investigation and boundary-pushing.

Decisive understanding of choosing the appropriate thermal methodology, such as lamp mass versus finite element, is crucial, shaped by specific needs and result quality. Importantly, comprehending the modelling of complex powertrain systems, such as V-type engines, and studying critical areas, including the exhaust side of the head, engine block interbore, and exhaust valve bridge, is paramount.

The challenges associated with hybridization, especially regarding the thermal management of batteries, controllers, and generator units, present opportunities for optimizing integration. The multifaceted obstacles ahead necessitate a global perspective on the thermal management system, as cooling systems evolve in complexity. Addressing stringent regulations requires flexible strategies capable of understanding the actual operating conditions of the engine and representing reality.

In summary, this research aims to implement a methodology for creating a 1D simulation engine thermal model that not only enhances various aspects of engine performance but also contributes significantly to reducing future engine development costs. The ultimate goal is to expedite the introduction of cleaner propulsion systems to the market.

Chapter 2 - Literature review

The following section presents previous work and knowledge in the research field used in the thesis. The broad use of modelling techniques is important to this work and covers a wide range of approaches and objectives. It introduces several fundamental engine technologies that have been implemented in the field of thermal Management 1D modelling and identify the research gap that this work will contribute to.

2.1 Summary

This chapter explores the main research area of interest to implement the current work:

I. Introduction

- A general overview of the challenges that face in terms of global warming, the role of the transportation sector and the importance of simulation tools.

II. Thermal Management Systems

- Setting the scene for thermal management systems: what they are and why they are fundamental to the engine development process.

III. Thermal Management 1D Simulation Systems

- In depth analysis of the current state of the art for thermal management 1D simulation models. Critical analysis and identification of gaps for the implementation of the thesis.

IV. Engine Warm-up

- Overview and understanding of the most critical engine phase for developing an appropriate engine thermal management system.

V.   Discussion

- A critical review of the previous paragraph and highlights of the main findings over the years.

VI.   Research Questions

- Finalisation of the thesis research questions to fill the gaps identified in the literature review.

2.2 Introduction

Global GHG emissions sources are usually attributed to five broad sectors, characterised by the Intergovernmental Panel on Climate Change (IPCC) Working Group III (WG3) as energy systems, industry, buildings, transport, and AFOLU (agriculture, forestry and other land uses). Together, these sectors cover aspects of energy supply (energy systems), energy demand (industry, buildings and transport), non-energy related process emissions (industry), and land-based emissions and removals (AFOLU) [8]. There have been few attempts to describe global and regional emissions trends and drivers on a consistent and comprehensive sectoral basis[8]. There is a substantive literature that compiles global emissions inventories for carbon dioxide (CO2) [9], methane (CH4) [10], and nitrous oxide (N2O), sulphur hexafluoride (SF6) and hydrogen (H2) emissions[11] [12]. The CO_2 levels in the atmosphere are one of the main concerns for future and reducing emissions represents the main driver for technology in energy-related transformations. The automotives sector accounts for 30/35% of the overall CO_2 emissions. A broad portfolio of new technologies is being considered as a short -to midterm response to the CO_2 concerns.

Governments around the world have, therefore, set limits on carbon dioxide emissions from vehicles and imposed fines on manufacturers who fail to meet the target. In Europe, emissions from new cars will have to be reduced by 37.5% and vans by 31% by 2030, compared to 2021 [13].

In addition, pollutant emissions (HC, CO, NOx and PM) will take into account new Real Drive Emissions (RDE) cycle tests, more difficult to meet the emissions limits [14].

A large proportion of engine-out emissions (both CO_2 and harmful pollutants) are generated during cold start [15] and in the first 75% of engine homologation duty cycles [16]. This is mainly due to higher engine internal friction losses [17], ineffective combustion and low efficiency of catalytic converters [18].

Information on the overall efficiency of an engine can be obtained by applying the first law of thermodynamics examples of which can be found [19][20][21][22] in these works and it can be seen that the relative amount of rejected heat at the steady-state conditions depends significantly on the engine load. The lower the engine load, the highest the proportion of rejected heat. This is important because most vehicle certification cycles and real-life usage occurs at relatively low engine loads. Furthermore, in these cases, the engine warm-up process accounts for a large proportion of the event. Consequently, the engine's thermal inertia plays an important role in the final distribution of the rejected heat [23][24].

Utilising a update version of the traditional thermostat, water pump and radiator fan with servo motor driven actuators permit real time computer control to improve temperature regulation and reduce power consumption [25]. Electrically Heated Catalyst (EHC) reduce the cold start emission since it enables fast light off for the Three Way Catalytic converter (TWC) [26]. The benefits of close coupled after-treatment systems are the ability to reach optimal operating temperature more rapidly, they enhance the efficiency of catalytic converters by minimizing heat loss between the engine and the emission control device Improving performance during the cold start phase can be done utilising thermal engine encapsulation. This is an effective design to reduce engine friction in application with frequent cold start [27]. Fuel and thermal efficiency can be achieved combing cooled EGR and high compression ratio in a turbocharged gasoline engine [28], and trough combustion retard via advanced calibration. This will have a benefit on emission control, knock mitigation, combustion stability especially at low speed and high loads [29].

Improving fuel economy without compromising engine performance can be done from new injection systems and new strategies passing through inlet air temperature [30] energy recovery system up to improvement of engine external system [31].

The design and optimisation of the engine thermal management system (TMS) is a key element in engine process development to address these issues and find a simple and viable way to achieve a profitable solution. The potential to increase the efficiency on the engine side correlates with a reduction in overall emissions, making thermal management a priority in the engine development process.

2.3 Thermal Management Systems

The following literature review provides wide background information to understand the intricacies of thermal engine management and the trade-offs involved. Thermal Management System (TMS) investigation has been performed since the 19th century [32][33][34].Over the years the development of powertrain TMS has been conducted by isolating singular modules and focusing on their individual efficiency improvement rather than looking at the global system. Traditionally, the cooling system is mechanically connected to the crank shaft. In this configuration to avoid overheating the system is usually over-sized [35].

A proper thermal management of the engine has the following objectives [39][40][41]: maintaining the internal combustion engine in its optimal temperature range in wide ranging working condition and in transient condition [40] avoiding overheating in any situation [42], reducing exhaust pollutant [43] and reducing oil viscosity by reducing warm up time always maintaining a correct temperature [44], decreasing power dissipation in engine auxiliaries and improving combustion boundary conditions [41].

With the advent of electrical components, thermal management for engine cooling tends towards electrification, featuring modularization, integration and calibrated control [45][46][47].

Electric water pump systems allow independent control over the coolant flow around the engine and aim to reduce fuel consumption by lowering the pumping

work when the high flow is not necessary [48]. These systems generally work by controlling the metal temperature of the block or cylinder head, the temperature of the top hose as with a conventional thermostat. This metal temperature based strategy allows the engine cooling to operate hotter at low load conditions. This method results in greater efficiency, as it is preferable to have higher coolant temperatures at low load and, of course, higher oil temperature to achieve a faster warm-up and reduce friction and hydraulic viscosity losses [35].

The cooling system development continues with several studies investigating the effect of heating different parts of the powertrain or even decoupling the coolant flow rate from the engine speed. The aim is to improve system efficiency. This choice has been made because the development of the thermal system has always been carried out under the two most extreme engine operating conditions. In general, these thermal systems work by controlling a metal temperature (e.g., engine block) rather than controlling the coolant temperature with a thermostat. This allows the engine cooling system to run hotter under low-load operating conditions. However, it is better to have higher coolant temperatures and higher oil temperatures in low load conditions to reduce friction losses and allow the engine to warm-up faster [49] [50] [51]. The effect of warming parts of the powertrain or decoupling the coolant flow rate from the engine speed to improve the system efficiency has deeply analysed by Janowsky [52]. Decoupling the coolant flow rate is typically realised by swapping the mechanically driven pump and thermostat with an electric pump and control valve. It depends on a conventional engine cooling system being designed to manage the engine's temperature in the most demanding condition. As a result, it operates overly during most driving conditions.

The benefits of splitting the coolant circuits are that it is possible to reduce the coolant pump power consumption by distributing the coolant more effectively to the cylinder head and cylinder block. Another advantage of this strategy is that the cylinder head can be run cooler than the cylinder block without an additional thermostat or coolant pump through controlled coolant flow rates [53].

More advanced thermal management technologies and strategies are being implemented to make the engine more flexible and to better match, the demands corresponding to different engine operating conditions. In addition to the reducing

emissions and fuel consumption, thermal management technologies and strategies achieved important benefits. Besides, engine durability will also been improved [53]. Considering also a significant reduction in terms of CO_2 [54] and reduction of pollutant emission in test cycles [55].

Hyundai introduces the principles behind the design of the new Smartstream engine. This powertrain for price-sensitive A and B segment models has a number of efficiency measures, including dual port injection, high-energy ignition, an EGR system with external cooling and continuously variable valve timing. The Smartstream G 1.0 and G 1.2 engines apply various new technologies to improve fuel efficiency and performance. The medium to high load fuel efficiency was significantly increased by cooled EGR supported by high energy ignition and dual port injection. The low load fuel economy was improved through high compression ratio, low mechanical friction and mid-position lock cam phasers. The newly designed cross flow cooling cylinder head enabled earlier spark timing and the cylinder head with integrated exhaust manifold reduced the exhaust temperature significantly. These measures provide a potential method for stoichiometric combustion in all operating conditions for Euro 7 [56].

Some of the theoretical and experimental works related to the study of cooling system improvement are for example Luptowski [57], where a fully coupled engine and cooling system model was applied to develop and simulate an actively controlled electric cooling system for a Freightliner FLD120 with a Detroit Diesel Series 60 engine. The cooling system is controlled to reduce power consumption while simultaneously reducing cylinder wall temperature fluctuations to reduce thermal stresses and stabilize oil film temperature to reduce piston sliding friction. Cortona [38] proves that the substitution of the mechanically driven cooling pump with an electrical one and at the same time, of the thermostat with an electrically actuated valve makes it possible to reduce the coolant pump energy need. It is also possible to reduce the duration of the engine cold-start phases and to operate the engine under optimal thermal conditions. Improved fuel economy can be attributed to lower drive power requirements for the electrified cooling system components and the controllability of these components, used in the advanced thermal management system [58] and also with the usage of new electrical water valve[59] by reducing the vehicle airflow restriction and distributing the cooling load from

the transmission and EGR to two smaller heat exchangers fuel efficiency can be reduced [60]. Engine cooling system also allows efficient control of cooling through the flow control valve. Rapid warm-up, increased cooling water temperature and cooling around the combustion chamber reduces friction loss and suppress knock tendency. It is possible to improve fuel efficiency by increasing the heat efficiency at the high compression ratio [61].

Power consumption and engine warm-up time can be improved by evaluating the interaction between the smart valve, variable flow coolant pump and electric radiator fan [62]. An advanced thermal management system can simultaneously improve both engine and cabin warm-up, heater performance with an advanced thermal management system is significantly improved by maintaining the coolant temperature at a higher level and by increasing the coolant flow rate to the heater through system modification [50]. A secondary cooling system offers opportunities to improve cooling system performance for both the secondary circuits and the engine cooling, in addition to benefits in temperature controllability [63]. The integration of split cooling and precision cooling with controllable elements to run a cooler head and warmer block is singled out as the most promising concept to meet expanding requirements on the performance of the ECS [41].

Empirical models can provide realistic component data used in simulation tools during the development process. Introducing a coolant rail to accommodate specific cylinder temperature control defined by an on-demand cylinder-dependent cooling strategy gives benefit in terms of combustion and energy consumption [64]. New cooling prototype which uses a coordinate control strategy to achieve precise control of engine coolant temperature, heat rejection regime using minimum flow rates and the advanced impeller design allow a simplified valve to control flow to the heater and radiator. The system considerably reduces pump power consumption whilst maintaining good control of coolant temperatures. Increased engine temperature leads to reductions in fuel consumption and emissions [65].

The Otto cycle is often applied in SI engines where fuel and air are mixed in the

intake manifold or engine cylinder, and then the premixed mixture is ignited actively by a spark plug.

When the stoichiometric mixture is compressed, a fuel resistant to the auto-ignition, such as gasoline, must be used to avoid engine knock. Some drawbacks limiting the thermal efficiency of SI engine are as follows: Lower compression ratio, longer combustion evolution, gas exchange losses by throttle valves and lower specific heat ratio.

The theoretical thermal efficiency of the Otto cycle can be determined employing Equation (1) [66] [67][68] [69]

$$\eta = 1 - (\text{CR})^{1-\gamma} \qquad \text{Equation (1)}$$

where CR is the compression ratio and γ is the specific heat ratio. In general, two effective methods are used to improve thermal efficiency. The first one is increasing the CR through enlarging compression stroke or retarding exhaust valve opening timing. The second way is using lean burning to modify specific heat ratios. Dilution combustion is an efficient technique for overcoming engine knock and reducing heat loss. These obvious advantages have motivated the extensive applications of dilution combustion in IC engines in recent years [29].

As for specific technologies, raising the mechanical compression ratio, retarding the exhaust valve opening timing and using lean burn can be considered [70][71][72].

Lean burn combustion is an effective means of achieving the latter goal, but its application remains limited to the issue of NOx emissions and the challenges for aftertreatment systems operating under non-stoichiometric conditions. The limitations are given by the increase of the cost of aftertreatment systems as well as emission control [73] and the reliance of AdBlue [74].

On the other hand, the thermal efficiency of an actual engine's also depends on factors such as mechanical, pumping, cooling heating, exhaust and unburned losses due to incomplete combustion processes.

In work by Smith et al. [75] and Jones et al. [76], typical approaches to reducing each loss are examined.

Lowering the mechanical loss is a fundamental target for the engine design and several technologies have been developed such as lowering the piston ring tension

and optimizing the bearing axis and width. Decreasing pumping loss can be achieved by optimising the valve system train system and by using EGR and lean-burn combustion. Since these types of combustion technologies lead to decreased combustion temperature, they also contribute to a lower cooling loss. Reducing the surface area of the combustion chamber by using a long-stroke design and optimising the combustion chamber design is also important for reducing heat loss. For low exhaust loss, raising the expansion ratio is essential. In the case of raising the compression ratio, it is required to improve engine antiknock quality.

All these systems have a high cost and will reflect on the technology but as it becomes more widespread the cost will be reduced. An example of this can be found in the electric pump technology, which is used in more than just the engine thermal management system. The same aspects appear in the EV(Electric Vehicle) and Hybrid electric vehicles, where mechanical drive is not available [77].

Improving the engine cooling system serves the purpose of advancing the vehicle's cold start fuel economy by enhancing engine efficiency. Several methods can be employed to achieve this objective, such as reducing parasitic loads on the engine, for instance, by replacing the mechanical coolant pump with an electric one. In addition, a variable flow oil pump can be used as another viable option.

2.4 Thermal Management 1D Simulation Systems

The capability to research and develop engine TMS is given by simulation tools, which engineers use to pursue these challenges more efficiently and intelligently. Digital modelling and optimisation algorithms can be implemented to reduce costs, time and to improve the engine development process.
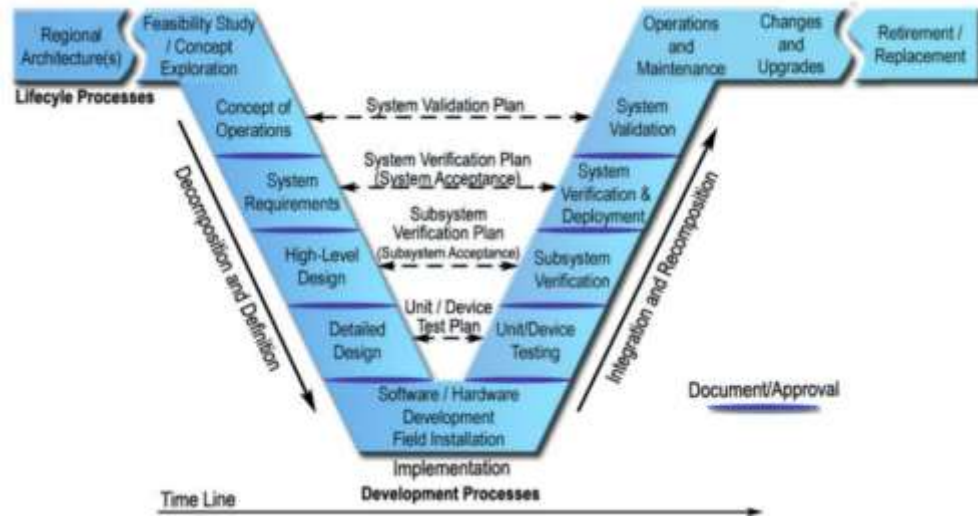
Figure 2: V-Model development process [78].

Figure 2 shows the OEM classical development process. Simulation software can play a fundamental role at the bottom of the V-Model development process where, for example, a detailed design is defined, implemented and verified. This is a crucial step in engine development. Saving time, or using it wisely, can be a step towards a better design process final validation. Most importantly will have a significant impact in reducing cost in prototyping and testing phase [79].

Simulation models for engine cycles are mainly classified into quasi-dimensional, zero-dimensional and multidimensional [80]. These models are extensively used to predict engine performance and fuel economy. Zero-dimensional models cannot accurately predict engine emissions. On the other hand, multidimensional models provide precise prediction. A multidimensional thermodynamic model is used to accurately describe engine performance and emissions [81]. All these software tools are used to study and implement new solutions for engine thermal management system to meet the requirements of future powertrain and comply with new regulations.

Simulation tools are largely used to study the thermal management process. The three-dimensional computational fluid dynamics (CFD) tools are used to study the flow of fluid inside engines and they are capable ensuring detailed analysis. One-dimensional thermal fluid analysis, on the other hand, does not provide detailed fluid flow analysis inside the engine but it enables the entire cooling system control

to be studied and the general system to be optimized [82]. 1D and 3D simulation softwares serve different purposes and are often used in different stage of thermal modelling process. Each type of simulation has is advantages and limitations, and the choice between them depends on the specific goals of the analysis. 1D simulation software are more appropriate than 3D simulation software in certain cases [83] [84]:

1) Computational efficiency: 1D simulation focuses on simplified representation of the engine components, such as pipes and manifolds. This simplicity allows for faster computational times compared to the more detailed and computationally intensive 3D simulations. 1D simulations are advantageous when quick design iteration or parametric studies are needed.

2) System level analysis: 1D simulation are well-suited for system level analysis, providing an overview of the entire engine thermal management. This includes coolant flow, oil circulation, and heat exchange between various components. Such system level insights are valuable for understanding the overall thermal behaviours of the engine.

3) Early design exploration and reduced model complexity: During the early stages of the engine development, when broad design decisions are being made, 1D simulations allow for rapid exploration configuration and thermal management strategies. This also because is possible to involve simplified representation of components. Making easier to manage and interpret the results. This reduced complexity is advantageous when aiming for a balance between accuracy and computational efficiency.

4) Parametric studies and conceptual designs: 1D simulation are effective for conducting parametric studies, where multiple variables are systematically varied to understand their impact on the thermal performance of the engine.

5) Resource efficiency: 1D simulations require led computational resources than 3D simulations. Making them more accessible and practical in the initial stage of the design process.

While 1D simulations are beneficial for certain aspects of thermal modelling, CFD simulations become essential when a more detailed and accurate representation of complex geometries and fluid dynamics is required.

Over the years, the engine cooling system has been designed to ensure sufficient heat removal under the most demanding operating conditions. In general, these would be at low vehicle speeds coupled with high power demand at high environmental temperatures. However, these points will represent only 5% of the total conditions during the lifetime of the vehicle [85] [86] [31]. This approach leads to the design of an oversized thermal management system for the most typical operating conditions including those corresponding to type approval drive cycle, such as the NEDC (New European Drive Cycle) and results in slow engine warm-up, with obvious drawbacks in terms of emissions and fuel consumption.

The more the system became complex with a variety of heat exchangers, indirect intercoolers, water-cooled exhaust manifold and Waste Heat Recovery (WHR) technologies, the more 1D software tools became vital for the optimal design of the cooling system. These systems are also relevant at an early development phase, especially in terms of the transient behaviours [87].

The need to further reduce fuel consumption and emission and to increase engine thermal efficiency is a key challenge that all OEMs are facing. Being able to develop a study methodology that allows this issue to be considered globally provides a great advantage in terms of development and know-how. To do this all the modules involved in thermal efficiency must be taken into consideration simultaneously [88][89][90].

To do so a realistic simulation model of an engine in steady and transient condition requires a coupling between a combustion model and a thermal model of the engine cooling system [91].

Sangeorzan et al. [92] developed an engine thermal management model to predict piston, oil and coolant temperature in a 3.5L direct-injected turbocharged SI engine. The 1D simulation model presents a detailed lubrication system, a detailed coolant system, a turbocharged model and lumped thermal models for engine components. The cooling system includes a water pump, heater core, turbocharger sub-system, water-jacket and cylinder block and head cooling passages, oil cooler and water

tower. The hydraulic calibration of the system conducted by modelling the flow resistance in the turbocharger system, water jacket and cylinder and head cooling passages with various surface roughness and appropriate length and diameters. In the block cooling jacket, an area equivalent to length and diameter was also calculated.

The model uses experimental coolant energy to estimate energy input. Heat transfer in the turbocharger sub-system and in-cylinder block and cylinder head water jacket was handled using a typical heat transfer correlation of the form:

$$N_{u_D} = cRe^a Pr^b \qquad\qquad \text{Equation (2)}$$

Sageorzan's model predicts oil sump temperatures and peak piston temperature in a steady-state condition, in WOT condition across a speed range.

Lauerta and Samuel [93] developed a detailed cooling system model to investigate the thermal management of a 4-cylinder 1.6 l turbocharged and intercooler GDI engine. The simulation model, developed using GT-Suite, includes a predictive combustion engine model and an engine thermal model.

The modelling approach by Lauerta is as follows. The cylinder structure is defined with the geometrical parameters of the piston, head, valves and ports and the initial temperature of the component. The calculation of temperatures is based on a finite element model of the head, valve, cylinder liner and piston. Surrounding this geometry there is the water jacket gallery, modelled as a thermal pipe where the coolant goes through. The heat transfer is estimated from the fluid to the wall using the convection coefficient between the wall and the fluid. The engine block is modelled as a homogeneous isotropic and lumped mass. This component is linked to the water jacket and cylinder galleries to exchange heat with the fluid circuits. The cylinder head gallery is modelled and linked with the cylinder, water jacket and head block through a heat convection coefficient: it is defined in the same way as the water jacket gallery. The head block and the engine block are linked through thermal conductance. The pump is modelled as a fixed mass flow rate, calculated through a heat balance. All the geometrical data necessary to complete the model (water jacket, pipes cylinder head) were measured from the engine.

The fully integrated model was validated against experimental data by comparing the engine-out coolant temperature at a single-engine point: 2000rpm and 20Nm. Once validated, this model was used to investigate the sensitivity of the numerical simulations. This was done using two different heat rate multipliers. These parameters allow calibration of the amount of heat transferred from the cylinder through the cooling system and the results show that the higher the mass flow rate lower the gradient temperature. More importantly, the influence of heat rate from cylinder to coolant is significantly higher than the influence of mass flow rate of coolant.

Kitanoski et al. [82] have analysed the thermal engine model using a lumped mass discretisation of the engine and through coupling between cooling and combustion models was able to simulate the time-dependent warm-up behaviour of the engine and the cooling system.

Millo et al. [94] developed, in GT-Suite environment, a numerical model of an advanced cooling circuit of a European passenger car diesel engine to obtain a virtual engine test bench for the assessment of the impact of different thermal management strategies on the engine warm-up. The engine used is a DI Turbocharger Diesel EURO 6 1.6L (4 Cylinder). In his work, he utilised a detailed representation of the engine structure, the water jacket and the lubrication system. This approach ensures higher accuracy and a reduced calibration effort, although it requires significantly higher modelling effort. The simulation model for the engine combustion chamber uses a detailed parametric finite element cylinder model. It will include liner, head, valves, ports, pistons and rings. HTCs (Heat Transfer coefficient) and temperature are used to calculate the heat rate into the engine structure. Meanwhile, from the gas side, HTCs and temperature were calculated from an engine performance simulation model and mapped as a function of engine speed and load (BMEP). In the thermal model, all cylinders interact with the coolant jacket. This allows transmitting the heat generated by combustion to the coolant. The average heat transfer coefficient between the engine structure and coolant jacket for each region of the engine has been calculated based on a 3D CFD analysis. Millo demonstrated a basic modelling methodology on how to discretize the coolant water jacket, see Figure 3.
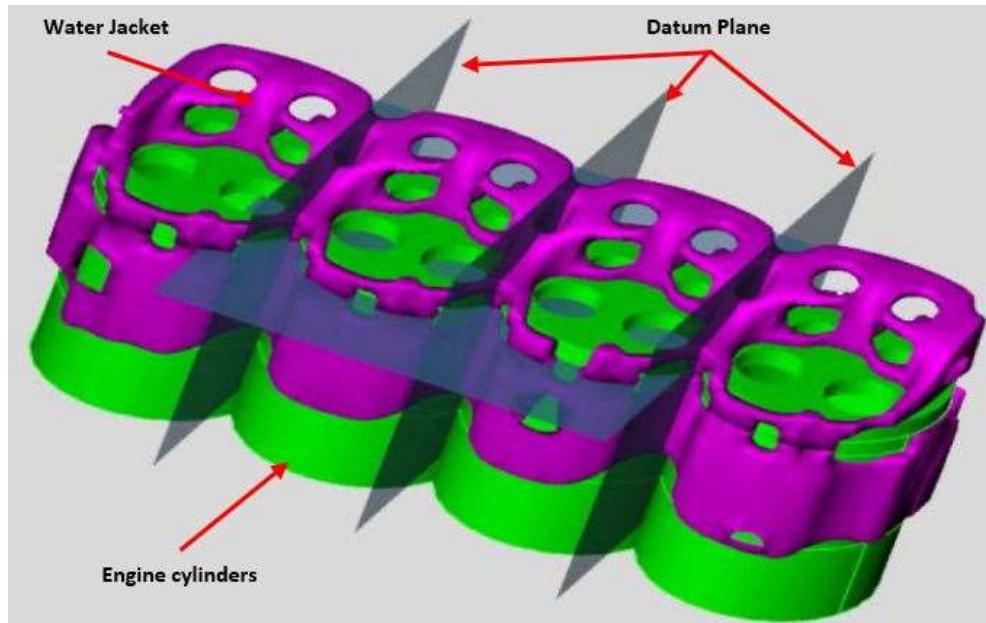
Figure 3: Coupling between cylinders and coolant jacket in the pre-processing tool by Millo [94].

As a result of the discretisation, the hydraulic model was unable to catch the 3D characteristic of the flow and ensure the correct heat rate distribution. A hydraulic calibration was necessary. The proposed calibration methodology uses two orifices on the main outlet and the bypass line of the cooling jacket. By manipulating the diameters of these two orifices, it is possible to reproduce the pressure drop across the engine.

The thermal mass of the engine, such as the block and the head, were considered as lumped masses. Moreover, here a thermal calibration of the model was required to ensure the correct heat rate distribution from the engine to the fluids and external environment.

A sensitivity analysis was carried out to understand the importance of the parameters involved in the thermal calibration. Factors such as HTCs between engine structure and coolant or oil, HTCs between engine structure and environment and the conductive resistance of thermal masses were considered in the analysis. Following the sensitivity analysis, Millo concluded that HTC can be treated as a calibration parameter and can be adjusted during the calibration. The thermal calibration methodology was refined due to the requirement to match the correct heat distribution in the engine structure.

This was modelled by acting on the resistance to conduction of the lumped thermal mass. The thermal resistance of the lumped mass is calculated as follows:

$$R = \frac{L}{k * A}$$

Equation (3)

where:

- R is the thermal resistance between the centre of the mass and the heat exchange area.

- L is the distance between the centre of the mass and the heat exchange area.

- k is the thermal conductivity.

- A is the heat exchange area.

The heat transferred from the coolant to the engine structure was calibrated by acting on the L parameter in the above equation.

The 1D thermal engine simulation model development continues with Bryakina's work [83]. The 1D model developed demonstrates the modelling engine is improved. It appeared like the state-of-the-art approach to simulate structure temperature for the prediction of fuel economy considering NEDC and WLTP cycles. The simulation model showed a significant step towards higher accuracy engine warm-up. Fasters model built compared to lumped mass approach and reasonable run time for typical fuel consumption drive cycle analysis.
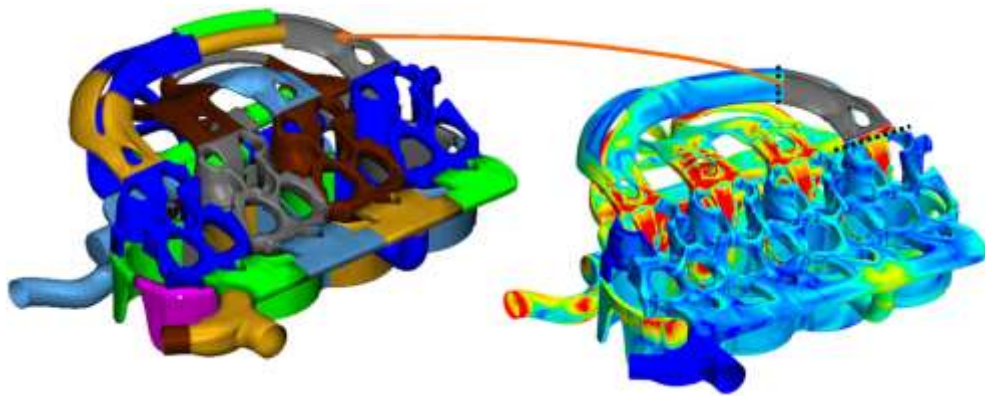
Figure 4: Head cooling jacket proposed by Bryakina [83]. A division between intake side and exhaust side in the block is present. Head water jacket are considered as single volume. Head pipe in the exhaust side are divided for each cylinder.

Based on the innovative approach to the modelling of a 3D custom mesh of the engine thermal structure to discretise the engine model from 3D to 1D, Graziano et al. [95] use his model to advance the moment at which reliable heat rejection calculations can be effectively used to support the engine cooling design.

The approach (used by Brvakina) compared to the parametric cylinder approach (shown by Millo) implies the possibility to mesh the overall engine structure based on the real geometry. Graziano has implemented a modelling methodology on how to discretise the coolant water jacket. As is shown in Figure 5 the headwater jacket is represented by 3 flow volumes. For the block, there are two flow volumes. This was done to capture the real flow distribution through the water jacket passage. Although flow restrictions placed along the coolant path have been used to calibrate the pressure distribution.
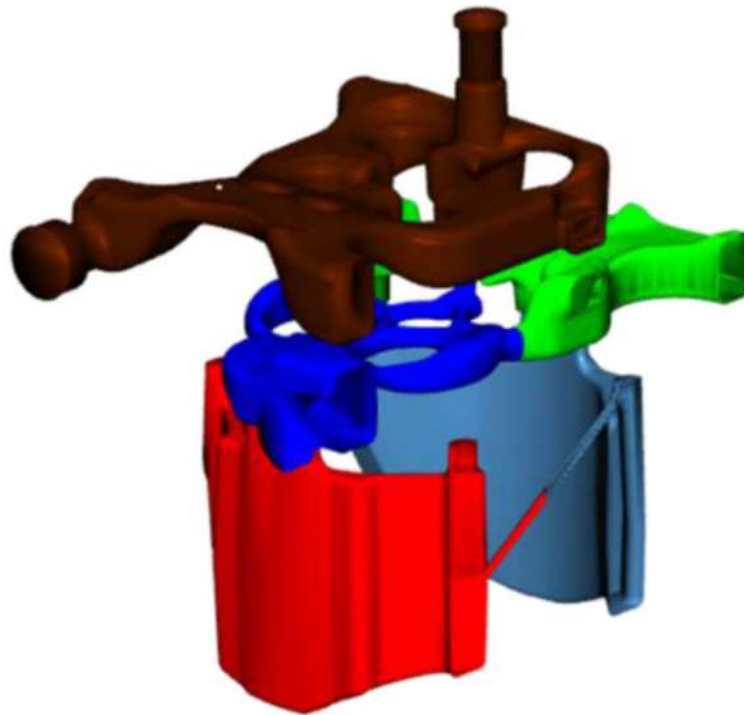
Figure 5: Water jacket discretization scheme adopted for each cylinder by Graziano [95]. *This is an example from Graziano on how the cylinder block water jacket can be modelled. The split between the exhaust and the intake side is evident and the approach of considering the upper side and the lower side of the water jacket head is taken into consideration.*

The 3D Custom Mesh GT-Suite used by Graziano demonstrated the possibility to mesh the entire engine structure based on real geometry. This thermal modelling

technique allows for defining heat transfer to the whole engine head and block, as well as for the liners, pistons, and valves. As well as defining the fluid wall heat transfer coefficient, this work was calculated from a 3D-CFD conjugate heat transfer analysis. The cylinder water jacket modelling is shown in Figure 5.

In this work, since the coolant and oil HTCs were imposed in the model, the tuning of its calibration parameters was limited to the conduction resistance characterising the head gasket and the magnitude of heat loss to the external environment which shows a small impact on heat rejection results, limited to a few percentages of the overall heat transfer figures.

The 1D model calibration and validation were realized by integrating the thermal model with the engine performance model. The integration of the models allows the performance model to calculate the gas side in-cylinder boundary conditions and passes this information directly to the thermal model.

The thermal calibration was realized following a sensitivity analysis to understand different model calibration levers. A single set of parameters working for both the performance and thermal model was defined and tuned to calibrate the overall model. With this work and this modelling methodology, Graziano proved that it is possible to refine the engine model to have a more precise thermal predictivity.

Previous works have shown how the modelling technique is developed to find the best trade-off between modelling effort, calibration methodology and result accuracy. In his work Bovo [96] developed a 1D engine thermal model using a pre-developed 3D model as a reference. The modelling methodology that was used was driven mostly by the CFD results. The hydraulic methodology applied for the model was driven by geometrical convenience.

Rather, it is interesting the effect the thermal approach had in the model. The cylinder head cold side is represented with a single thermal mass and the head hot side is divided into one thermal mass per cylinder. The block is also divided into four thermal masses. These thermal masses were considered lumped masses in the 1D model. These modelling strategies will allow lump masses to be at different temperatures when running the engine are different strategies, for example for cylinder deactivation.

The calibration proposed by Bovo is set up to characterise the total heat transfer between the different heat sources and sinks. Consequently, heat fluxes are the variables used to calibrate the model. Therefore, the model calibration target is set to minimise the normalised difference between the heat flux calculated in the 1D model and the reference given by the 3D model. The mathematical expression of the error to be minimised for each of the following steps is:

$$error = \sum \frac{Q_{3Di,j} - Q_{1Di,j}}{Q_{3Di,j}} \qquad \text{Equation (4)}$$

Where Q is the heat flux, i is the heat sink represented by coolant, oil and external environment and j is the engine load case.

The first step is to implement all the engine's solid thermal masses and their connections. The calibration was taken by adjusting the distance between the flame deck and the cylinder head coolant jacket.

The second step of the calibration will simply calibrate heat transfer coefficients in the 1D model. In the third step, the radiation heat transfer coefficient will be calibrated, due to its importance especially at low load as well as for the HTC for external convection. The next step of the calibration process is carried out on the coolant system. The coolant domain is discretised with three objects for each cylinder. Each object is connected to the corresponding thermal masses with an appropriate convection thermal connection. For each thermal connection, appropriate heat transfer coefficients need to be specified. The heat transfer coefficient is calculated using the coolant inlet temperature as a reference and the values are implemented as a table in the 1D model. The calibration in this step is achieved by multiplying the entire heat-transfer coefficient table with a single multiplier. For the surfaces in contact with oil as mist, uniform values for heat transfer are used matching those used in the 3D model. The last step of the calibration implies the system study in transient conditions. The coolant heat transfer coefficient is a function of its temperature. A linear correlation between the heat-transfer coefficient and coolant temperature is derived and implemented.

Using complex thermal management strategies, it is possible to make the heat distribution of the engine more accurate and dynamic, thereby increasing efficiency [97]. A more accurate modelling methodology was investigated using a 2.0L diesel

engine for a passenger car. The methodology expressed is based on the behaviours of a test engine which was recorded by thermal and optical measurements and represented by validated 3D CFD simulation models. Considering the three-dimensional flow effect within a 1-D model when discretising the volumes, the reliability and the validity of the simulation can be significantly increased.

The hydraulic modelling approach is shown in Figure 6. This is based on the basic flow behaviour of the water jacket and the different thermal loads in the engine block and cylinder head. The block was divided between the exhaust and intake side, while interbore sections were also modelled to better capture the flow rate. The head jackets were divided per cylinder and divided per intake and exhaust side.
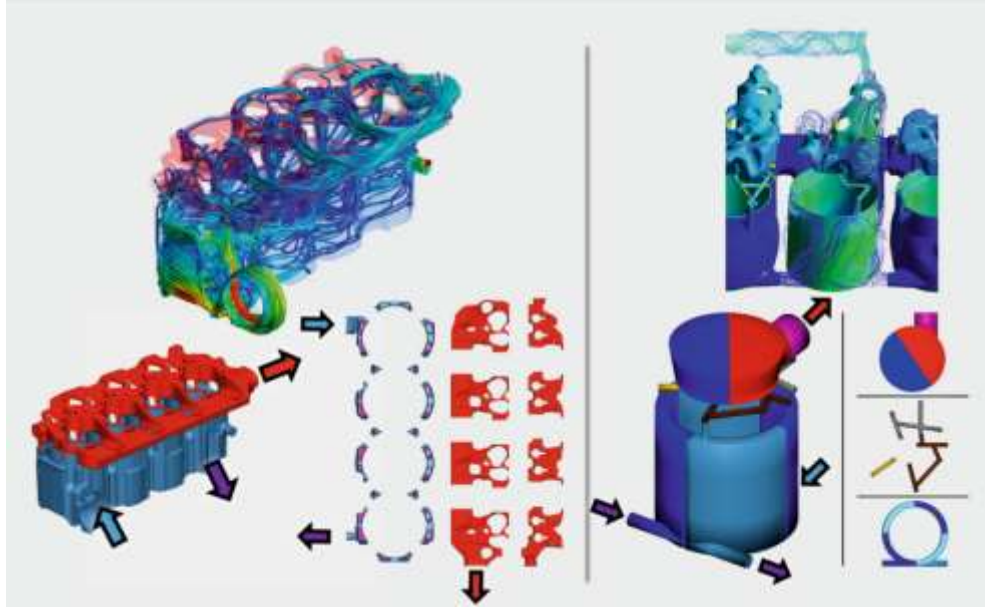
Figure 6: Flow characteristic (3-D CFD) of a passenger car, and water jacket discretization [97].

The calculation of the heat flow Q between wall and fluid in 1-D simulation is based on Netwon's approach with the heat transfer coefficient α, the area A, the wall temperature T_w and the fluid temperature T_F:

$$\dot{Q} = \alpha \cdot A \cdot (T_F - T_w) \qquad \text{Equation (5)}$$

To formulate α with its dependencies on the thermal conductivity λ and the characteristic length L, an approach with dimensionless numbers from the similarity theory is chosen:

$$\alpha = \frac{\lambda}{L} \cdot Nu \; ; Nu = Nu(Re, Pr) = a \cdot Re^b \cdot Pr^c \qquad \text{Equation (6)}$$

The above equation shows the relationship between α and the Nusselt number Nu, which described the forced convective heat transfer between a solid surface and flowing fluid. The Nusselt number can in turn be described by the Reynolds number and the Prandtl number. This so-called Nusselt correlation is described in equation 2 in a general form with three parameters a, b and c. For the work, this correlation does not provide satisfactory accuracy, so it is necessary to determine the parameter using 3D CFD simulation. The cooling water jacket is modelled in the 1D simulation with general 1D flow volumes. A heat transfer coefficient is calculated for each flow interface (FIF) of the 1D volume (Equation 3). The common heat transfer coefficient for the 1D volume results from a mass flow weighted average m:

$$\alpha_{FIF} = \frac{\lambda}{D_{char,FIF}} \cdot \left(a \cdot Re_{FIF}^b \cdot Pr_{1-DVol}^c \right) \qquad \text{Equation (7)}$$

Further modifications to this basic approach, such as the consideration of the transition between laminar and turbulent flow, the refined weighting of the individual flow interfaces and extended output variables, lead to more accurate results:

$$\alpha_{1-DVol} = \frac{1}{\dot{m}_{tot}} \sum_{FIF} \alpha_{FIF} \cdot \dot{m}_{FIF} \qquad \text{Equation (8)}$$

The parameters a, b, and c of the Nusselt correlation are ideally calibrated by varying inlet mass flow and the inlet temperature. In this case, separate parameter sets are derived from the 3D CFD for the engine block and cylinder head and for the large engine, a third parameter set is additionally derived for the pipe network in the combustion chamber roof.

2.5 Engine Warm-Up

Improvements in engine performance have increased demands on the engine cooling system over the last two decades where the overall rate of heat transfer in internal combustion engines has increased by 50-100% [98] [41].

Engine thermal efficiency is a key factor in the automotive industry. To pursue this objective, one of the areas that can be further implemented is the warm-up of the engine.

Warm-up and cold start are the critical phases in any type of approval regulatory test as they determine the time spent with almost uncontrolled tailpipe emissions until the catalyst light-off temperature is reached. This process may take several minutes to heat the exhaust gas system and is strictly dependent on the influence of heat transfer between the hot gas of the pipes by the thermal inertia of the pipes and heat losses to the ambient. It also depends on the heat up and thermal management of the engine and how the entire vehicle is driven. Thus, the principles guiding the cooling system design do not rely anymore only on the need to provide enough cooling capacity in all circumstances, but also on the speed of the warm-up phase targeting the nominal engine operating temperature [99]. This is one of the main reasons why engine thermal management systems have been constantly evolving.

A major trend in the automotive field is that modern vehicles are gradually incorporating electrification to evolve from conventional vehicles to hybrid electric vehicles (HEV), plug-in hybrid electric vehicles (PHEVs) and fully electric vehicles (EVs). The trends towards electrification will increase and last longer in the future.

Choukroum and Chanfreau introduced electronic control to an engine coolant circuit to optimise the warm-up rate of the engine. The use of electric water pump, thermostat valve and a variable speed fan shows greater control over the coolant circuit. This also implied that the system was able to delay the thermostat opening in the engine at a higher temperature. In this case until 110C during the part-load condition. It allows the system to a reduction in fuel consumption by 2 and 3% over an NEDC drive cycle [100].

Replacing the mechanical water pump and wax thermostat valve with an electrical model, was a strategy developed also by Cortona et.al. In their study, they reached a 3% saving in terms of fuel consumption over the NEDC drive cycle [38].

Another approach consists in using a variable flow oil pump as well as a second oil coolant EGR cooler in parallel with a coolant EGR unit. This method has been investigated by Burke et. al.[101] The work shows that the saving in these experiments was given by the variable flow pump with the EGR coolant giving a lower benefit. An amount of 22 grams of fuel was saved over the NEDC drive cycle which is a 2% saving for the engine under consideration.

There have been several investigations into the use of thermal stores as ways to improve the engine warm-up rate of engines.

Among them, there is the work completed by Shatz [102]. A thermal battery that relied on a phase challenge salt mixture was used inside an insulated tank. This layout allows the salt solution to melt during engine operation and maintains the solution temperature overnight before the cold fluid is flushed through the tank causing the solution to solidify and provide heat to the coolant. The heating reported to be available for 10 seconds was in between 50 and 100kW. This was before heat transfer levelled off. Regarding fuel economy, this approach relies on an improvement of 14% over the first phase of the FTP-75 cycle. Using only a single phase of a drive cycle the fuel penalty is proportionally larger than it would have been if the technology was evaluated over a full cycle, expanding the percentage of fuel economy gains [102].

However, there are considerations such as weight, size and cost, that need to be taken into account. Regarding the weight of a thermal battery can be a concern in vehicles where minimising weight is crucial for fuel efficiency and overall performance. The additional weight may offset some of the fuel efficiency gains achieved through improved warm up phase. The side of the battery is another factor. Integrating a thermal battery without compromising other components or reducing passenger and cargo space is essential. The cost of implementing a thermal battery system can be a significant consideration. The cost of materials, manufacturing process and integration into the vehicle's thermal management system all contribute of the overall costs [103] [104] [105].

Meanwhile, the use of a tank that does not rely on a phase change solution and instead captures hot coolant in an insulated tank, was analysed by Kuze [106]. This system was able to maintain coolant temperature above 50°C for more than 36 hours from a starting temperature of 90°C. However this approach led to a 5 – 6% of improving fuel economy over a ten minute drive from the cold start that was seen using this tank [106].

Exhaust heat recovery is another method which has been explored for improving engine warm-up. One example utilized a coolant-to-exhaust gas heat exchanger before the oil-to-coolant heat exchanger. This system yielded an 8 – 10% fuel consumption benefit when comparing a cold-start test with a hot start test with an impact on the specific fuel consumption of 14% during the first six minutes from a cold start [107].

2.6 Discussion

Reducing emissions and fuel consumption are two of the main goals that OEMs and researchers have pursued in recent years. Developing the cooling system of the engine brings several benefits in this direction. The development starts with improving the system by considering engine parts separately and trying to implement them to the best thermal efficiency. This strategy allows reaching some benefits even though with the increase in the engine technology involved in the engine cooling, it has shown its limits.

Taking into consideration the whole system, several studies understood the capability to highly improve thermal efficiency and reduce emissions and fuel consumption.

 This was achieved using newly available technologies:

- Electronic control.

- Variable-speed fan.

- Wax thermostat valve with an electronic model.

- Variable flow oil pump.

- Thermal battery.

- Exhaust heat recovery.

- Split cooling.

All these new technologies studied and developed into whole system solutions gave real benefits regarding thermal efficiency and fuel consumption. However, it is not enough to address the challenges that future powertrain systems will face in the next years.

In this scenario, virtualisation tools have a predominant role searching possible solutions for powertrain system challenges.

As discussed in the previous paragraphs, it is possible to identify three main families of simulation tools used to develop thermal management systems: 3D CFD model,

1D model and 0D model. All three are extensively used and all of them will provide the information needed to understand a particular problem and how to solve it and implement new solutions. To do this, "time" is an important factor that researchers and engineers need to consider in their development process. Not only "time" is important but also "robustness" is fundamental as well as "flexibility".

These factors can be summarised perfectly in the 1D model simulation tools world.

The benefit of having a 1D model, for thermal management usage are:

- Perform system analysis at all levels.

- Computational simulation run time.

- Easy to fix debug problem solution.

The ability to perform a system analysis or to use the model to validate engine performance and cooling assessments, even though it might lack some spatial resolution when looking are localised phenomena, is central to the engine development process. This shortcoming has been addressed by software development solutions with new features in how to implement the modelling work. One of these features is the possibility to discretise a 3D CAD model into a 1D model. This was a breakthrough in thermal management system development.

The research in these fields is wide and, as has been said in previous paragraphs, the focus has been only on the development of engine cooling systems mostly done with the discretization technique from 3D to 1D using GT-Suite.

The modelling phase, using the discretization technique from 3D to 1D, is first connected to the software availability options. Secondly, there are multiple ways to achieve the same result. This means that there is no perfect way to model an engine cooling system.

The first approaches on how to discretise a 3D model into a 1D model were given by Lauerta and Millo. Based on the previous works they were in the position to offer first clear guidelines and give a first modelling technique to develop a 1D thermal engine model. To validate the model Lauerta used experimental data being of a lack of CFD data but did not show how the model was hydraulically calibrated while Millo showed a first hydraulic calibration approach using two orifices

positioned in the main outlet and in the bypass lane of the coolant jacket to calibrate the system. For the thermal calibration, Millo used to adjust the thermal resistance of the lamped mass calibrating the distance of the mass centre for each lumped mass used in the model.

Based on previous work, Bryakina improved the modelling methodology showing a clear trend on how to model a water jacket and how to discretise it. The modelling approach on the hydraulic side shows a higher level of accuracy. No clear explanation was given and not all the engine water jackets were displayed. The higher accuracy of the model is due to the fact that CFD data were available and helped the user in the modelling phase. This work also shows a clear step towards the modelling development because the authors show the usage of the "Customised FE Cylinder Structure Objects". This is a Finite Element Cylinder structure model that can be used in the 1D model tool. Bryakina's results show that having a higher fidelity model will give higher accuracy results in studying engine warm-up in a shorter time compared to CFD models.

The works presented by Graziano and Bovo have shown advanced methodology to support engine cooling design. This was done based on the approach of modelling a 3D custom mesh used by Graziano and a detailed lumped mass used by Bovo for the engine thermal structure to discretise the engine model from 3D to 1D. Both show a more detailed methodology on how to discretise the head and block the water jacket. Both divided the block water jacket into exhaust and intake sides, while for the head Graziano choose to divide the lower part of the cylinder head into exhaust and intake sides and considered the upper part as another flow volume, Bovo instead considered having a single volume for each cylinder.

This modelling approach will have advantages in terms of capturing flow distribution and allowing more degree of freedom in hydraulic calibration but most important in thermal calibration. Graziano's model will use HTCs calculated from a 3D-CFD analysis and not specific thermal calibration was required by the model. Meanwhile, Bovo expresses a clear process methodology to calibrate the model using an error function that will minimize the normalised difference between the heat flux calculated in the 1D model and the reference given by the 3D model. More specifically for the coolant domain, the heat transfer coefficient was calculated by

the 3D model for each thermal connection used in the 1D model. These parameters were adjusted during the calibration process using a single multiplier.

2.7 Research Questions

The literature review highlights the importance of simulation tools in addressing research and development challenges, by providing a variety of approaches to tackle complex problems. This study focuses on a specific research area, which centre on the use of GT-Suite simulation software. The research demonstrates how simulation tools have been helped to overcome new powertrain challenges through the developing of various modelling and calibration techniques. Furthermore, the trend suggested that 1D models will be increasingly used for heat rejection prediction, utilising CFD data for validation.

This work aims to establish a robust modelling methodology for V engine. Focusing on modelling the cooling water jacket for different V engine geometries and developing a hydraulic calibration methodology validated against CFD data and a thermal calibration methodology validated against experimental data.

The research to be undertaken is constrained by three important research boundaries as follows:

- Hydraulic modelling methodology for V engine.

- Thermal modelling methodology for V engine.

- Calibration methodology for Hydraulic and Thermal model.

High performance engine and especially those with a V architecture must always face the challenge to have a coolant mass flow well balanced between the banks. This implies a better flow distribution along the water jacket as well as per the coolant heat release. From a hydraulic 1D modelling prospective this is a major challenge due to the major assumption that must be taken in terms of flow pressure drop and volume discretization. From a thermal perspective V engines must run with almost the same temperature for each bank. This allows a better engine efficiency and will prevent the engine from having knocking events localised to

individual hot cylinders. Based on this, three main questions are to be answered in this work. They are closely relating to the research gap identified in the literature review. The questions are:

- How can the hydraulic 1D modelling methodology be further implemented and renew to achieve a minimum calibration work on V type engine ensuring a flow rate a pressure distribution?

- In the context of power dense V engines, what novel approach can be explored within the thermal 1D methodology to optimise the calibration process, utilising experimental engine metal temperature and dedicated heat transfer multipliers for the engine block and head, and how can this methodology be validated across different engine operating points?

The first question will challenge the difficulties on achieving balanced water mass flow across the two banks of the V engine. This will require a comprehensive understanding of the fluid dynamics within the engine, Factors such as geometrical intricacies and varying operating conditions contributes to the complexity of achieving an optimal mass flow and pressure distribution.

The second research question will address the challenge of accurately capturing the intricate heat transfer dynamics. The need to integrate experimental engine metal temperature data and establish a dedicated heat transfer multiplier for different engine components introduces complexities as well in understanding and modelling the thermal behaviour under diverse operating conditions.

Chapter 3 - Hydraulic Modelling Methodology

In this chapter, the hydraulic modelling technique used in two different V gasoline engine geometries is introduced. Furthermore, a hydraulic calibration methodology is outlined, implemented and validated, Finally, a comparison discussion is provided to compare different methodologies.

3.1 Summary

This chapter focuses on the application of hydraulic modelling methodology to two different engine geometries: A-Sample, C-Sample.

I. Introduction

- The chapter starts by highlighting the importance of 1D simulation tools and thermal models in the engine development process. It also introduced the two engines under study.

II. Hydraulic Modelling methodology – A Sample

- This section presents the hydraulic modelling methodologies used for the A-Sample engine. Three different hydraulic modelling methodologies are developed, implemented and compared. The selected hydraulic methodology is simulated and validated against CFD data.

III. Hydraulic Modelling Methodology – C Sample

- Based on the finding from the A Sample and the chosen hydraulic methodology, the C-Sample case study is implemented. The hydraulic model is calibrated and validated against CFD data.

IV. Conclusion

- The chapter concludes with a final discussion on the benefits of the hydraulic methodology for both the engine and the selection

of the final simulation model to be used for the thermal methodology.

3.2 Introduction

Developing an engine simulation model is a complex task and a challenge for researchers and engineers. The importance of such models lies in their extensive use in the engine development process to reduce fuel consumption and emissions while improving the performance and reliability of the powertrain system. A thermal management system is central to the design and optimisation of the engine development process. The ability to solve engine thermal behaviour and optimise the system in a relatively short time frame can help OEMs, engineers and researchers to discover new, more efficient solutions, leading to achieving the net-zero emission target.

Simulation software tools can be categorised into zero-dimensional, quasi-dimensional and multidimensional domains, which are all used to implement new solutions. Over the years, software developments have paved the way for new strategies in modelling engine thermal models. One of the most innovative ways, as seen in the previous chapter, is the possibility to discretise the actual 3D CAD into a 1D model. This modelling methodology can be performed using different software available on the market or with open-source codes. In the present work GT-Suite is used for the entire modelling technique and calibration. The literature review presented has shown the current state of the art and this work aims to fill the research gaps identified. In this chapter, a hydraulic modelling methodology and its calibration methodology is implemented and validated.

Three different methodologies are developed and compared to assess the best procedure to model the coolant water jacket.

The "Method One Volume" approach that consists in modelling the engine block, head and gasket as a single volume flow, which is then discretised into a 1D model. This method simplifies the modelling process, but it may not accurately capture the complex geometry and flow restriction of the engine.

The second approach is "Method Separate Vol 1". This methodology splits the engine block into the exhaust and intake side and each cylinder is treated separately. This allows for more detailed modelling of the engine geometry, but it may increase the computational complexity and the number of parts in the model.

The last approach is "Method Separate Vol 2". This is a hybrid of the previous two methods, where the engine block and gasket are modelled as one volume flow, while the head is divided into separate volumes for the intake and exhaust sides and cylinders. This approach aims to balance the accuracy of the modelling with computational efficiency.

The CFD simulation results will refer to an hydraulic analysis conducted by an external research centre, commissioned by the engine manufacture. Quality assurances were integral during the simulation phase reviewing initial and boundary condition with empirical and real world measurement data and validated against industrial standard

These methodologies are based on the literature review and implemented for the following case of studies. The engine primary data are listed in Table 1, while A Sample and C Sample will differ from coolant jacket geometry.

Table 1:Engine type: Four stroke, V-Type, six cylinders turbocharged, GDI engine.

Configuration	120deg V6
Displacement (L)	3.0
Bore (mm)	84
Stroke (mm)	90
Compression ratio	9.415
Material	Aluminium head and block
Target Max Torque (Nm)	585
Target Max Power (kW)	435
Max Engine Speed (rev/min)	8250
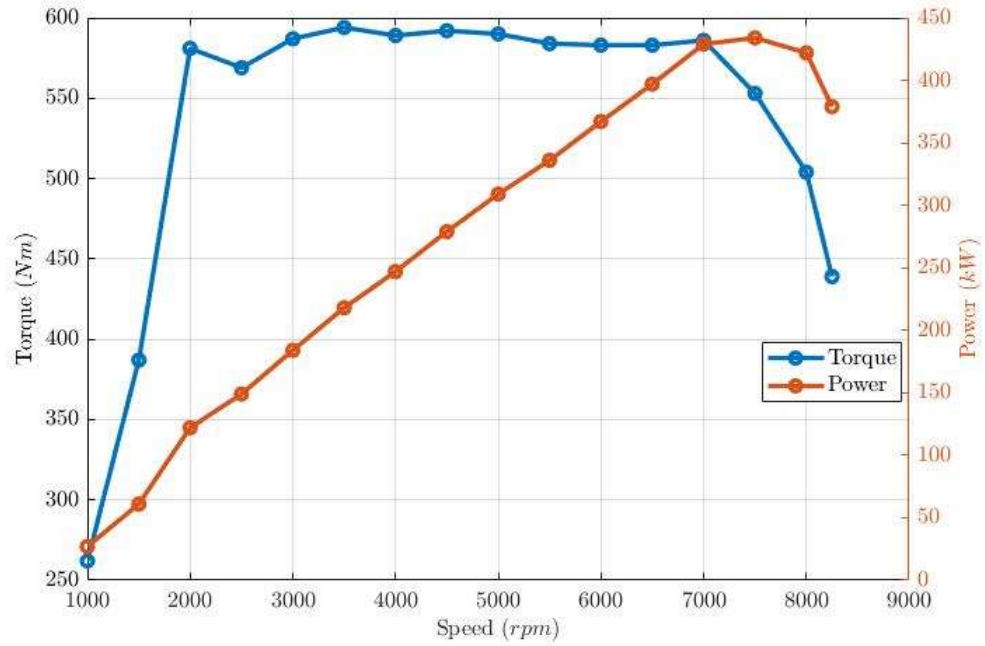
Figure 7: Engine Torque Power Curve.

The main steps in the creation of a complete thermal engine model can be summarised as follow [108]:

1. Definition of flow volume

2. Definition of thermal masses

3. Definition of Cylinder structure

4. Assembly of the model

5. Calibration (Hydraulic and Thermal)

6. Connection to engine

7. Addiction of a friction model

In this current work, these steps are divided into three main stages. Stage one involves the implementation of hydraulic modelling, while stage two focuses on thermal modelling. Stage three comprises the validation of the engine thermal model.

Figure 8 illustrates the workflow during the hydraulic methodology stage. The procedure is divided into two phases. In the first phase, the hydraulic model is optimized to accurately estimate coolant pressure and flow rate, minimizing calibration efforts. Once phase one is completed, a set of calibration parameters is defined and optimized in the model to meet validation criteria. The model is then considered validated, marking the commencement of the second modelling stage.
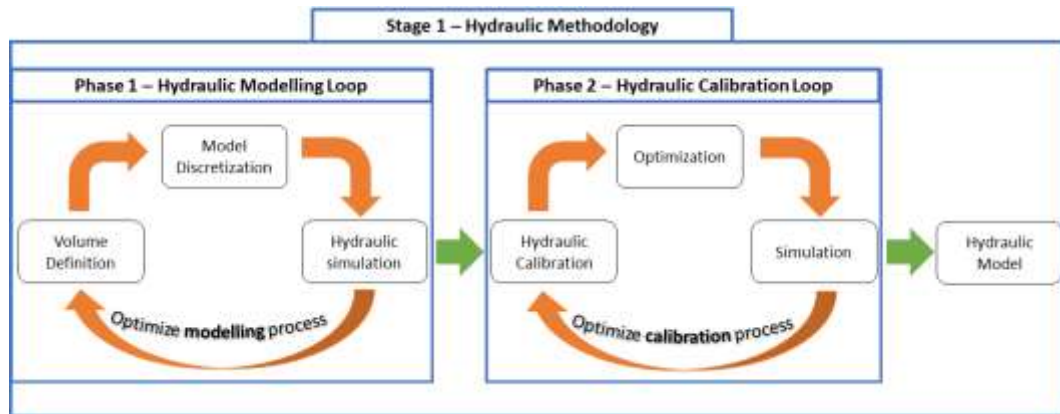
Figure 8 : Hydraulic modelling stage workflow.

Stage two, depicted in Figure 9, consists of two phases akin to the hydraulic methodology. Phase three involves the implementation of the hydraulic model with thermal masses of the engine, followed by a simulation run to validate the model's correct procedure and implementation. Upon completion of this phase, phase four ensues. In this phase, the model is implemented with a set of calibration parameters and undergoes optimization. The phase concludes when the results meet the validation   criteria.
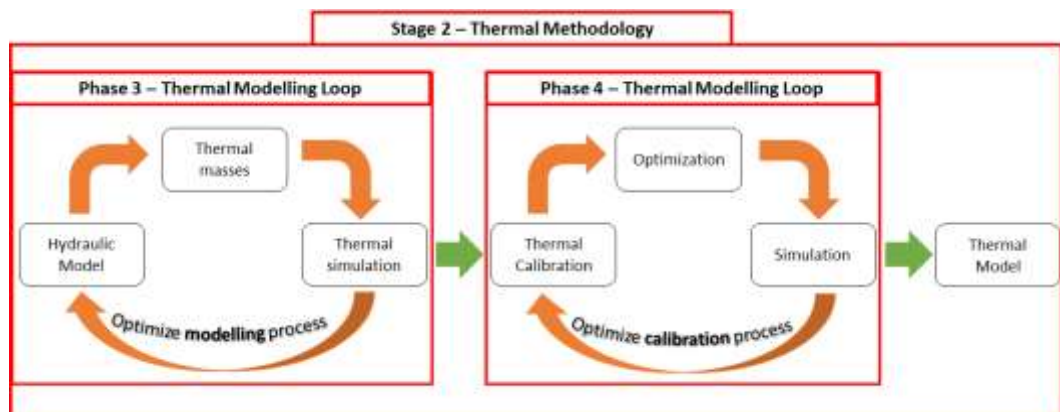
Figure 9: Thermal modelling workflow.

The final stage, as shown in Figure 10, encompasses phase five. This phase begins with the overall engine thermal model using parameters calculated and estimated in stage two, concluding with simulation and data analysis. Results are compared against experimental data, and at the end of this stage, the overall engine thermal model is considered validated.
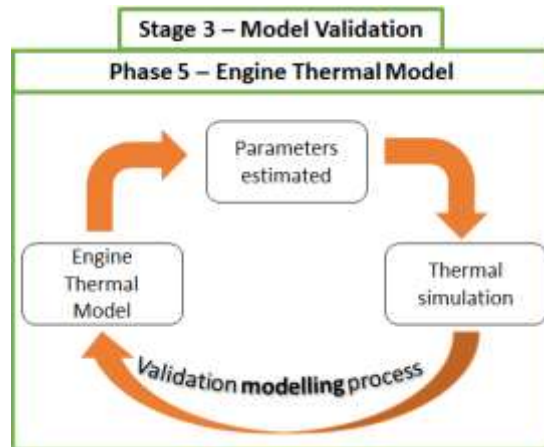
Figure 10: Model validation workflow.

3.3 Hydraulic Modelling Methodology – A Sample

The modelling process can be summarised in the following three main steps:

1. Extraction of water jacket geometry from CAD.

2. Definition of flow volumes.

3. Discretization.

The first step in the modelling process is to extract the engine water jacket volume, which is done using a pre-processing tool within GT-Suite SpaceClaim. A geometry check is then performed to ensure that the CAD geometry is free of any errors or inconsistencies that could affect the accuracy of the model. This includes a thorough analysis of all solid parts to ensure that they are properly defined and ready for the next phase of the process, which is performed in GEM3D.
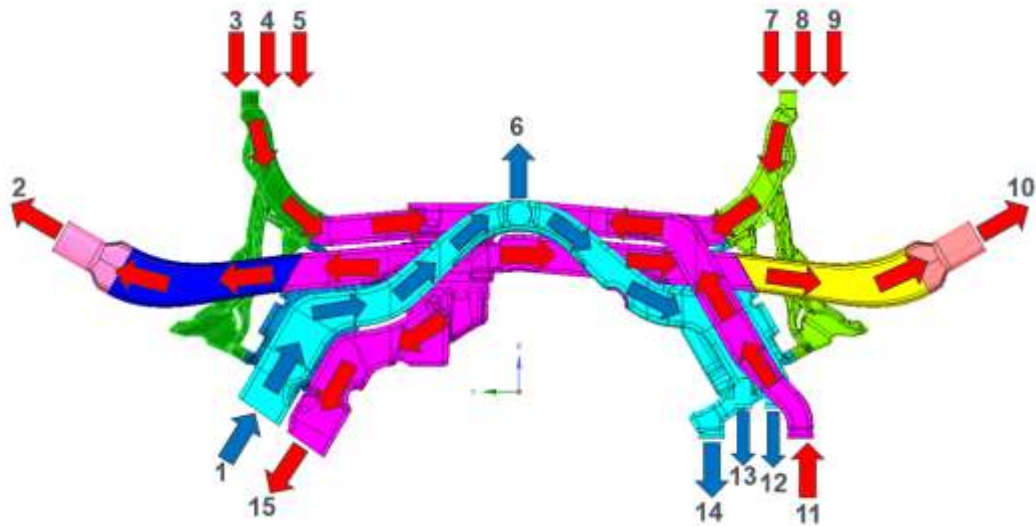
Figure 11: A Sample - Coolant flow circuit frontal view.
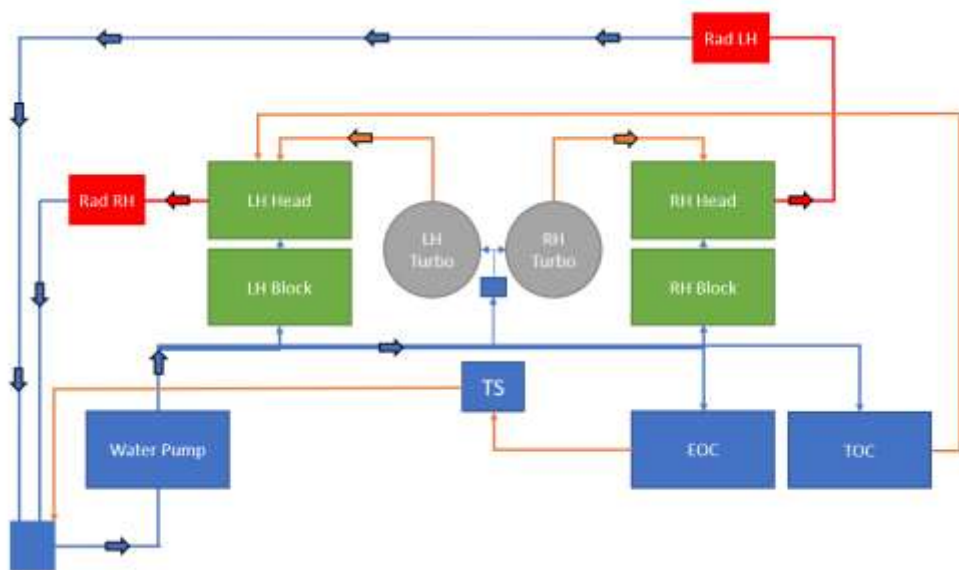
Figure 12: A Sample coolant flow diagram.

The complexity of the overall water jacket can be seen in Figure 11, which shows a front view of the entire coolant circuit for A-Sample, while in Figure 12 is showed the coolant flow system diagram. The inlet pump is located on the bottom left of the engine and has two main entrances, which split the flow into two-thirds for the bank comprising cylinders 4-5-6 and one-third for the bank where cylinders 1-2-3 are located. The flow then goes directly to cylinder one and cylinder four passing through all the cylinder blocks and moving to the head from the exhaust side of the block. The gasket closes the passages from the intake side of the block and the head.

Next, the flow enters the head and goes to the upper side of the cylinder head via the two rails before returning directly to the thermostat and exiting to the radiators. Various inlets and outlets which play a crucial role in the cooling process, are located in the cooling circuit.

These inlets and outlets are listed below:

1. Block LH Inlet.

2. Radiator RH Out.

3. Not used (closed off).

4. Turbo RH Inlet.

5. Degas.

6. Second turbo take-off.

7. Transmission Inlet.

8. Turbo LH Inlet.

9. Degas.

10. Radiator LH Out.

11. Oil cooler Inlet.

12. Turbo Out.

13. Transmission Out.

14. Inlet flow to the pump (radiator bypass).

15. Pump Return.

In the following section the explanation of the three methodologies used for the hydraulic modelling is provided. In the table below a summary of the methodologies and the models are listed.

Table 2: Hydraulic methodologies and models.

Methodologies	Models Name
Method one Volume	MA – MB
Method Separate Volume 1	MC - MD – ME
Method Separate Volume 2	MF – MG - MH

3.3.1 Method One Volume

In this paragraph the first methodology, named "Method One Volume" is presented. It is based on the general approach [108] suggested in the GT-Suite manual for modelling the water jacket and Millo's work [94].

Four assumptions are needed to model the water jacket with this approach:

- Only the water jacket for the cylinder block, head gasket and cylinder head are considered with One Volume.

- The water jacket for each bank is considered as two coolant circuits. (Due to the two different inlets in the geometry).

- The water jacket gasket volumes are merged with the block water jacket (due to the small volume).

- Frontal pipes are treated separately.

Before starting the procedure, it is important to understand the step-by-step procedure within the pre-processing CAD software. Firstly, the CAD geometry is imported into the pre-processing tool, GEM3D, and it has the status of a Solid Shape. The Solid Shape can be converted into a part, which is a fundamental step. The Solid Shape can also be converted to a General Flow Volume, which allows the software to continue the modelling procedure. Alternatively, it can directly convert the Solid Shape into Flow Splits of Pipes, giving two different ways to carry out the modelling work.

Model A

As previously mentioned, the upcoming methodology treats the primary water jacket volume as a General Volume Flow. The modelling process began by defining the inlet and outlet of the water jacket using conventional naming convention, while the model was still in Solid Shape mode.

The tools that have been used are:

1. Three points cutting plane: place three points on the block water jacket solid to create a cutting plane, select the geometry to be cut and then with the clip option the solid will be cut.

2. Restore Cutting plane: restore the precious cutting plane and with the drag and move option it is possible to be more precise in the zone to be cut.

3. Pipe normal cutting plane: this tool analyses the centre line of shape and follows the centre line so that cuts perpendicular to the flow direction can be made.

An example of the plane used are shown in Figure 13.

During the modelling process, the three cutting options mentioned were extensively used. The next step involves defining the inlet and the outlet solid parts of the water jacket in Solid Shape mode. Subsequently, the water jacket volume of the block, gasket and head were then merged and the entire water jacket was converted to a General Volume Flow, except for the inlet and outlet. Additionally, the frontal pipe of the water jacket was separated from the water jacket bank.

The next step is to model the water jacket volume flow. The approach is used to discretise the three cylinders separately by dividing them using Datum planes features.

Datum planes are:

- Global datum Plane (it exists independently in the model tree) so it refers to all the parts.

- Child Datum Plane (it belongs to a specific component) so it only refers to the component where it is applied.

Datum planes are divided into:

- Pipe Normal.

- Snap to feature.

- 3 Points.

- Single point and Vector.

In the modelling methodology, the Child Datum Plane option is chosen because it allows a higher degree of flexibility during the modelling procedure. Moreover, all four options were used where the geometry required special attention.
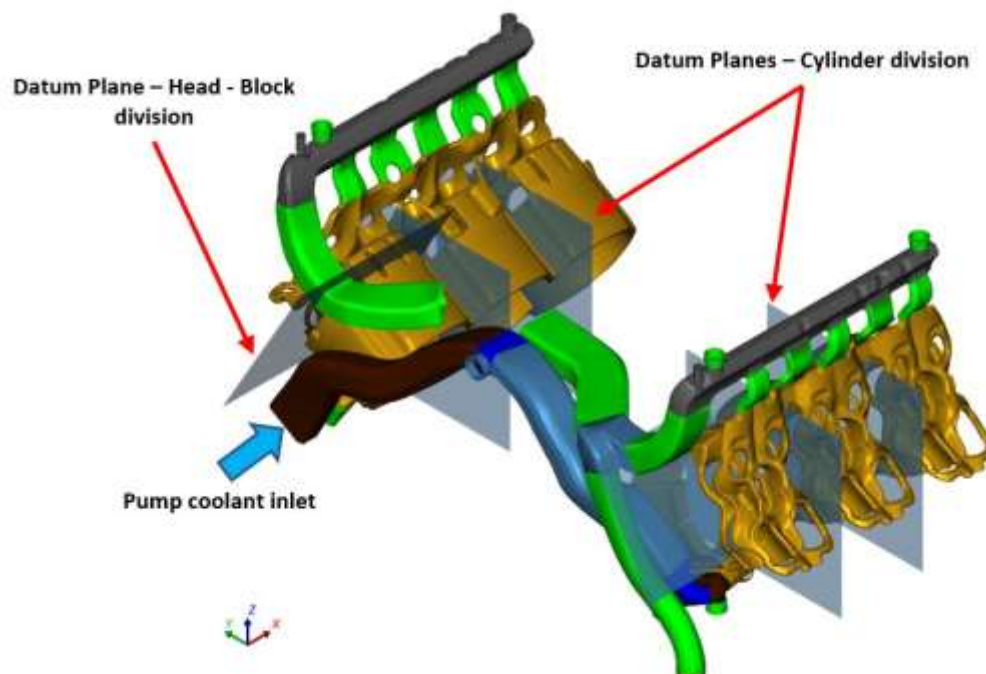
Figure 13: A Sample – Model A -Datum Planes definition.

Figure 13 shows how the water jacket volume flow is divided. Two Child Datum Plans are defined in the cylinder interbore to divide each cylinder. One plane is placed at the gasket height to capture the inlet geometry of the gasket and control the coolant flow. The fourth plane is placed at the exit of the head where the rail pipes start. In the modelling procedure, the planes must be as orthogonal to the flow as possible to ensure better conversion of the solid and better discretisation of the geometry. This procedure was repeated for the other engine bank.

The front pipe, which was separated from the engine block, was modelled in a Solid Shape state for ease in defining the different inlet and outlet sources of the engine. The thermostat volume and the outlet pipe to the radiator were not included in this model because the CFD simulation model was not implemented.

At this point, the model is ready to be discretised into a 1D model using a discretisation length of 40mm.
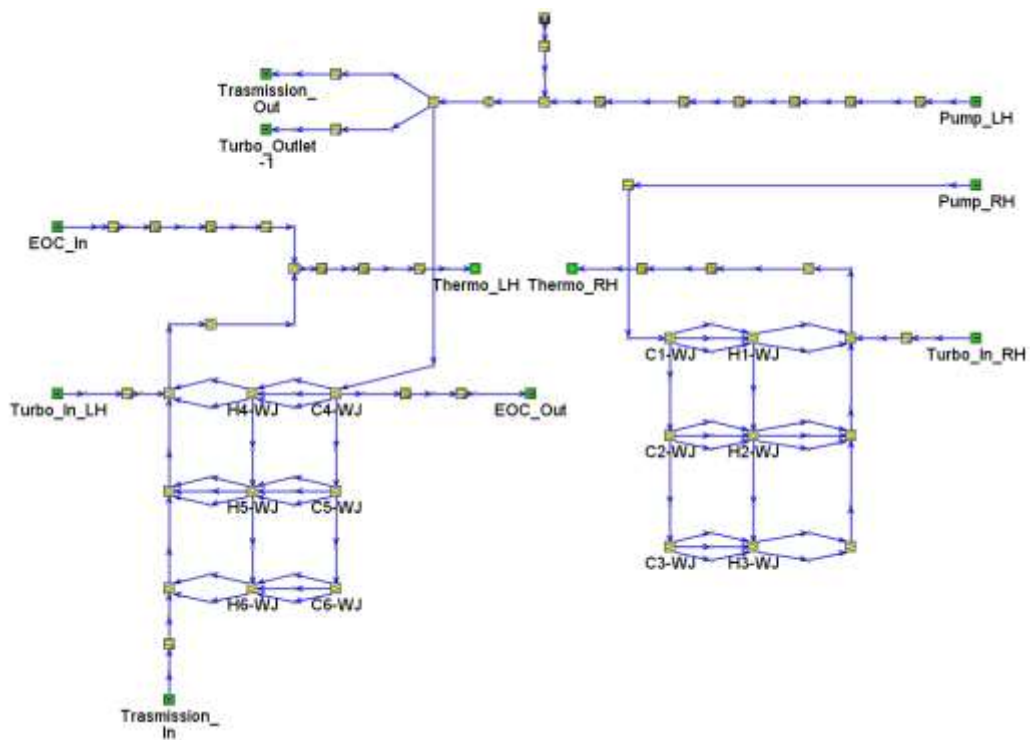
Figure 14: A Sample - Model A- Discretisation using Method One volume.

Figure 14 shows the model discretised from GEM3D to GT-Suite. The two engine banks can be easily recognised. The water jacket is represented by two separate cooling circuit, one for the right bank of the engine: cylinder 1-2-3 and the other for the left bank: cylinder 4-5-6. It's worth noting that the model includes two different coolant circuits for each bank of the engine.

To have a clearer understanding of the model's discretisation and how child datum planes are defined, Figure 15 graphically shows how the upper part of the model is discretised.
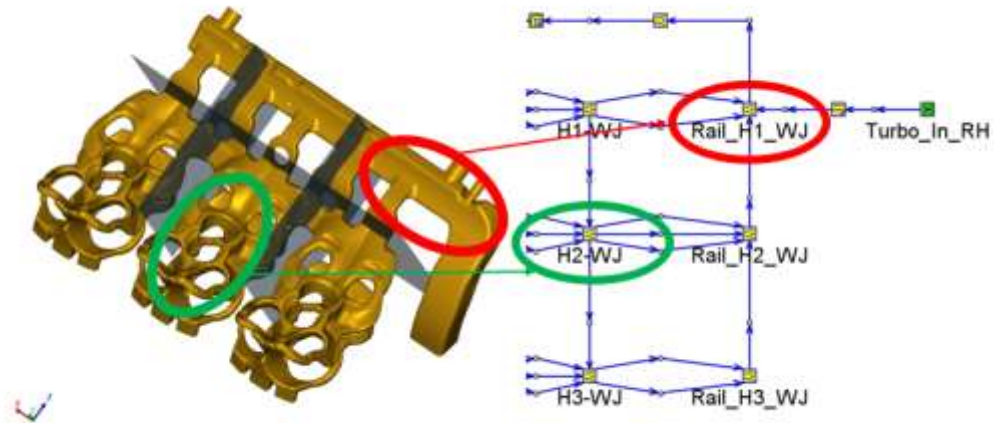
Figure 15: A Sample – Model A - Rail analysis.

In Figure 15, it can be observed that certain simplifications are made with this strategy, particularly for the upper side of the head, while the block and head will certainly be discretised as a general flow split. This is because the main passages between the upper side of the rail are not captured and their geometrical properties do not accurately represent the real CAD geometry.

The discretisation from 3D CAD to a 1D volume flow part are not enterly able to capture the complexity of the engine head geometry. This may lead to a not effective capturing of the volume flow rate in the head region and consequently to the coolant pressure. This simplification will also have an impact on the temperature estimation in an important region of the V engine. More in particular, part discretised in the 1D tool, is represented as a volume sphere with inlet and outlet described by diameter calculated from the section had using the cutting plane.

Model A – Hydraulic Simulation

The objective of the simulation is to gain a deeper understanding of the model behaviour which will inform the modelling methodology and guide decisions on which areas require more detailed modelling work and which areas can be considered acceptable with simplified models. To achieve this, the 1D model results are compared against hydraulic CFD results.

53

Part	Unit	7500 rpm	5000rpm	2500rpm
Pump Inlet	L/min	378	252	126
Bank RH Out	Bar	4	4	4
Bank LH Out	Bar	4	4	4
EOC Out	L/min	67	45	23
Transmission Out	L/min	33	22	11
EOC Inlet	L/min	67	45	23
Transmission Inlet	L/min	33	22	11
Turbo Out	L/min	8	5.3	2.7
Turbo RH Inlet	L/min	4	2.7	1.35
Turbo LH Inlet	L/min	4	2.7	1.35

Three engine operating points considered in the simulation process are shown in Table 3. The water coolant fluid used is the glycol 5050. These three engine operating points are mainly selected for low, middle and higher coolant flow condition.

Results are shown in the following figures. Pressure comparison is made between the 1D model and the CFD model.
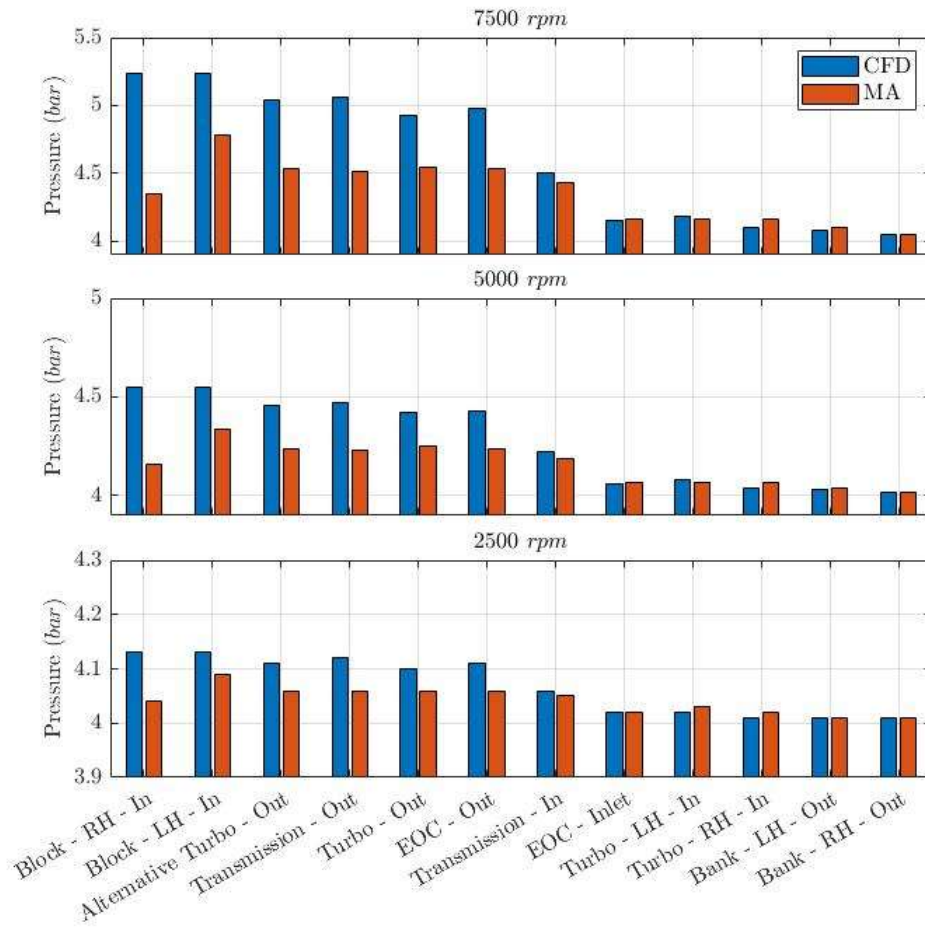
Figure 16: A Sample - Model A - Pressure Results.

The initial results presented in Figure 16, have been thoroughly analysed to assess the pressure distribution along the 1D model. However, the 1D model with the current layout exhibits a considerable deviation from the CFD results. Specifically, the pressure difference at 7500 rpm, the block inlet pressure is 0.89 bar for the right bank and 0.46 bar for the left bank. This trend persists even at lower engine speeds. Moreover, the transmission outlet pressure shows a difference of 0.5 bar, while the turbo outlet pressure exhibits a difference of 0.38 bar. All these inlets and outlets are located in the front pipe. A significant difference of 0.45 bar is detected for the EOC (Engine Oil Cooler) return. On the other hand, the results trend for other outputs appears reasonable. It is important to note that the discretised model fails to detect the pressure as deduced from the detailed analysis.

The reason of this difference between the CFD results can be explained by the over simplified volume flow geometry discretised. This first attempt considered large

portion of the volume coolant jacket both for the head and the engine block. This also means an oversimplification in the discretization that lead to a poor estimation of the coolant pressure along the engine water jacket.

Model B – Implementation and comparisons

Further modelling work is necessary due the limitations of the previous 1D model, which failed to capture the pressure along the main inlet and outlet points. To address this issue, the water jacket rails have been separated from the main water volume flow. This is achieved by converting the model to Solid Shape mode and cutting and separating the rail region. Additionally, the engine block gasket and head are now considered as one volume, while the transmission and the turbo outlet have been given a better definition in Solid Shape mode, as the difference between CFD results and 1D was too high. These improvements enable the model to capture the flow and the pressure more accurately. The procedure for discretising the model remain the same as described in the previous paragraph and the final model is presented in Figure 17.
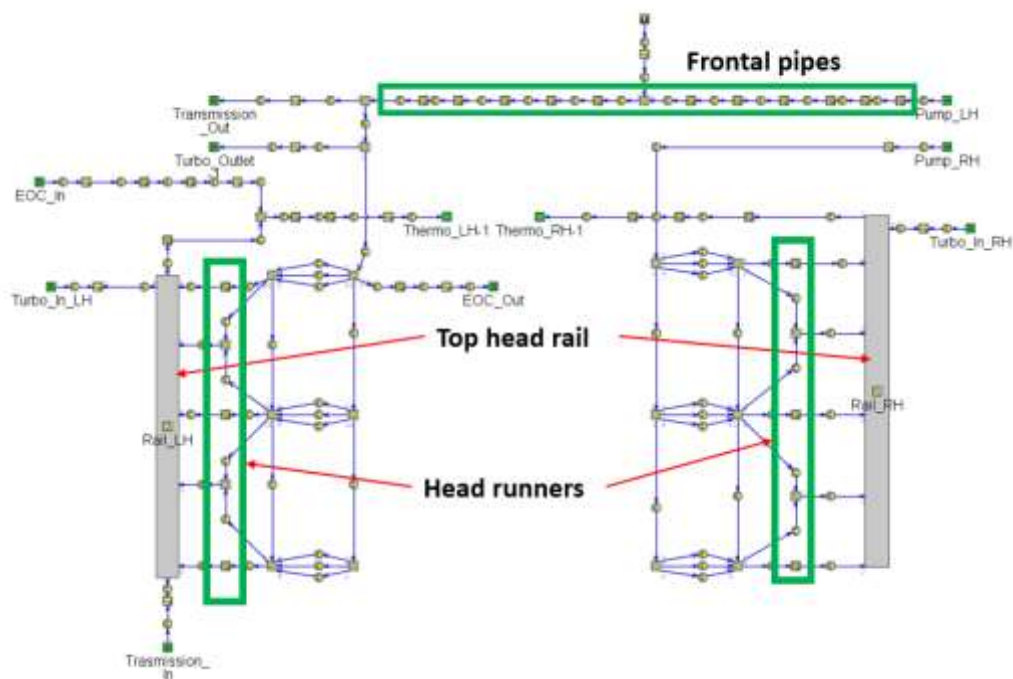
Figure 17: A Sample – Model B -Method One Volume implemented.

Considering the large portion of volume flow that was taken into consideration in Model A, in Model B an extensive studied were performed in the main coolant rail presents in the coolant jacket. This as show in Figure 17 are represented by the frontal coolant jacket pipe and the two head rails. In this model a detailed approached to model the frontal pipe was used based from the Model A results that showed a quite significant difference in the inlet of the two engine banks. Regarding the head rails a more simplistic approach was taken, due to not over complicate the model understanding the benefit only in modelling the head runners and how effectively they capture the pressure between the engine block and the head.

After the implementation with the same initial conditions, another hydraulic simulation is carried out.
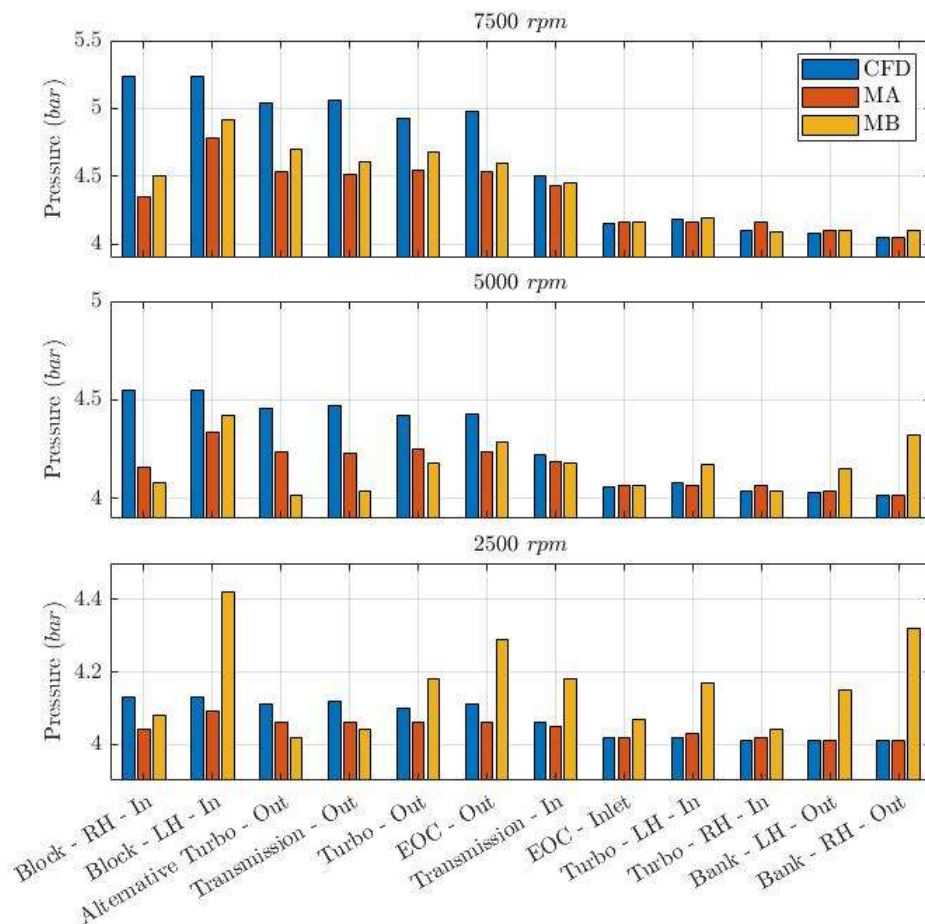
Figure 18: A Sample - Model A and Model B comparison.

With the recent implementation, an overall improvement can be observed in Figure 18. However, there is still a considerable difference between the 3D model and the 1D model. It is important to note that the 1D model assumes two coolant circuits.

A clear difference is showed at 2500 rpm in the LH inlet engine block. This can be explained by the discretization of the coolant frontal pipe. This pipe is distressed in the 1D model with a series of pipes, each of them that capture the diameter in the cutting section. Having such multiple pipes also lead to multiple restrictions and consequently to an increase of pressure. It also can be explained by the surface roughness of the pipes. Where is possible to see at higher speed the pressure remain as well as the lwer case for the left inlet block. This also imply further modelling development.

A possible improvement would be to model a single coolant circuit by designing an appropriate flow split with the geometrical properties of the CAD and integrating it into the model. This modification may lead to better capture the flow and pressure in the frontal pipes, as well as the pressure distribution on the left bank of the engine. The results demonstrate the significant advantages of this modelling approach, as the gap between the 1D and CFD results is significantly reduced.

3.3.2 Method Separate Volume 1

After observing the positive impact of implementing additional modelling work on pressure calculations, a new approach has been adopted. Instead of treating the entire water jacket as a single volume, it is separated into distinct volumes. This modelling process is carried out in Solid Shape model, which enables more precise cutting and shaping. This approach is expected to result in more accurate calculations and better overall performance of the model.

Method Separate Vol 1:

- Consider the water jacket separately.

- The modelling procedure will be conducted in Solid Shape modes.

Model C

The engine block has been the initial focus of the implementation process. Although its geometry is relatively simple, there are certain geometric restrictions that control the flow, which can be captured during the modelling phase. Furthermore, the block's water jackets are connected through two interbores via small water pipes, which can also be implemented in the modelling process. The waterjacket of the block is divided into exhaust and intake sided and the connecting parts between cylinders were defined as well. Figure 19 depicts the appearance of the water jacket after the implementation.
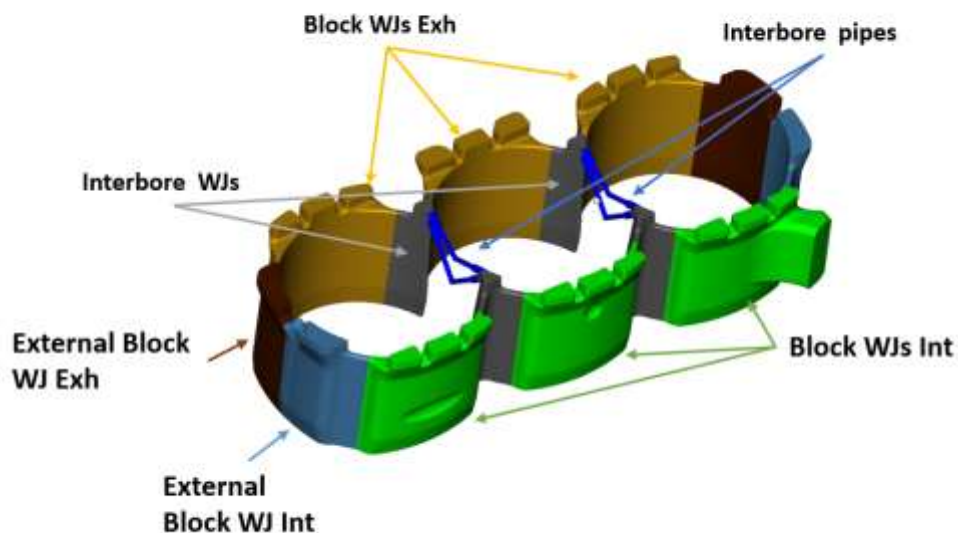
Figure 19: A Sample - Model C Block - water jacket division.

As for the head, additional modelling work has been done to overcome the difficulty in matching the CFD results. A better discretisation of the geometry is expected to aid the 1D simulation model. The three-cylinder heads are divided and cut into two volumes, one represents the intake part and the other the exhaust part. It is important to note that the coolant flow goes from the exhaust side of the block through the exhaust side of the head. The rail is separated from the cylinder head and is treated as in Method One Volume, while the rail is divided into several parts, one for each entrance of the rail pipe. This will help the discretisation to match the real geometry.

The overall model, ready to be discretised into a 1D model, is depicted in Figure 20.
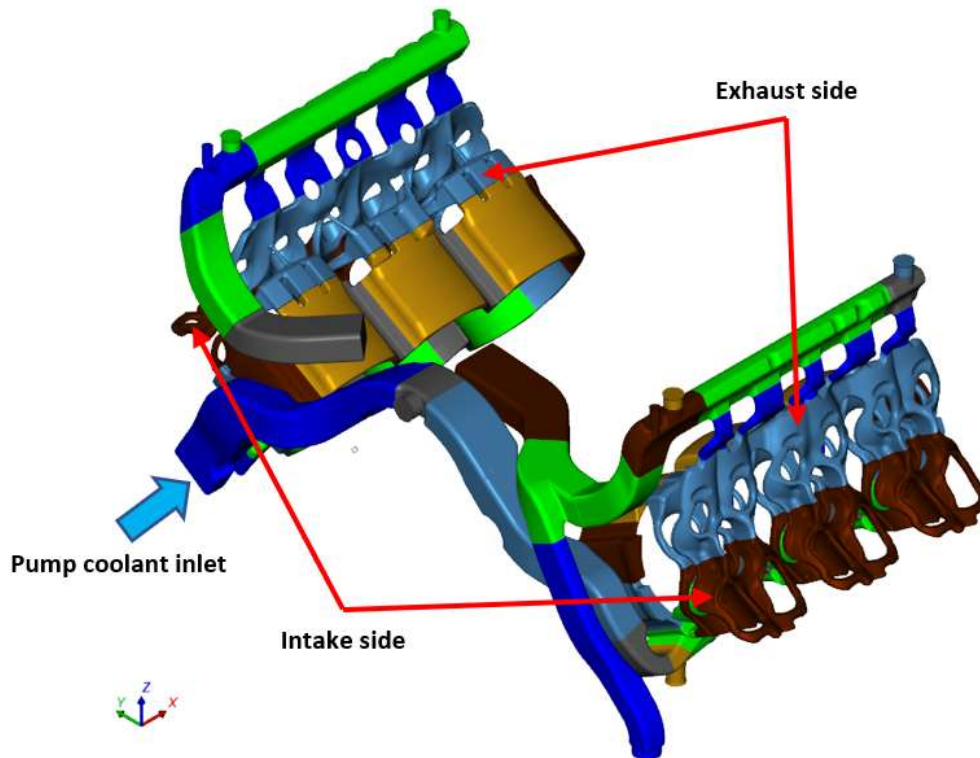
Figure 20: A Sample -Model C - Assembly water jacket definition.

Model C – Hydraulic Simulation

The hydraulic simulations have been executed following the same procedure as before. Figure 21, clearly indicates the improved results achieved with the new modelling methodology. Although this approach leads to an overestimation of pressure in the main frontal pipe, it provides significant benefits in terms of evaluation. With further adjustment and implementation, this methodology can continue to be refined and improved.
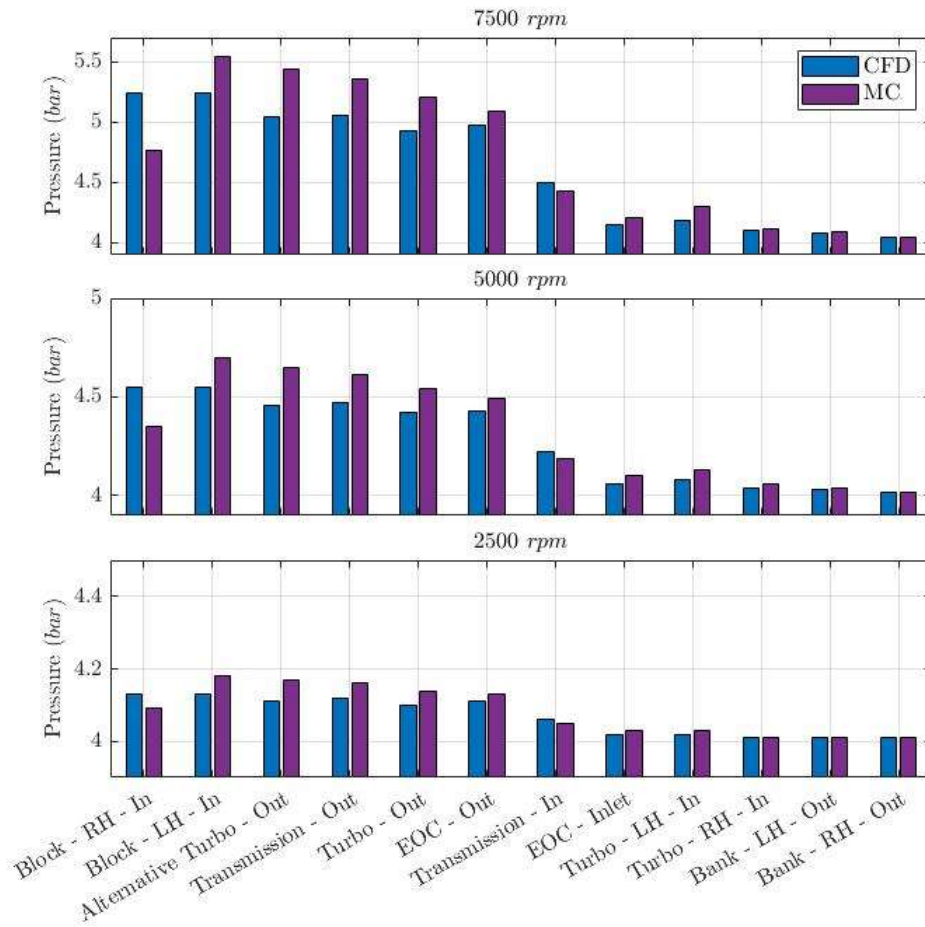
Figure 21: A Sample - Model C pressure results.

Model D

Model C has proved to be challenging to simulate due its complex geometry and the presence of numerous restrictive parts. As a result, the previous modelling approach let to an overestimation of the pressure within the cooling jacket. To address this issue, the two external flow splits of the engine block have been merged, and the block has been divided into exhaust and intake sides, as shown in Figure 22. This new modelling configuration aims to provide a more accurate representation of the flow and pressure distribution in the system.

61
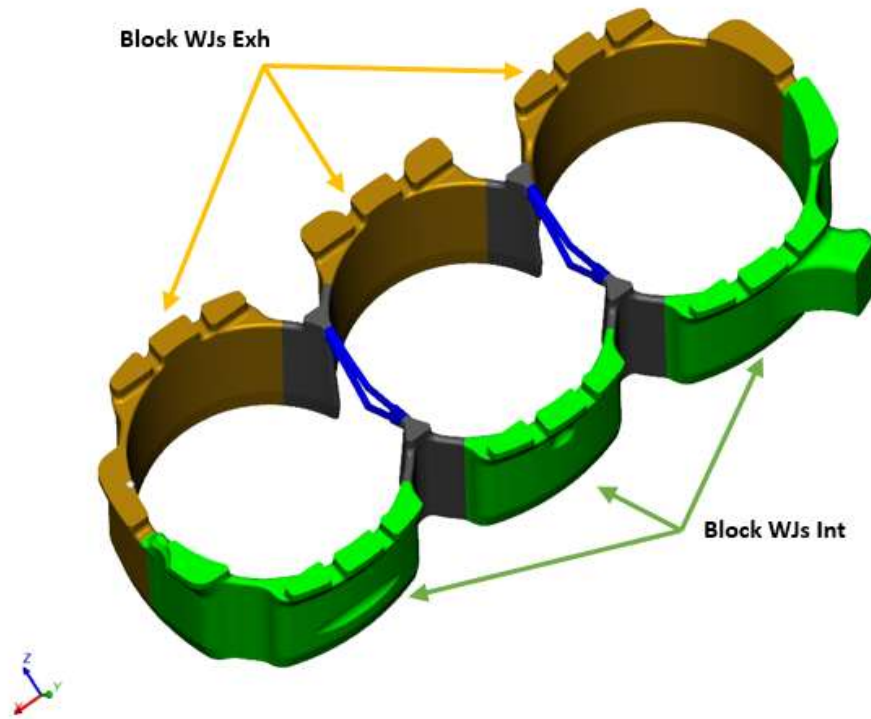
Figure 22: A Sample - Model D implementation. The external block waterjacket for cylinder 1 and three, as well per cylinders four and six were incorporated in the cylinder block waterjacket intake side and exhaust side.

Model D – Hydraulic Simulation and comparison

The implemented model shows some improvements in reducing pressure, especially in the frontal pipe of the engine block. However, the reduction is still insufficient, as shown in Figure 23.
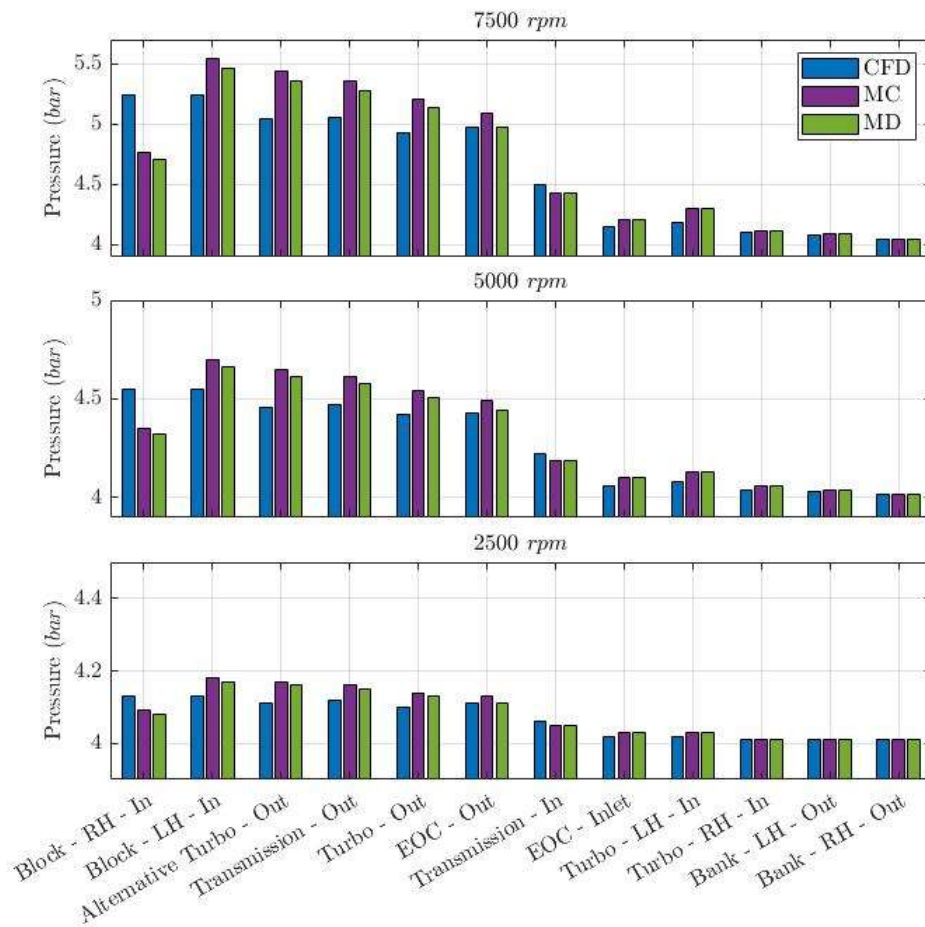
Figure 23: A Sample - Model C and Model D pressure comparison.

Model E

Further modelling work has been carried out on the head side of the cooling jacket as it presents the most complex geometry and a better implementation can enhance the model's ability to predict the pressure along the cooling circuit. To achieve this, the head has been divided into the exhaust and intake sides, with the upper side being separated from the bottom side, resulting in the head being divided into four flow splits. This approach is expected to provide more accurate results by better capturing the flow dynamics and pressure distribution within the head.

Model E – Hydraulic simulation and comparison

Despite the implementation of additional volume parts, the pressure in the main frontal pipe increased instead of being reduced. It seems that increasing the complexity of the model did not provide the intended benefit. While this approach may be worth exploring in the future, it is worth noting that the returns were not affected by this change, as shown in Figure 24.
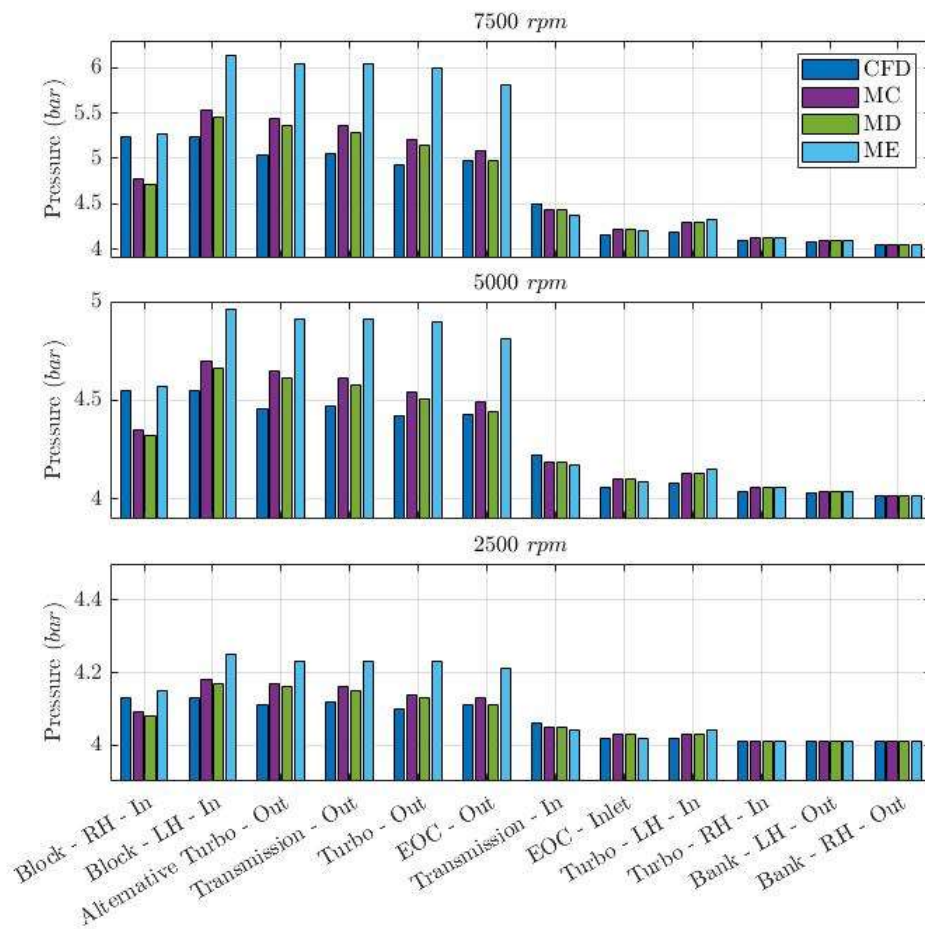
Figure 24: A Sample - Model C, Model D and Model E pressure comparison.

3.3.3 Method Separate Volume 2

The latest approach developed in this study combines the best features from the previous two methods to improve estimation of pressure along the cooling jacket and enhance the overall modelling work.

The modelling phase with this approach can be summarised as follow:

- The modelling of the main parts (block, gasket and head) starts after converting them to a general flow volume.

- The volume of the rail will be also treated as a general flow volume. However, the pipes that connect the head to the rail is treated separately.

- The main pipe is treated separately from the main water jackets.

Model F

This model marks the first implementation where the block, gasket and head water jacket are treated as separate entities, each converted into a general volume flow after utilising the datum plane definition. In the case of the block, the datum planes are defined similarly to the position definition used in Method Separate Vol 1. Then, the head is split into its intake and exhaust side and then subdivided into individual cylinders.

Model F – Hydraulic Simulation

The results of the model using the new methodology are presented in Figure 25. By considering the block, gasket and head water jacket separately and then converting them into General Volume flow, the model achieves a good overall estimation of the pressure along the entire cooling circuit. The cutting strategy chosen in the previous methods is applied here as well and the head model helps to increase the pressure along the cooling jacket.
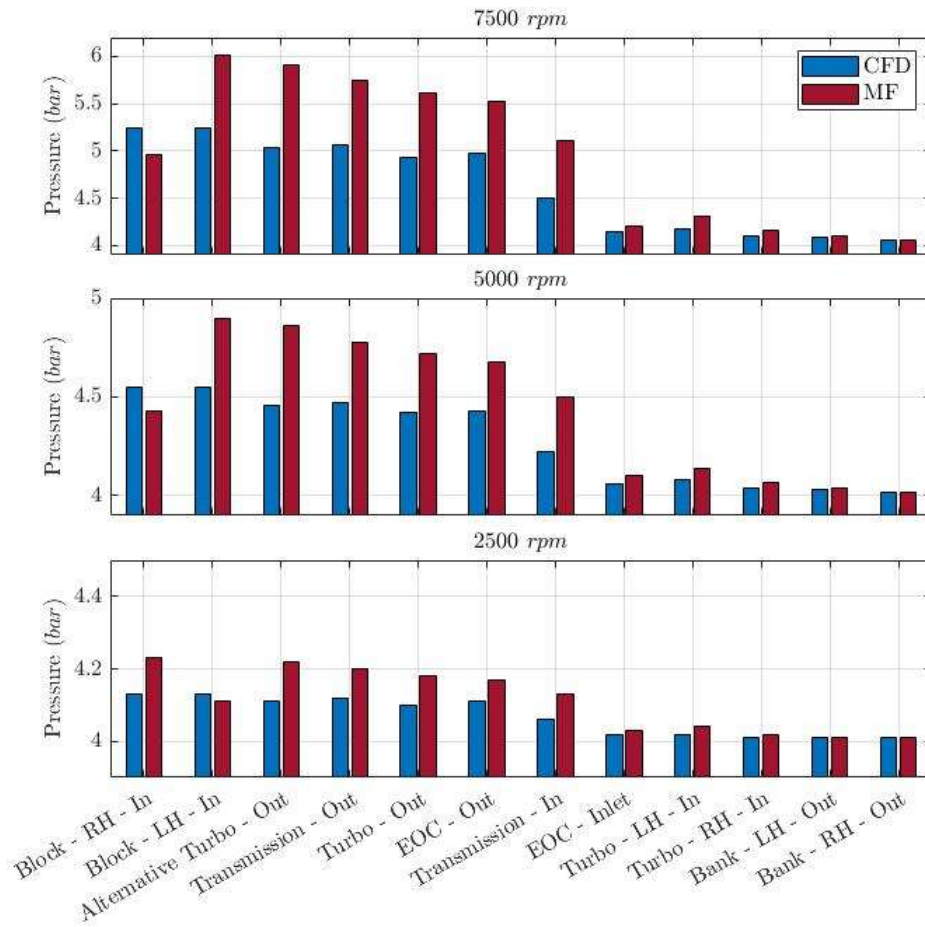
Figure 25: A Sample - Model F pressure results having the intake head water jacket discretised as in Model F increases the pressure given the fact the flow distribution is not well modelled in the 1D model. This because part of the coolant flow rate remains trapped in the head waterjacket intake part.

Model G

Model F focuses mainly on the head side of the engine and does not separate it into exhaust and intake side. Additionally, the gasket has been merged into the block general volume flow to improve the model's ability to capture the geometrical properties of the gasket. This implementation appears to be effective in calculating the pressure along the block water jacket.

Model G – Hydraulic Simulation and Comparison

Figure 26 shows the simulation results obtained with the implantation of model F. As expected, the discretization of the gasket as part of the block helps to better capture its geometrical properties resulting in a more accurate pressure prediction along the block water jacket. Additionally, the decision to treat the head as a single volume also leads to an improvement in the overall performance of the model. However, despite this adjustment, the pressure prediction is still not sufficient, suggesting that further refinements may be necessary.
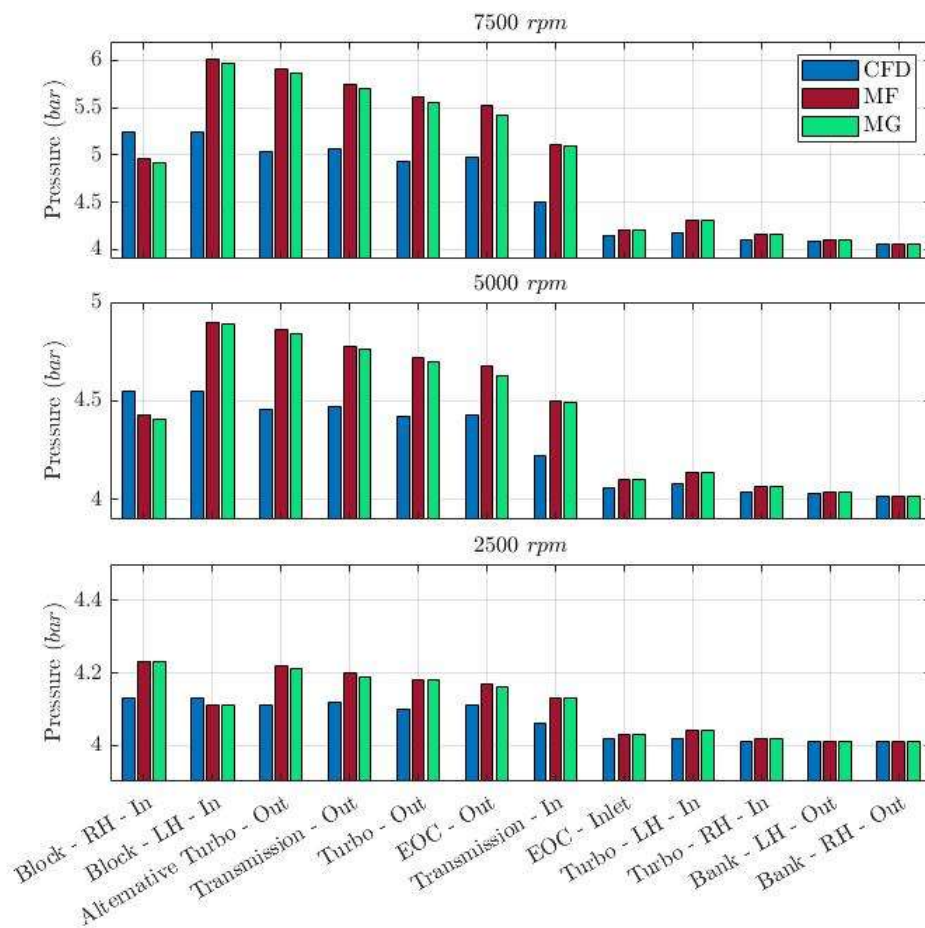
Figure 26: A Sample - Model F and Model G pressure comparison.

3.3.4 Methodology Comparison

Before delving into the data analysis, it is worth summarizing the key features of the three methods under consideration.

The "Method One Volume" approach consists in modelling the engine block, head and gasket as a single volume flow, which is then discretised into a 1D model. This method simplifies the modelling process, but it may not accurately capture the complex geometry and flow restriction of the engine.

In contrast, the "Method Separate Vol 1" approach splits the engine block into the exhaust and intake side and each cylinder is treated separately. This allows for more detailed modelling of the engine geometry, but it may increase the computational complexity and the number of parts in the model.

The "Method Separate Vol 2" approach is a hybrid of the previous two methods, where the engine block and gasket are modelled as one volume flow, while the head is divided into separate volumes for the intake and exhaust sides and cylinders. This approach aims to balance the accuracy of the modelling with computational efficiency.

In terms of results, the "Method One Volume" approach is the simplest but provides the least accurate pressure prediction along the cooling circuit. The "Method Separate Vol 1" approach shows an improvement in pressure results, but it may increase the computational complexity due the number of the parts in the model. The "Method Separate Vol 2" approach provides a good balance between accuracy and computational efficiency, showing a good overall estimation of the pressure along the cooling circuit.

As shown in Figure 27, Method One Volume (MA and MB) tends to under-estimate the flow pressure, while Method Separate Vol 2 (MF – MG – MH) tends to over-estimate the pressure. In general Method Separate Vol 1(MC – MD – ME) performs better than the other two methods in calculating the flow pressure. Therefore, it was adopted as the most suitable methodology for the modelling process. However, further analysis is needed to determine which model is the most suitable for hydraulic estimation. As seen in Figure 24, all three models estimate correctly the

pressure in the return areas. Model C and D perform better than Model E in the inlet zone. Model E is over-estimating the pressure, this may be due to the division of the exhaust and intake parts of the head.

Thus, the last comparison is between MC and MD implemented with Method Separate Vol 1. There is no significant difference in pressure results, but MD has a better match to the pressure. This choice is also made for further consideration, such as implementing the hydraulic calibration and how to connect thermally the water jacket part to the engine thermal masses.
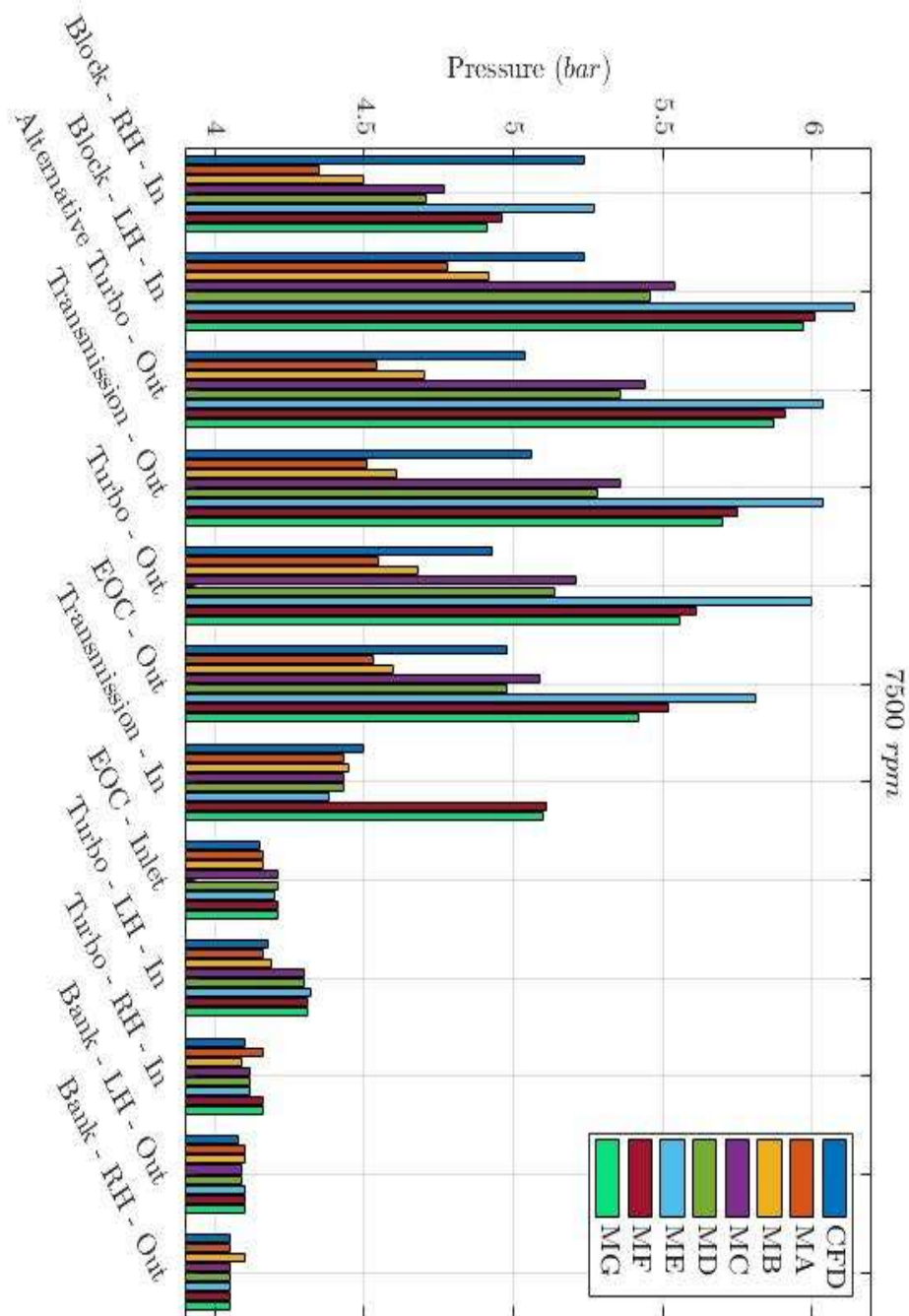
Figure 27: A sample - Hydraulic Models comparison - 7500 rpm.

3.3.5 Hydraulic Calibration Methodology

The A sample model has been thoroughly studied to determine the most effective methodology for generating a highly calibrated model of the water jacket hydraulic circuit. This involved simplifying the complex 3D geometry by converting it to a 1D representation, which should help to reduce the level of required hydraulic calibration. The goal of this study is not only to minimise the effort required for the hydraulic calibration but also to identify the optimal methodology and the most accurate 1D model for conducting the calibration. Further work is needed to fine-tune the hydraulic calibration and connect the water jacket thermally to the relevant thermal masses.

In this section a strategy of how to hydraulically calibrate the model is explored. The purpose of this calibration is to better distribute the flow along all the cooling jackets, resulting in a more even distribution of pressure, flow rate and flow velocity. This, in turn, affects the calculation of heat rejection.

There are several ways to perform hydraulic calibration, such as defining a pressure drop characteristic, using orifices, or manually changing the geometry of the actual part. In this case, before performing the calibration, a single cooling circuit is defined, resulting in a flow split design for the inlet pump (see Figure 28). The geometry of the entrance section of the two pipes remained the same and the main inlet geometry section of the pump is the sum of the two outlet sections.
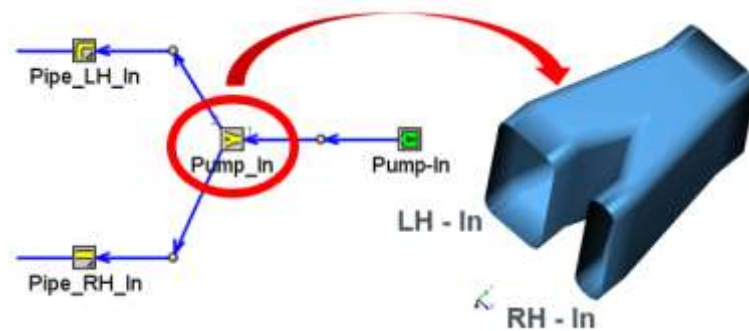
Figure 28: A sample - Model D - Inlet pump flow spilt implemented and design.

Figure 29 shows the results of the model D implemented with the inlet pump flow split. This made model D as a one coolant circuit which demonstrate the model's ability to calculate the pressure. In Figure 30, we can see the distribution of the

percentage error for the three cases, which is below 5% overall, indicating that the hydraulinc model is predictive. It is important to note that the comparison and validation were done against CFD results.
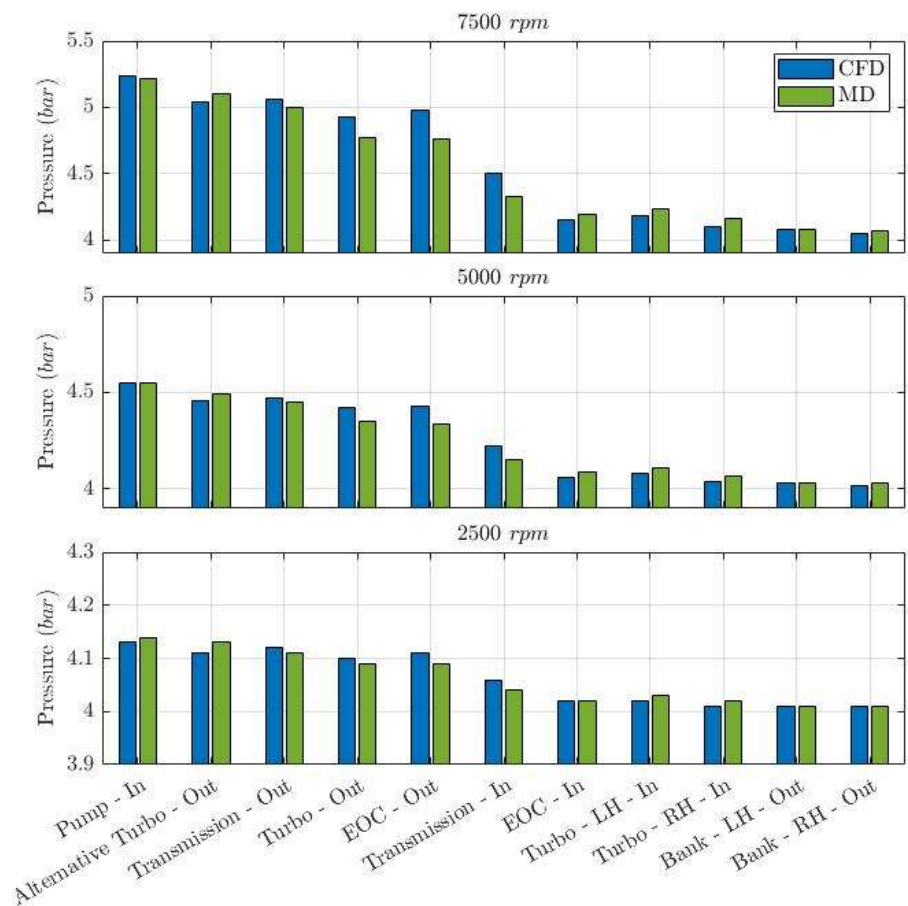
Figure 29: A Sample - Model D - One coolant circuit.
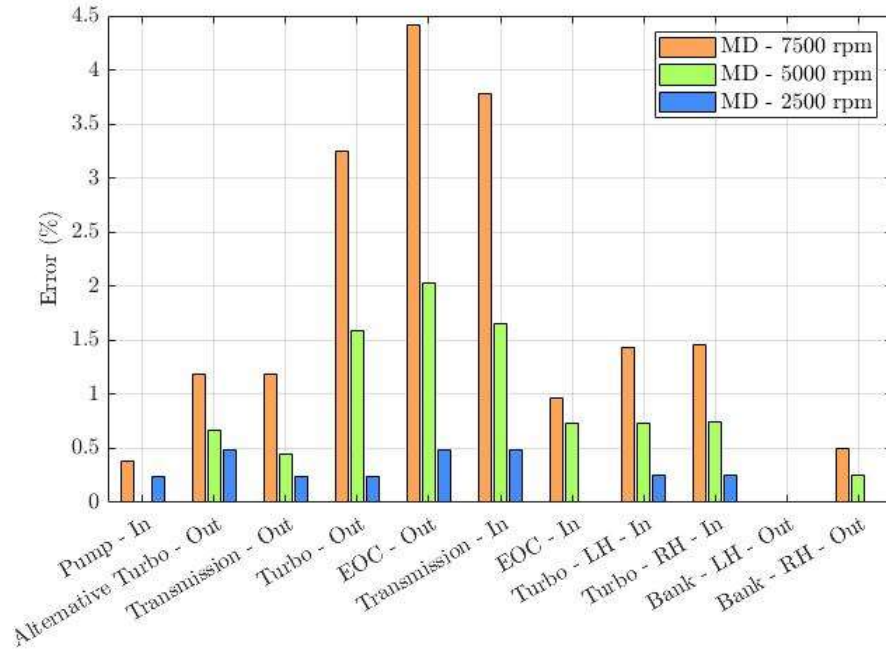
Figure 30: A Sample - Model D One coolant circuit - Error % comparison between cases.

Hydraulic calibration is required to improve the flow distribution. To achieve this, ten orifices are defined inside the model and their diameters are calibrated to reduce the pressure error and improve coolant flow rate distribution. The position of these orifices are mainly studied with the simplest model represented by Model A (which used the Method One Volume) to understand which areas are more affected by the changes. The orifices were mostly defined in the block interbore section and in the main entrance of the two banks (see in Figure 31).

The reason why the orifices are defined in the block area is because the interbore pipes have an important role in balancing the flow between the intake and exhaust side of the cooling block jacket. Another important reason is because the discretization in this part of the engine coolant block is quite complex, and the volume flow is not well captured by the sotware. The position of the other two orifices was selected because a better control on the coolant inlet flow was needed based on the discretisation results of the inlet diameter of the block component. Based on the flow results from the 1D model and compared to the validated CFD model (voumetric flow rate can not be showed for confidentiality reason) is possible to say that there is an overall match between the 1D volumetric flow rate and the CFD flow rate. The diameter of the orifices where adjusted accordingly to match as possible the coolant flow rate in the engine block.
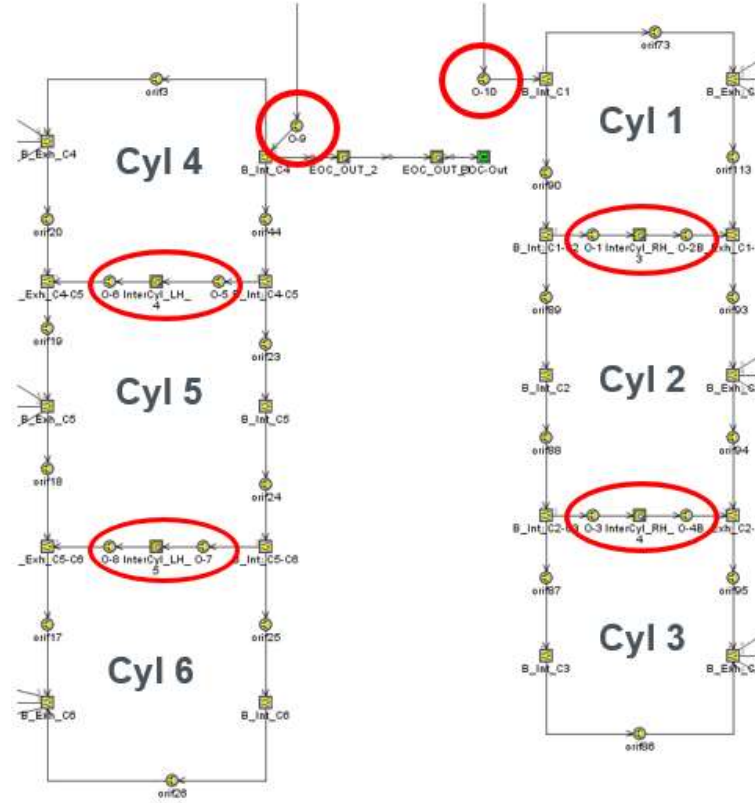
Figure 31: A Sample - Model D - Hydraulic calibration. Definition of orifice.

After implementing this calibration methodology, the pressure and flow distribution become more homogeneous, as shown in Figure 32. The results demonstrate a significant improvement in reducing the error in all zones of the cooling jacket. Although there was a slight increase in the inlet pump, it was less than 2%.

This calibration strategy works and can be implemented in other types of geometry.
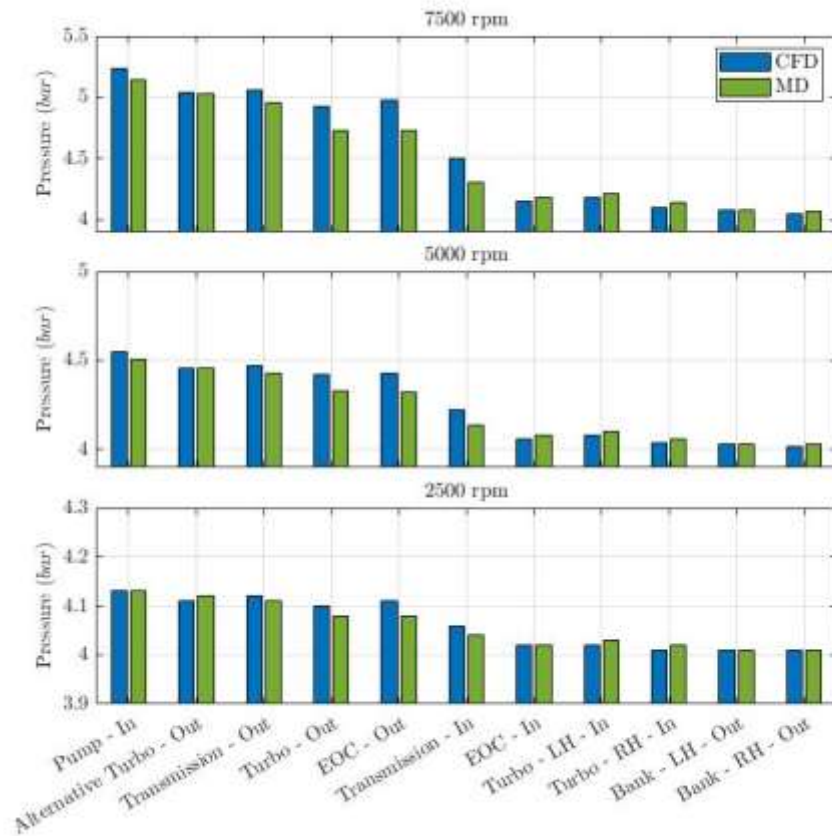
Figure 32: A Sample - Model D One coolant circuit - Hydraulic calibration - Pressure results.
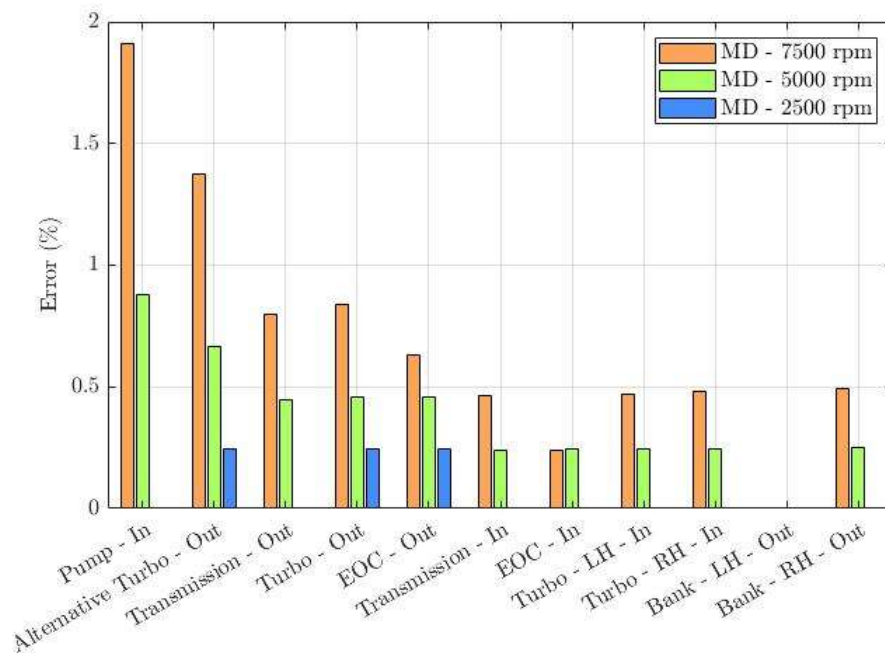
Figure 33: A Sample - Model D One coolant circuit - Hydraulic calibration – Error percentage
results in comparison.

3.4 Hydraulic Modelling Methodology - C Sample

The next phase of the hydraulic modelling methodology involved the processing of a second design iteration of the engine, which shares a similar overall structure to the A Sample. However, the cooling strategy differs, with the coolant flow inlets and outlets positioned in a different zone than in the A Sample. Additionally, there is a new feature where the coolant flow from each bank does not go directly to the thermostat. Instead, a frontal pipe collects the flow from both sides and thanks to a valve, it opens a passage to the flow for the thermostat. Another change in this engine is the positioning of the turbo returns in the middle of the head rail. The interbore cylinders have also been modified to be larger and allow better flow between the sides. Furthermore, the coolant flow that enters the banks for this engine is divided with the flow entering from cylinder 1 and 2 for the right bank and cylinder 4 and 5 for the left bank. The coolant boundary conditions were represented from Table 3.

3.4.1 Method Separate Volume 1

For the C Sample, shown in Figure 34, it is used the same methodology used for the A Sample. However, there are some minor differences in the modelling process due to a different cooling strategy, particularly in the frontal pipes and inlet side of the blocks. To achieve the most predictive 1D simulation model possible, it is used the Method Separate Vol 1, which was also used for Model D.

The cutting modelling procedure is carried out in the Solid shape mode, which provides increased flexibility and accuracy. The pipes conversion required significant work, especially for the main frontal pipe, which required a more detailed cutting procedure due to its complexity. However, the overall methodology process remains the same.
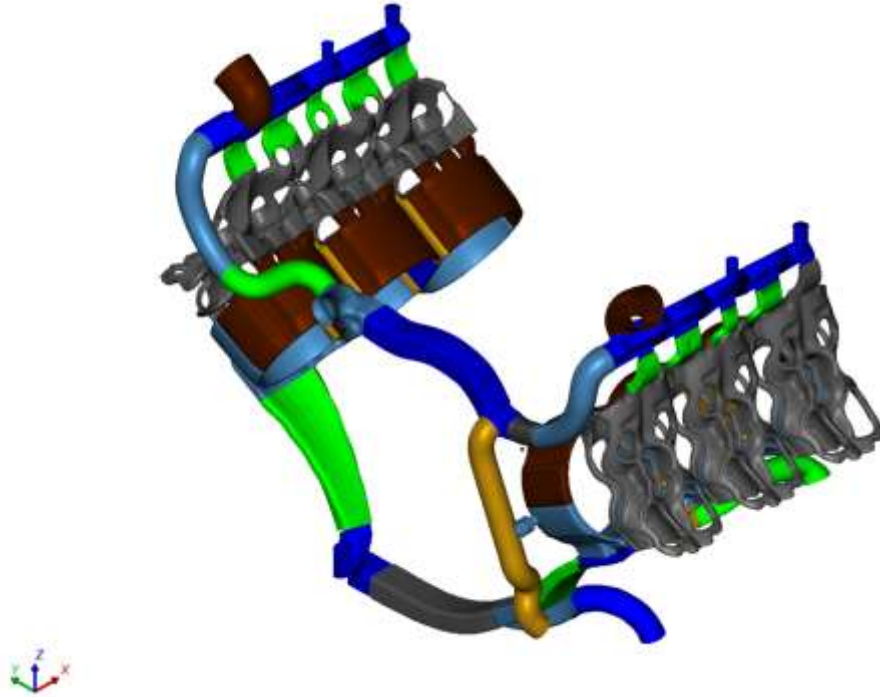
Figure 34: C Sample - Model H - Water jacket modelling. Method Separate Volume 1 is used to model the water jacket volume flow. Cylinder water jacket are considered for intake and exhaust side. Every cylinder head water jacket is considered as a single volume.

The complete model geometry has been processed with Method Separate Volume 1, with discretisation made using the same length of 40mm as the other models. No inlet pump design was necessary in this case since the CAD geometry already provides the inlet. The complete 1D model is already a single coolant circuit due to the discretisation of the CAD geometry. The overall 1D model discretised is represented in Figure 122 Appendix A.

Model H – Hydraulic Simulation

Hydraulic simulations are conducted for the same three engine operating points as those used for the A Sample. The CFD initial boundary conditions were mostly the same as those used for the A Sample engine (Table 2), with the flow inlet and outlet remaining unchanged. The overall flow was split equally between the two banks. The only difference in this simulation model is represented by the bypass outlet. At 7500 rpm, the initial pressure boundary condition for the bypass outlet is 4 bar, while for 5000 rpm and 2500 rpm, the system is considered closed.

The first run of the simulation is depicted in Figure 35. The results, shown in Figure 36, indicate a significat improvement in the model's accuracy. Although there are differences in pressure estimation, the model appears to be robust overall. The main error is found in the inlet zone of the EOC, where the coolant circuit piping system is complex and the 1D siscretisetion is not accurate. However, even for the worst-case scenario (7500 rpm), the error is less than 10%. The error in the TOC (Transmission Oil Cooler) feed and Turbo feed is acceptable, although it exceeds 5%, as the difference between CFD and 1D results is only around 0.2 bar.
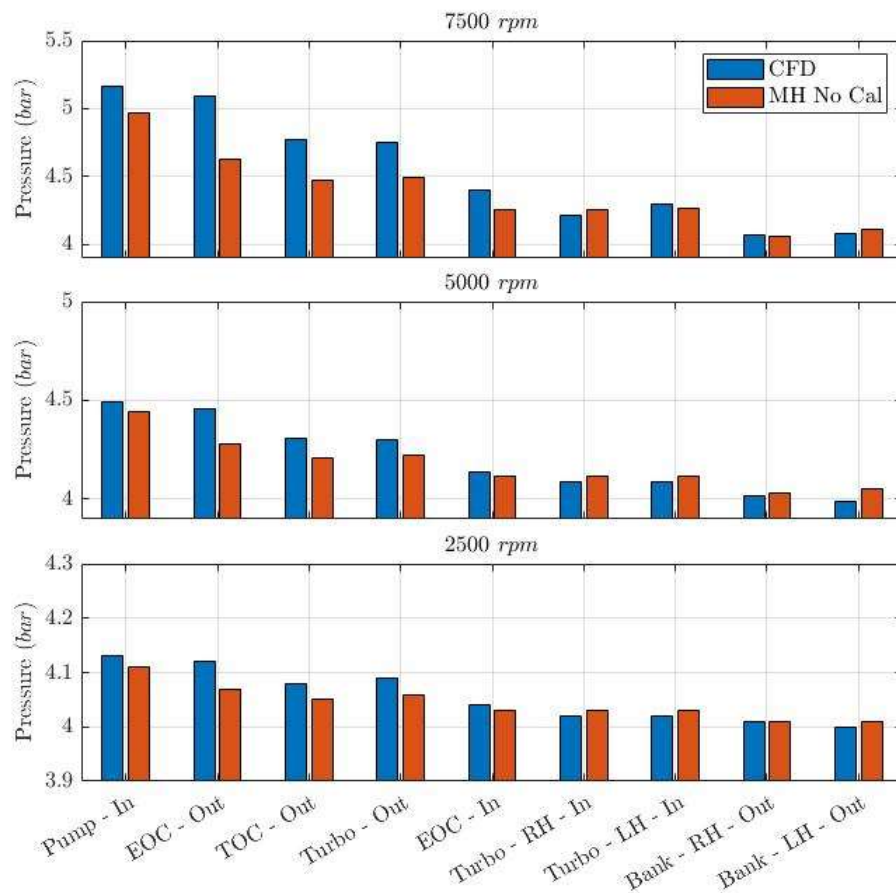
Figure 35: C Sample - Model H - Model without hydraulic calibration - Pressure results.
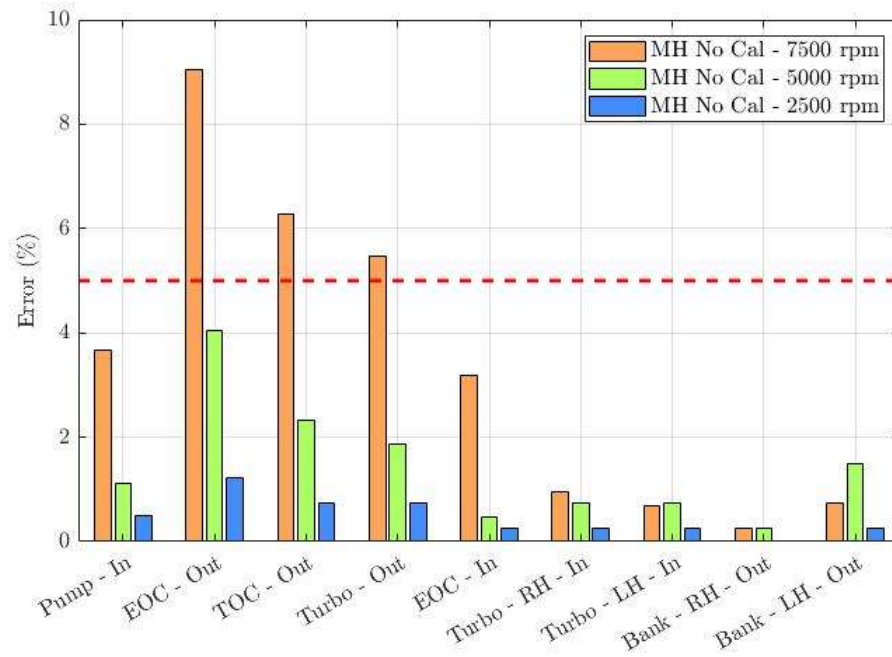
Figure 36: C Sample - Model H - Model without hydraulic calibration - Error % results - 7500 rpm.

Based on these findings, the model is calibrated using the methodology explained previously to better match the hydraulic pressure and the mass flow rate.

Model H - Hydraulic Calibration

To calibrate the model, the same 10-orifice approach used for the A Sample MD model is adopted.

Two types of calibration strategies are used for this model:

I.   Pressure target – matching the best pressure possible along the coolant circuit.

II.   Flow target– matching the best flow rate possible along the coolant circuit.

The former aims to match the best pressure possible along the coolant circuit, while the latter aims to match the best flow rate possible. Figure 37 shows the orifices defined in the model. Two orifices are assigned to each interbore in the block area to better control the flow, while two orifices are assigned to the inlet of the fourth and fifth cylinders due to the complexity of the geometry in that area. The entrance

of the first and second cylinder, on the other hand, is well discretised in the non-calibrated model.
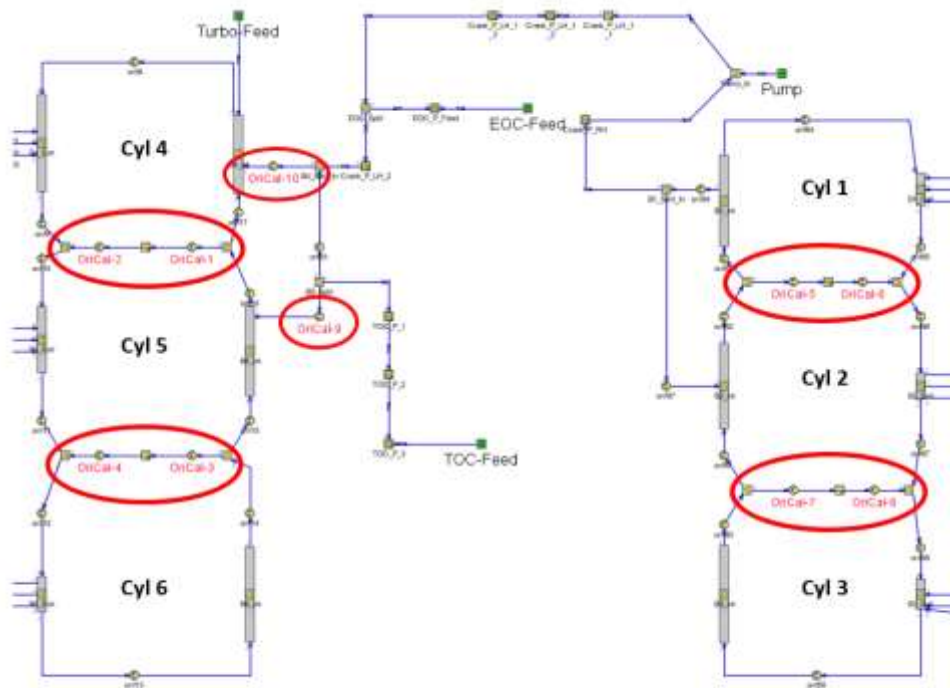
Figure 37: C Sample - Model H - Hydraulic calibration. Orifices definition. Two orifices per interbore are defined. One at the entrance of the cylinder four and one at the entrance of cylinder five.

Simulation results are presented in Figure 38 and Figure 39, and from the worst-case scenario at 2500 rpm, it can be observed that the model targeting the best pressure achieved the target to whithin less than 5% along all cooling circuits. Meanwhile, for the best flow model, there is still up to a 5% error in the EOC feed zone, despite some benefits to the calibration. These benefits are slightly lost in the turbo feed, which is positioned in the fifth cylinder jacket. At 5000 rpm, the overall error is below 5% in every section of the engine, with really good results for the best pressure model.
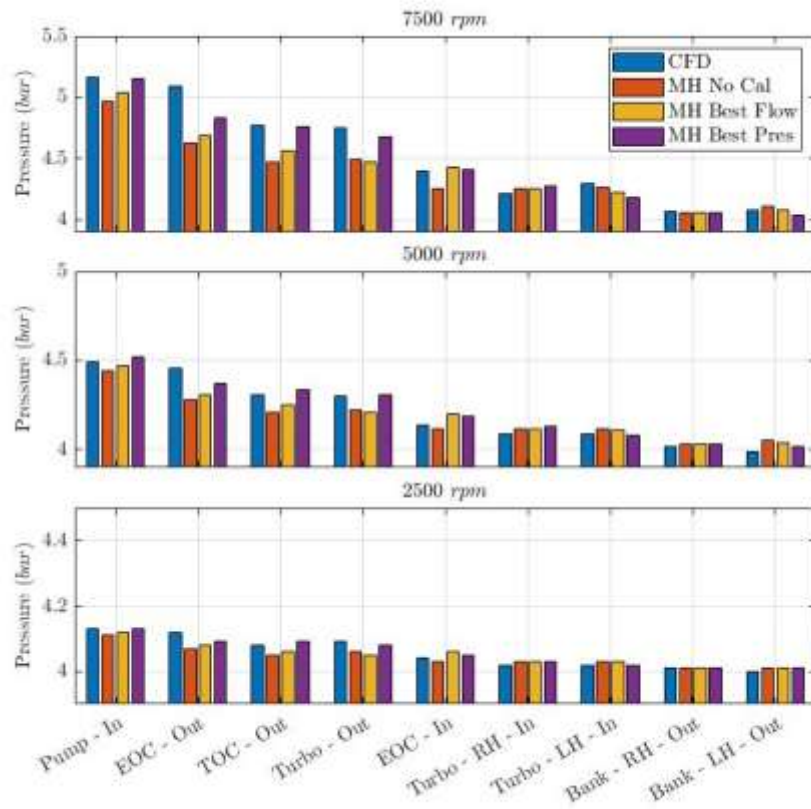
Figure 38: C Sample - Model H - Hydraulic calibration strategy comparison – Pressure results - 7500 rpm.
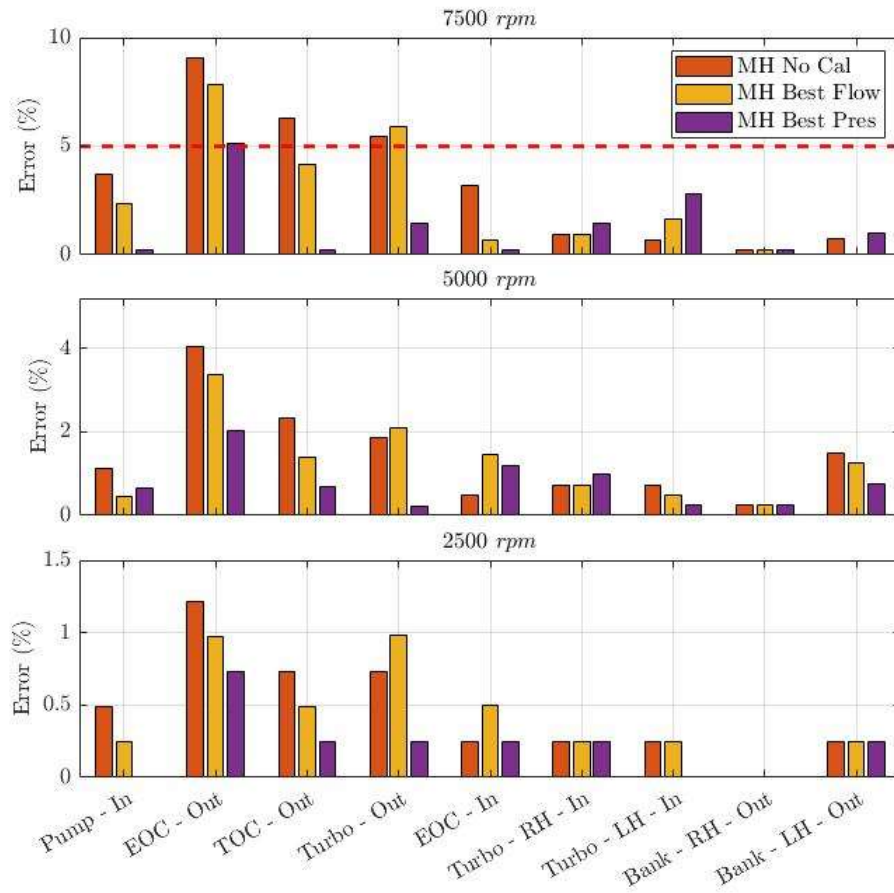
Figure 39: C Sample - Model H - Hydraulic calibration strategy comparison - Error % results.

The aim of implementing this methodology is to reduce hydraylic calibration to a minimum. And the final reults presented a model that was still flexible and reliable in calculating the coolant flow pressure with a restrained error.

3.5 Conclusion

In this chapter, a methodology for hydraulic modelling is developed to create a cooling flow model for two different water jacket geometries from the same engine family. Three different methodologies were investigated, including Method One Volume, Method Separate Volume 1 and Method Separate Volume 2. Each method showed a high modelling work impact and could be used for hydraulic modelling. The purpose of this work is to find the best methodology to create a hydraulic model that would be efficient in terms of simulation computational time and as precise as possible.

After considering the benefits and the limitation of each method, the Method Separate Volume 1 developed in Model D was chosen. This method offered the best pressure calculation along the coolant circuit, precise modelling, easy hydraulic calibration, flow balance, pressure control, and capacity for further work. The methodology is validated against CFD results, with the maximum acceptable error during validation set at 5%. This target is achieved for the A Sample Model D, but not for the C Sample Model H, where the error in one of the inlet part of the coolant (the EOC feed) is approximately 8%. Nevertheless, this error is deemed acceptable for the methodology.

The hydraulic calibration strategy is found to be efficient, requiring little effort, and allowing for flow control inside the coolant circuit. Orifices are defined in the model to support this calibration strategy. The usage of ten orifices to calculate the coolant flow rate and the pressure along the coolant jacket results to be effective. The difference between sample A and sample C was the positioning of the two orifices outside the cylinder water jacket. For Model D, one orifice was defined at the entrance of cylinder one and one at the entrance of cylinder four. While for model H instead of setting one orifice at the entrance of cylinder 1 it has been chosen to set the orifice at the entrance of cylinder five. While all the other orifices are in the same place the methodology is now validated and the work will continue with the implementation of the thermal model part. Overall, this work developed a methodology for hydraulic modelling that can be used to predict cooling performance in complex engine geometries.

Chapter 4 - Thermal Modelling Methodology

In this chapter, a thermal modelling methodology is introduced, built upon the hydraulic model selected in the previous chapter. Two different thermal modelling approaches are presented: Lumped Mass methodology and Finite Element methodology. A comprehensive analysis of both methods is provided to determine which approach is the most effective for the present case.

4.1 Summary

The following chapter describes the thermal modelling methodology in detail:

I.   Introduction

- The introduction presents an overview of the two modelling approaches, highlighting their respective advantages and limitations in terms of modelling efforts and potential outcomes.

II.   Integration with Engine Performance Model

- The interaction between the 1D engine performance model and the thermal model is explored. Two different interaction approaches are described, the direct and indirect interaction between performance model and thermal model. The indirect approach was adopted given the benefit and the purpose of the current work.

III.   Model H – Lumped Mass

- A lumped mass model developed using the hydraulic model previously created for the C Sample.

IV.   Model H – Finite Element (FE)

- An explanation of the overall modelling methodology and the development of the thermal model using the FE methodology in the 1D simulation tool is presented.

V.   Thermal Calibration Strategy – Model Setting

- Before describing the calibration methodology, an analysis of the experimental thermal data survey is conducted to gain a comprehensive understanding of the key factors that need to be defined in the simulation tool, including boundary condition settings in the model. The calibration strategy deployed for both thermal approaches is described in a step-by-step process.

VI.   Thermal Calibration – Results

- The analysis and discussion of the thermal calibration results for the three engine points used in model calibration is presented.

VII.   Heat Transfer Multiplier Analysis

- The heat transfer multiplier results is presented, along with a first and second order correlation analysis to determine the heat transfer multiplier for additional engine points that are utilised to validate the thermal methodology.

VIII.   Conclusion

- The overall thermal modelling methodology and the calibration approach used is summarised and discussed in the concluding section.

4.2 Introduction

This chapter presents two different thermal modelling procedures that are applied to the C Sample Model H developed in the previous chapter:

I.   Lumped Mass Methodology

II.   Finite Element (FE) Methodology

The Lumped mass methodology involves converting the engine's thermal masses into lumped masses, including a representative cylinder, head, piston and port structure. The engine cylinder structure is created parametrically from user input

and a finite element method is used to calculate the structure temperature and the resulting heat transfer rate [108].

On the other hand, the Finite element methodology converts each engine part into finite element parts using a template called "EngCylStructCustom". This includes the cylinder block, cylinder head, piston, intake and exhaust valves [108].

Both methodologies are implemented using indirect modelling integrations which means that the engine performance model and the cooling system will not interact simultaneously during the same simulation. Information will be transferred in one direction only, from the performance simulation to the thermal engine simulation model.

The primary purpose of the thermal calibration is to ensure the correct heat transfer rate distribution from the engine to the coolant, oil and external environment. Thermal calibration is performed over three engine load conditions using experimental data provided from an engine thermal survey, covering a full range of engine speed. The overall engine data will be used later for model validation. A data sanity check of the thermal survey is executed.

4.3 Integration with Engine Performance Model

The implemented thermal model uses a fully physical 1D engine performance model. The performance model was given by the project partner. This baseline model featured a detailed geometrical representation of the intake and exhaust lines, wall temperature solvers along the gas path and in the cylinders and imposed combustion profiles mapped as a function of engine speed and load.

The baseline model was established in GT-Power software and calibrated and valibdated by the engine manufacturer partner against industry standards. It needs to be mentioned that parameters in the combustion, valve and fuel injector templates are load dependent with look up table based on the engine speed and BMEP. The combustion model present in the model is the SIWiebe model using and in cylinder heat transfer model based on WoschniGT. The BMEP controller will be using a

PID controller of wastegate and throttle handle while the exhaust temperature controller will be done by the PID controller f fuel enrichment.

The simulation faces a critical challenge concerning the coupling between the engine model, responsible for simulating the thermodynamic cycle and defining boundary conditions related to the combustion chamber and the engine thermal model, where this boundary condition must be applied. To address this, two distinct approaches can be adopted: Indirect (partial) and Integration direct (full) Integration [57].

In the indirect type of integration, the engine model and the cooling system model operate independently during the simulation, with the information flowing in one direction only, from the engine model to the cooling model. Consequently, changes in coolant and oil temperature do not impact engine performance and the boundary conditions at the combustion chambers walls, as imposed by the engine model, remain unaffected.

To utilise this method effectively, the engine model must be executed across a range of operating points, representative of various driving conditions, to obtain gas temperatures and convective heat transfer coefficient. These parameters are then used as boundary conditions for the finite element cylinder of the cooling model, based on the engine speed and load.

In the direct approach, the engine performance model and the thermal model are run simultaneously, enabling the engine model to directly determine boundary conditions at the cylinder walls for the cooling model. This integration involves updating the Indicated Mean Effective Pressure (IMEP) based on the calculated heat transfer between the gas combustion chamber walls. While this configuration accurately simulates the interactions between engine combustion and the cooling system, it comes with significant computational demands due to the small-time step required for the engine fluid dynamic simulation. To mitigate these computational requirements, a Fast Running Model (FRM) is preferred for direct integration. The FRM simplifies the detailed engine model by lumping flow volumes and increasing their discretisation lengths. This leads to larger time-steps and reduced computation time for the simulation [109].

As adopted by Millo [94] and recommended by GT-Suite [108], in the current work the indirect integration approach was adopted. This because the present study wants to implement a first a thermal calibration strategy over two different modelling approaches: lumped mass and finite element. To be consistent and explore different simulation strategies, run time was considered as a key decision factor.

The direct approach shall be considered in the future work. As explained this technique makes the model more accurate and being able to explore transient simulation such as warm up phase.

4.4 Model H – Lumped mass

The engine parametric template discretised the structure surrounding the combustion chamber into smaller elements, including ports for coolant, oil and structure. It is used in engine models with coolant/oil boundary conditions imposed and in cooling system models with gas-side boundary condition imposed. The thermal solution can be studied for each part, including the cylinder, head, piston and valves.

The cylinder has two sides for thermal connections as it is possible to see in Figure 40. The first one is related to the combustion side, where there are four zones. Cylinder Zone 1, 2 and 3 are surfaces that contact combustion gas while Cylinder Zone 4 is not an internal gas zone but is used for connection to the oil.
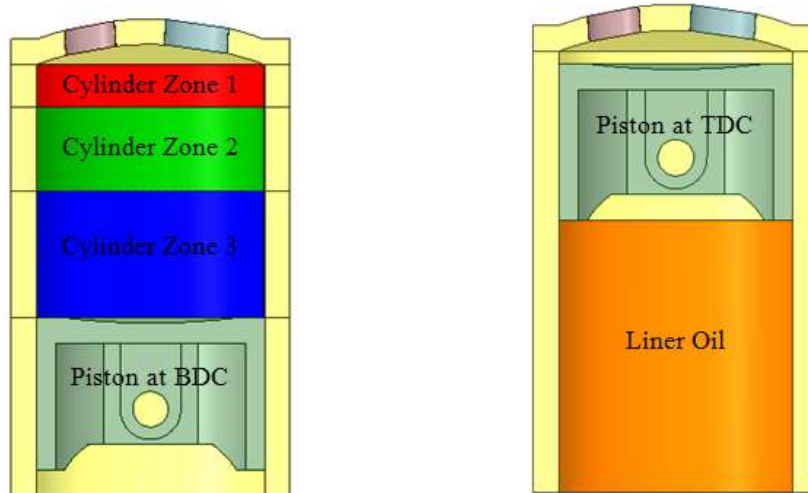
Figure 40: Cylinder temperature zones and liner oil zones.

A representation of the heat transfer area in the inside liner of the cylinder is presented in Figure 41,where it is possible to recognise the external area of the cylinder: Wjkt1 and Wjkt2 are the heat surface area that will be connect to the water jacket part discretised.
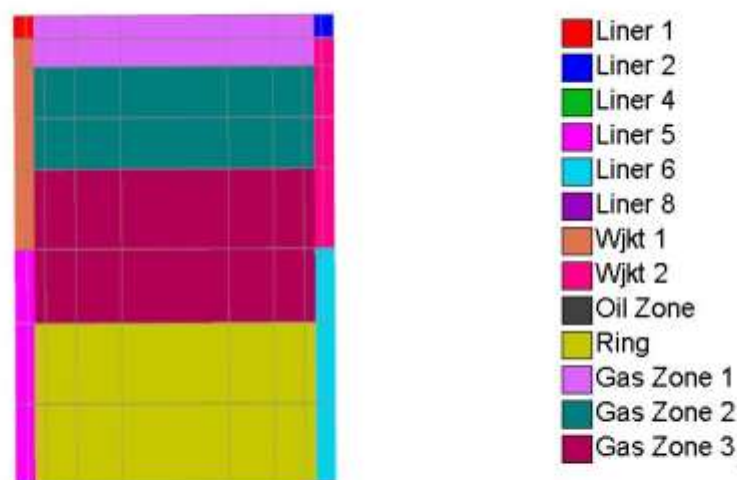
Figure 41: Cylinder heat transfer zone, inside liner.

Figure 42 shows the area defined for the cooling jackets. The geometrical data of the coolant jacket is defined in the EngCylStrucCond part of the simulation model.

Regarding Cylinder Zone 4, the liner oil is the only internal surface that can be connected to an oil flow volume. This zone extends from the bottom of the cylinder liner to the bottom of the piston at top dead centre (TDC) and may overlap cylinder gas zone 3. The cylinder from the outside is divided into three main zones: top side, middle side, bottom side. The top side considers the liner of the cylinder, the middle side considers the coolant jacket and the bottom side considers the oil.
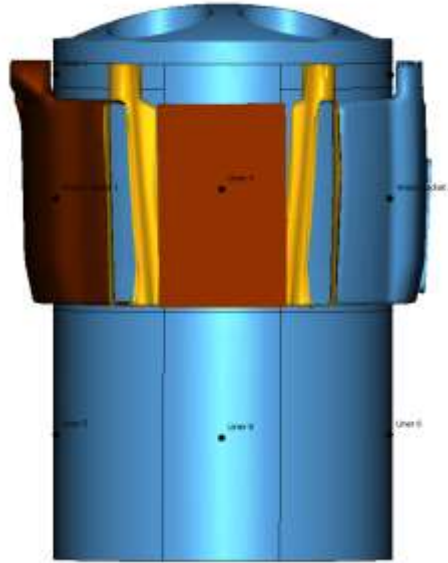
Figure 42: Cylinder 1 coolant jacket.

For the cylinder head, there are two sides: the combustion side and the coolant side. For the combustion side, the head is divided into three zones as shown in Figure 43. There is also the cylinder gasket zone that is connected to the cylinder structure. The upper side of the cylinder is the coolant area and it is connected externally to the head coolant jacket.
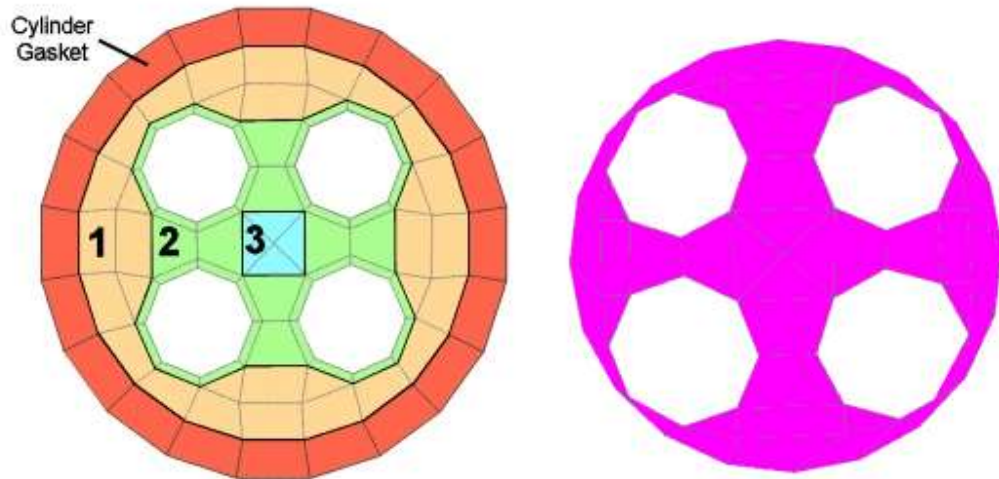
Figure 43: Head temperature zone and head coolant heat transfer zone.

Regarding the piston, a similar structure to the one shown in Figure 44 is used. The upper side of the piston is utilised to connect the combustion boundary conditions while the lower side of the piston represents the oil zones. For the valves the heat transfer zones connected with the coolant flow are represented Figure 45.
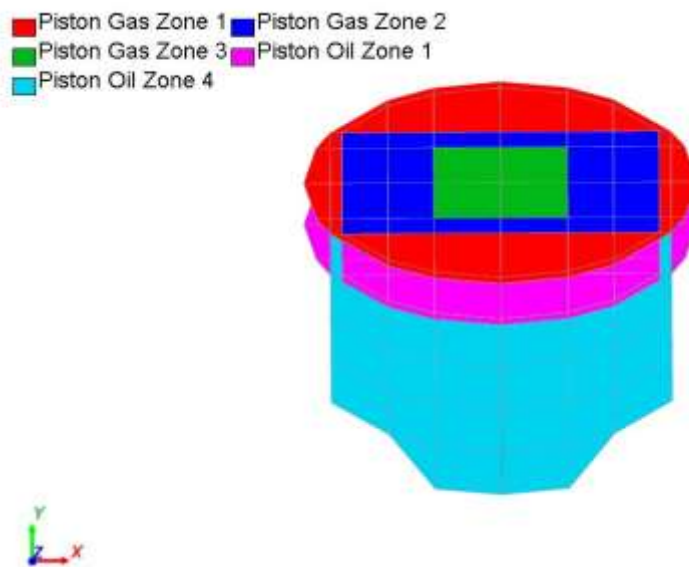
Figure 44: Piston heat transfer zones.
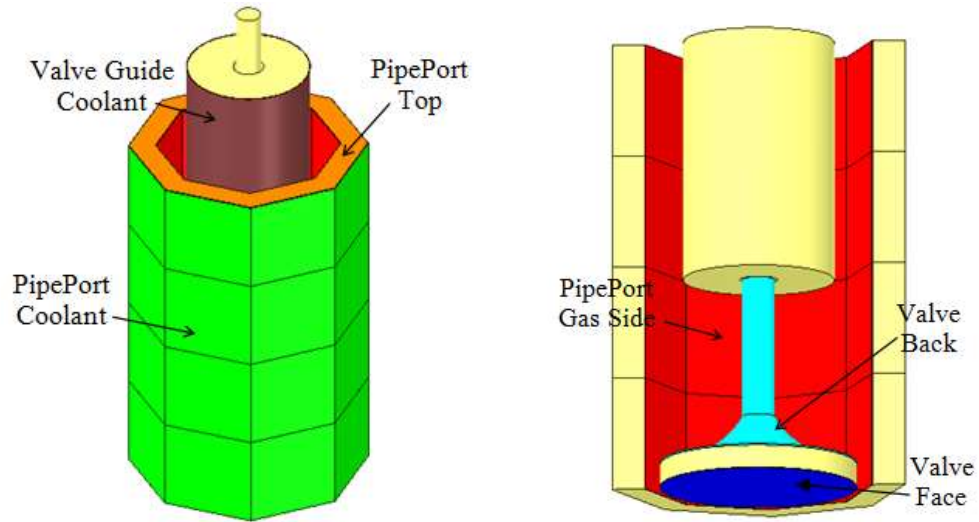
Figure 45 : Valve heat transfer area coolant side and gas side port and valve zones.

Overall, the engine parametric template discretises the structure surrounding the combustion chamber into small elements, allowing the study of the thermal solution for each part of the engine. The different zones of the cylinder, head, piston and valves are connected internally and externally through convection and conduction convection, allowing accurate thermal modelling of the engine.

4.5 Engine Thermal Model

The coolant circuit selected for further modelling is Model H, which has been calibrated to achieve the best flow rate across the water jacket. This decision was made after a thorough analysis conducted in the previous chapter. At this stage of the process, the thermal masses of the block and head geometry are converted into lumped mass using GEM3D. Before proceeding with the conversion, pre-processing is performed by dividing the engine geometry into two separate banks – left and right – and then dividing each into a cylinder block and cylinder head. These new parts represent the thermal masses of each engine cylinder.

However, converting the geometry to lumped masses alone does not provide the representative cylinder head, pistons and port structure of the engine. The process of creating the six cylinders begins by defining the position of the first one using a

template. It is also important to define the location of the water jacket and the surface connected to the mass structure. After defining the cylinders, the next step is to thermally connect the lumped masses to the cylinders and the water jacket to the cylinder and lumped mass.

To achieve this, convection and conduction connections are used. A convection connection specifies the heat transfer convection coefficient and surface area to calculate the heat transfer between two components using Newton's law of cooling Equation (9). The temperatures are obtained from the neighbouring thermal components and this connection supplies the convection coefficient (h) and surface area.

$$Q = hA(T_1 - T_2)$$ Equation (8)

The heat transfer connection connects the cylinder to the water jacket. Between the thermal masses a conduction connection is also defined. The values used for this parameter was 50000 W/(m^{2}K), based on simulation experience. While the lumped mass of the block and the head are connected to the ambient via a heat transfer connection set as 20 W/(m^{2}K). When defining conduction between the block thermal mass and the head thermal mass, a formula Equation 9 is used instead of a single value to represent the gasket conductance:

$$gasket\ conductance = \frac{1}{hg_{resistance}}$$ Equation (9)

The final thermal model using the lumped mass methodology is shown in Figure 123 in Appendix A after being discretised.

4.6 Model H – Finite Element (FE)

This paragraph outlines the implementation of the thermal model using the "Custom Mesh" template in GEM3D. The hydraulic model utilised is Model H, previously used for the lumped mass. The FE mass structure should allow for a better study of heat transfer throughout the engine geometry.

Firstly, the solid geometry of the engine is used as the basis for the finite element mesher. This conversion process generates separate meshes for the head, block,

piston and valve components of the engine. Multiple conversions are required to complete the cylinder structure with each mesh requiring a local origin component to define local coordinates. These local origins are defined in GEM3D by entering single coordinates for each part of the engine.

While the mesh size can be chosen, local refinement as with typical CFD software are not allowed. Instead, a minimum and maximum element size must be selected. The size of the finite elements is set between 10 and 20 mm and the elements are considered tetrahedral. For computational reasons and estimation result this was assumed as a suitable trade off. Further work could consider implementing the mesh size and also studying the relation between the temperature error estimation versus the mesh density.

The final mesh used for the engine is displayed in Figure 46.
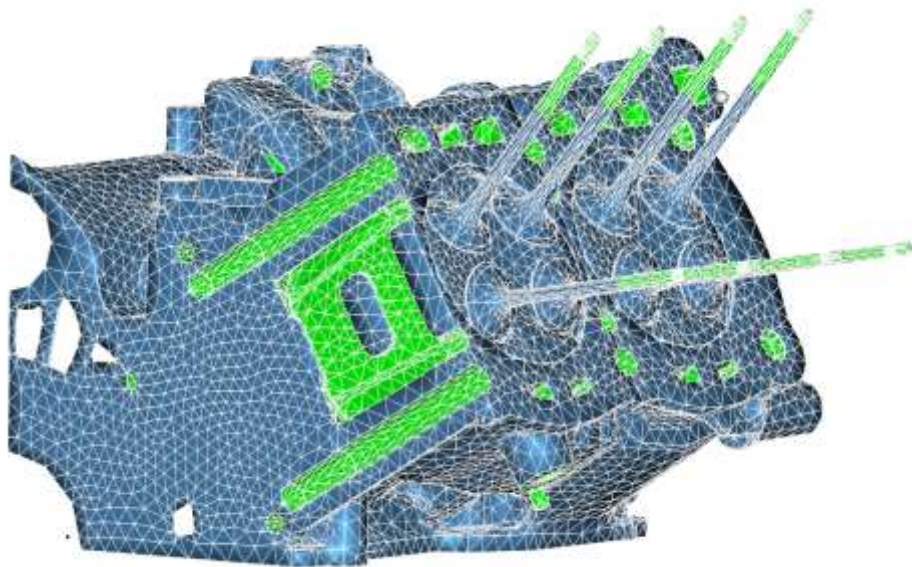
Figure 46: C Sample - Model MH - Finite Element engine conversion.

In this model, the same procedure for convection and conduction connections is applied as in the lumped mass model. However, the use of FE model allows for greater accuracy in the definition of convection and conduction connections due to the use of the actual engine geometry.

4.6.1 Engine Thermal Model

In this model the heat transfer zones are defined using GEM3D. In Table 4 all the heat transfer areas defined in the FE model are listed. The selection of all these surfaces is done manually using the tool available in the software. A meticulous approach is taken to ensure that of all heat transfer surfaces are truly captured.

Table 4 : Heat transfer contact area for the FE Model.

		Engine Parts		
	Bock	**Head**	**Piston**	**Valves**
Heat Transfer Surface area	Bore – Gas and Oil	Combustion Gas 1 – 2- 3	Combustion 1 -2- 3	Front
	Gasket	Gasket	Oil	Back
	Coolant	Upstream intake port gas	Cylinder contact	Seats
	Oil	Downstream exhaust port gas	Ring groove	Guide contact
	Ambient	Valve seat contact		
	Custom	Valve guide contact		
		Coolant		
		Ambient		
		Oil		
		Custom		

A graphical representation of these surfaces and how the software represents those surfaces are showed in the following Figures.
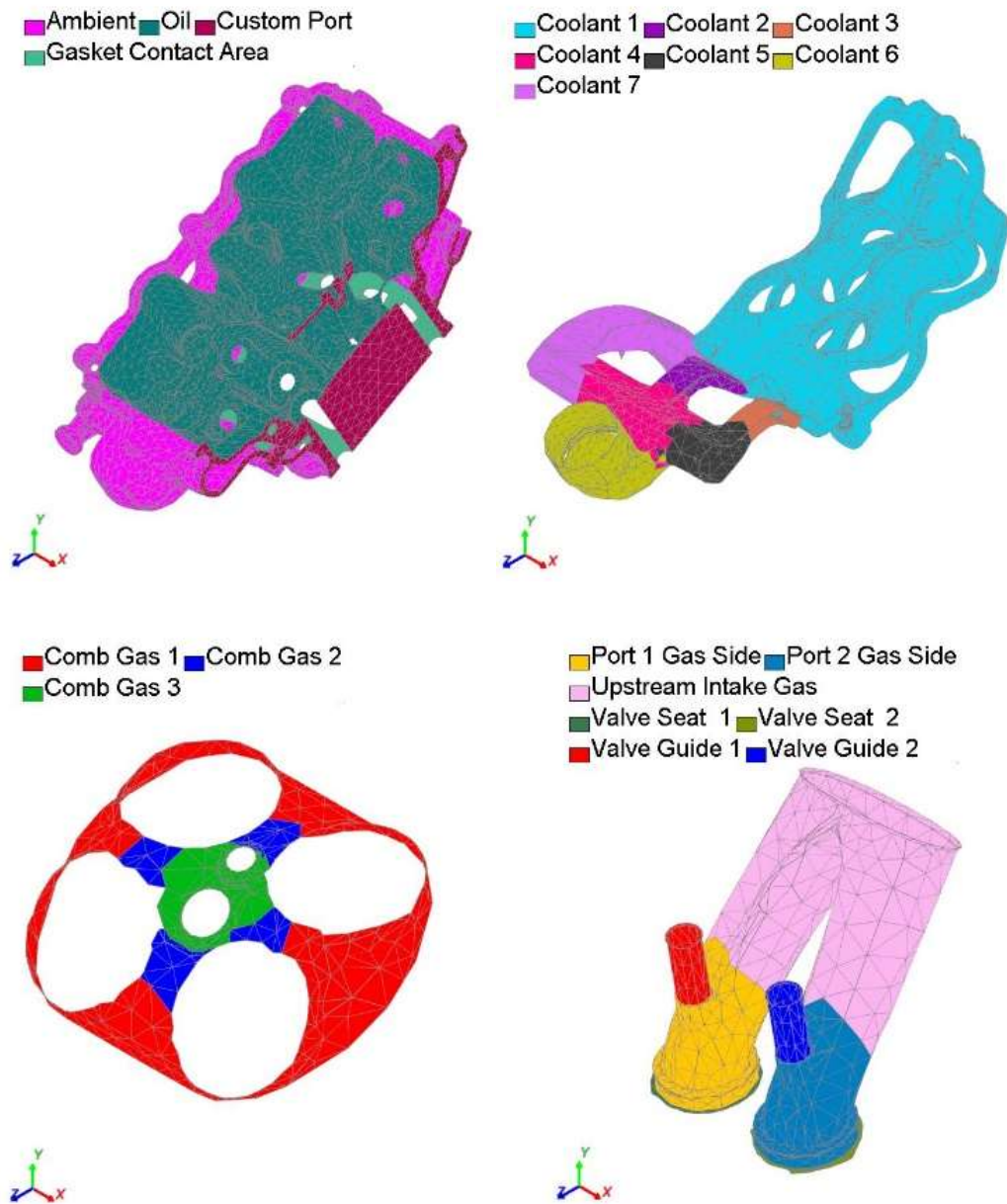
Figure 47: Head heat transfer zone for FE model.

Figure 47 shows the head heat transfer surfaces.
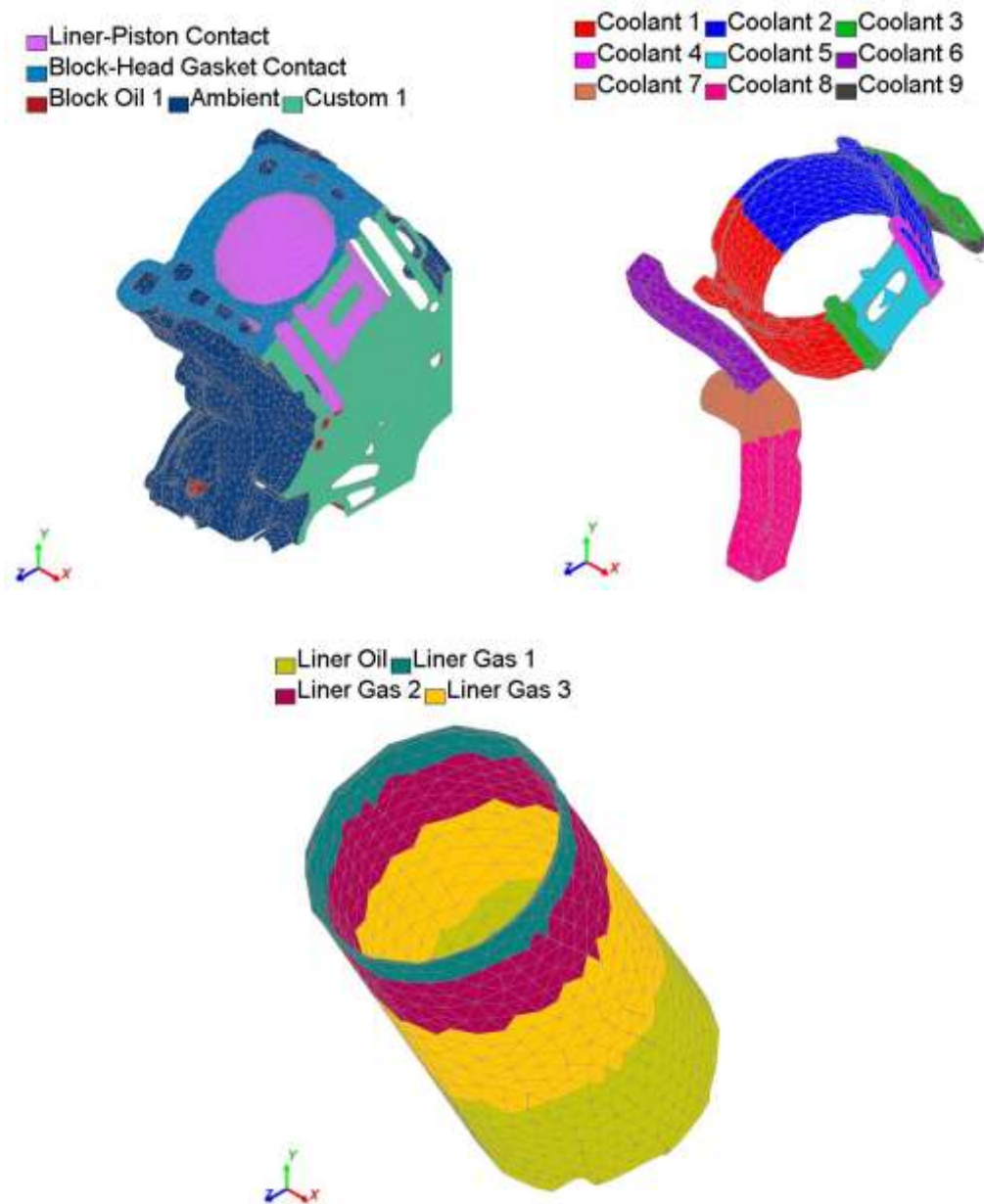
Figure 48: Cylinder 5 heat transfer surface area definition.
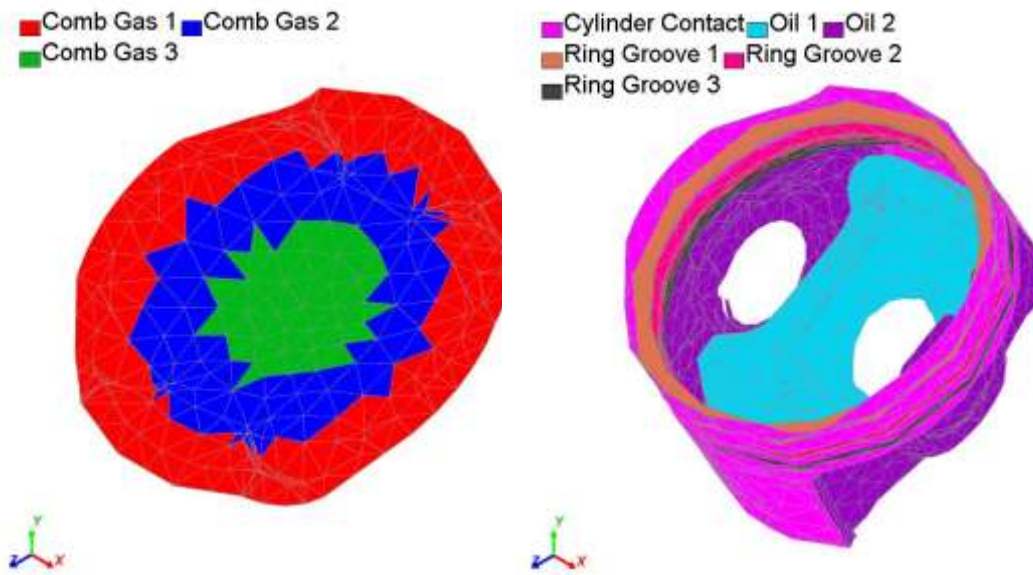
Figure 49: Piston heat transfer zone in the FE model.
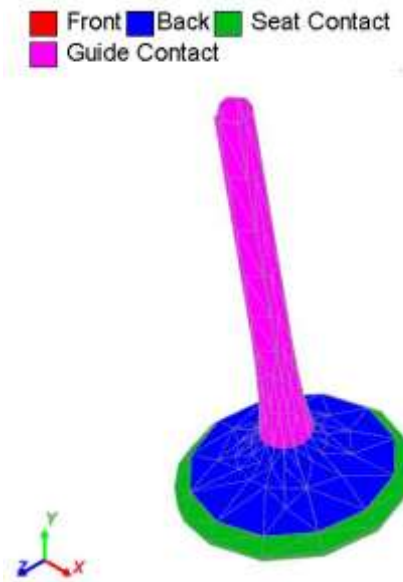
Figure 50: Valve heat transfer surface area definition.

The overall engine thermal model discretised is shown in Figure 124 in Appendix A.

4.7 Thermal Calibration Strategy – Model Setting

The following paragraph describes the thermal calibration strategy that is used for both the Lumped Mass and Finite Element models. Although the parameters utilized in the calibration differ between the two models, the setting used for both approaches remain unchanged. Before starting the calibration strategy, it is crucial to analyze the experimental data to ensure the consistency and reliability of the data to identify and exclude any thermocouple failures. Furthermore, this analysis helps to determine the optimal strategy and thermocouple data to include in the calibration process.

4.7.1 Experimental Data Sanity Check

In this study, the thermal engine experiment campaign was meticulously conducted in collaboration with an esteemed external research center, commissioned by the engine manufacturer. The external research center, renowned for its expertise in thermal engine research, played a pivotal role in overseeing and executing the experimental procedures. The collaboration ensured the application of rigorous methodologies and adherence to industry best practices throughout the entire campaign.

The experimental setup, conducted at the state-of-the-art facilities of the external research center, featured advanced instrumentation and equipment specifically chosen to meet the high standards required for precision in thermal engine measurements. The engine manufacturer actively participated in defining the experimental parameters and closely monitored the entire campaign to guarantee the accuracy and reliability of the acquired data.

Quality assurance procedures were integral to the experiment campaign, including regular calibration of measurement instruments and strict adherence to established industry standards. The transparency of data collection was maintained through

comprehensive documentation of each step, allowing for traceability and auditability of the entire process.

Furthermore, the results obtained from the experiment campaign underwent an independent verification process, involving external experts and peer reviews. This additional layer of scrutiny not only reinforces the credibility of the data but also ensures that the findings withstand rigorous scientific validation.

For confidentiality reason in this work are present part of the the experiment campaign, along with detailed methodologies and supporting documentation. We acknowledge the limitations inherent in any experimental study and provide a transparent discussion of these limitations in the subsequent sections. Through this collaborative and rigorous approach, we aim to instill confidence in the quality, reliability, and validity of the thermal engine data presented in this study.

Figure 51 shows the general test cell installation for the engine in the research facility.
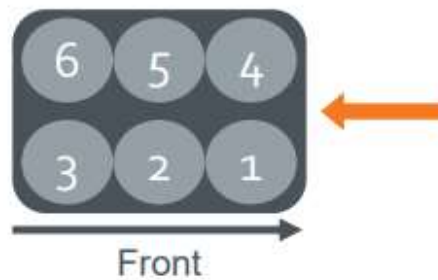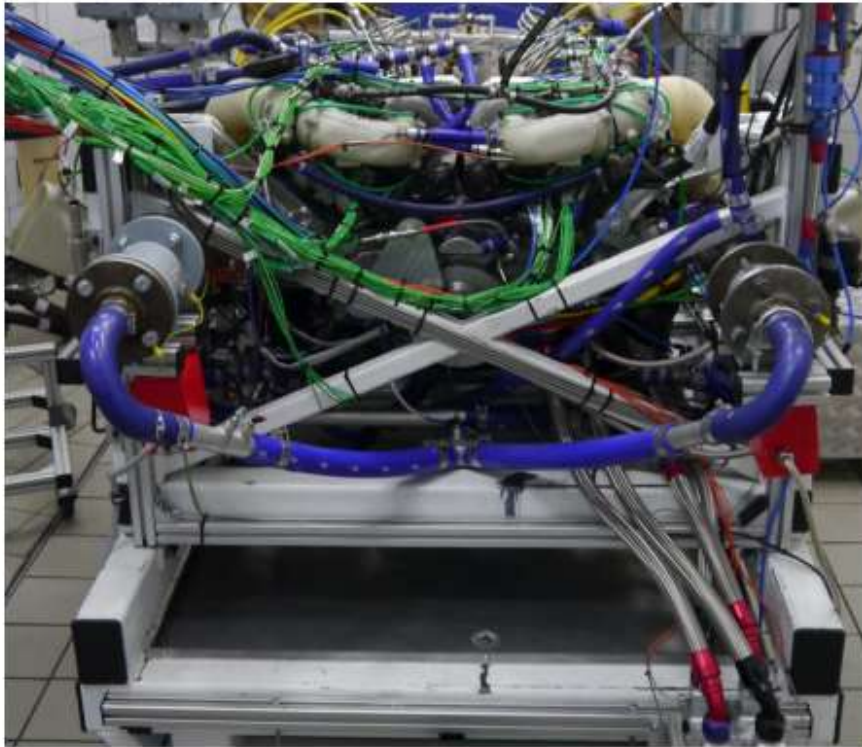
Figure 51: Engine Cell installation.

The engine was heavily instrumented with a broad range of sensors. A list of the sensors is available in Appendix B. The thermal survey engine used k-type thermocouples of either 1.5mm or 3mm diameter depending on location and durability considerations. This type of thermocouples are stable for thousand hours below 700°C but only for about 20 hours at above 900 °C, though the exact temperature is highly dependent on wire diameter [110]. Absolute temperature accuracy is dependent on a number of elements of the data acquisition chain, including cold junction compensation, but k-type thermocouples are generally accepted as the most robust approach to thermal surveys with metal temperatures. Higher temperature accuracy could be achieved with resistance thermometry i.e PT100 sensors, but these were out of scope for this work.

The thermal survey data has been thoroughly analysed to ensure the reliability of the thermocouple data used for the calibration. Figure 52 shows the data from the upper cylinder block thermocouples which are seen to be consistent and robust across all the engine speed cases. Cylinders one and four register as the coldest due to their contact with coolant flow from the pump. All data was collected at WOT full load conditions across the speed range from 1000-8000 rev/min.
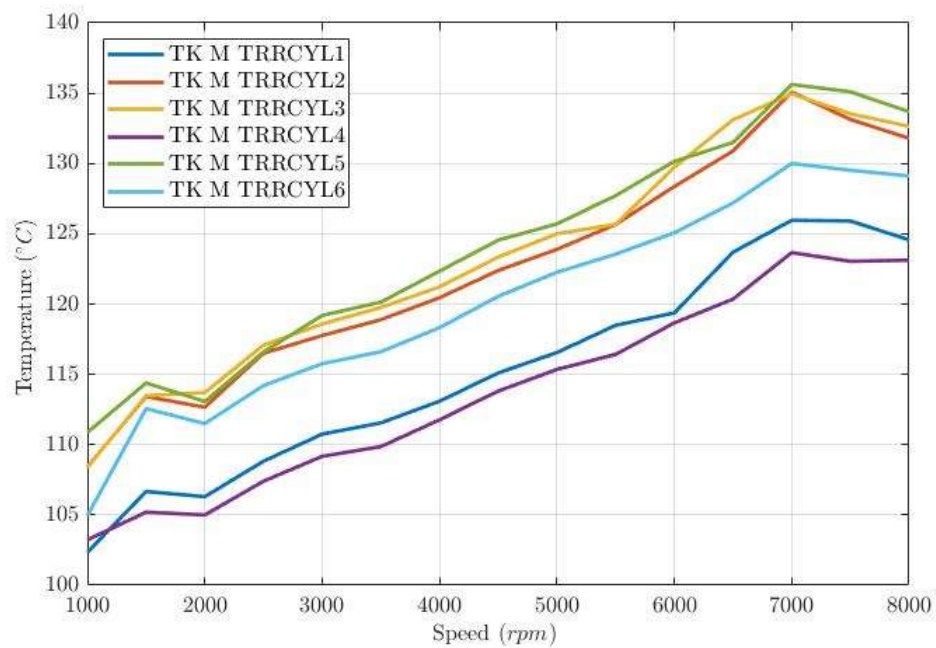
Figure 52: Top cylinder thermocouple temperature - thermal survey data.

The middle cylinder thermocouple data is depicted in Figure 53, revealing that cylinder one is consistently cooler than cylinder four, while cylinder five is the hottest with an average delta from the other cylinder of 5°C. The cylinder bank comprising cylinder 4,5 and 6 is consistently hotter than the other bank throughout the speed range.
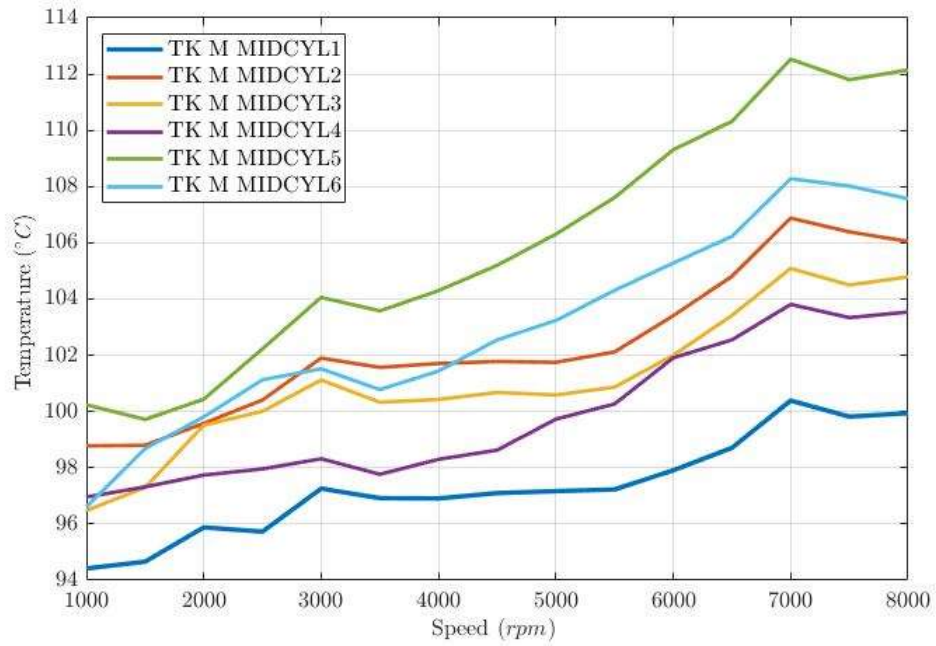
Figure 53: Mid cylinder thermocouple temperature – thermal survey data.

Figure 54 shows the results of the bottom thermocouples, indicating that TK_M_BRRCYL1 and TK_M_BRRCYL3 are not reliable for consistent data collection.
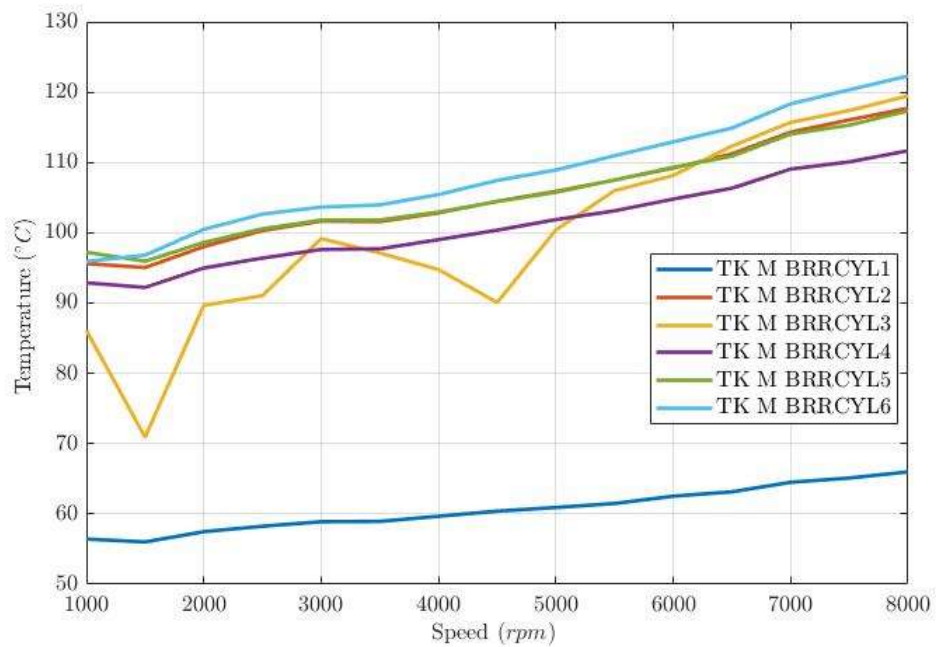
Figure 54: Bottom cylinder thermocouple temperature – thermal survey data.

In contrast, the interbore data for the top and middle thermocouples, shown in Figure 55 and Figure 56, appear reliable.: Interbore middle cylinder thermocouple temperature – thermal survey data.
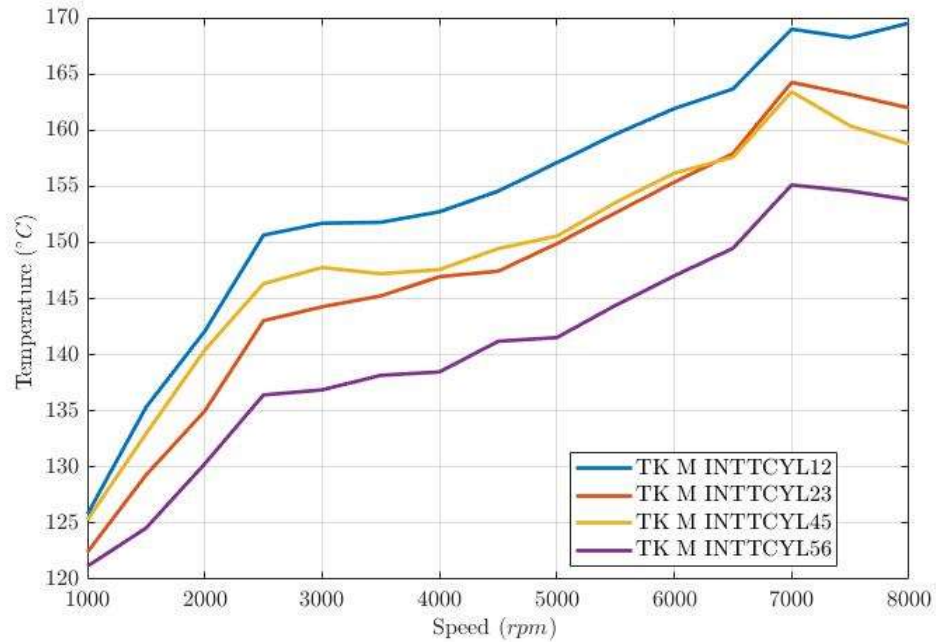
Figure 55 : Interbore middle cylinder thermocouple temperature – thermal survey data.
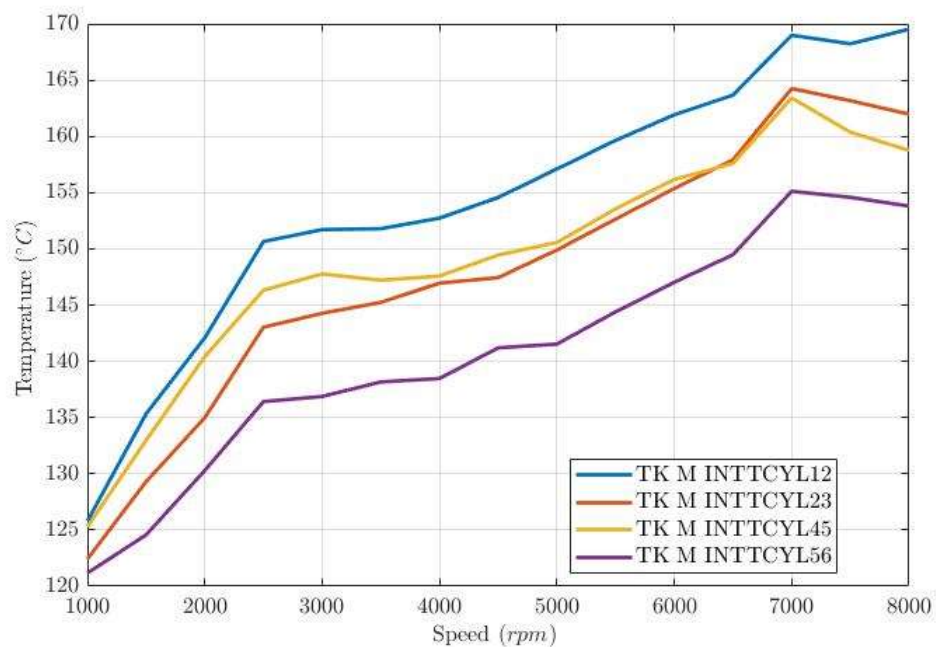
Figure 56: Interbore top cylinder thermocouple temperature – thermal survey data.

Figure 57 shows that all cylinder temperatures are consistent except for cylinder five, TK_M_EBCYL5, which runs lower than the others at all engine speed. The

difference between cylinder five and cylinder four and six for high rpm is ~20°C. This can be explained by a thermocouple that might be located poorly, or not have good thermal contact with the surface or has a small air pocket in the measurement hole.
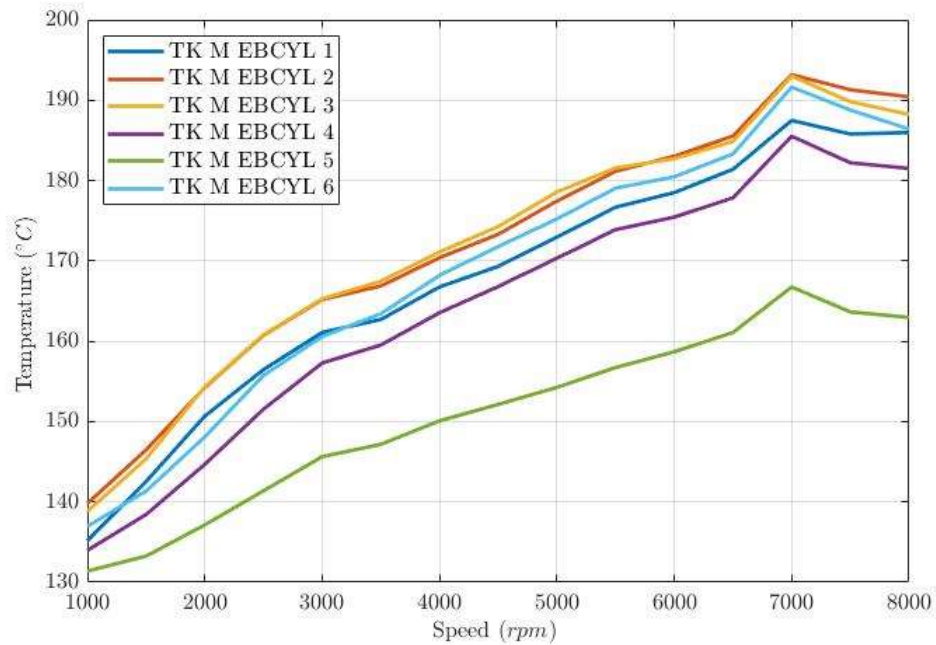
Figure 57: Exhaust valve bridge thermocouple temperature – thermal survey data.

Figure 58 shows the intake bridge and intake-exhaust thermocouples data. The intake bridge valve seat thermocouples were only installed in cylinder head two and cylinder head four. It is interesting to note the difference between TK_M_IBCYL2 and TK_M_IBCYL5. The second cylinder runs hotter than the fifth cylinder with a delta temperature of ~10°C. Meanwhile, the results for the intake-exhaust bridge for cylinder one and four show similar trends in temperature.
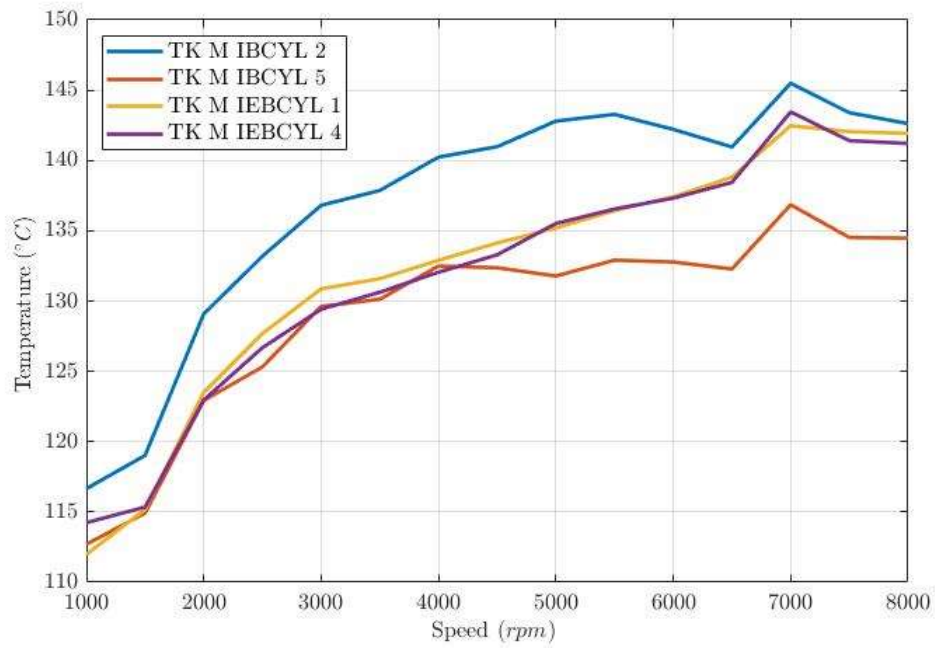
Figure 58: Intake valve bridge thermocouple temperature – thermal survey.

The exhaust valve seats in Figure 59 and Figure 60 show consistent data, except for TK_S_EV10 in cylinder 5.
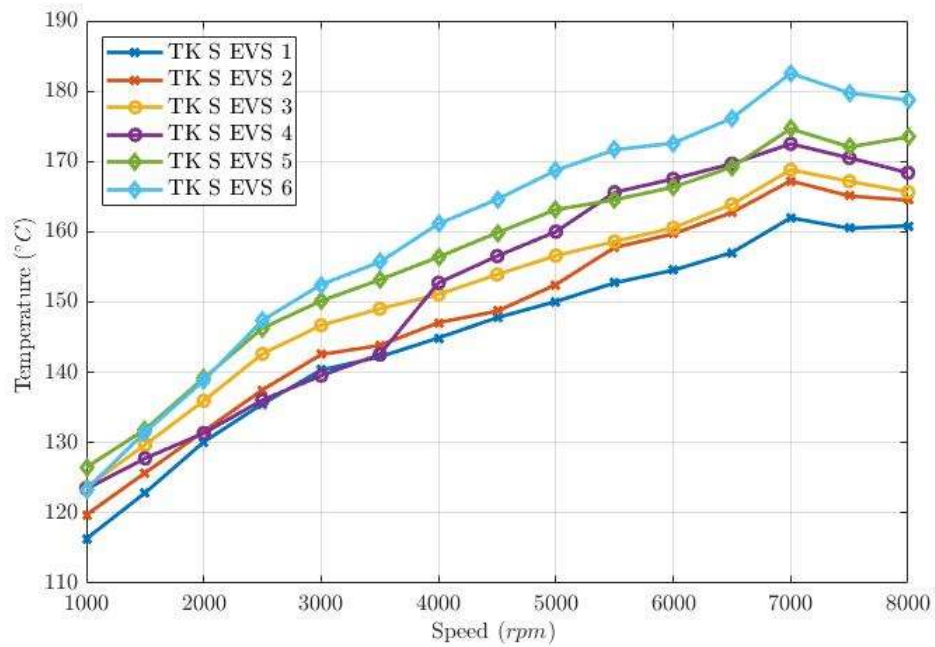
Figure 59: Exhaust valve seats thermocouple temperature - Cylinder one two and three.
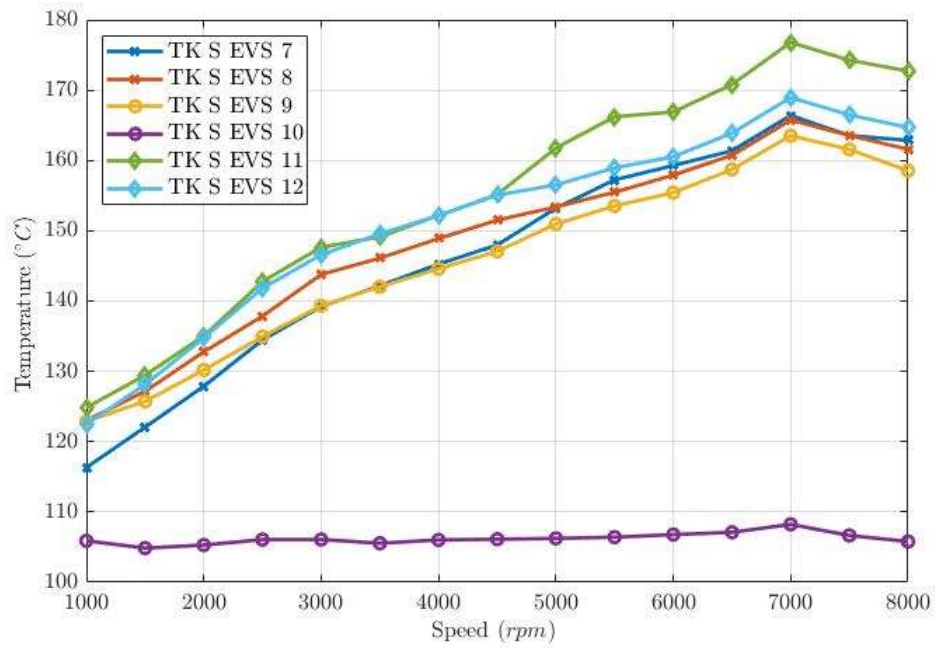
Figure 60: Exhaust valve seats thermocouple temperature – Cylinder four five and six.

The intake valve seats in Figure 61, Figure 62 are working correctly showing a robust trend for all the engine thermocouples.
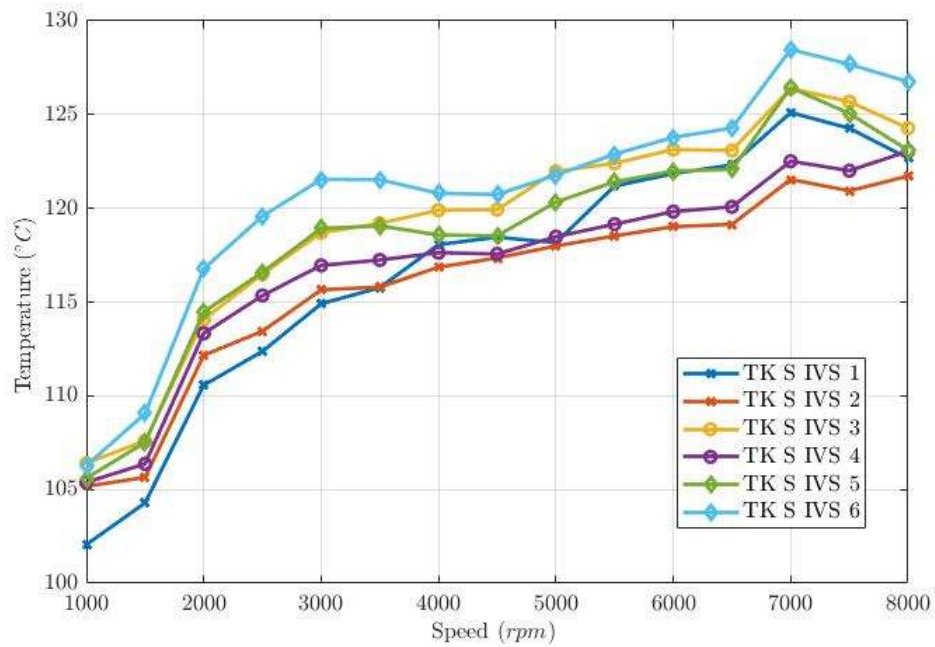
Figure 61: Intake valve seats thermocouple temperature – Cylinder one two and three.
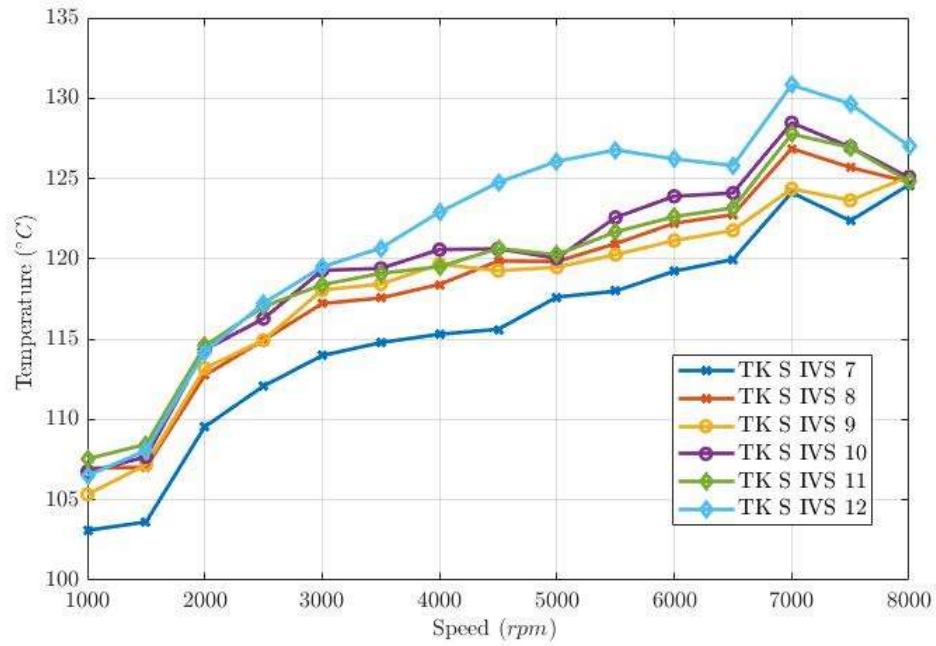
Figure 62: Intake valve seats thermocouple temperature – Cylinder four five and six.

The head coolant jacket temperature shown in Figure 63 indicates that the cooling system is effectively and efficiently working along the banks. Thus, overall, the thermal survey is reliable for thermal calibration, except for TK_MBRRCYL1, TK_S_EV10, and TK_M_BRRCYL3, which are not recommended for use.
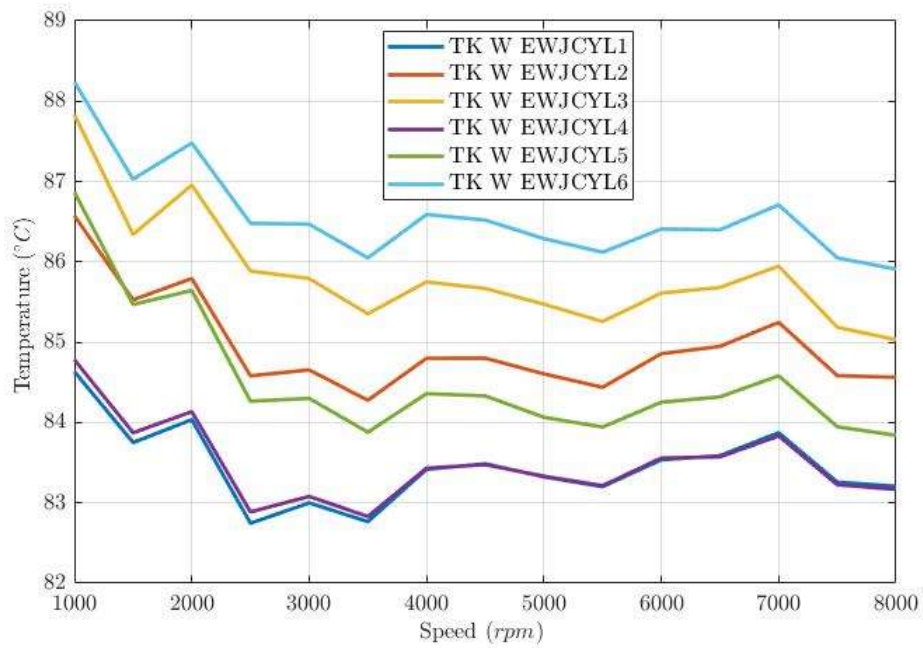
Figure 63: Top rail head coolant jacket temperature.

4.7.2 Friction and Oil included in the Model

Engine friction modelling is commonly achieved using experimental data or semi-predictive model like the Chen-Flynn friction model, which provides sensitivity to engine speed and peak firing pressure but relies on a fixed coefficient calibrated from experimental data. However, this model has limited capabilities in considering the temperature dependency of the oil and the friction measurement. In this project, a friction model was not developed and the friction was applied to the piston ring and skirt as a heat source term, which was then divided equally across each cylinder. Figure 64 shows the partition of the friction power.
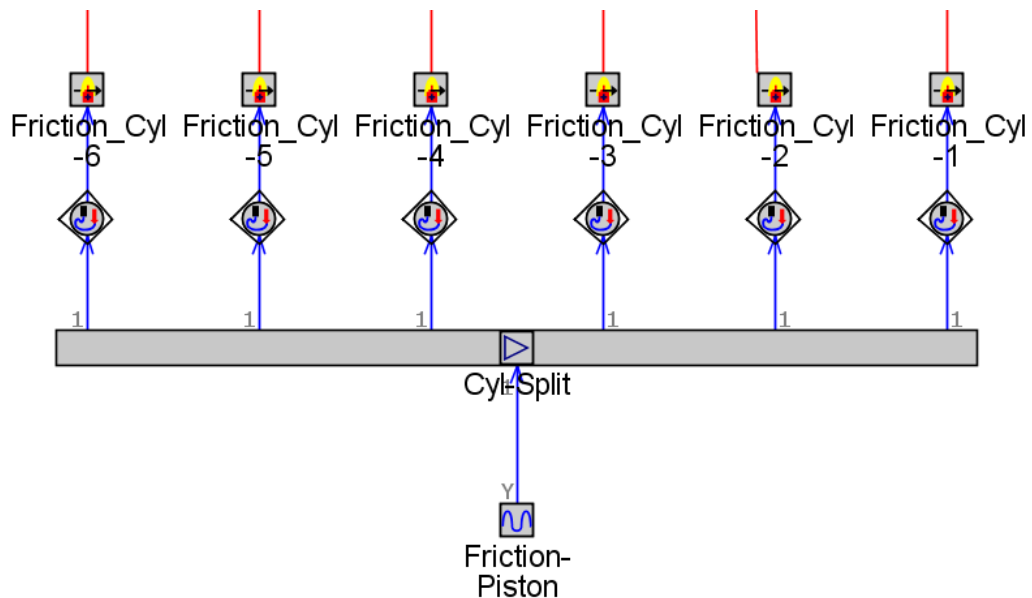
Figure 64: Friction split in the thermal model.

To discretise the oil circuit, a single flow split is used and the area considered for the heat transfer is shown in Figure 65. Although a detailed model is not provided, the surface area is calculated in SpaceClaim from the engine CAD geometry.
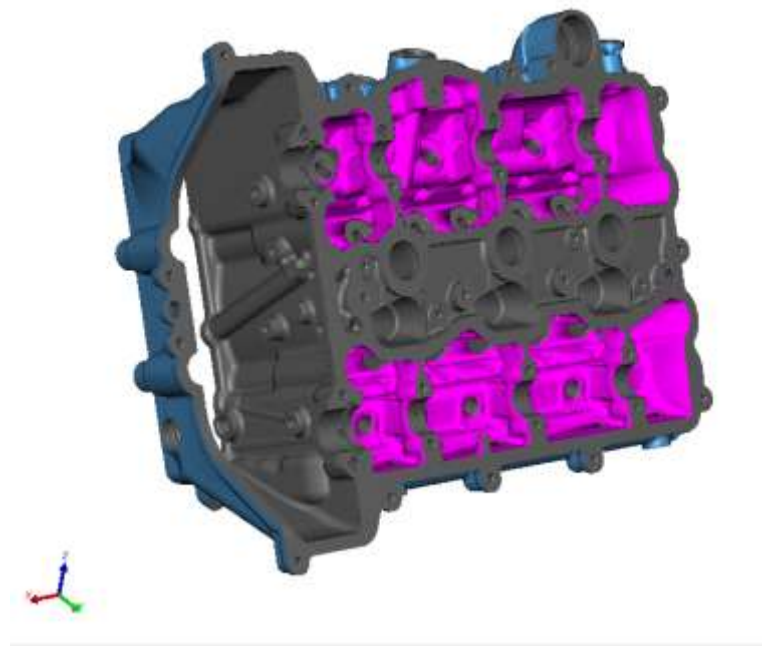
Figure 65: Head RH, oil surface contact.

Figure 66 depicts the oil surface area for the engine block. The oil flow split is connected through the blocks and head by convection connections, where the heat transfer coefficients were applied based on previous experience and therefore not considered as a calibration parameter.
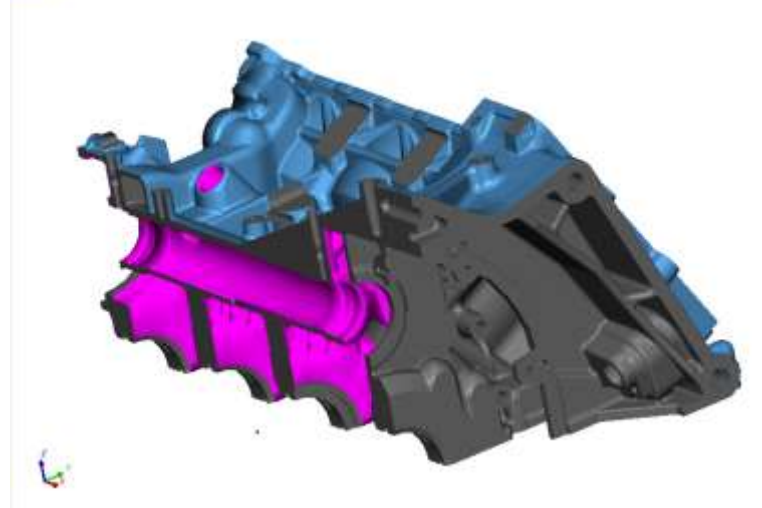
Figure 66: Bloch RH, oil surface contact.

Specifically, the block oil heat transfer coefficient was set at 1000 W/m²K and for the head, it was set at 400 W/m²K, those values were imposed based on simulation experience and third party knowledge. Finally, the initial condition for the oil flow rate, temperature and pressure were taken from the test bench data results provided and they are shown in Table 5.

Table 5: Oil initial condition.

	2500 [rpm]	5000 [rpm]	7500 [rpm]
Oil Pressure [bar]	3.92	6.71	7.41
Oil Temperature [°C]	93.54	99.54	110.52
Oil Flow rate [L/min]	49.23	74.8	83.53

4.7.3 Thermocouple Position in the Simulation Models

The primary objective of thermal calibration is to ensure that the heat transfer rate distribution from the engine to the fluids, coolant, oil and external environment is accurate. In the simulation mode, the heat transfer coefficient (HTC) is calculated using the Colburn analogy [108]. The HTC multipliers are as a calibration parameters in the coolant jacket volumes. The heat transfer coefficient is calculated at every simulation time step using fluid velocity, thermos-physical properties and wall surface roughness. The Colburn analogy is expressed by Equation (11).

$$h_g = \left(\frac{1}{2}\right) C_f \rho U_{eff} C_p P_r^{\left(-\frac{2}{3}\right)}$$

Equation (11)

where:

C_f is the fanning friction factor.

ρ is the density.

U_{eff} is the effective velocity outside the boundary layer.

C_p is the specific heat.

P_r is the Prandtl number.

If the surface has an imposed roughness, the coefficient is still calculated with the correlation above but with the following correction showed in Equation 12 and Equation 13:

$$h_{g,rough} = h_g \left(\frac{C_{f,rough}}{C_f} \right)^n \qquad \text{Equation (12)}$$

$$n = 0.68 * Pr^{0.215} \qquad \text{Equation (13)}$$

where:

$h_{g,rough}$ - *the heat transfer coefficient of a rough surface*

$C_{f,rough}$ - *the Fanning factor of a rough pipe*

It is important to note that the software also calculated additional enhancement factors for each flow split based on the ratio of the characteristic length to the port reference, typically the expansion diameter. These factors are not included in the "Reference HTC, without multiplier" results. Therefore, the value without the multiplier cannot be calculated simply from the multiplier and factor. The calculation for the pipe is more straightforward and the heat transfer multiplier would be the difference between the reference and the calculated heat transfer coefficients. To correctly calibrate the model, it is necessary to know the exact boundary condition for the experimental tests. The simplification made for 1D conduction in the head and block also requires adjustment to match the correct heat distribution in the engine structure. By acting on the resistance to conduction of the lumped masses, it is possible to compensate for the error resulting from the simplified modelling of the engine structure.

Another calibration parameter is the distance L, which is the distance between the centre of the lumped mass and the heat exchange area. Within the model, it is possible to modify the thermal resistance of a single thermal mass and consequently, the heat transferred from the coolant to the engine structure. In the Lumped Mass Model the engine block and head are modelled using lumped mass (homogeneous and isotropic) and thermal resistance of the lumped thermal is calculated using Equation (14):

$$R = \frac{L}{k * A} \qquad \text{Equation (14)}$$

where:

> *R - the thermal resistance between the centre of the mass and the heat exchange area.*

> *L - the distance between the centre of the mass and the heat exchange area*

> *k - the thermal conductivity*

> *A - the heat exchange area.*

The engine block parts and the head parts are represented by thermal masses and are linked via convective connections to the corresponding section of the coolant jacket. These connections represent the rate of heat transfer from the coolant to the engine structure. Conduction between the head, the cylinder block and the structure is considered using a conductive connection.

The calibration strategy involves imposing experimental temperature data on the simulation model by applying the temperature directly to the cylinder structure. Specifically, the temperature was defined on the thermal node that composes the cylinder structure. To achieve the best thermal calibration, we optimize the heat transfer multipliers defined in the model. Before starting the calibration process, a comprehensive thermal survey of the engine is analysed. It is crucial to ensure that the physical position of the thermocouples in the experimental setup correspond to the defined nodes within the cylinder structure to achieve accurate thermal calibration.

To optimise the selection of the thermocouples, an initial analysis is performed for the following reasons:

- To gain a better understanding positioning of the thermocouples in the engine.

- To identify the most suitable thermocouples and nodes that would facilitate thermal calibration.

- To minimise the number of thermocouples chosen, thus reducing the overall cost of the calibration process.

Figure 67 illustrates the positioning of thermocouples on the engine block's exhaust side for the thermal survey. The thermocouples are placed strategically to ensure accurate measurement of the cylinder's temperature. Specifically, a single thermocouple is positioned at the top of the cylinder block to cover the top liner section, while another one is placed in the middle to measure the coolant jacket's temperature. Additionally, a bottom thermocouple is located to measure the cylinder block's oil area temperature. The interbore thermocouples are also included: one positioned at the top and the other in the middle of the cylinder, both measuring the cylinder's metal temperature.
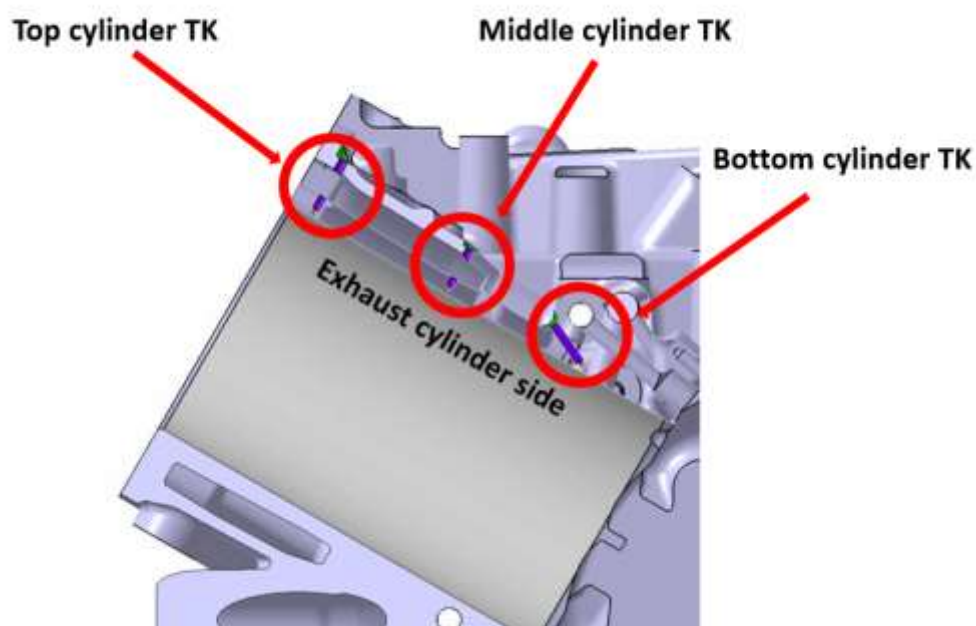
Figure 67: C Sample - Thermal engine survey, thermocouple position in the cylinder block.

In Figure 68, the engine's structure (EngCylStructCond) used in the lumped mass model is displayed, including the thermocouples indicated by coloured diamonds and the nodes. This gives an overall understanding of the thermocouple positions, allowing the user to verify the correct coordinates of the FE cylinder in the simulation model.
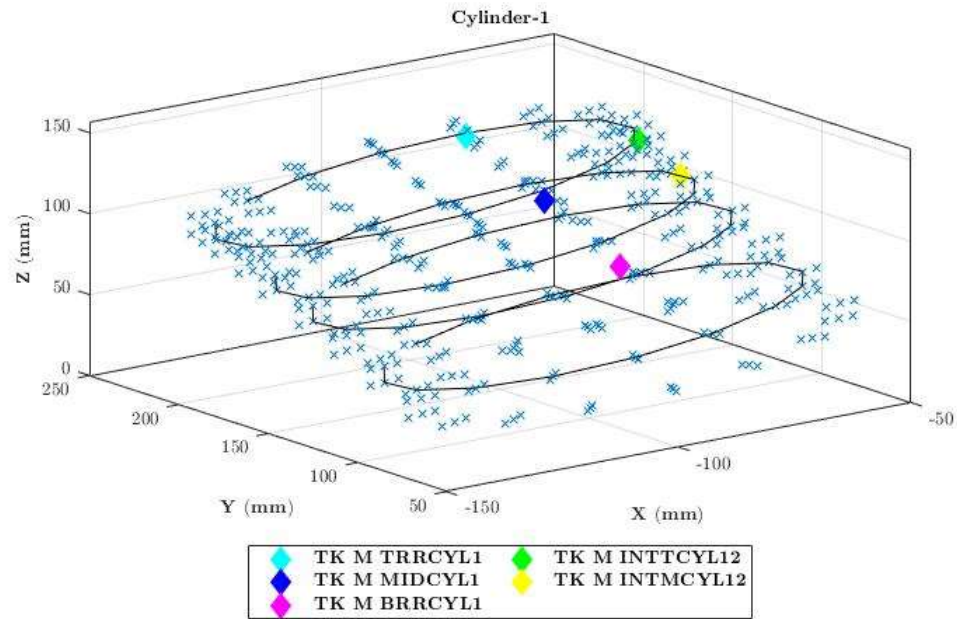
Figure 68: Engine Cylinder structure, nodes definition.

Table 6 shows the complete list of the thermocouples presents in the engine. There is a symmetry between the two engine banks. Cylinder one is equipped as cylinder four, cylinder two is equipped as cylinder five and cylinder three and six as well.

Figure 69 shows an example in which the thermocouples are placed within the cylinder structure head of the lumped mass model. The stars represent each node of the cylinder structure, while the diamonds represent the engine thermocouple. The head structure even if itis a basic representation, correctly captures the position of the thermocouple.

Table 6: Cylinder head thermocouples.

	Cylinder 1	Cylinder 2	Cylinder 3	Cylinder 4	Cylinder 5	Cylinder 6
Intake Seat	2	2	2	2	2	2
Exhaust Seat	2	2	2	2	2	2
Intake Bridge		1			1	
Exhaust bridge	1	1		1	1	
Intake - Exhaust Bridge	1			1		
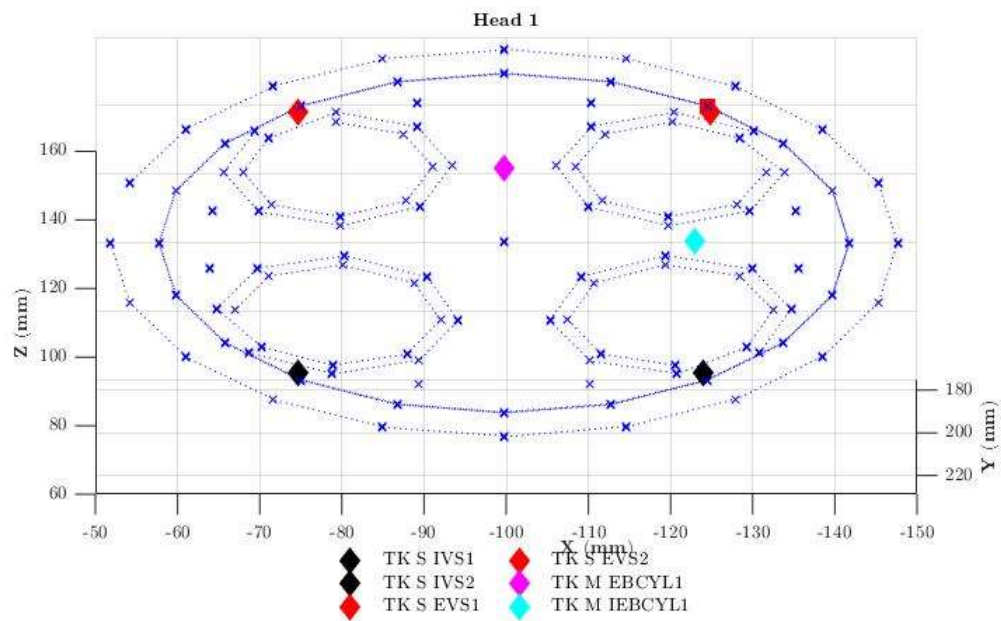
Figure 69: Head thermocouples cylinder one.

Several factors were taken into consideration when selecting the thermocouples to be used for thermal calibration. Firstly, it was determined that only thermocouples measuring metal temperature should be used, so the coolant jacket thermocouples were excluded. This is also one of the first assumption of the current methodology. Calibrating and validating the thermal model are performed using thermocouples that measure only the metal temperature of the engine. Secondly, to simplify the data management and because the information from a lumped mass model was deemed sufficient, only one valve seat and one exhaust valve seat thermocouple are used. The intake-exhaust bridge thermocouple is also excluded due to difficulties in temperature detection within the lumped mass model, which will be discussed in more detail later.

The following thermocouple positions were selected for calibration:

- Top cylinder block.

- Middle cylinder block.

- Bottom cylinder block.

- Top interbore cylinder block.

- Intake valve seat head.

- Exhaust valve seat head.

- Exhaust valve bridge head.

- Intake valve bridge head.

The thermal calibration objective is to match the lumped mass model and the finite element model to the metal temperature in the cylinder structure. That will be EngCylStrucCond for the lumped mass model and EngCylStrucCustom for the Finite element model. To achieve this, the closest FE node in the cylinder structure is identified and the test data temperature is imposed to it. A minimum distance Equation (15) is used to calculate the minimum distance between the nodes and the thermocouple position.

$$d = \sqrt{(x_1 - x_2)^2 + (y_1 - y_2)^2 + (z_1 - z_2)^2} \qquad \text{Equation (15)}$$

where:

x_1, y_1, z_1 - are coordinate for the engine thermocouple position.

x_2, y_2, z_2 - are coordinate for the FE cylinder node.
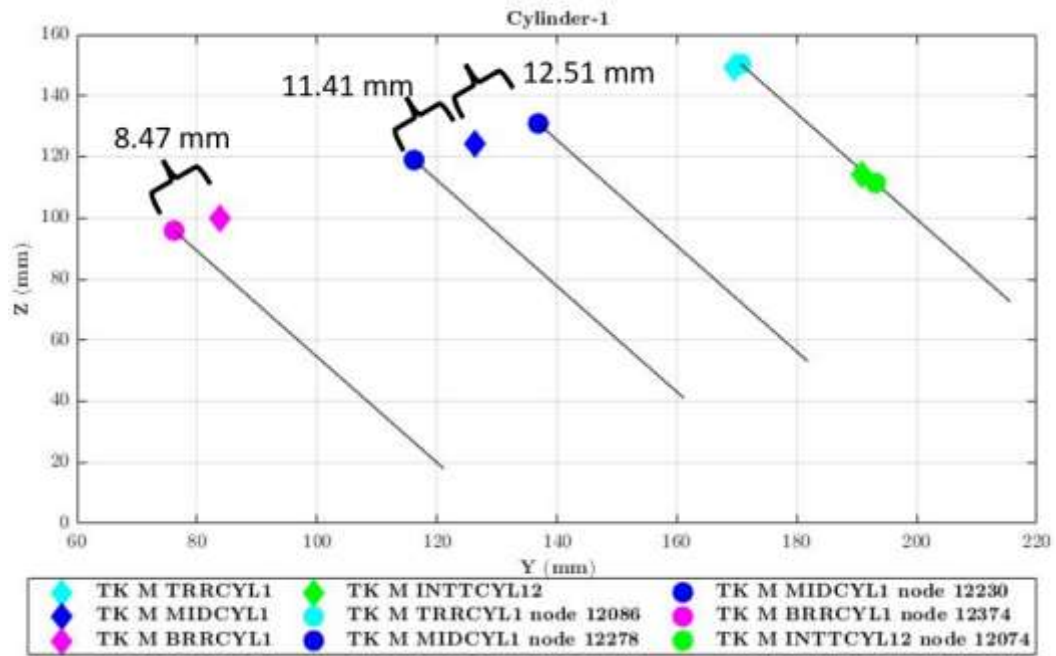
Figure 70: FE cylinder one thermocouple and nodes.

Figure 70 displays the selected nodes and thermocouple positions for the thermal calibration process. For the top thermocouple, the selected nodes are near the thermocouple position, with a distance of 1.57 mm. For the middle thermocouple, two nodes are considered (for the lumped mass model) as the thermocouple is positioned between the two nodes of the EngCylStruc. The distance from node 12278 to the thermocouple is 11.41 mm, while the distance to node 12230 is 12.51 mm. The temperature will be calculated as an average of the two selected nodes, and this average result must align with the thermocouple temperature data.

For the bottom thermocouple, a single node is deemed sufficient, given its proximity to the thermocouple position, with a distance of 8.47 mm. Similarly, the top interbore thermocouple was closely matched to the selected node, which is 120474, at 3.68mm.

The selection approach for cylinder one is duplicated for all other cylinders, with the only variation being for cylinders three and six, where the interbore nodes were not considered since they were already considered in cylinder two and four.

The thermal calibration of the lumped mass model involved considering a set of thermocouples and nodes for each cylinder. The selection of thermocouples and nodes for cylinder heads is more complex due to the simplicity of the cylinder structure. After investigating several different strategies, a method is implemented to consider the head and valves either as a single mesh or with separate discretised meshes.

As with the engine block thermocouples, Equation 15 is used to calculate the minimum distance between the head thermocouples and the nodes. Figure 71 shows cylinder head one with the thermocouples used for the calibration and their respective nodes.
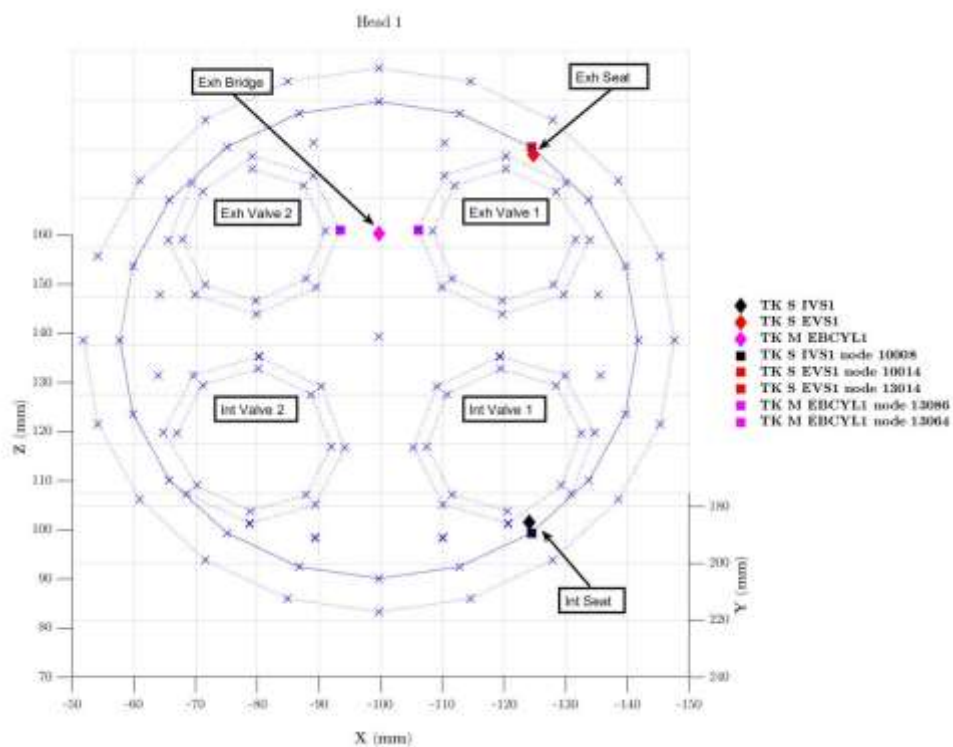
Figure 71: Cylinder head one, thermocouple, and nodes.

For cylinders two and five, the only difference is the intake bridge thermocouple which will be part of the calibration process.

The thermal calibration process involved 41 thermocouples distributed as follows:

Table 7: Total thermocouples used for the calibration. The total thermocouples number is 41.

	Cyl 1	Cyl 2	Cyl 3	Cyl 4	Cyl 5	Cyl 6
BLOCK	TK Top	TK Top	TK Top	TK Top	TK Top	TK Top
	TK Midt	TK Midt	TK Midt	TK Midt	TK Midt	TK Midt
		TK Bot	TK Bot	TK Bot	TK Bot	TK Bot
	TK Int Top 1-2	TK Int Top 2-3		TK Int Top 4-5	TK Int Top 5-6	
HEAD	TK Int Seat	TK Int Seat	TK Int Seat	TK Int Seat	TK Int Seat	TK Int Seat
	TK Exh Seat	TK Exh Seat	TK Exh Seat	TK Exh Seat	TK Exh Seat	TK Exh Seat
	TK Exh Bridge	TK Exh Bridge	TK Exh Bridge	TK Exh Bridge	TK Exh Bridge	TK Exh Bridge
		TK Int Bridge		TK Int Bridge		

In the Finite element model, a similar approach is used to impose the thermocouple temperatures on the engine. However, unlike the lumped mass model, the position of the nodes in the engine are more accurately represented in the finite element discretisation. This increases the likelihood that the thermocouple node will be placed in the correct position. The Equation 16 is used to find the closest engine node in this model. In the FE model no average temperature calculation was used during the calibration process. This is due to the more accurate meshing of the cylinder block and head of the engine.

4.7.4 HTC Multiplier Definition

The process of the thermal calibration involves setting up the temperature node in the FE cylinder structure and using a heat transfer coefficient multiplier to achieve the desired temperature. Several iterations were needed to determine the heat transfer multiplier strategy in the engine model, considering the different parts of the engine and their varying heat transfer properties.

Initially, it was tried using a single multiplier for all engine models, but this did not yield satisfactory results. Then, two different multipliers were used, one for the block one for the head. A third strategy, not shown in this work, was to use a dedicated heat transfer multiplier for cylinders block and head two and five, while for the other cylinder were used one heat transfer multiplier for the block and the head cylinders. The final strategy adopted is to use separate multiplier for each cylinder block and cylinder head.

The heat transfer multiplier is set as a parameter in the thermal folder of each water jacket volume part in the 1 D simulation model. The final setting is listed below (where HTC stands for Heat Transfer Coefficient):

- HTC-1-Block-Mult.
- HTC-1-Head-Mult.
- HTC-2-Block-Mult.
- HTC-2-Head-Mult.
- HTC-3-Block-Mult.
- HTC-3-Head-Mult.
- HTC-4-Block-Mult.
- HTC-4-Head-Mult.
- HTC-5-Block-Mult.
- HTC-5-Head-Mult.
- HTC-6-Block-Mult.
- HTC-6-Head-Mult.

Each cylinder has its unique multiplier. In the interbore waterjacket volume part the multiplier it is not applied due the complexity of the coolant jacket in that area and the small volume of it.

4.7.5 Design Optimizer

The calibration process optimises the factors involved in thermal calibration to match experimental results. An error function is calculated which sums the average of each error calculated for each thermocouple used in the thermal calibration. Equation (17) calculates the single error, where e1 is the absolute difference between the simulated temperature and the target temperature imposed for the thermal calibration, expressed as a percentage:

$$e1 = abs\left(1 - \left(\frac{HEAD\ 1\ T}{HEAD\ 1\ T\ Target}\right)\right) * 100 \qquad \text{Equation (16)}$$

where:

HEAD 1 T - the simulated temperature.

HEAD 1 T Target - the data temperature imposed for the thermal calibration.

To minimise and optimise the total error output for the thermal calibration, the summed average of all 41 errors is calculated (due to the number of the thermocouples), as shown in Equation (17):

$$e_{tot} = \frac{(e_1 + e_2 + \cdots \ldots \ldots \ldots + e_{41})}{41} \qquad \text{Equation (17)}$$

The model in the calibration process will be considered fully calibrated when the total error is less than 5% and calibrated when the total error is between 5% and 8%. Higher than that, the model should not be considered calibrated and a better modelling strategy should be considered.

The Designer Optimizer tool from GT-Suite is used to perform the thermal calibration, which finds an optimal output by varying one or more model factors. The Design Optimizer runs simulation, evaluates the responses, uses an algorithm to update the factors values and runs again. This process is repeated for multiple designs until the optimal value is found according to certain convergence criteria or until the maximum number of designs specified by the user is reached.

The Genetic Algorithm, specifically the non-dominated sorting genetic algorithm II (NSGA-III), is used as the search algorithm in the calibration, as it is recommended for problems of medium to high complexity, resulting from many factors, the presence of one or more constraints and nonlinear characteristics. The population size is determined by the number of independent variables, the number of active cases and the number of "Sweep" variables. Table 8 provides a recommendation for the population size, which was considered in setting the population size to 60 and the number of generations to 20 for the current model, based on experience and optimization simulation.

Table 8: Population size recommendation.

N	Population size
3	10
4	16
5	20
6	26
7	30
8	40
9+	50

The heat transfer multipliers are defined in the lumped mass model and the finite element model design optimizer, and upper limit as a value of 9 and lower limit as value as 1 for the factors are applied. The lumped mass model has one additional parameter used for calibration, which is the distance to the mass centre used for the block and head.

4.8 Thermal Calibration – Results Discussion

The thermal calibration has been completed using three engine operating points, represented by 2500 rpm, 5000 rpm, and 7500 rpm. A direct comparison between the lumped mass model and finite element model is being performed. The analysis starts with the cylinder block temperature followed by the cylinder heads. An overall model error of 5% is considered acceptable for both thermal and hydraulic calibration. For individual location, a maximum error of 10% between the thermocouple data and simulation data is acceptable.

During results analysis, it is important to note the following:

- TK_M_BRRCYL1 is not considered a temperature target during calibration, but its results are shown to illustrate trend results.

- TK_M_BRRCYL3 is considered reliable for the three cases used in the calibration, and the data will be treated carefully.

- TK_M_EBCYL5 does not work properly, so the average temperature between TK_M_EBCYL4 and TK_M_EBCYL6 will be used for the calibration (this hard assumption must be taken due the importance of the thermocouple position). The average temperature will be used in the results graph.

The right bank of the engine model (cylinder one, two and three) is shown in Figure 72. The graph shows the top thermocouple, the middle thermocouple and the bottom thermocouples. Overall, the results for the cylinder block are satisfactory. It can be inferred that the top thermocouple exhibits a high degree of calibration, as there is almost no error in the results. However, for the middle thermocouples, the model tends to underestimate the temperature at low speeds. On the other hand, for the bottom thermocouple, the models overestimate the temperature.
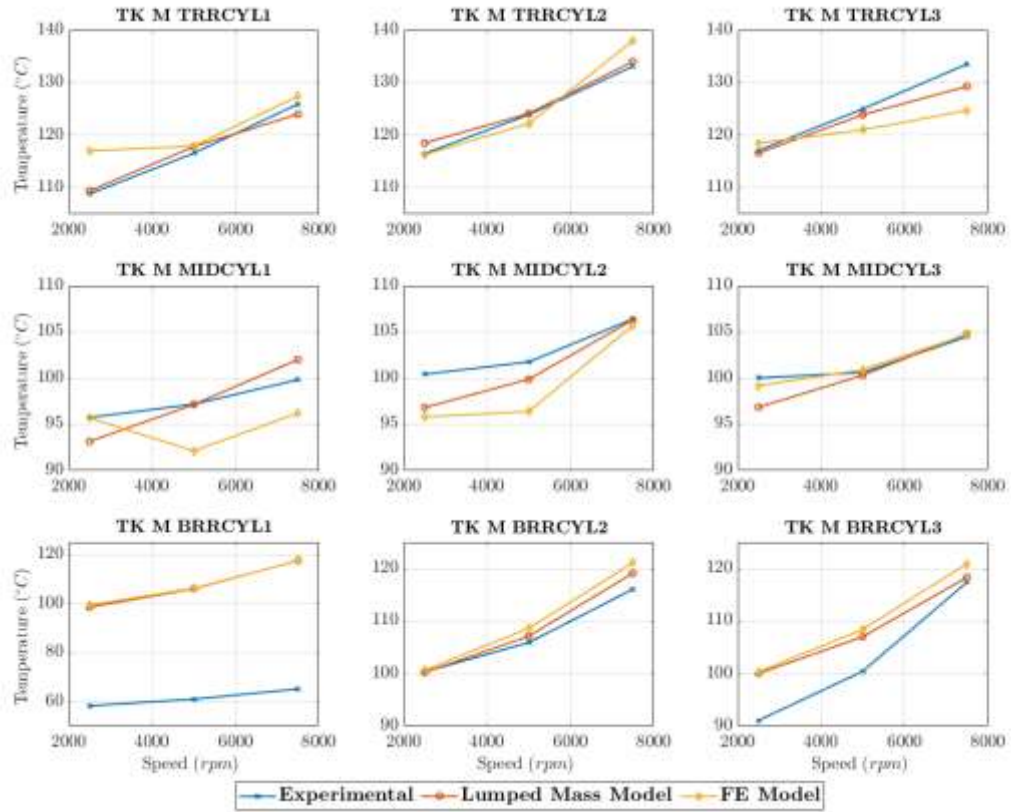
Figure 72: Block RH (Cylinder 1-2-3)temperature result. The TK M BRRCYL1 is a faulty thermocouple. This will not be considered in the calibration process.

Figure 73 shows the top thermocouple of the right bank, where the differences between simulation results and test data can be seen more clearly. The model is sufficiently calibrated from the top liner of the cylinder. Cylinder three shows at higher rpm an underestimation of the temperature and the error is 3%. The FE results appear to be less accurate than the lumped mass for the three cylinders, also showing an overestimation of the temperature for the first cylinder at lower engine speed.

126
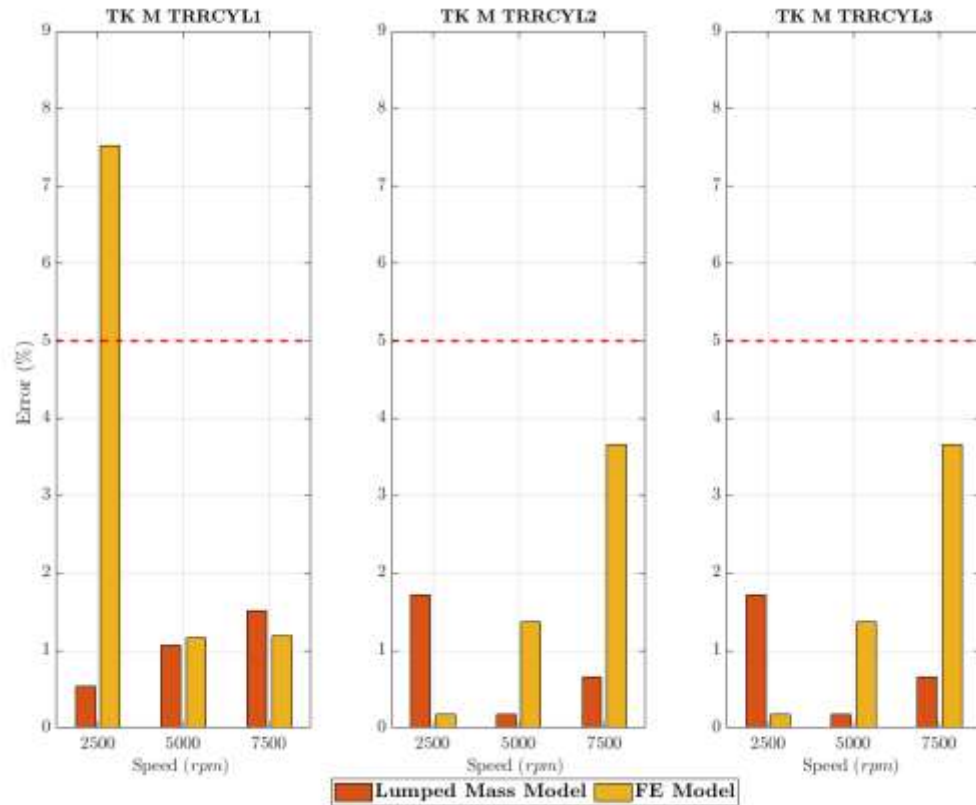
Figure 73: Block RH - Top cylinder thermocouples. The Lumped mass model for all the three engine load point show an error trend below the 2%. The Finite Element model as for the first cylinder at low engine point an error higher than the 5% limit acceptable, while the other cases are showing an higher accuracy given the fact is always below the error margin.

Figure 74 displays the middle thermocouples and the calibration process uses two thermal nodes in the cylinder structure, with their temperatures averaged to match the experimental temperature during simulation. However, the model faced challenges in matching this crucial temperature throughout the calibration process as it is measured in the coolant jacket area and it is sensitive to changes. Eventually, the two chosen nodes matched correctly the temperature. Nevertheless, the results show that cylinders two and three are hotter than the first one, as indicating by the top thermocouple results, mainly due to the impact of the coolant flow path. Cylinder two is also influenced by a portion of coolant from the coolant pump, which may affect the simulation and result in differences for lower speed cases in cylinder two, but not in other cylinders.
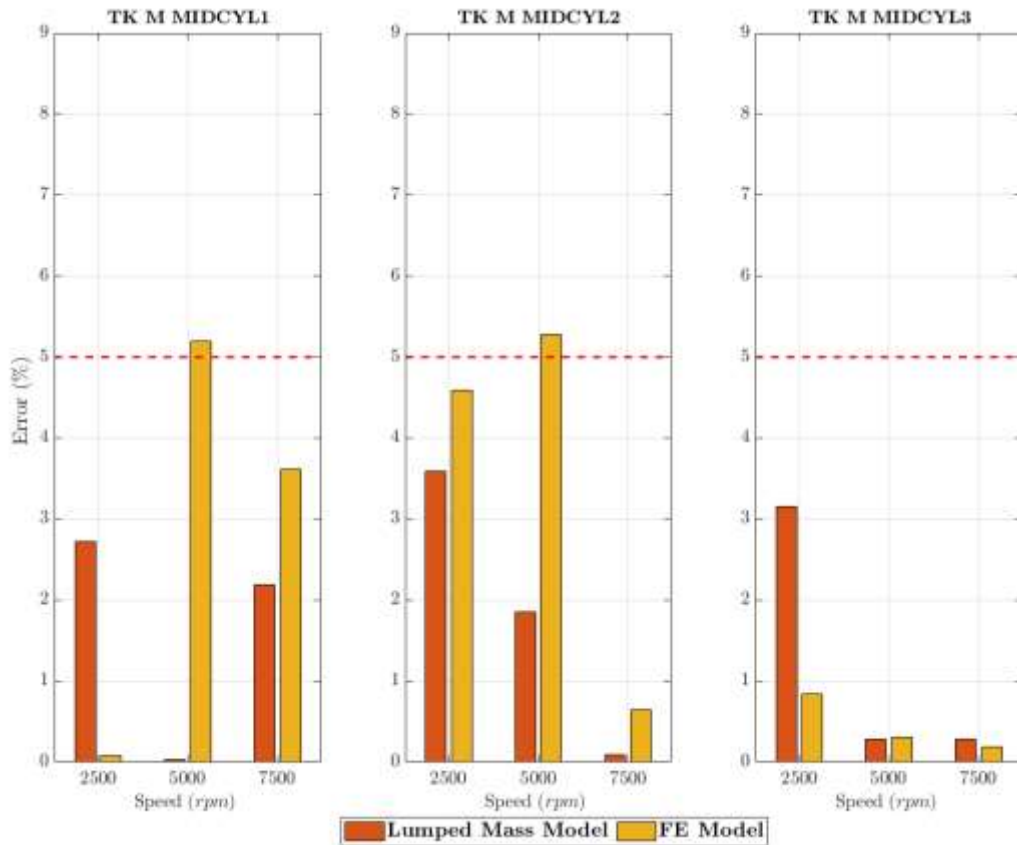
Figure 74: Block RH - Middle thermocouples.

The bottom thermocouples, shown in Figure 75, measure temperatures in the area that comes in contact with the oil and are typically hotter than the area influenced by coolant flow. During calibration, TK_M_BRRCYL1 is not taken into consideration whileTK_M_BRRCYL3, despite being a faulty thermocouple, is used. The second cylinder demonstrates the reliability of the thermal calibration. For cylinder three, the model remains within the calibration range with a maximum error of less than 10% for the 2500rpm case.

The temperatures trends inside the cylinder block for the 7500-rpm case provide an understanding of the temperature distribution. The maximum temperature is in the interbore area of cylinder two, reaching 172.5°C. Cylinder one has lower temperature, as explained earlier, while the third cylinder on the right-hand side of the graph exhibits a higher overall temperature.
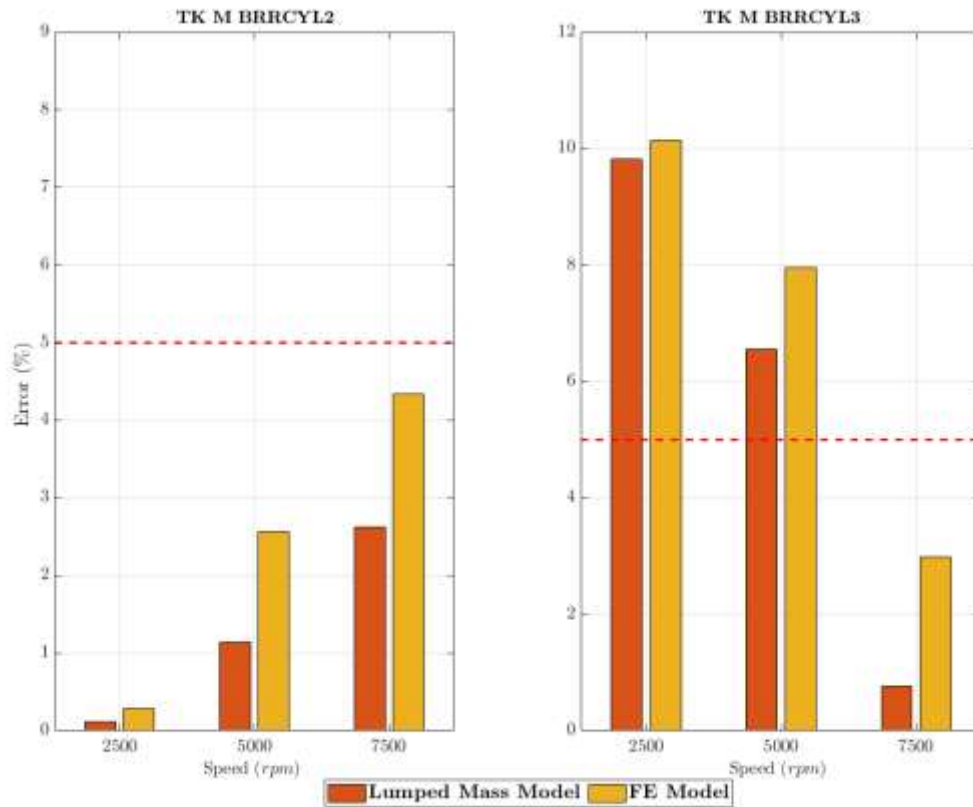
Figure 75: Block RH - Bottom thermocouple, The bottom thermocouples for the first cylinder is not considered in the error analysis.

Figure 76 displays the results of the intake valve seat for the right bank of the engine. These valve seats are calibrated using only the nearest node to the engine thermocouple. In the lumped mass model, the valve part is challenging to calibrate due to the single heat transfer area, which is connected to the head volume coolant jacket. Based on this, the calibration strategy aims to target the hottest temperature rather than the lower ones. The lumped mass model, however, overestimates the temperatures observed in the experimental program. The worst-case scenario is represented by the 5000 rpm, particularly by TK_M_IVS5, TK_M_IVS7, and TK_M_IVS11 (intake valve seats for cylinders three, four, and six respectively). The percentage error for these three nodes is 10-12% for the lumped mass model. The first and second cylinders show a reliable and robust trend, while for cylinder five, TK_S_IVS9, the temperature seems to match the test data. The Finite element model, as well as the lumped mass, has difficulties in being calibrated in the intake valve sitting region. The main difference is that the model underestimates the

temperature, running colder than the experimental data. The best trend is shown for lower speed cases, as confirmed by Figure 77.
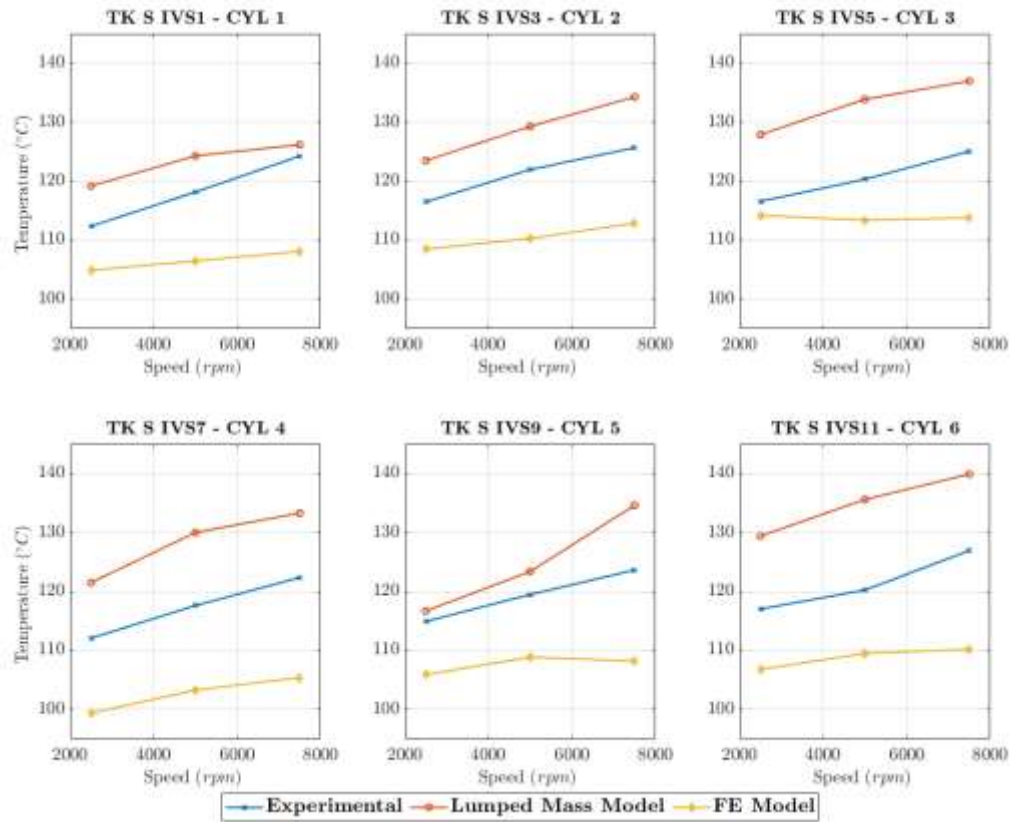
Figure 76: RH Bank – Intake valve seat temperature results.
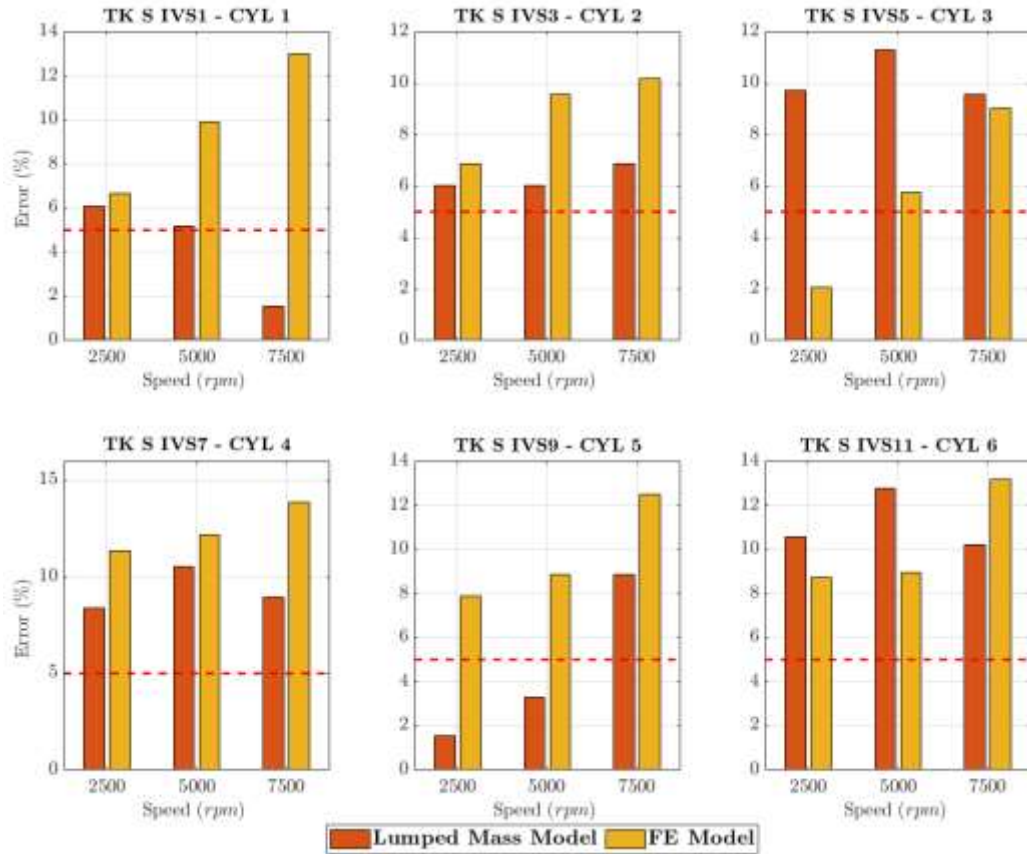
Figure 77: RH bank, Intake valves seats error.

Figure 78 presents the results for the exhaust valve seats. The lumped mass model is calibrated using two nodes in the head structure, with a focus on accurately representing the hottest part of the cylinder head. In contrast, the finite element model is calibrated using only one thermal node. In the lumped mass model, all the exhaust valve seats are well matched with the experimental data, with only a slightly difference observed in cylinder five between engine speed 2500 rpm and 5000 rpm, where the simulation runs colder than the test data. However, it matches perfectly at higher speeds. For the sixth cylinder, the model falls short of the target temperature by 5°C. In comparison, the FE model underestimates the temperature for the exhaust valve seats, similarly to what was observed for the intake valve seats.

As discussed earlier, it was noted that the finite element (FE) model possesses a fixed-size mesh, which may prove disadvantageous in certain regions of the engine geometry, such as the intake valve seat area. Additionally, it is important to consider that the FE model utilizes only a single thermal node for specific thermocouples.

Despite these considerations, the statement suggests that the FE model remains a promising candidate for further development.

The point raised underscores potential limitations in the FE model, but it also articulates the reasons for favoring it in future development efforts. The flexibility for improvements is outlined, including the prospect of conducting a mesh size study for the head region to address current limitations. Furthermore, the potential for enhancing the thermal calibration strategy by incorporating various thermal nodes is highlighted to improve accuracy. The integration of the hydraulic model in specific regions of the engine geometry is also mentioned as part of potential advancements.
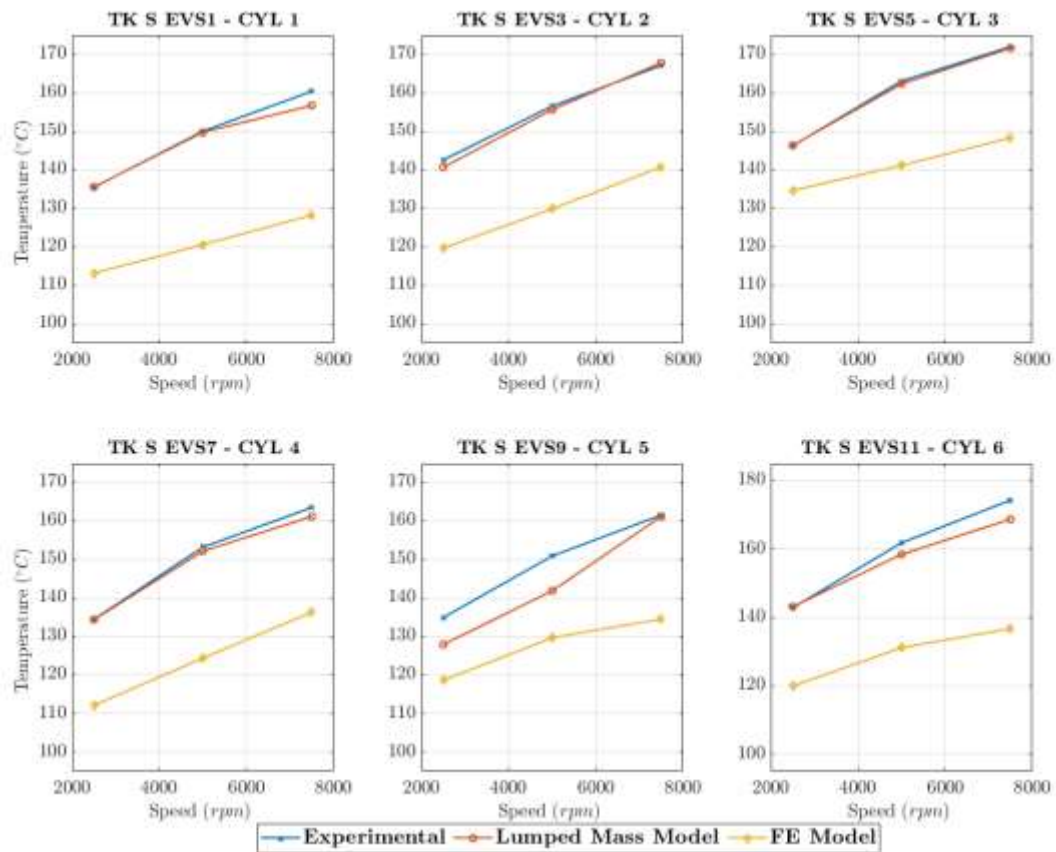
Figure 78: V6 Engine Exhaust valve seats.

In Figure 79, the percentage error for the exhaust valve seats is presented, showing how the thermal calibration matches the test data. Overall, the lumped mass model performed correctly, with the maximum error occurring in the fifth cylinder at 5000 rpm, and being ~5.5%. However, the error remains within acceptable range

establish at the beginning of the calibration process. On the other hand, the Finite element model struggles to predict accurately within the 5% error range and even the 10% range, indicating that it may not be as accurate as the lumped mass model for this component.
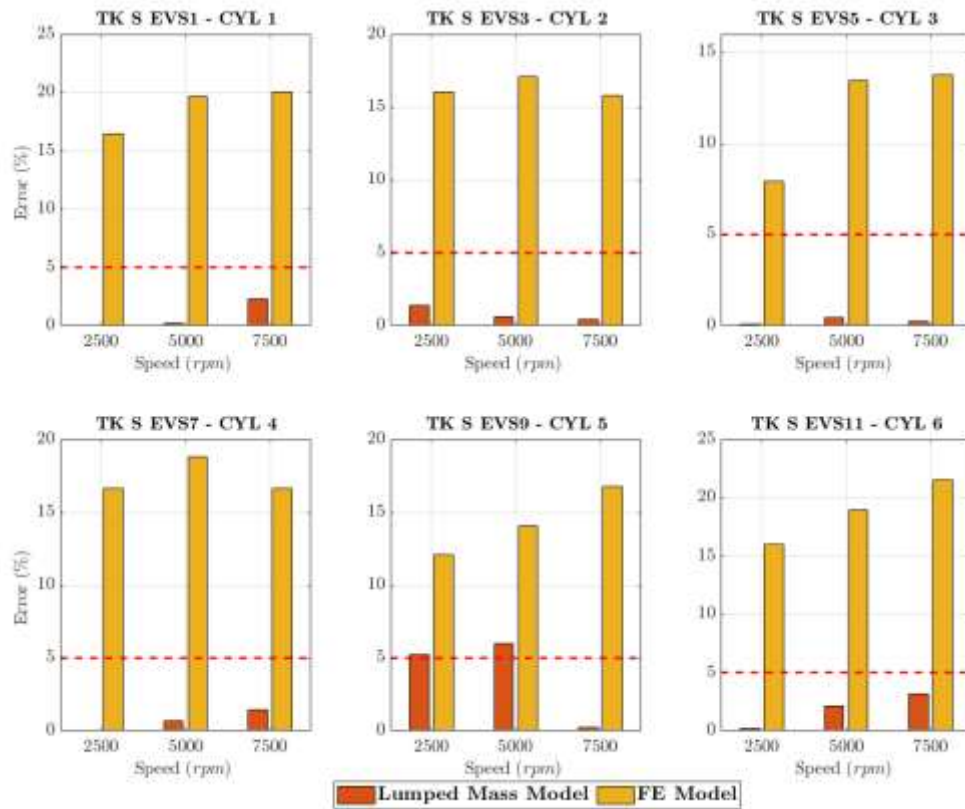
Figure 79: Exhaust valve seat error results.

Figure 80 represents the exhaust valve bridge temperature results. The lumped mass model calibration is carried out considering two nodes located in the head structure, which belong to the exhaust valves. Although the calibration is successful, it should be noted that the accuracy of the temperature match varies across cylinders. Specifically, cylinders one, two, and five do not show an accurate temperature match in the model.
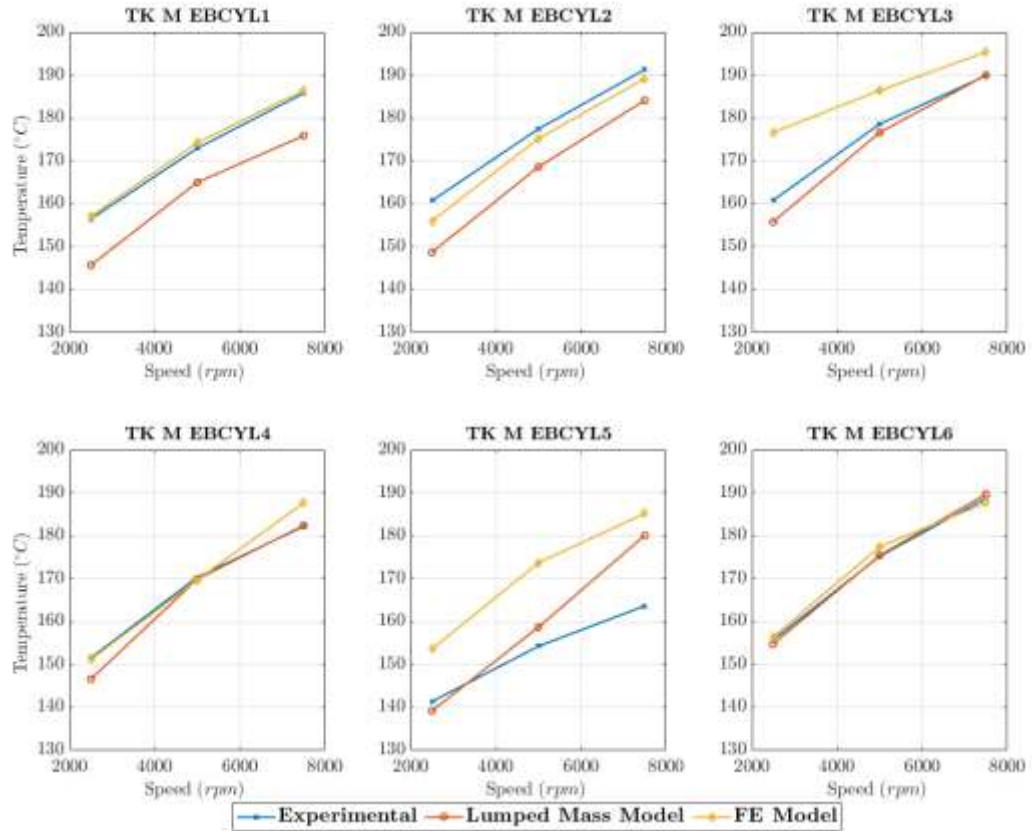
Figure 80: V6 engine – Exhaust bridge valve temperature results.

Figure 81 shows that the lumped mass model's estimation for the exhaust valve bridge temperature in cylinder five has an error of more than 5% indicating that it may not be reliable for this cylinder. The finite element model, which uses a single node, seems to provide more accurate temperature estimations. The exhaust valve bridge temperature is a critical factor in engine development and thermal management, making the reliability of its estimation essential. However, for cylinder five neither the lumped mass model nor the finite element model appears to be reliable.
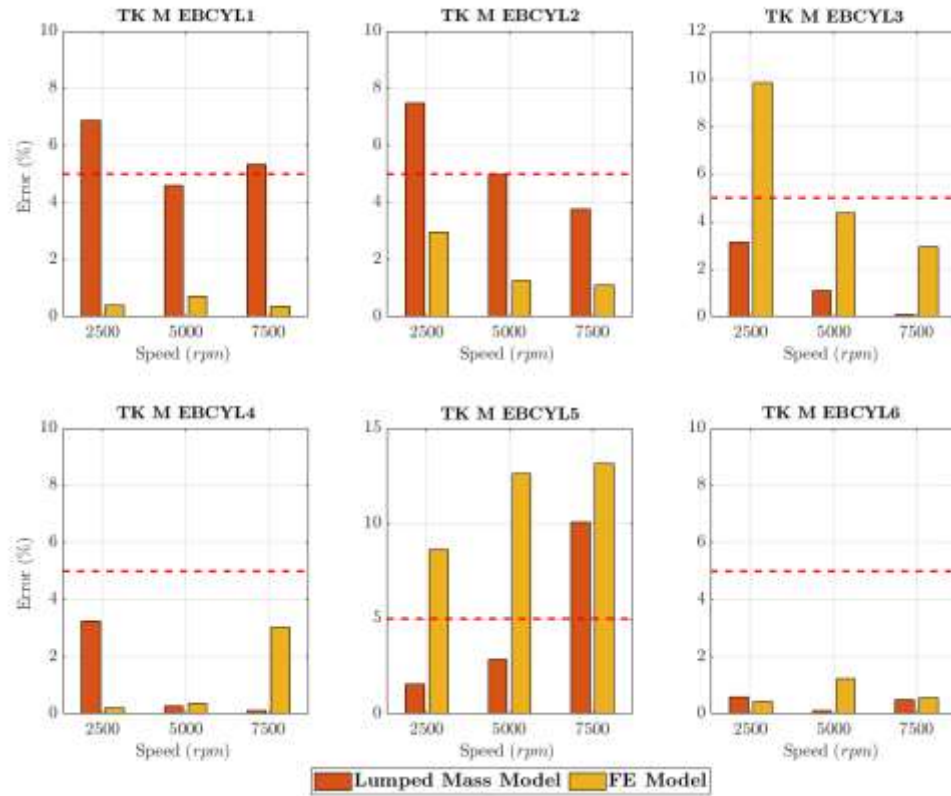
Figure 81: V6 engine – exhaust valve bridge temperature results. Cylinder six exhaust brigde zone have the maximum temperature as ~203°C.
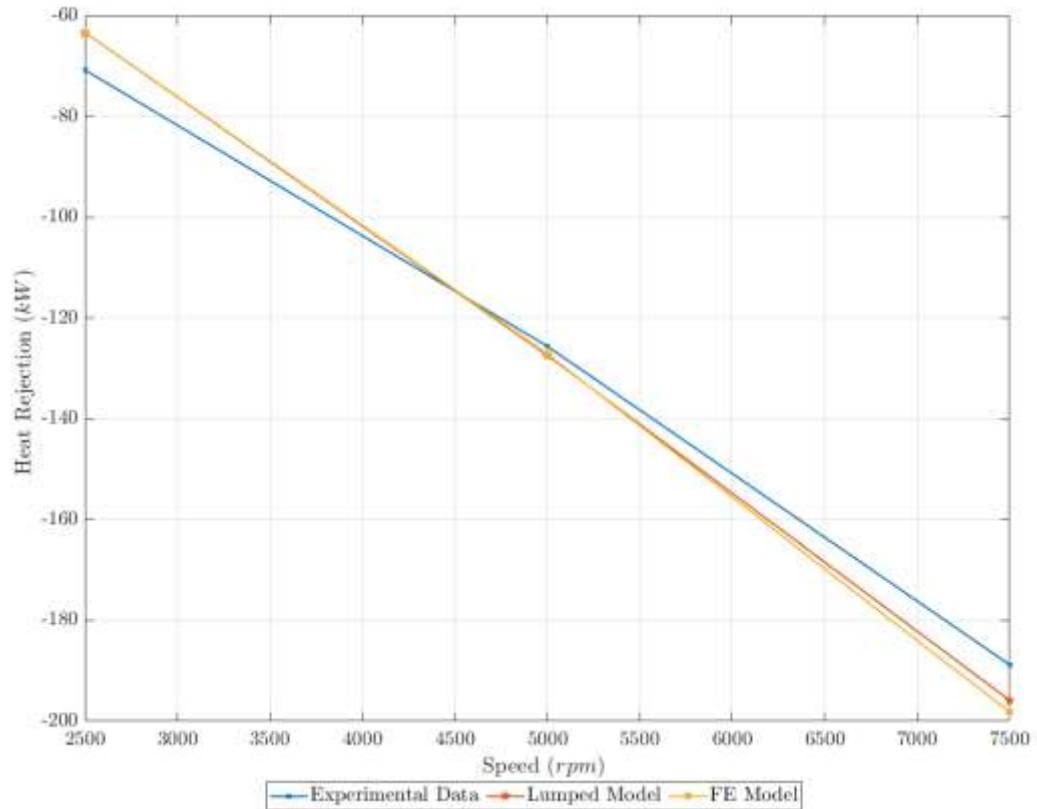
Figure 82: Engine coolant heat rejection.

Figure 82 illustrates the coolant heat rejection for the engine, which is not a target parameter for the thermal calibration, but it is considered in the thermal analysis to verify if the engine model is simulating the appropriate heat transfer to coolant. From the results it can be seen that the calibration strategy gives an overall suitable result in terms of heat rejection by the engine. Table 9 shows the error between the experimental data and the simulation results for the coolant heat rejection. At low load condition, as seen from Figure 82, the two models are underestimating the coolant heat rejection and the range of the error also indicates a warning but it still considerable acceptable because the two models at higher engine load conditions are capable to estimate with a lower error the coolant heat rejection.

	2500 [rpm]	**5000 [rpm]**	**7500 [rpm]**
Lumped Mass Model	10.52%	1.43%	3.72%
FE Model	9.89%	1.23%	4.96%

Figure 83 presents the results of the lumped mass model optimization in terms of the total error output function for three cases. The objective of this optimization is to minimize the total error by exploring a total of 1201 design cases. From the 800th case onwards, all three cases converged to the final error value. This number of design cases is deemed sufficient to ensure convergence and accurate optimization results.
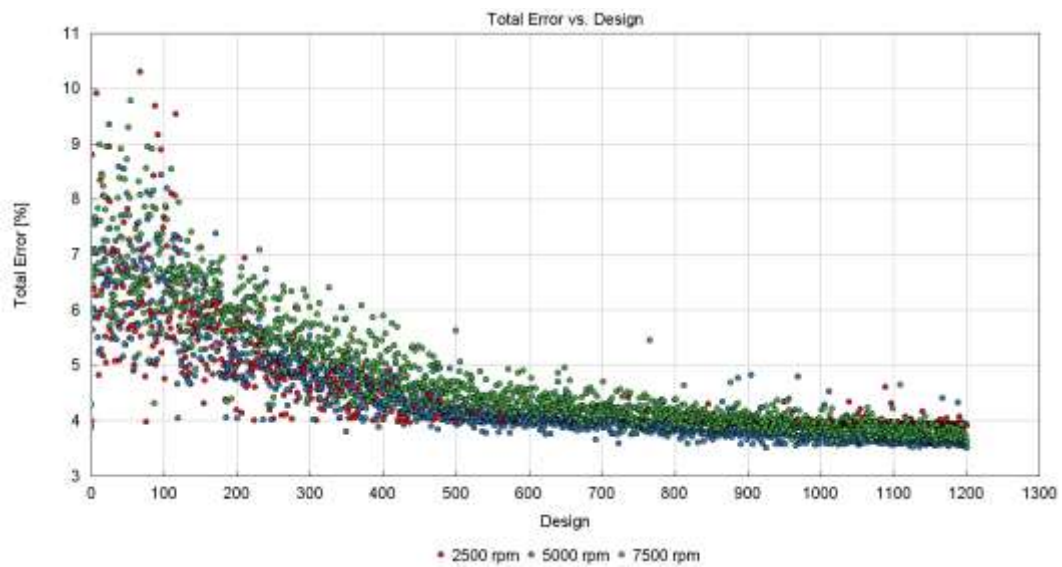
Figure 83: Lumped mass model Total error output.

Figure 84 displays the relationship between the total error and the factors for each cylinder in each case. For the engine 2500 rpm case, the block multiplier has the greatest impact on the total error, particularly for cylinder 1,4, and 6. At 5000 rpm, all factors have similar effects on the total error, except for cylinder 5 which has a value less than 0.04. At 7500 rpm, the HTC head multiplier has a more significant impact compared to the block multipliers.

137
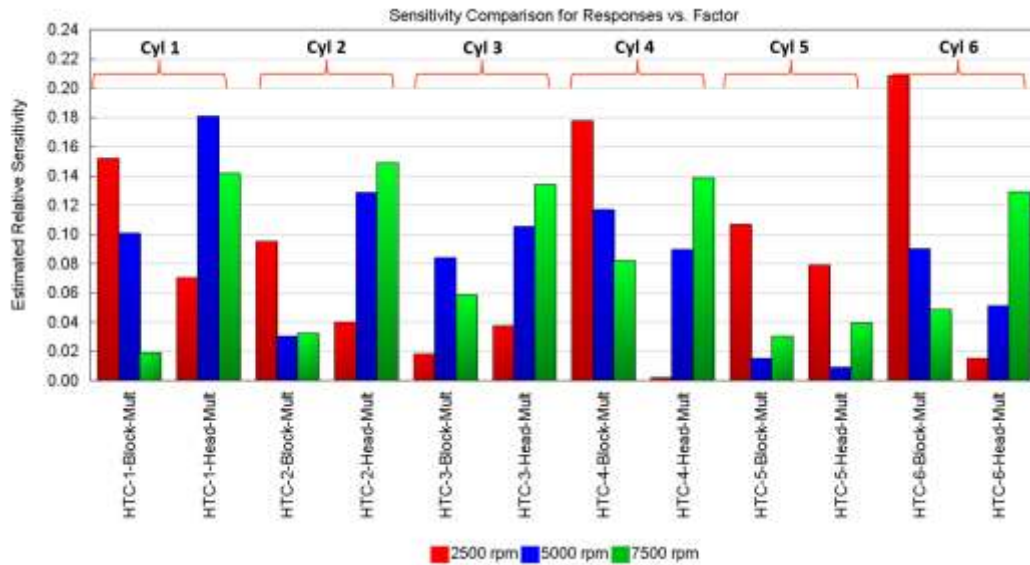
Figure 84: Lumped Mass Model. Estimated relative sensitivity – Responses vs Factor.

Figure 85 shows the total error output for the FE model. The total error output is calculated from Equation 18 and considers all the single errors for each thermocouple used for the calibration. This means that the optimisation is minimising the sum of all the single errors. For the FE model, as discussed previously, there are some parts of the engine model, such as the exhaust and intake valve seats, that have a higher error value compared to, for example, the cylinder block zone. This has a direct impact on the optimisation and of course on the results. The graph shows that at higher load conditions the error is higher than the case at lower load conditions.
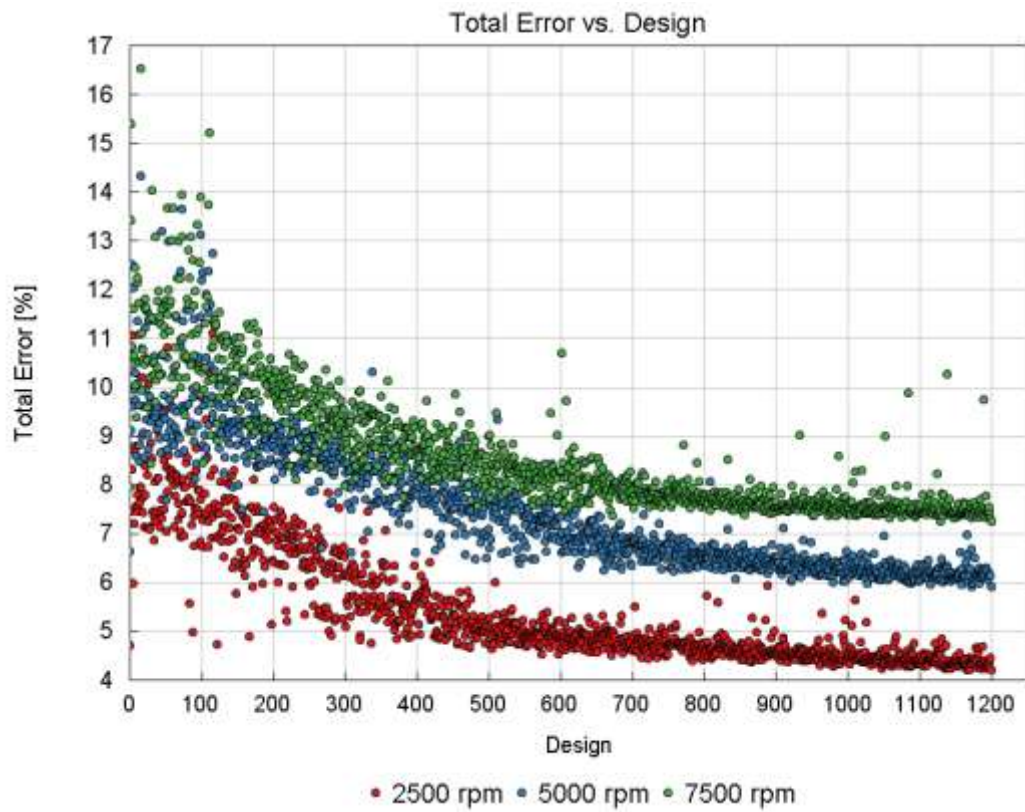
Figure 85: FE Model Total Error.

As shown in Table 10, the difference between the two cases is 3.04%. The case at 2500 rpm is below the 5% range and the case at 5000 rpm is slightly over 5%. The sensitivity analysis conducted and displayed in Figure 86 shows that head multipliers are more sensitive compared to the block multipliers. The left bank from exhibits a more sensitive factors at 5000 rpm compared to the right bank.
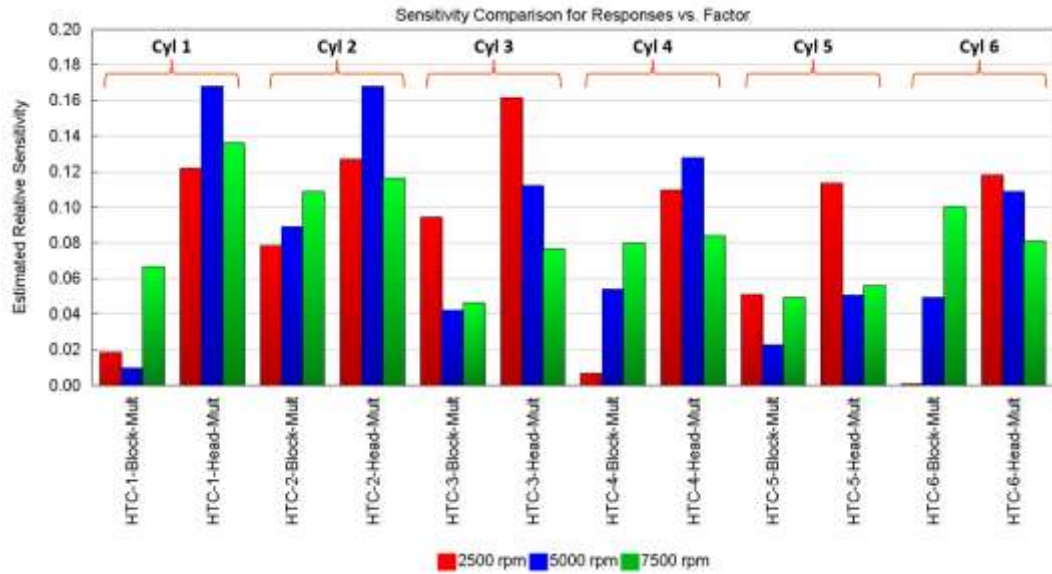
Figure 86: FE model, sensitivity comparison for Response versus factors.

This analysis also reveals how the current models can be implemented in the future. The lumped mass and the FE model have the potential for further implementation. The work could be done in the head area, considering the complexity of the geometry and the obtained results. It will also be possible to conduct a more extensive optimisation for future work considering a more implemented calibration methodology. This work aims to discover and implement a first robust modelling methodology and highlight the possible implementation solutions. Table 10 shows the final total error output comparing the two methodologies applied to the engine thermal 1D simulation model. The lumped mass model enters in the 5% error range set at the beginning as a parameter to consider the model fully validated. The FE model at lower load conditions can be considered fully calibrated and between 5000 and 7500 rpm enters in the range between 5- 8% of the total error that, as explained before the model can be considered calibrated.

Table 10: Calibration total output error, Equation 17.

	2500 [rpm]	5000 [rpm]	7500 [rpm]
Lumped Mass Model	3.9%	3.51%	3.61%
FE Model	4.18%	5.90%	7.22%

4.9 Heat Transfer Multiplier Analysis

After validating the thermal calibration strategy, a more detailed analysis of the heat transfer multipliers calculated during the optimization process is conducted. Figure 87 and Figure 88 illustrate the calculated multipliers and a trend can be observed from the low speed to the high-speed case for both thermal models. In addition, the block multipliers are generally larger than those for the cylinder head since the portion of the coolant volume connected to the heat transfer area is lower for the head and a higher multiplier is needed to achieve the target temperature. This trend is also observed in the sensitivity analysis, where the block multipliers were more affected in lower cases. A "high" multiplier value is not desirable for simulation model and based on the lumped mass model experience, a value less than 10 is acceptable, given the geometry's complexity. The head multipliers show suitable results, except for cylinder five, where the intake valve seats are not aligned with the test data (but always within a maximum error of 10% in each case).
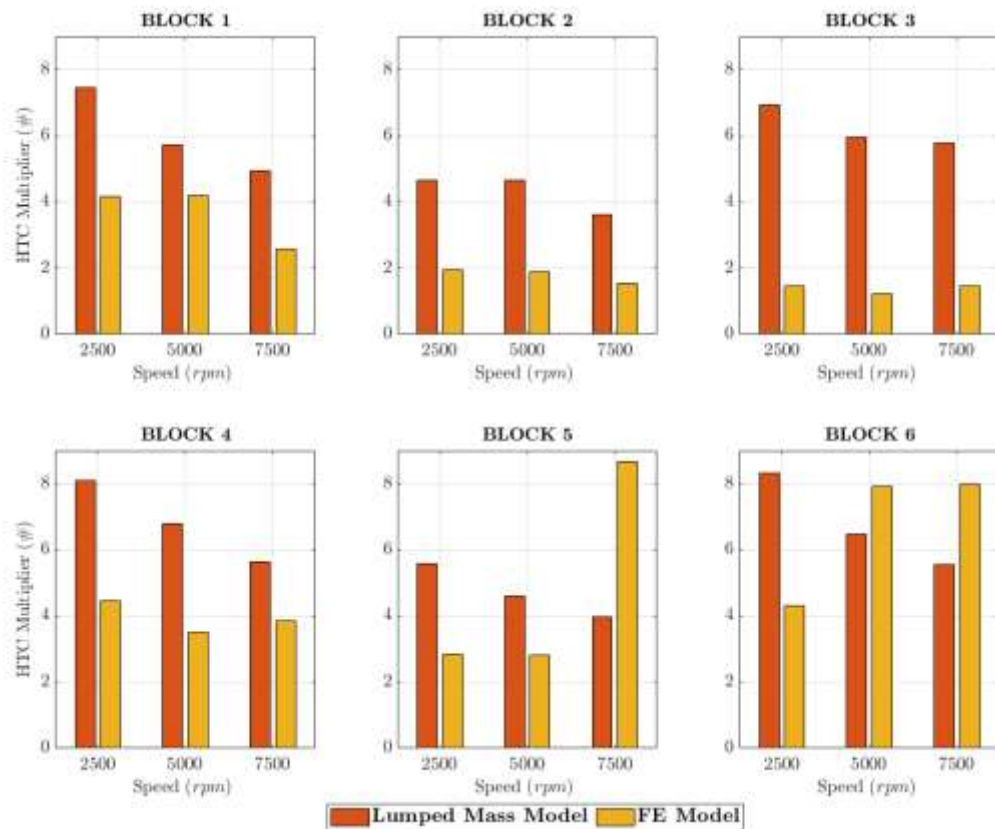
Figure 87: Calculated block heat transfer multipliers.
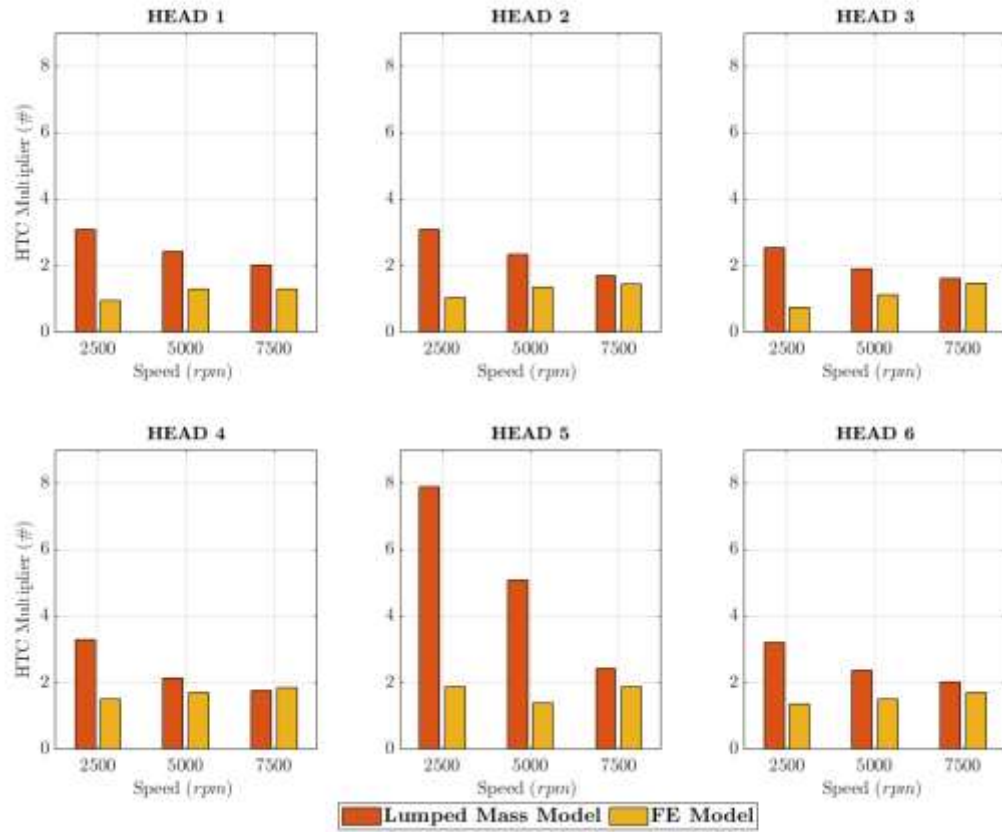
Figure 88:Calculated head heat transfer multipliers.

Figure 89 and Figure 90 show the heat transfer coefficient for the block and head coolant-jacket parts calculated without the multiplier. These coefficients are calculated with the Colburn analogy.
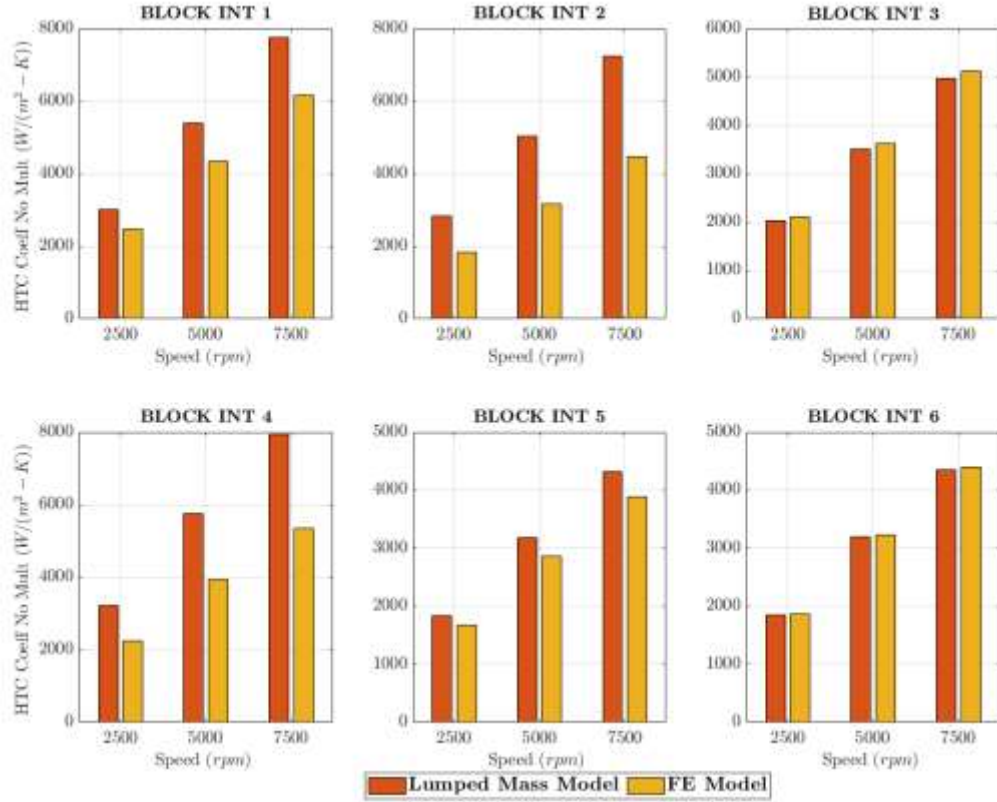
Figure 89: Block heat transfer coefficient without multiplier calculated.
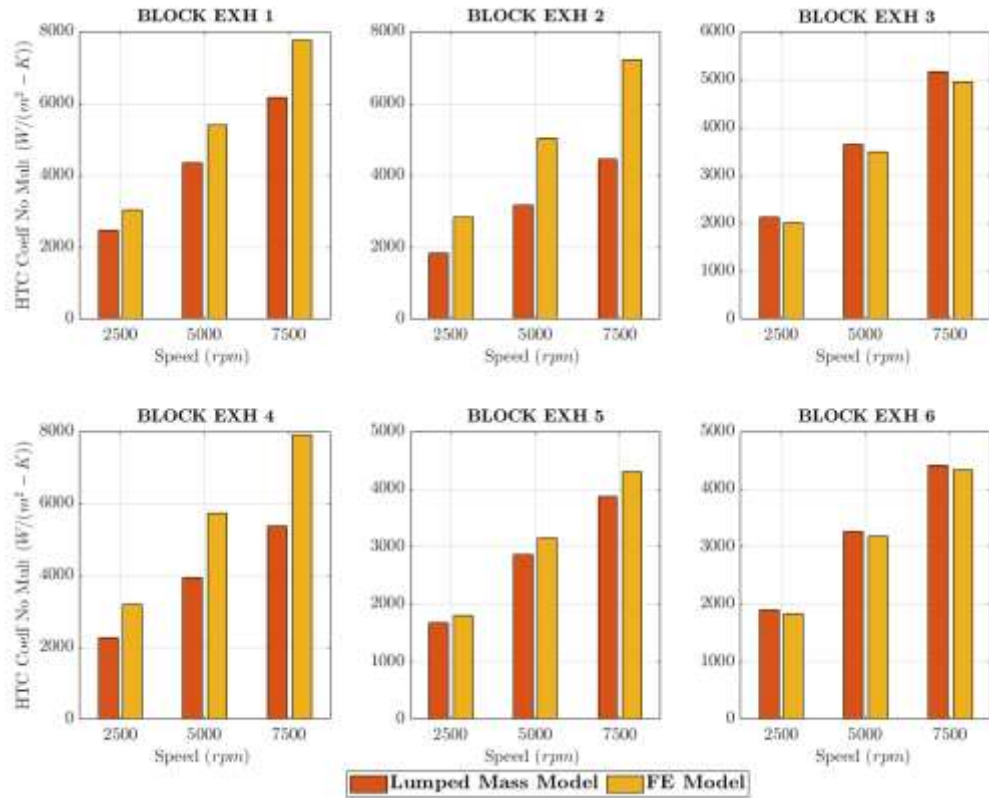
Figure 90: Block exhaust side heat transfer coefficient without multipliers.

143
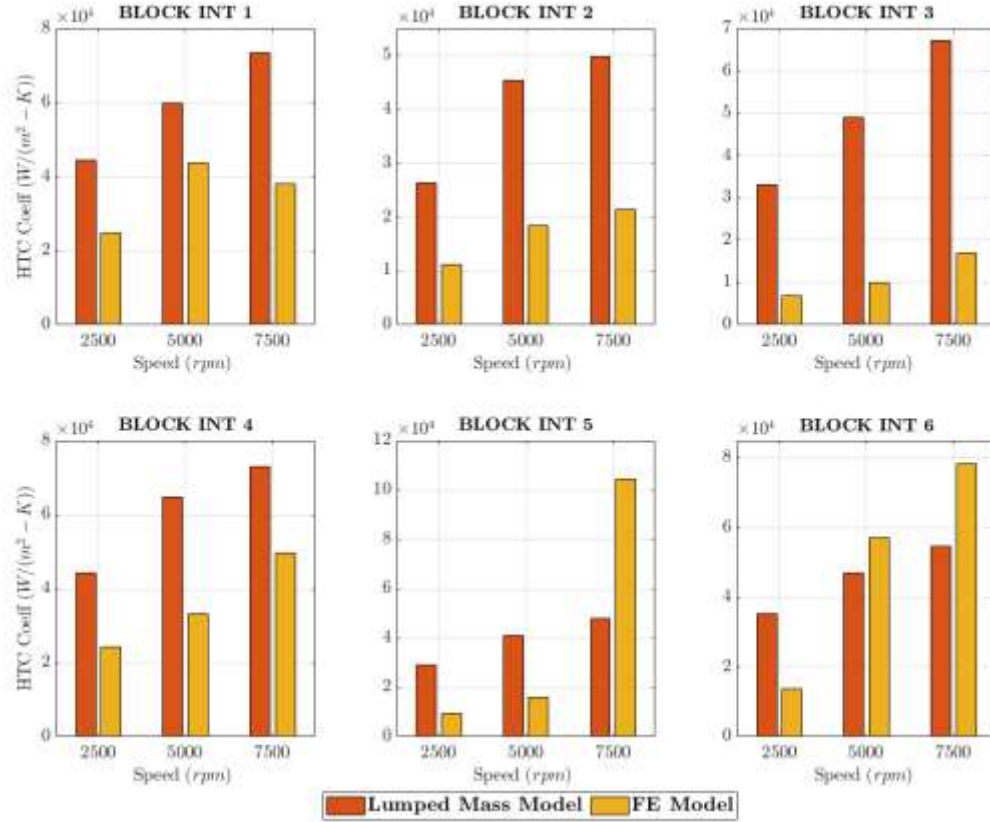
Figure 91: Block heat transfer coefficient with multiplier calculated.
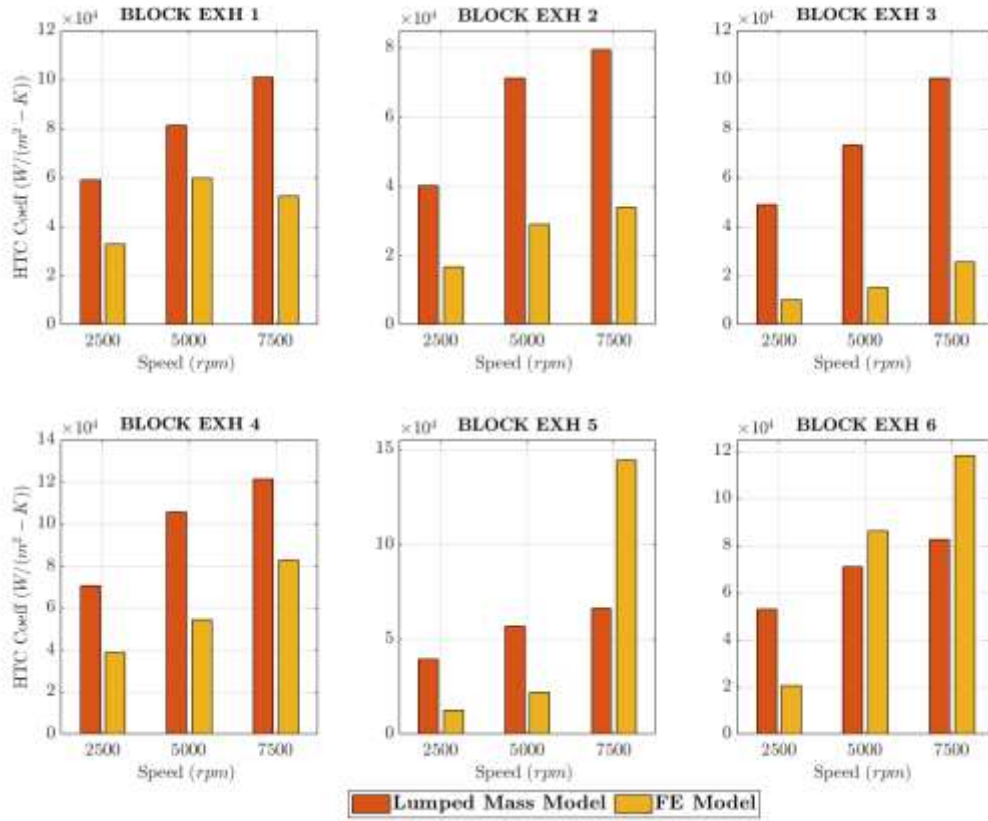
Figure 92: Block exhaust side heat transfer coefficient.

144

Figure 91 and Figure 92 illustrate the block heat coefficient with the multiplier, which is a key parameter in the engine thermal model. It is important to note that the software also calculates additional enhancement factors for each port based on the ratio of the characteristic length to the port reference diameter. However, these factors are not included in the "Reference HTC, without multiplier" variable, which is shown in Figure 89. For pipes, the heat transfer multiplier is simply the difference between the reference and calculated heat transfer coefficient.

To validate the accuracy of the 1D model, a comparison between the heat transfer coefficient calculated with the 1D model and the results of a 3D CFD simulation is also made.

The CFD simulation results will refer to a conjugate heat transfer analysis conducted by an external research centre, commissioned by the engine manufacture. Quality assurances were integral during the simulation phase reviewing initial and boundary condition with empirical and real world measurement data and validated against industrial standard.

Figure 93 shows the heat transfer coefficient results for the 7500 rpm case from the 3D CFD simulation, using the same engine geometry as used in the 1D models. The results reveal that the fourth cylinder in the intake zone has the highest heat transfer coefficient from both the 1D model and the CFD simulation. This is due to the coolant flow impacting the cylinder at a certain velocity to extract as much heat as possible. In addition, the CFD results indicate that the cylinder six has the lowest heat transfer coefficient.
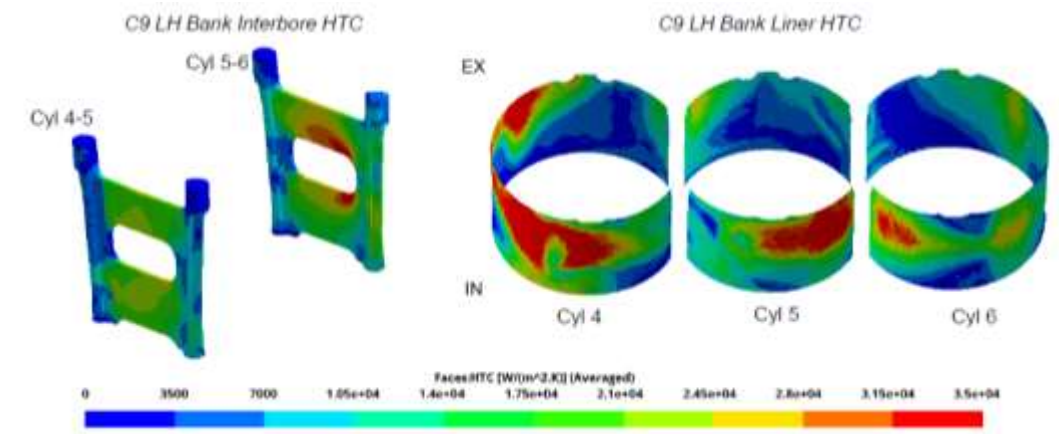
Figure 93: Heat transfer coefficient for 7500 rpm case obtained from 3D CFD simulation.

Generally, the intake side of the engine has a higher heat transfer coefficient than the exhaust side, as the 1D model illustrates in Figure 92. The trend is clear and the intake side of each block has a lower coefficient than the exhaust side.

The cylinder head analysis also provides valuable insights, as shown in Figure 94 which displays the heat transfer coefficient without the multiplier. Interestingly, a consistent trend is observed across all cylinders due to the uniform volume considered for the head in the simulation model. Figure 95 depicts the head heat transfer coefficient multipliers. Similarly, to the results without the multiplier, the graph displays a distinctive pattern. Notably, cylinder five, which operates at a lower temperature, exhibits a higher heat transfer coefficient, indicating more heat extraction from the region of the engine. As with the block analysis, a comparison with CFD results have also been conducted.
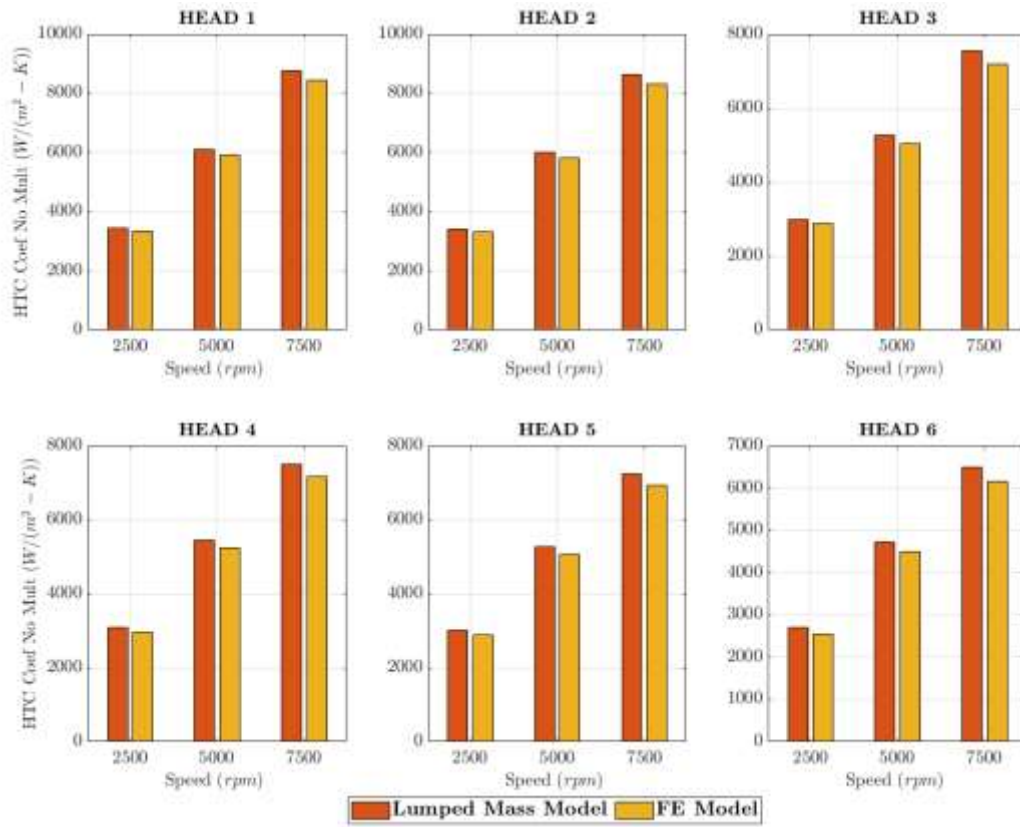
Figure 94: Head heat transfer coefficient without multiplier calculated.
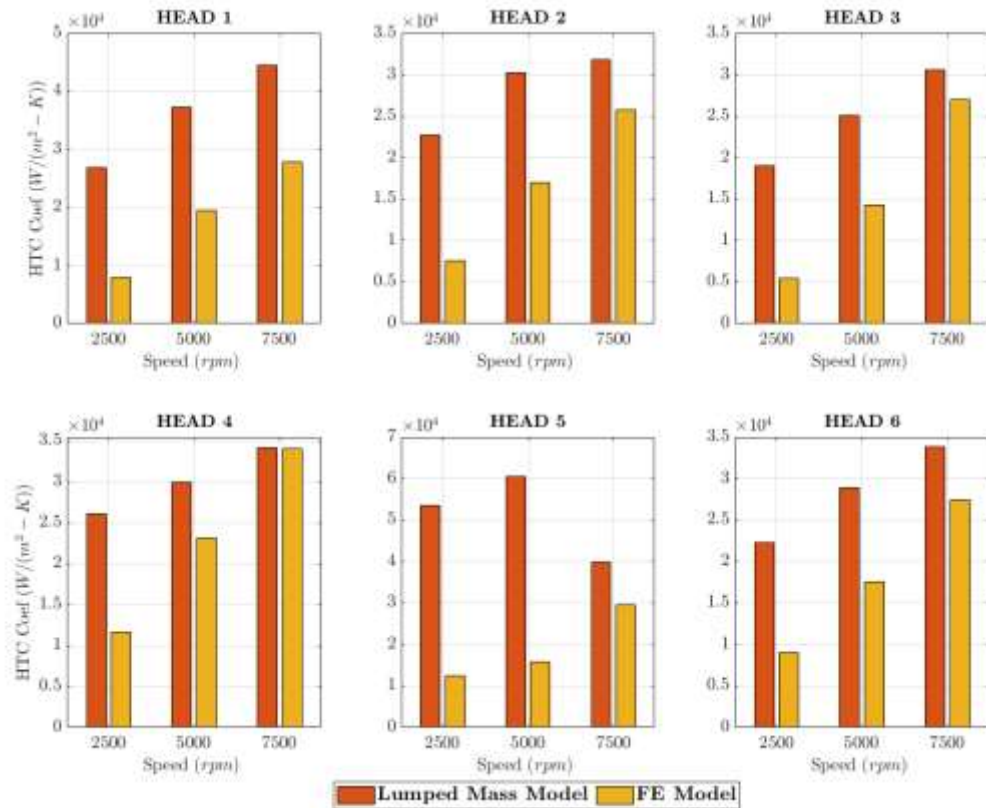
Figure 95: Head heat transfer coefficient with multiplier calculated.

147
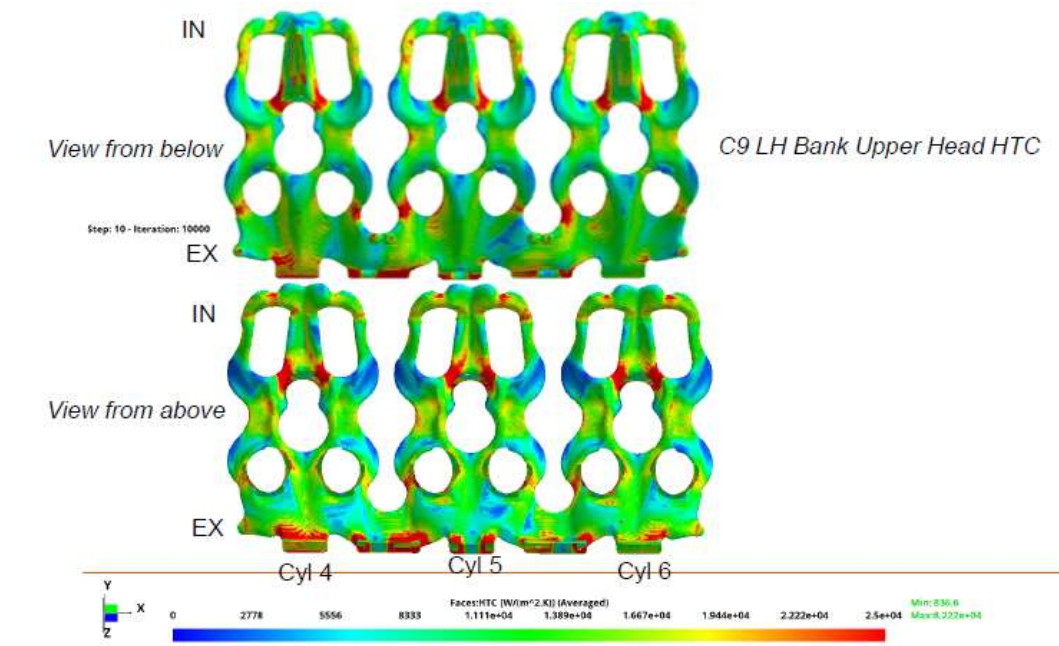
Figure 96: Cylinder head heat transfer results from CFD analysis.

Figure 96 displays the results obtained from the CFD analysis. The primary objective of this comparison is to evaluate whether the range of results obtained from the 1D model is equivalent to that of the CFD. The CFD analysis demonstrates that the maximum value of the heat transfer coefficient is 82220 W/m^{2}K, with cylinder five having the highest value. In comparison, the 1D simulation results for the left bank, at the same engine load condition at 7500 rpm, shows cylinder five having a value in the range of 80000 W/m^{2}K. These heat transfer coefficient values can be explained by a very high flow rate in a thin metal region around the exhaust valve bridge with a high temperature gradient and limited area. Unfortunately, CFD results are not available for the right bank, so a direct comparison is not possible.

In conclusion, the 1D simulation model has been shown to be reliable for calculating the heat transfer coefficients for the block and the cylinder head. The values obtained from the model are robust, although it should be noted that they are based on certain assumptions and the discretization of the volume flow from the 3D CAD. The heat transfer coefficients can be useful in the engine development phase to gain an initial understanding of the heat rejection from the block and head.

4.9.1 First Order Correlation

After completing the analysis on the heat transfer multipliers calculated in the thermal calibration using the Design Optimizer, the next step is to calculate the values for complete operating speed range of the engine. This range sweeps from 1000 rpm to 8000 rpm with a 500 rpm increment, giving a total of 15 cases. The calculation of the heat transfer coefficient multiplier is completed using two approaches: the first order correlation method and the second order correlation method. Figure 97 and Figure 98 show respectively the results of the two correlations.

During the analysis of the HTC multipliers, a clear trend was observed in the results, as seen in the figures. For cylinders one, four, five and six, the correlations match the data. However, for cylinders two and three there is room for improvement in the fit, although the difference in the actual value is relatively small. The cylinder head results, showed in Figure 98, displays a better trend for all six cylinders.
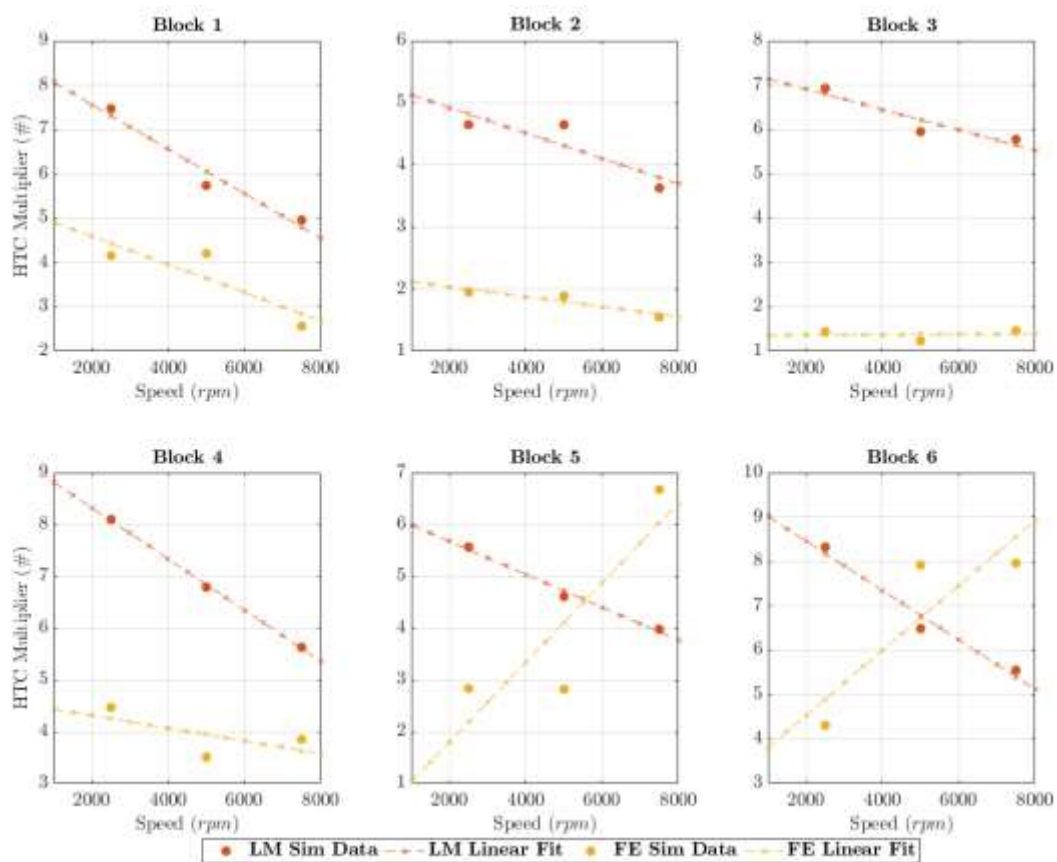
Figure 97: Block HTC multiplier – First order correlation.
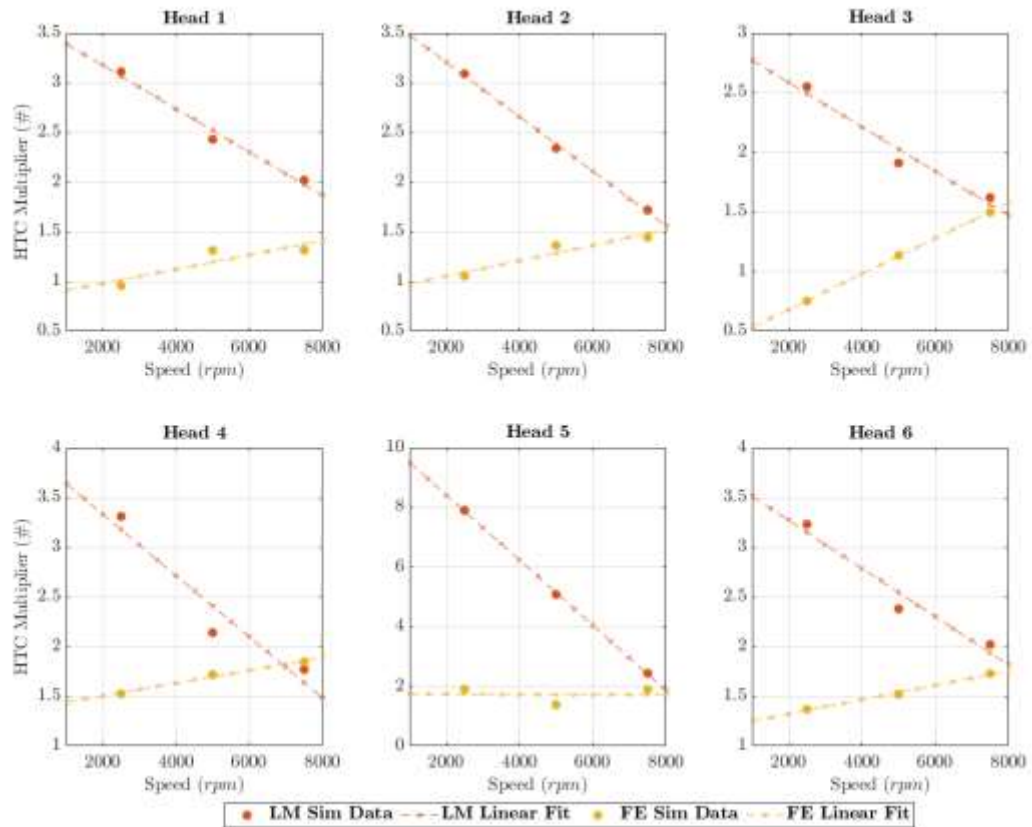
Figure 98: Head HTC multiplier – First order correlation.

4.9.2 Second Order Correlation

The methodology for calculating the heat transfer multipliers continues with a second order correlation calculation. The calibration methodology is still in early stages of development. Although only three points will always give a fitted curve, this allows a future fitting method to calculate more engine point results. In the following work it is also shown a relative change in heat transfer multiplier and how the thermal results would be sensitive.

The decision was driven mainly by the cylinder block multiplier. Figure 99 shows the block HTC Multiplier results. The second order correlation shows a better match and trend prediction in the block, but for example in case of cylinder two, the fitting curve is concave whereas the other cylinders show a convex curve. This concave curve is due to the two low-speed cases being almost equal, but for the first order, the trend was different. In general, for the other cylinders, the HTC multipliers calculated from the first and second correlation show no significant difference. The

results are shown in Figure 99 and Figure 100. For the cylinder head, the fitting curves do not show any trends.
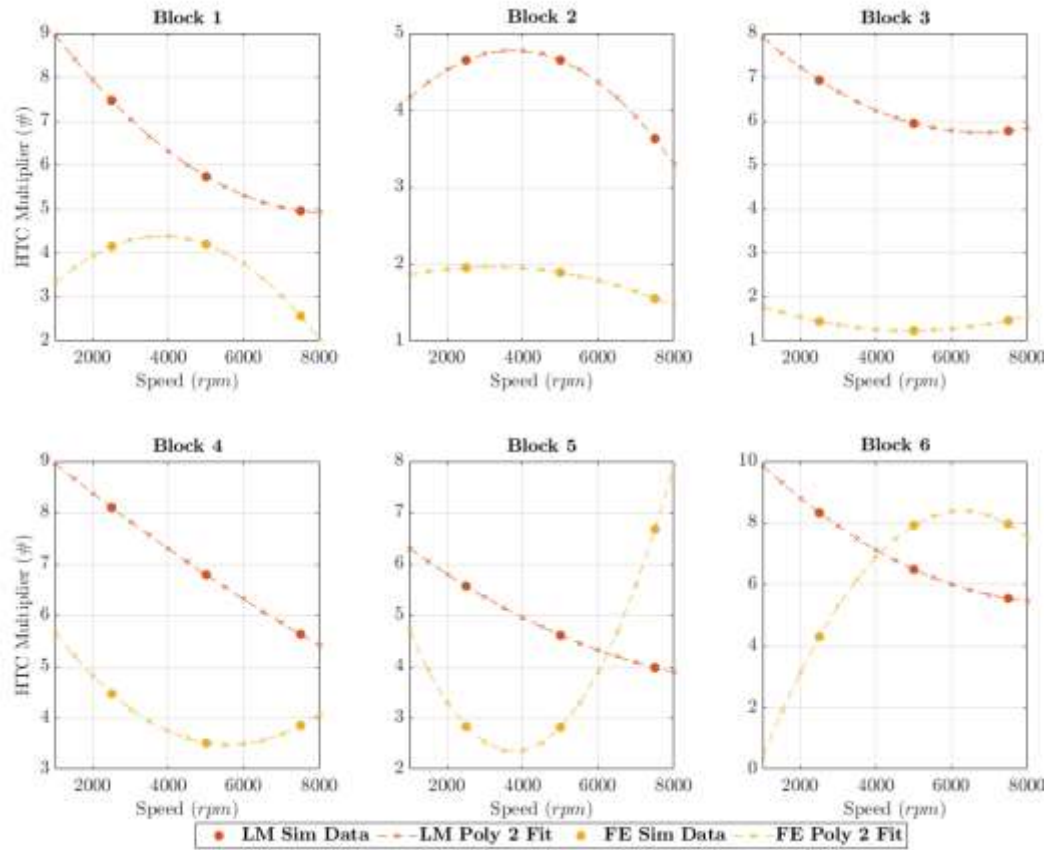
Figure 99: Block HTC multiplier. Second order correletion.
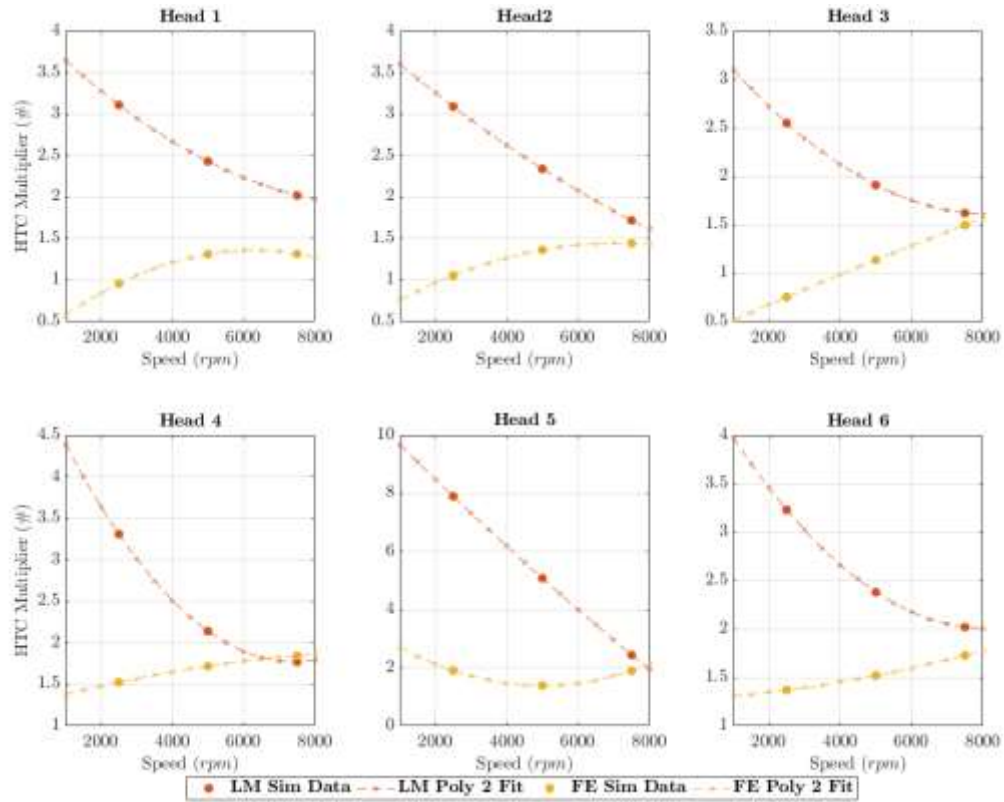
Figure 100: Head HTC multiplier. Second order correlation.

When analysing the calculated values, it is not expected to have such an impact during the engine sweep simulation as the values calculated from both correlations did not differ significantly. The engine sweep simulation is done using both the calculated multiplier and the analysing data, and the best correlation methodology is selected.

4.10 Conclusion

In this chapter a thermal modelling methodology is explored. First, the two thermal models, the lumped mass thermal model and the finite element model are explained, including the main characteristics and how to properly prepare the model for thermal calibration. The calibration strategy is then discussed, and a clear methodology is explained and followed for both the lumped mass and the finite element models. A thermal survey experimental data sanity check is performed, which helped to determine the calibration strategy and the thermocouples to be used. The Design Optimizer is described, explaining how the calibration is

performed and how to optimize the various parameters considered. Finally, a discussion of the results is given with a direct comparison between the two models, where both models performed efficiently during calibration. The lumped mass model seemed to be preferable in terms of absolute error, with the finite element model being excelling at estimating the exhaust bridge temperature, which is important for the engine development. In the last part of the chapter, a heat transfer multipliers analysis is performed and a comparison between the multipliers calculated during the calibration is made. The heat transfer multipliers are used to make a first and second order correlation fitting to calculate the multiplier for the engine sweep points.

In summary in this chapter, we embark on an exploration of a thermal modeling methodology tailored for engines, with a particular emphasis on innovation and novel approaches. The key highlights of novelty and distinct contributions are summarized below:

- Innovative Thermal Models

Introduction and exploration of two distinct thermal models—the lumped mass thermal model and the finite element model.

Comprehensive detailing of the unique characteristics of each model, showcasing a departure from conventional approaches.

- Calibration Strategy Advancements:

Proposing and implementing an advanced calibration strategy that considers a thermal survey of experimental data.

Application of a detailed sanity check on experimental data to guide the calibration process, demonstrating a novel and meticulous approach.

- Integration of Thermocouples:

Selection and integration of thermocouples for calibration, emphasizing their strategic placement for enhanced accuracy.

Novel use of thermocouples in optimizing the calibration process, contributing to the overall robustness of the methodology.

- Design Optimizer Application:

Utilization of the Design Optimizer for parameter optimization in the calibration process, showcasing a cutting-edge and efficient approach to model refinement.

- Comparative Analysis of Models:

Thorough comparative analysis of the lumped mass and finite element models, highlighting their respective strengths and novel applications in predicting engine temperatures.

Recognition of the finite element model's excellence in estimating the exhaust valve bridge temperature as a novel insight crucial for engine development.

- Heat Transfer Multipliers Analysis:

Calculation of heat transfer multipliers for engine points through first and second-order correlation fitting, introducing a novel and rigorous methodology for obtaining accurate multipliers.

- Validation and Future Perspectives:

Successful validation of the thermal calibration methodology, reinforcing its innovation in achieving accurate temperature predictions.

Laying the groundwork for future applications, providing valuable insights into optimizing engine performance through precise and novel thermal modeling.

This chapter stands out for its innovative approach to thermal modeling, from the introduction of distinct models to the application of advanced calibration strategies. The novelty lies in the meticulous integration of experimental data, strategic use of thermocouples, and the efficient application of optimization techniques. These innovations collectively contribute to a robust and reliable thermal modeling methodology, offering a paradigm shift in understanding and predicting engine temperature distribution. The chapter not only validates the methodology but also paves the way for future advancements in engine development through cutting-edge thermal modeling techniques.

Chapter 5 - Thermal Modelling Comparison – Results

This chapter presents the thermal results of the two 1D simulation models developed using the HTC multipliers calculated from the thermal calibration. A direct comparison between the models is presented and discussed.

5.1 Summary

The structure of the chapter is described as follows:

I.   Thermal Engine – Results Comparison

- A comprehensive comparison is made between the two correlations, one of the first order and the other of the second order, used for the thermal simulation throughout the engine speed range. The analysis includes a comparison between the lumped mass and the finite element models, followed by the selection of the final choice between the two models.

II.   Thermal Engine – Final Result

- The suitability of the lumped mass model and the finite element model is assessed through a final comparison, using the second order correlation process to calculate the heat transfer multipliers. The analysis focuses on the thermal performance of the engine, and a final discussion is held on the most appropriate thermal model.

III.   Conclusion

- A description of the methodology applied and the positive aspects in the simulation results are presented. Both the lumped mass model and Finite element model have been able to predict the engine temperature with no consistent difference between the two correlations used. The lumped mass model provides a finer estimation of the temperature in the block cylinder while

the Finite element model provides an excelling estimation in the head exhaust valve bridge. Both methodologies are considered validated based on the total given error.

5.2 Thermal Engine - Results comparison

The thermal simulation of the four engine models is performed by sweeping between 1000 rpm and 8000 rpm. The four models are named as follows: "Lumped Mass Linear Model" and "Lumped Mass Pol2 Model" for lumped mass model with first and second order correlation respectively, "FE Linear Model", and" FE Pol2 Model" explained in 4.9.1and in 4.9.2 for the finite element models with first and second order correlation. In Figure 101, the right block thermal model engine speed sweep is shown and it can be observed that the simulation results exhibit a satisfactory match with the test data. The two correlations show no significant difference in the calculated multiplier values and their trends are also similar. The middle thermocouples show a slight discrepancy in lower speed cases, but in general, the results match with the test data. For the third cylinder, the simulation results exhibit a robust trend in the lower engine points, which later matches the test data for the highest engine point. Although the finite element model underestimates the middle-block cylinder temperature, as observed during the calibration process, it correctly predicts the temperature for other zones of the engine. This could be explained by the limitation of the 1D simulation model, because the thermal solver calculates the temperature using the discretisation of the engine cylinder described in 4.4 and 4.6 and for both models this discretisation does not seem suitable to estimate the right temperature. This issue can be resolved partially in the FE model in the future utilising a more refined mesh in for the cylinder.
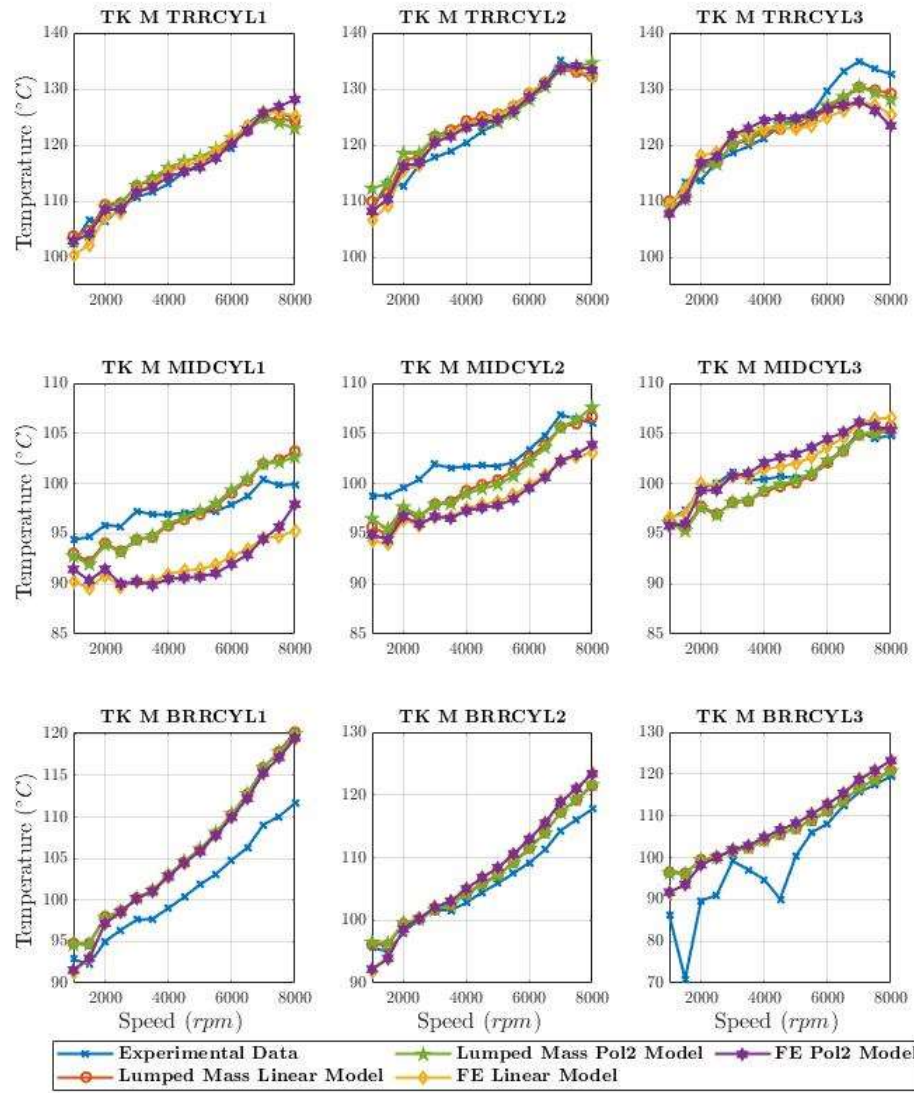
Figure 101: Right block thermal model engine sweep.

In the case of the left bank, as shown in Figure 102, the simulation results are similar to those of the right bank, but there is a noticeable increase in the temperature error in the middle thermocouples. In addition, the lower side of the cylinder, where the TK_M_BRRCYLs are placed, especially cylinder four, tends to overestimate the temperature for higher load engine points. However, there is no significant difference between the first and second order methods. Both correlation methods applied to the lumped mass and finite element show consistent results, but the second order correlation method appears to replicate the experimental trend.

157
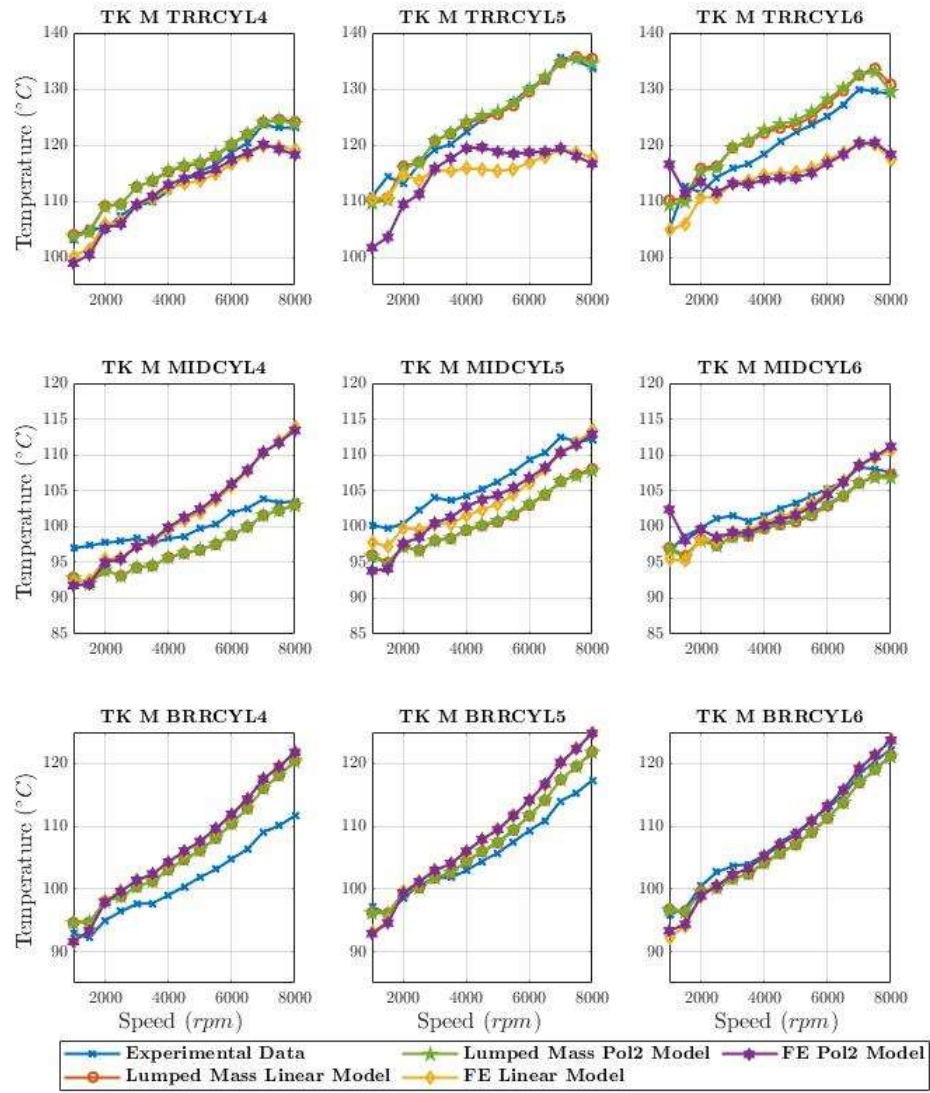
Figure 102: Left block thermal model engine sweep.

The analysis of the interbore thermocouples shown in Figure 103 reveals an adequate correlation in temperature in some areas of the engine, but discrepancies in others, as predicted during the calibration process. The temperature between cylinder one and two, on the top liner zone where the thermocouple is placed, shows an overestimation by the FE model. Both correlations overestimate the temperatures and the results are not affected by the heat transfer multiplier difference. The lumped mass model underestimates the temperature, but with a smaller difference compared to the FE model. The lumped mass matches the temperature between cylinders two and three and cylinder four and five. This means that, together with all the assumptions made in the previous chapters, the model is still able to estimate the correct temperature in an extremely important zone of the engine. For all the

considered cases, the FE model overestimates the temperature. The explanation can be that the discretization of the model is not satisfactory enough for this part of the engine block and likely with a mesh refine and a more detailed coolant volume jacket the temperature estimation can have a benefit. Overall, these results can be acceptable considering the simplification made in the model and the good prediction for the other two cylinders.
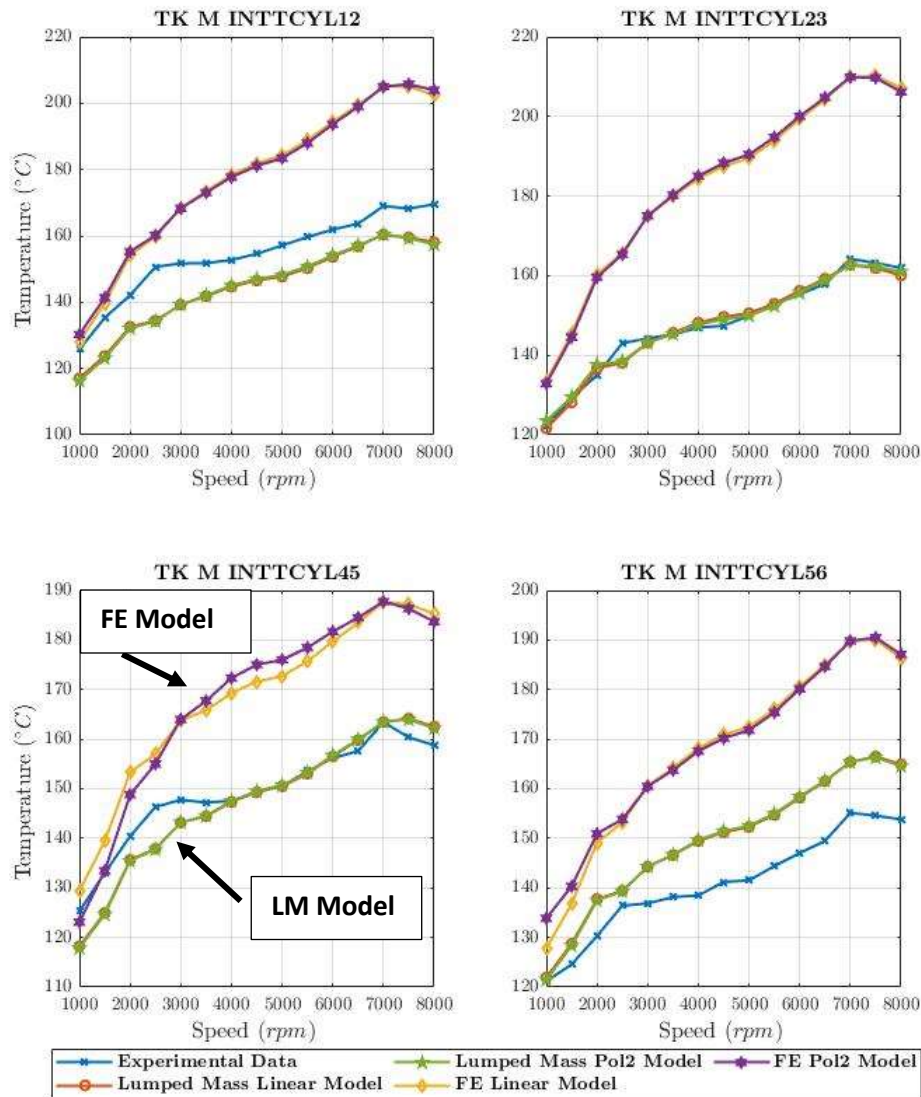
Figure 103: Interbore thermal sweep results.

The exhaust valves bridge temperatures are shown in Figure 104. There is a slight difference between the two correlation methods for cylinders three and four. The second order correlation performs better than the first order. Overall, the finite element model shows a better match across all six cylinders. It should be noted that

the calibration for this model considers a single node, whereas the lumped mass model averages between two nodes near the exhaust valve area. The exhaust bridge valve temperature is crucial for engine development because is usually representing the hottest part of the cylinder head.
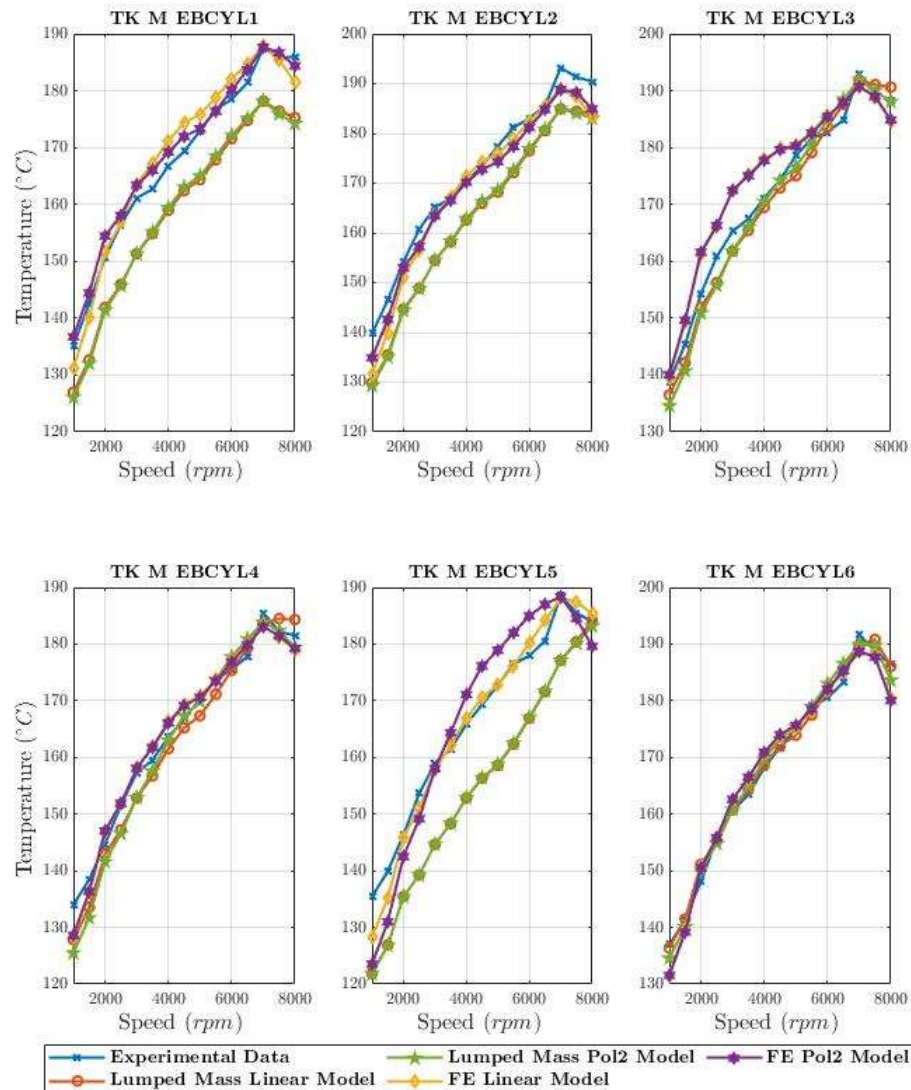
Figure 104: Exhaust valve bridge thermal sweep data.

The results for the intake valve seat are presented in Figure 105. Overall, the trend is similar between the two correlations methods both for lumped mass and FE model. The two modelling approaches showed a significant difference between the simulation results and the test data. This was also observed during the thermal calibration. Moreover, the lumped mass and the finite element model exhibit different behaviour for the intake valve temperature. The lumped mass model tends

160

to overestimate the temperature, while the finite element model tends to underestimate it. From the lumped mass perspective this can be explained by the discretisation of the head structure as seen in Figure 43. The discretisation for the cylinder structure is fixed by the software. It also explains why only one node was considered for the temperature calculation for the intake valve seat. The FE model instead tends to underestimate the temperature and this can be explained similarly for the parametrization of the engine. The size of the finite elements is set between 10 and 20 mm and the element are considered to be tetrahedral.
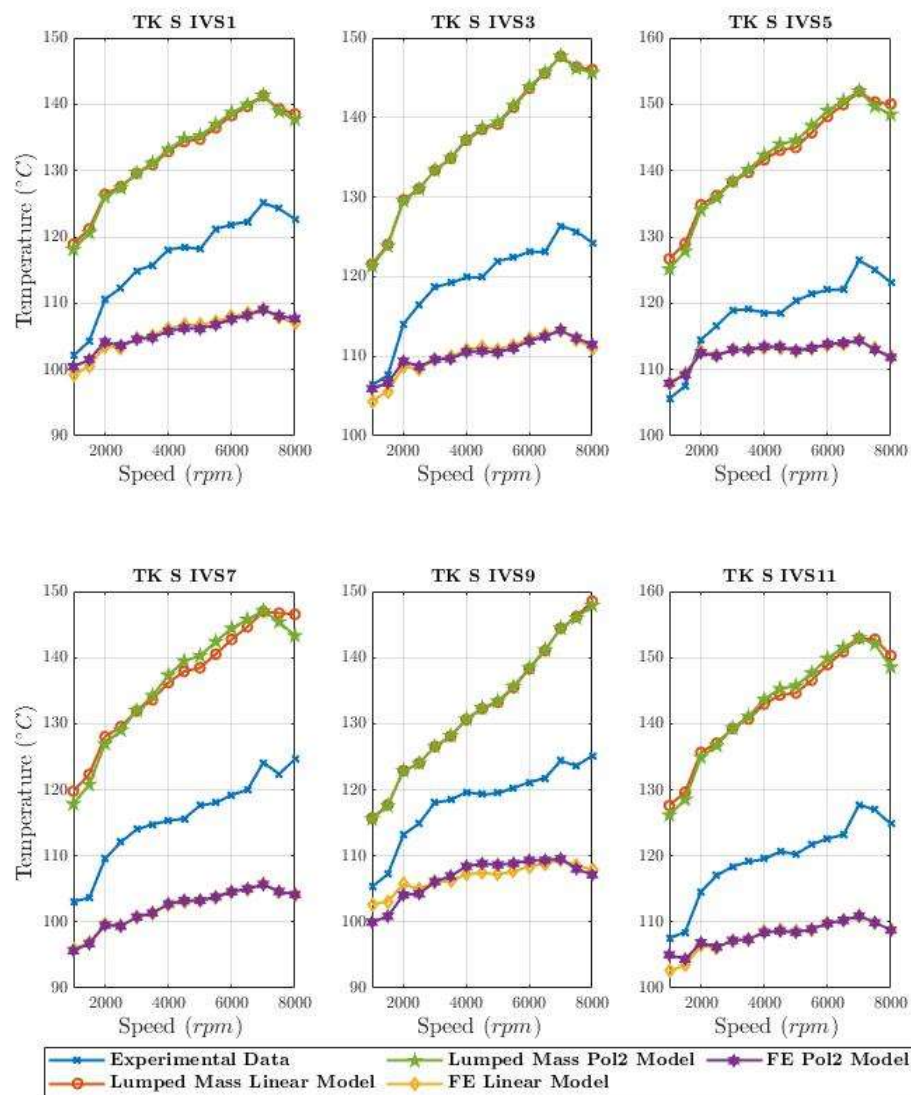
Figure 105: Intake valve seat thermal sweep results.

The exhaust valve seat simulation results, depicted in Figure 106, show good agreement for the right bank. However, the left bank results show some difficulty

in predicting higher speed cases, with a noticeable fluctuation for cylinder six between 5000 rpm and 8000 rpm. As explained before for the exhaust valve seat in the lumped mass two nodes are considered, while one node is considered for the FE model. This explains the suitable match for the lumped mass model but do not clarify the underestimation for the FE model. This can be likely described by the complexity of the geometry considered, plus the assumption made in terms of discretisation of the water jacket, and finally to the mesh resolution of the model. By implementing all of this it can be possible to make the model better estimate this important temperature.
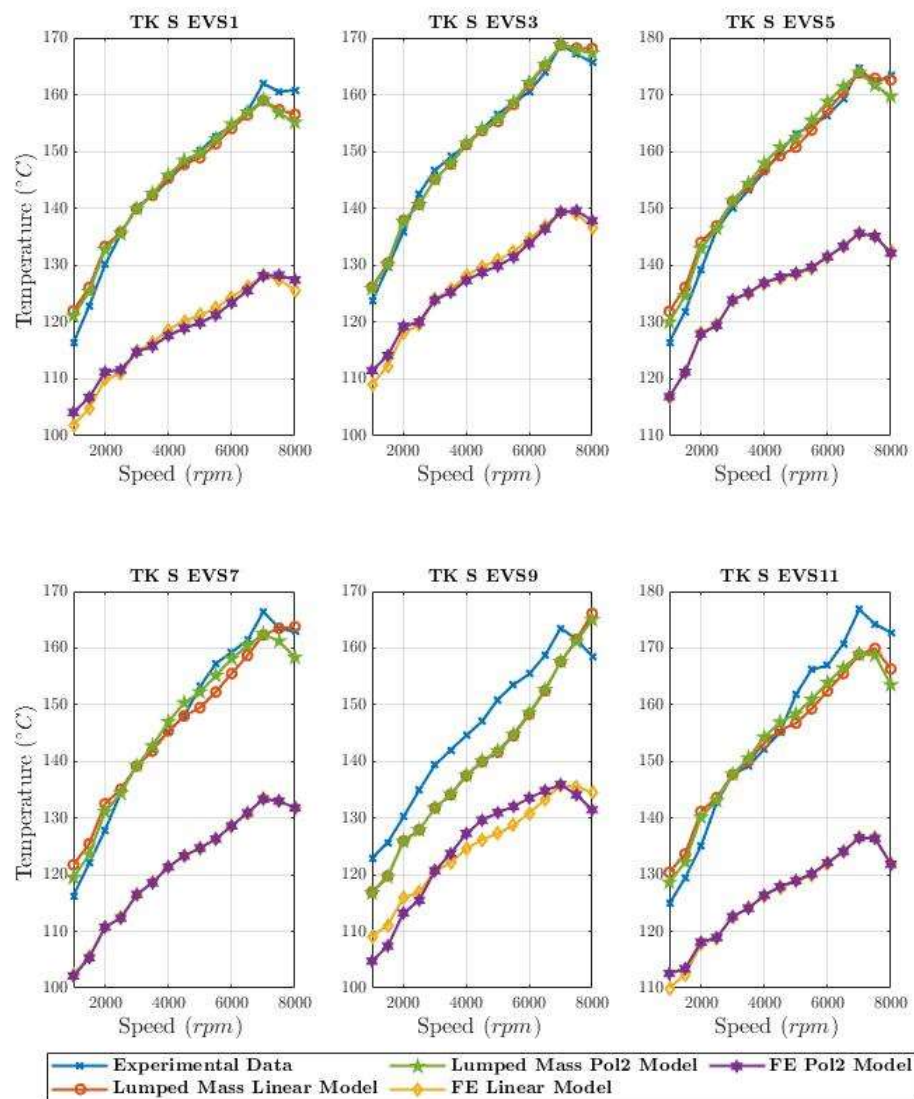
Figure 106: Exhaust valve set thermal sweep results.

5.3 Thermal Engine – Final Results

The thermal analysis is further detailed in the following results, which show how the model using the second order correlation matches the experimental temperature data. Figure 107 presents the temperature results for three thermocouples in cylinder one. Looking at the top cylinder thermocouple, a slight temperature fluctuation is observed at lower and higher engine points. However, the simulation model matches the data, with a small variation of ~3°C from 3000rpm to 5000rpm. For the middle thermocouple, the simulation model underestimates the temperature from 1000 rpm to 5000 rpm but overestimates it above this speed range, within ~3°C. As for the bottom thermocouple, it is used as a reference only since there is no test data available. In the graph the TK_M_BRRCYL1 is shown as a reference temperature.
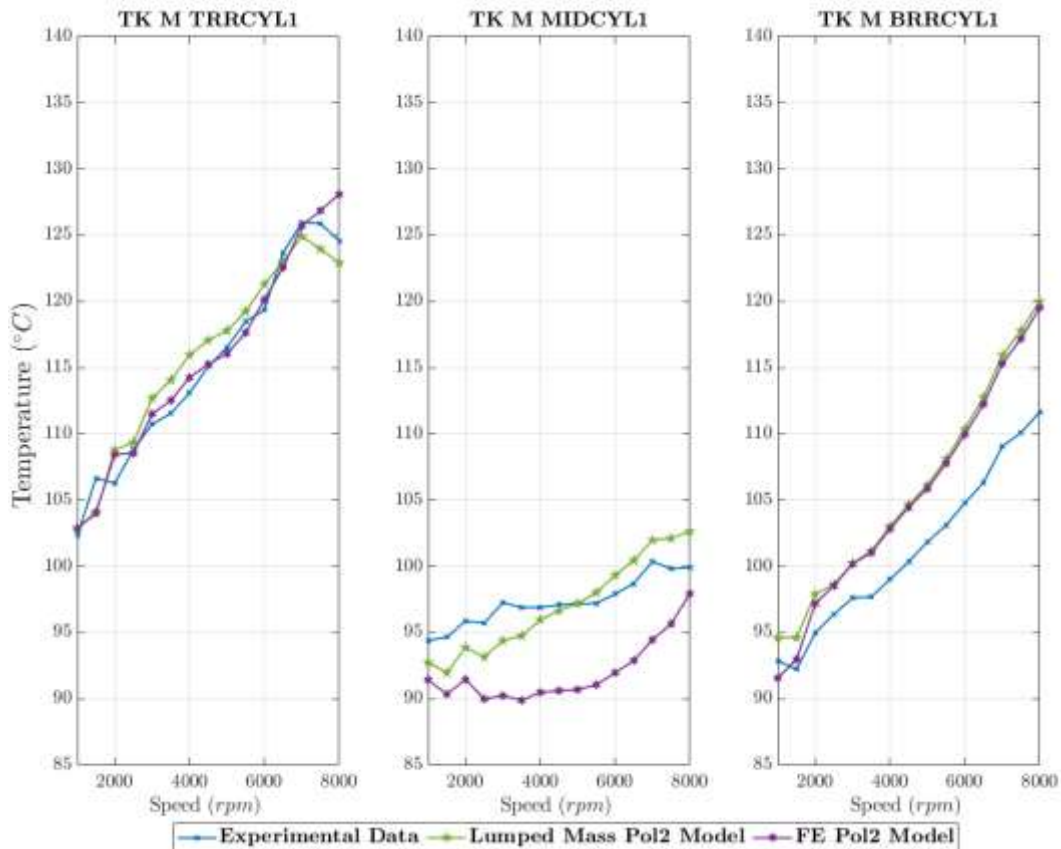
Figure 107: Cylinder one – Second order correlation thermal results.

In Figure 108, the error results for the two thermocouples used in cylinder one is displayed and it can be observed that the maximum error does not exceed 3% for

the lumped mass model. It is crucial to recall that the data for cylinder 4 were used in TK MBRRCYL1 and this thermocouple was not included in the calibration process, as agreed during the modelling phase. On the other hand, the finite element model shows a slightly higher error for the middle block cylinder thermocouple, particularly between 2500 rpm and 7000 rpm, but it never exceeds the 10% threshold.
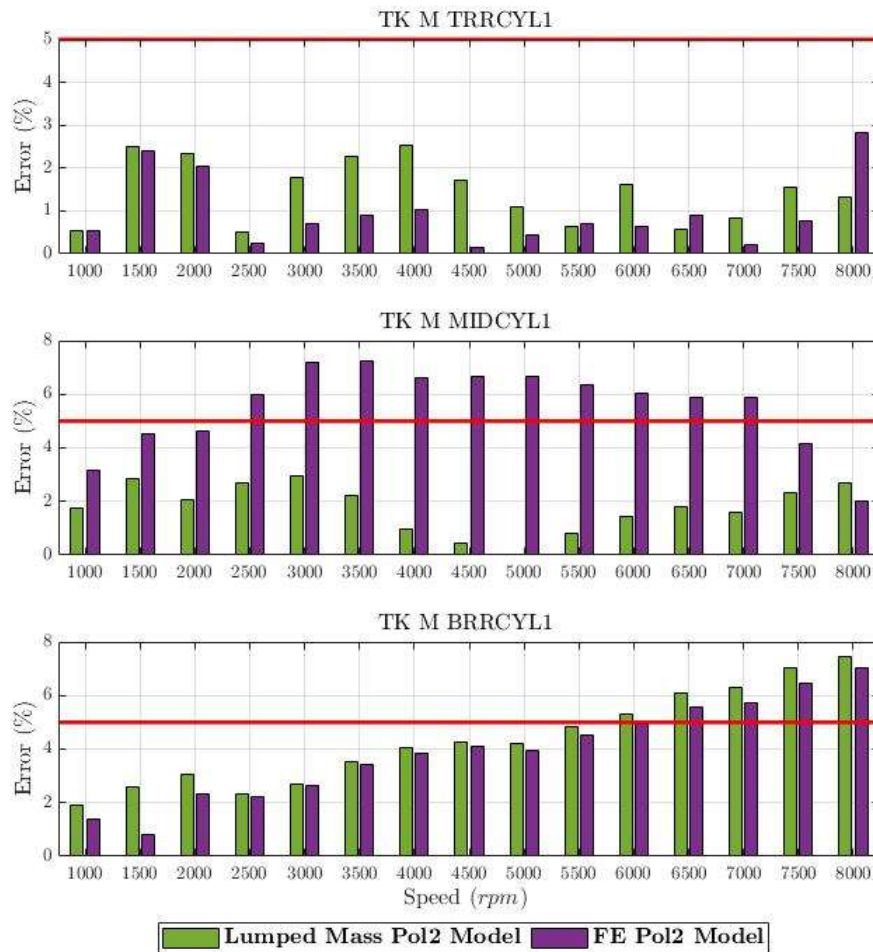
Figure 108: Cylinder one – Second order correlation error.

Figure 109 shows similar trend to cylinder one, for cylinder two in the lumped mass model. However, for the middle thermocouple, the model consistently underestimates the temperature, except for the 8000 rpm case. The largest error for this cylinder is observed at 2000 rpm, with a temperature difference of approximately 5°C, as shown in Figure 110. It is important to note that the engines are below the 5% error threshold, indicating that both models are capable of accurately predicting temperature in the top cylinder liner zone.
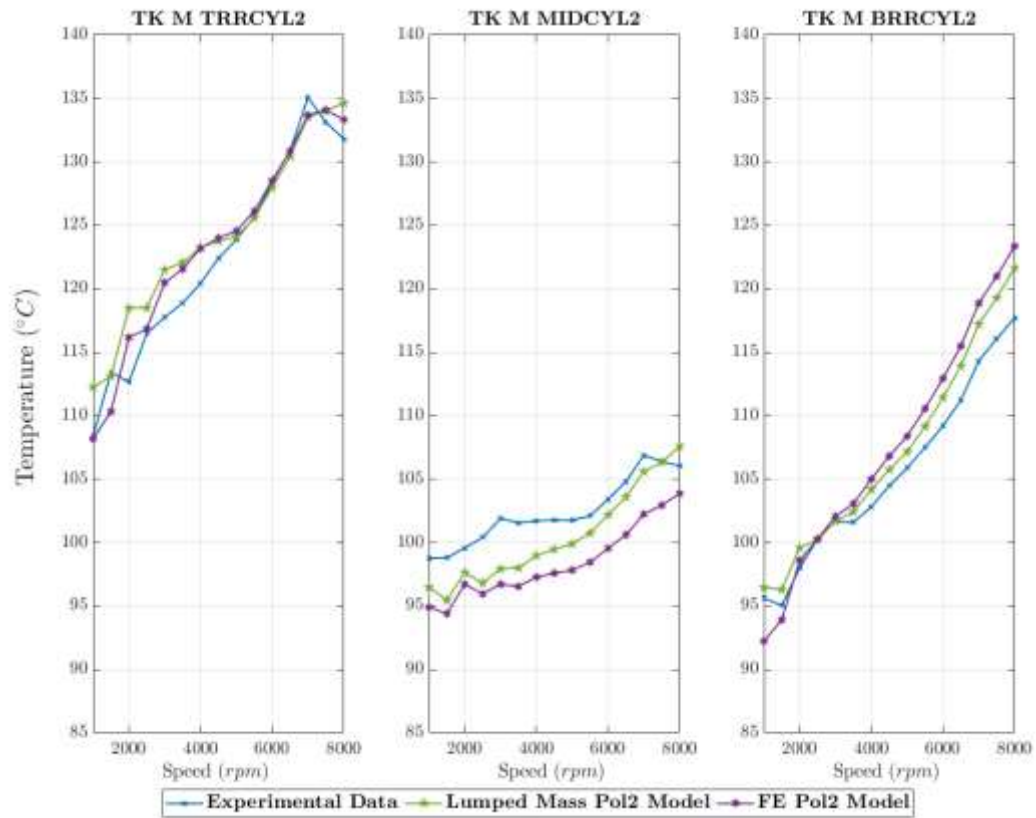
Figure 109: Cylinder two – Second order correlation thermal results.
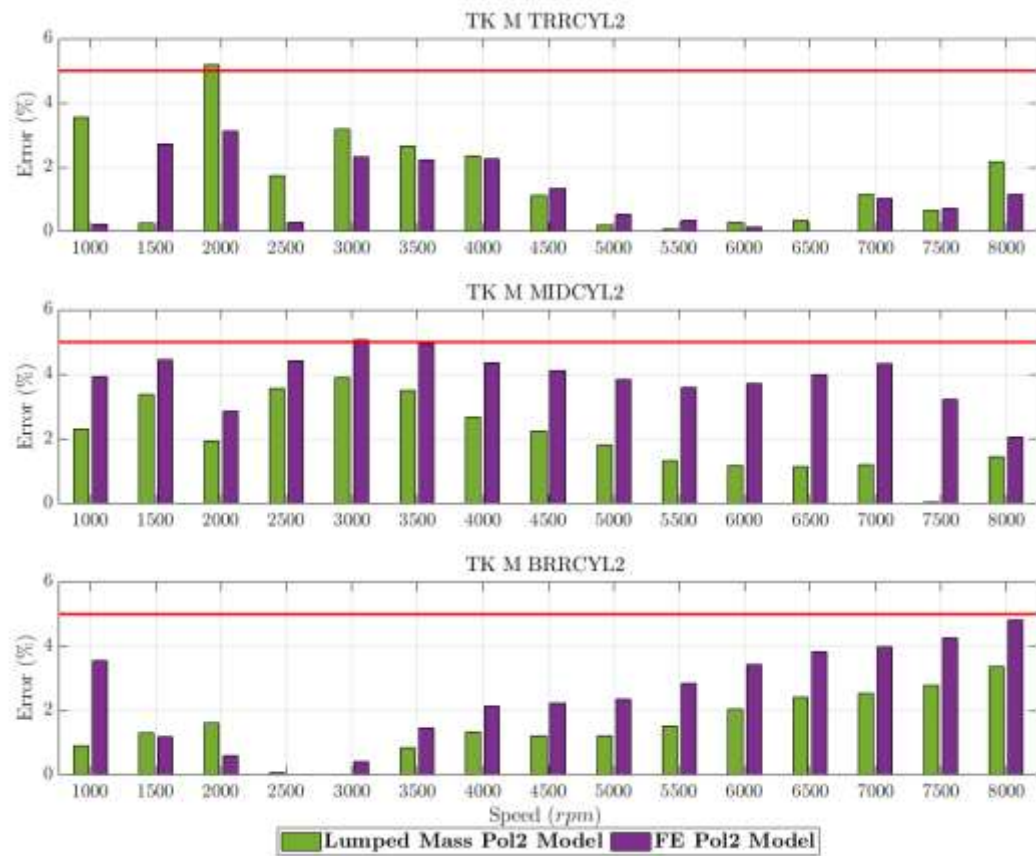
Figure 110: Cylinder two – Second order correlation error.

Figure 111 illustrates the results for cylinder three. The lumped mass model shows a consistent trend for the top thermocouple up to 5000 rpm, beyond which it underestimates the temperature by up to ~5°C at 7500 rpm. The match for the middle thermocouple is satisfactory in all cases, while the bottom thermocouples still exhibit fluctuations due to the engine thermocouple, but the simulation results demonstrate a robust trend. On the other hand, the finite element model tends to overestimate the temperature at the same engine load points but performs more effectively for the top liner temperature at higher engine points.
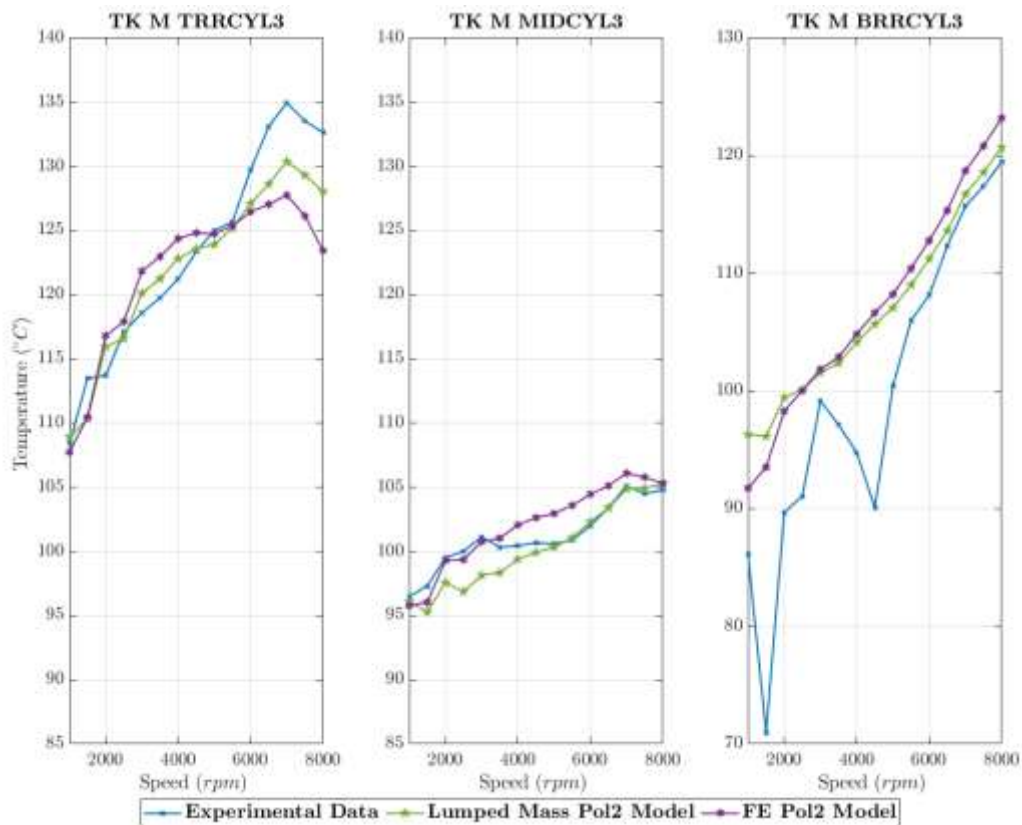
Figure 111: Cylinder three – Second order correlation thermal results.

Both models can predict the top liner cylinder temperature with less than a 5% error. The lumped mass model performs stronger than the finite element model for the middle cylinder temperature, but both models have errors below 5%, as shown in Figure 112.
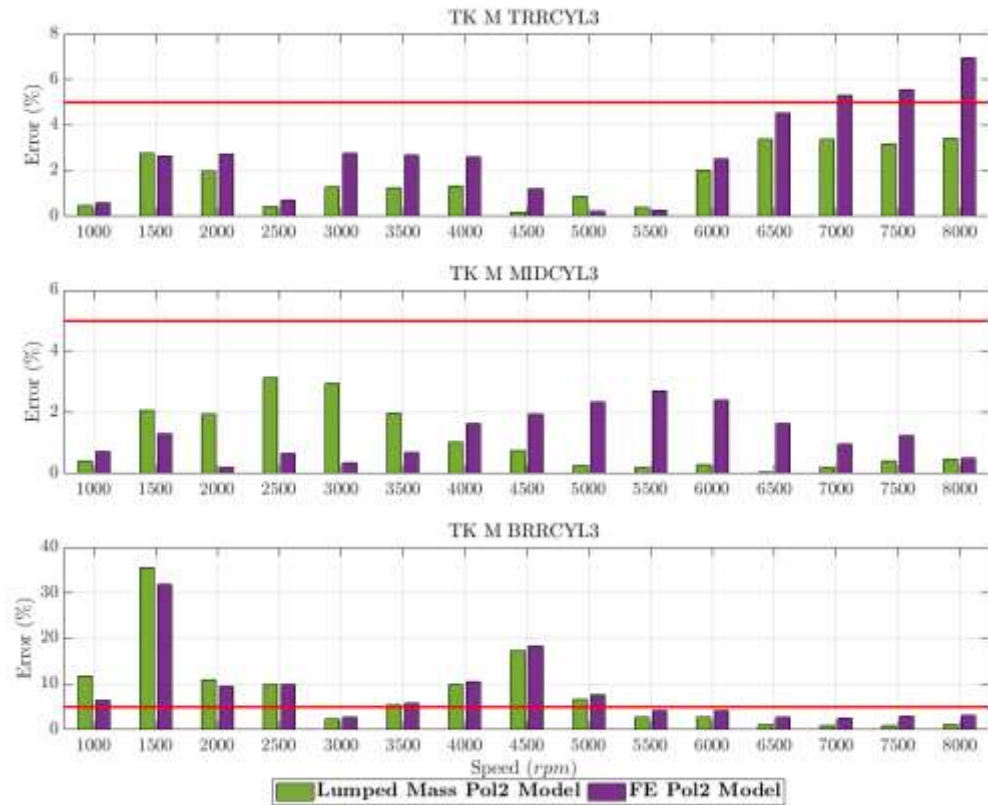
Figure 112: Cylinder three – Second order correlation error.

The intake valve bridge results are shown in Figure 113. The lumped mass model tends to overestimate the temperatures, while the FE model tends to perform better than the lumped mass model, even with a high error range. Both 1D models show the limitations of predicting metal temperature in complex head geometry. Given the oversimplification of the water jacket volumes and considering that the heat transfer multiplier is applied to the overall head volume, the temperature results are impacted. Also considering that the heat transfer area connections are different from lumped mass model and FE model as shown in Chapter 4 influence the results. The experimental data show an increasing trend from 1000 rpm to 4000 rpm, after which the temperature appears to converge to a certain level. For cylinder 2, the temperature is around 140°C, while for cylinder 5 it is about 135°C. The lumped mass model results follow a similar trend up to 4000 rpm, but after that, the model tends to overestimate the temperature.
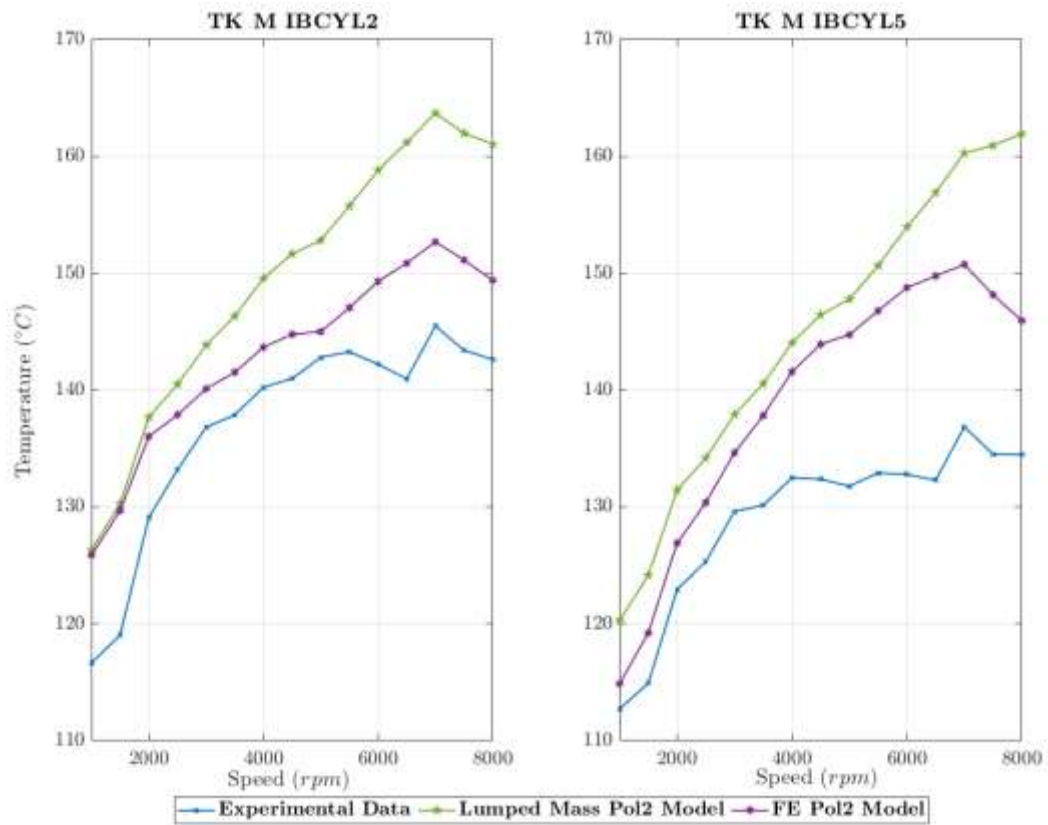
Figure 113: Intake valve bridge – Second order correlation results.

The error graph, Figure 114, highlights that the accuracy of the model for predicting intake valve bridge temperatures under high-speed operation is limited. The error values for cylinder five exceed 15% for higher speed cases, which is unacceptable. While cylinder two shows error values less than 10% for lower speed cases, it is around 10% for higher cases. The intake valve bridge is an important area in the cylinder head, but not as critical as the exhaust valve bridge with respect to material durability. The oversimplification of the water jacket part and consequently the calculation of the heat transfer multipliers performed before, make the two simulation models overestimate this temperature. From these results there is the possibility to consider in the future development of the methodology the prioritisation of the calibration to certain engine areas or making the assumption to not consider at all the thermocouple due to its difficulty to have the correct prediction.
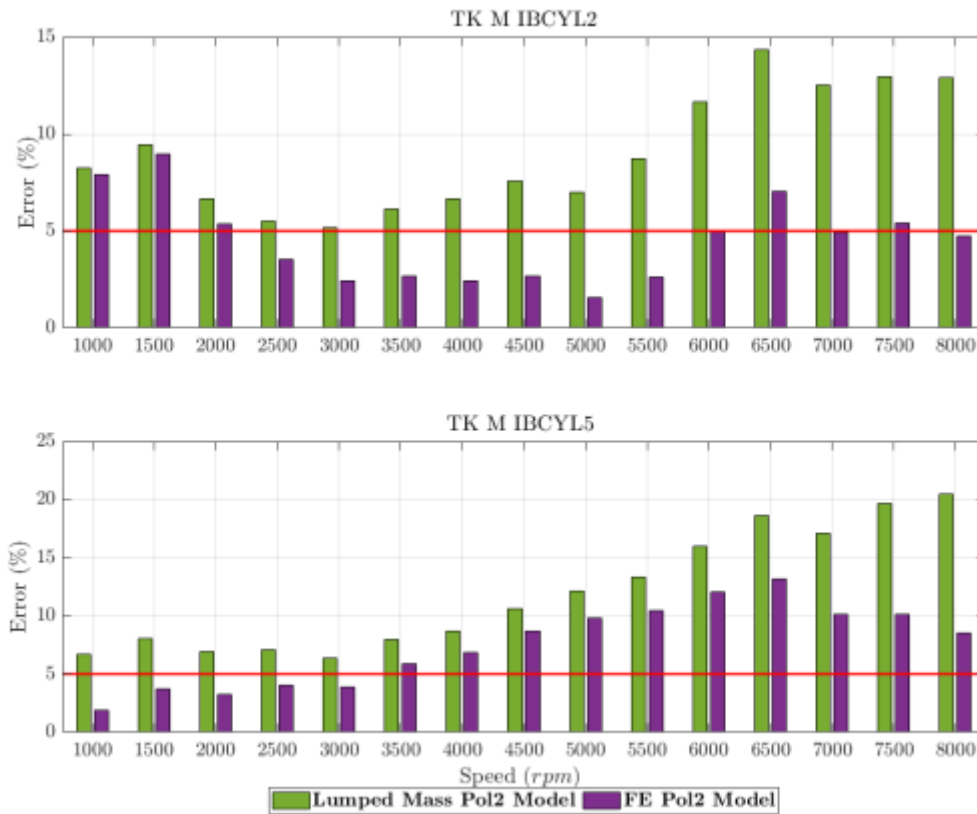
Figure 114: Intake valve bridge – Second order correlation error.

To provide a comprehensive view of the head temperature distribution, all three thermocouples are plotted in a single graph, as shown in Figure 115. The left plot depicts the temperature results for the intake valve seat, the middle plot shows the temperature distribution for the exhaust valve seat and the right plot displays the temperature data for the exhaust valve bridge.

From these results, the valve seat temperatures were challenging to match. From the intake side, where the engine head tend to be colder, the models perform in the opposite way. It can explain the fact that during the calibration process the decision to use only one thermal point for the intake seat was taken for both models. While for the exhaust seats the lumped mass model considers two thermal nodes, the FE model only considers one node. This decision was taken to favourite the lumped mass model in the calculation of an extremely important region of the head as per exhaust valve seats. While we anticipated the lumped mass model to match the exhaust valve seat, both models for the intake valve are off by an error range of more than 5%.

169
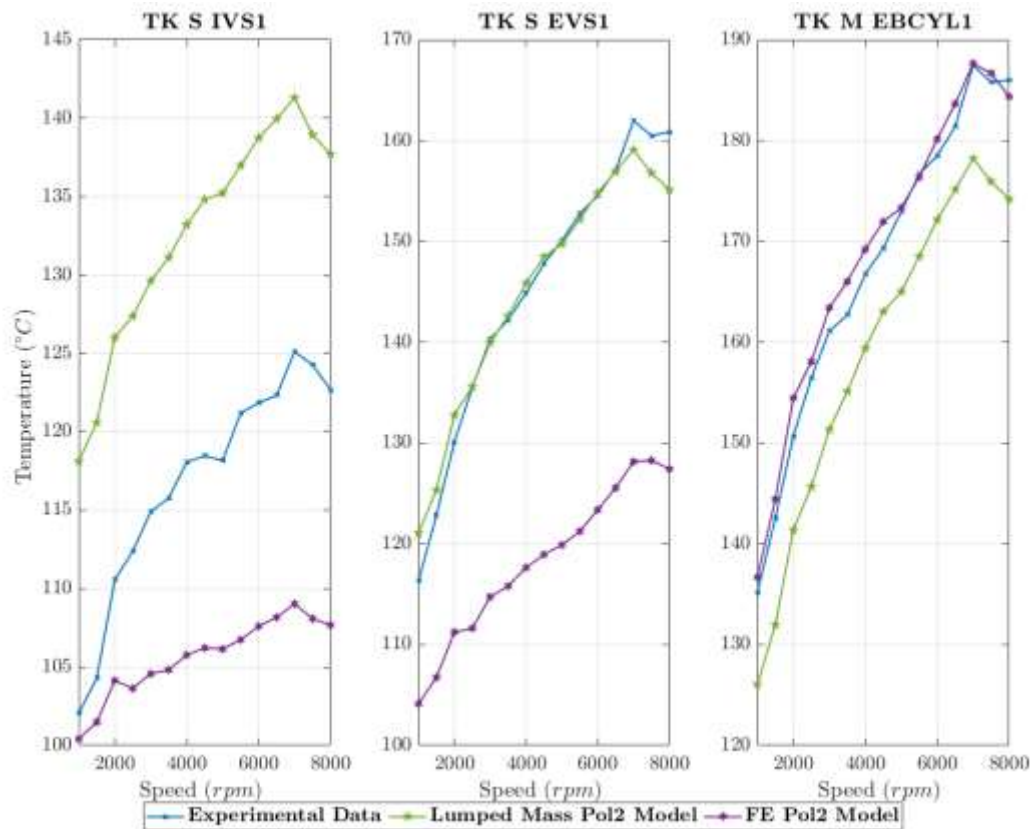
Figure 115: Head one – Second order correlation thermal results.

Figure 116 presents the error graph for the cylinder head analysis. While the intake valve seat temperature in the lower engine speed cases is outside the acceptable error range, the overall performance of the cylinder head meets the requirements. The finite element model for the exhaust valve bridge shows an error percentage below 3% for all engine speed, indicating excellent agreement with the test data.
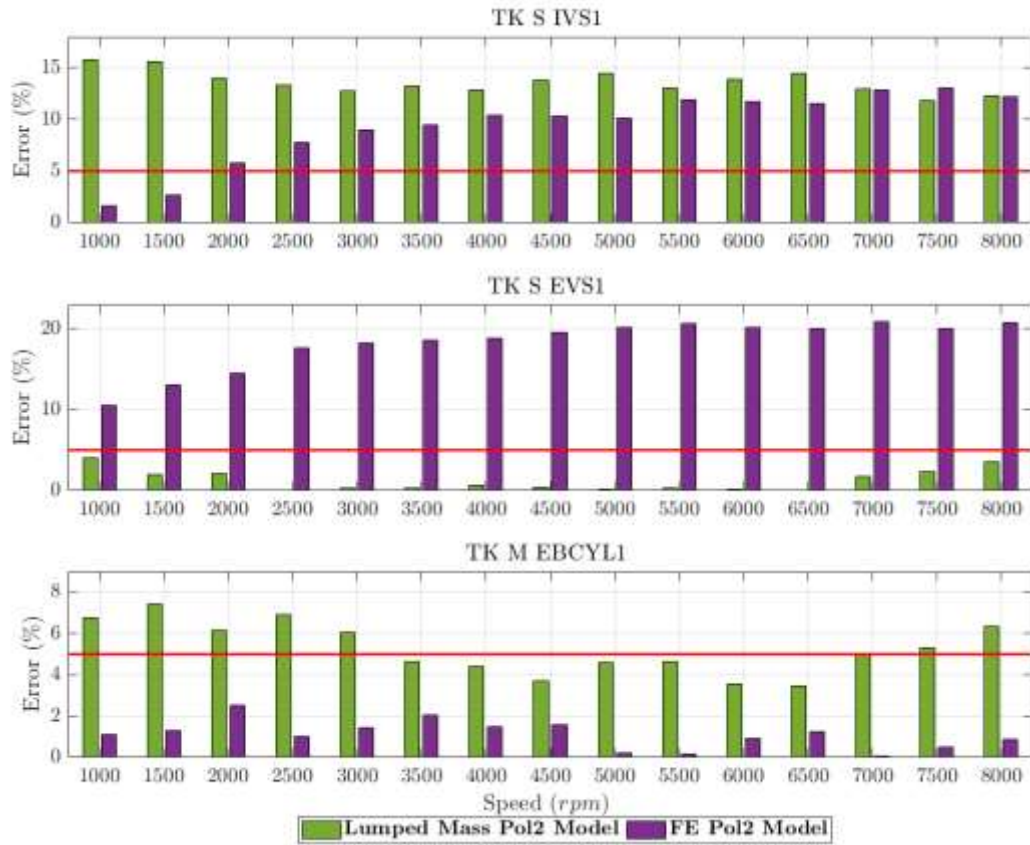
Figure 116: Head one – Second order correlation error results.

Figure 117 displays the results for the second cylinder head, which show a similar trend to those of the first cylinder head. The maximum error in the second cylinder is caused by the intake valve, as seen in Figure 118, but it is lower than that of the first cylinder, at around 10%.
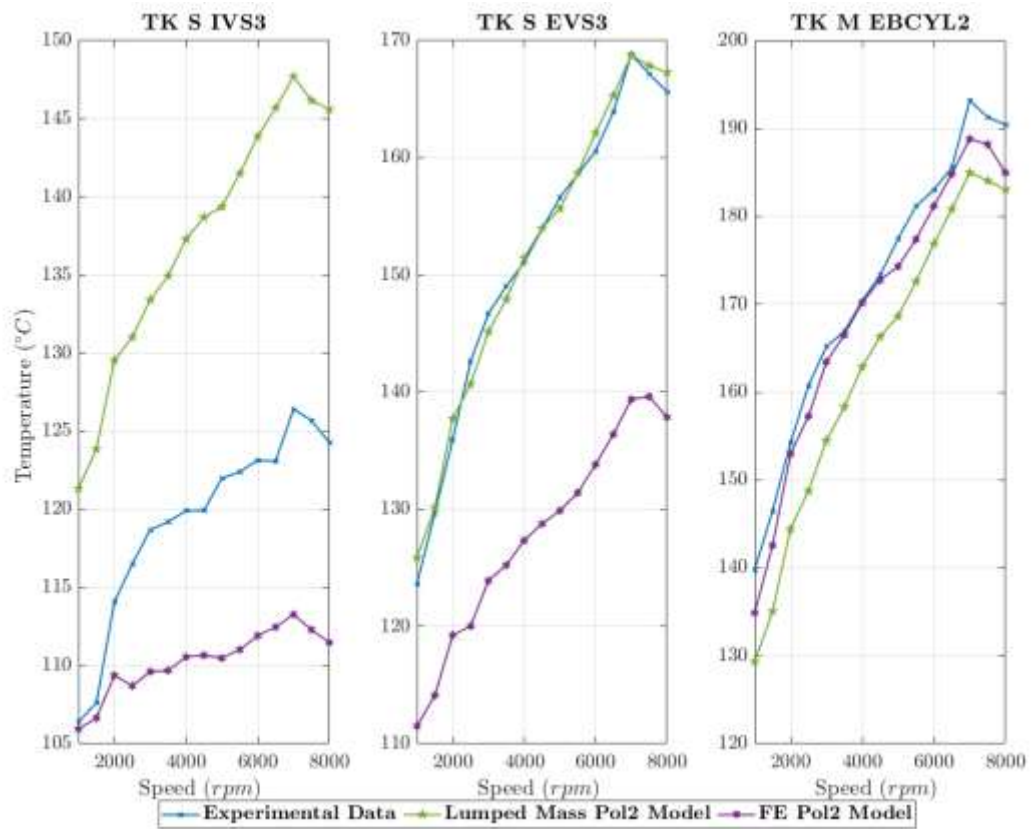
Figure 117: Head two – Second order correlation thermal results.
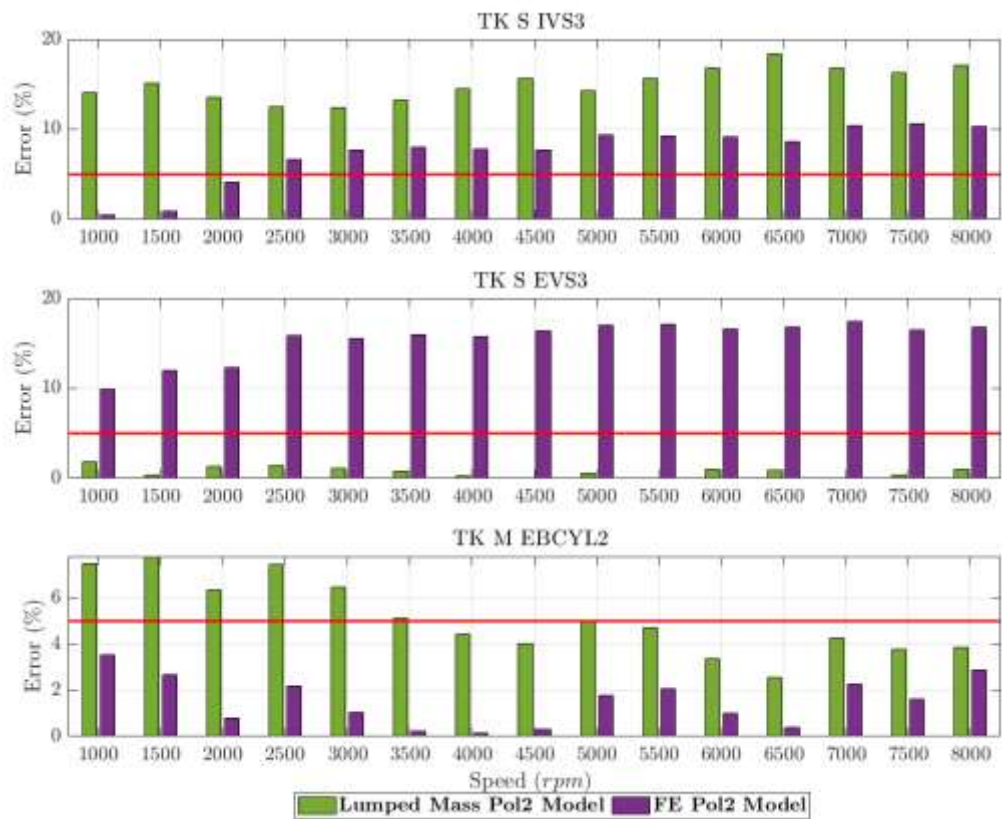
Figure 118: Head two – Second order correlation error results.

172

For the third cylinder, as shown in Figure 119 and Figure 120, the offset between the experimental data and the model is still present in the intake valve seat. In addition, the third cylinder runs hotter than the first, with experimental temperatures ranging from102 -107°C compared to the simulation temperature of 113-121°C. This consistent gap between test data and simulation data persists throughout the entire engine sweep and at all locations.
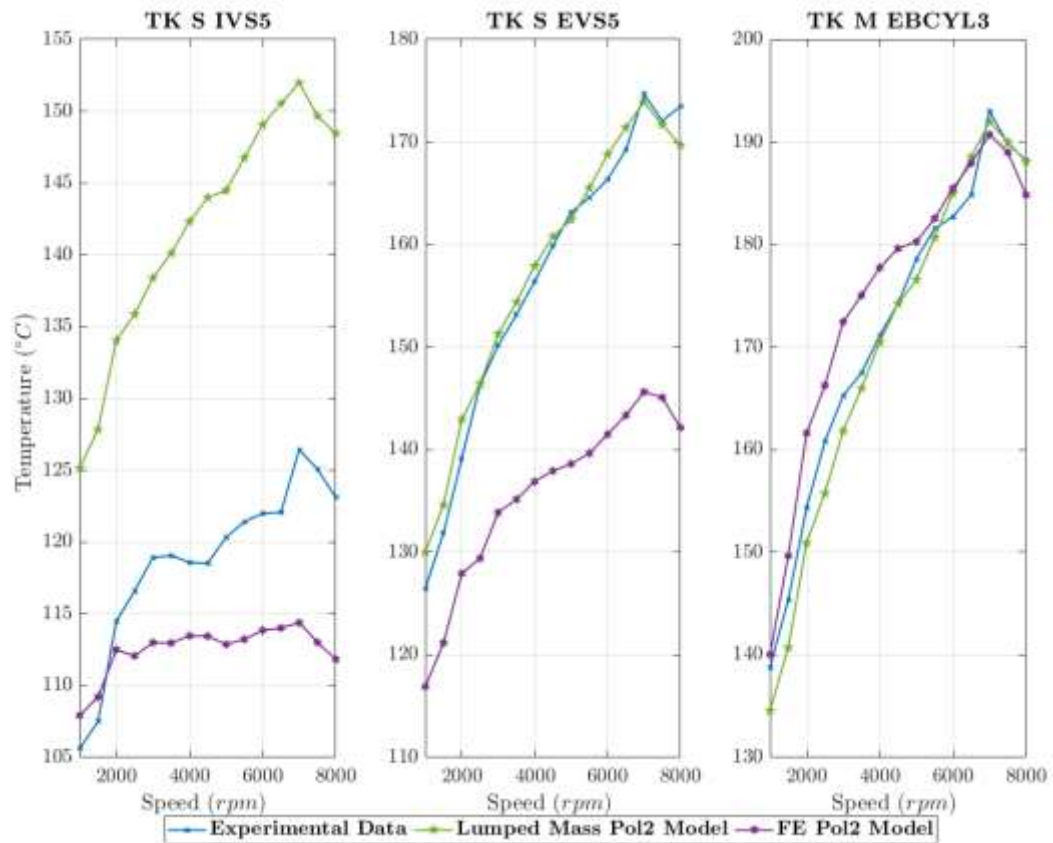
Figure 119: Head three – Second order correlation thermal results.
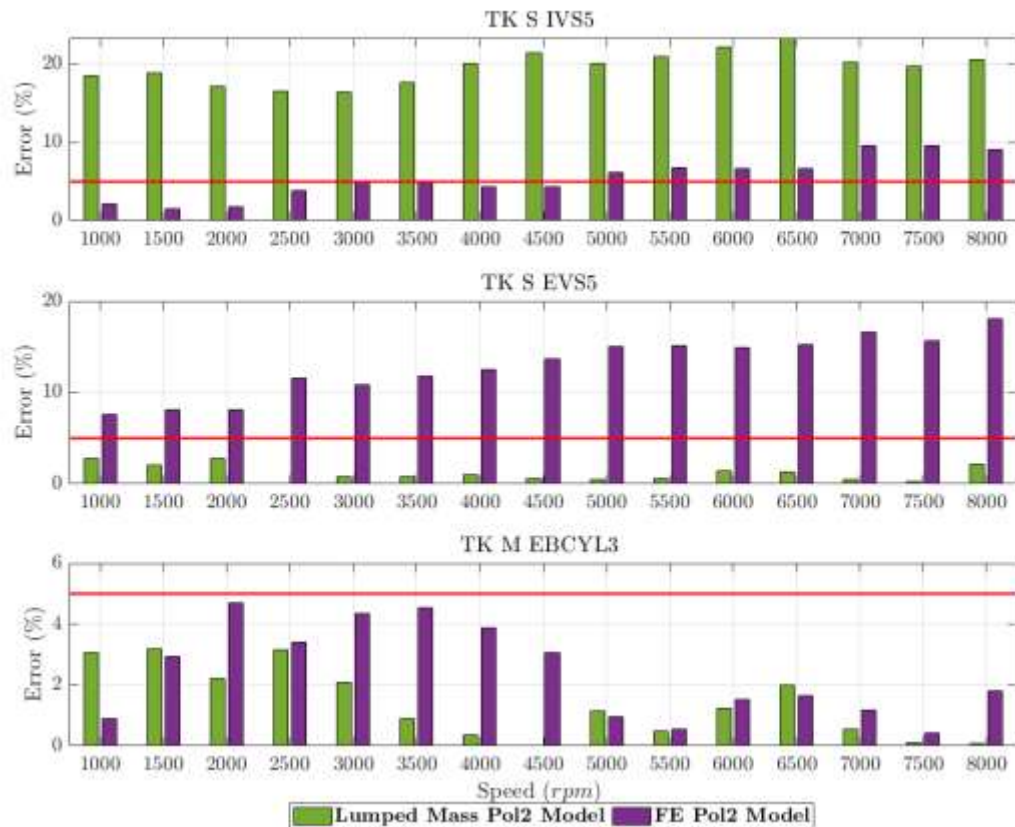
Figure 120: Head three – Second order correlation error results.

Figure 121 displays a comparison between engine heat coolant rejection for the two thermal models against experimental results. The results from the two models are similar, with fluctuations observed between lower and mid-high engine points. Between 1000 rpm and 2000 rpm, the simulation model underestimates the coolant heat rejection by approximately 5kW. However, from 2000 rpm to 3500 rpm, the model overestimates, with a difference about 10kW for the 2500 rpm case. From 4000 rpm to 6000 rpm, the model matches the coolant heat rejection. At the highest engine speed the lumped mass overestimate the coolant heat rejection by 10.20 kW more than the experimental data, while the FE model by 15.70 kW more the experimental data. It is important to remember that the coolant heat rejection was not taken into consideration as a validation factor. Those results were used to show the fidelity of the models and how they are capable to estimate such important factor. Even though the overall error percentage is less than the cases at lower engine speed, the two simulation models are overestimating the heat rejection. The engine thermal model can also be considered validated using the maximum

percentage error at 8%, as performed for the overall total error output in the previous chapter.
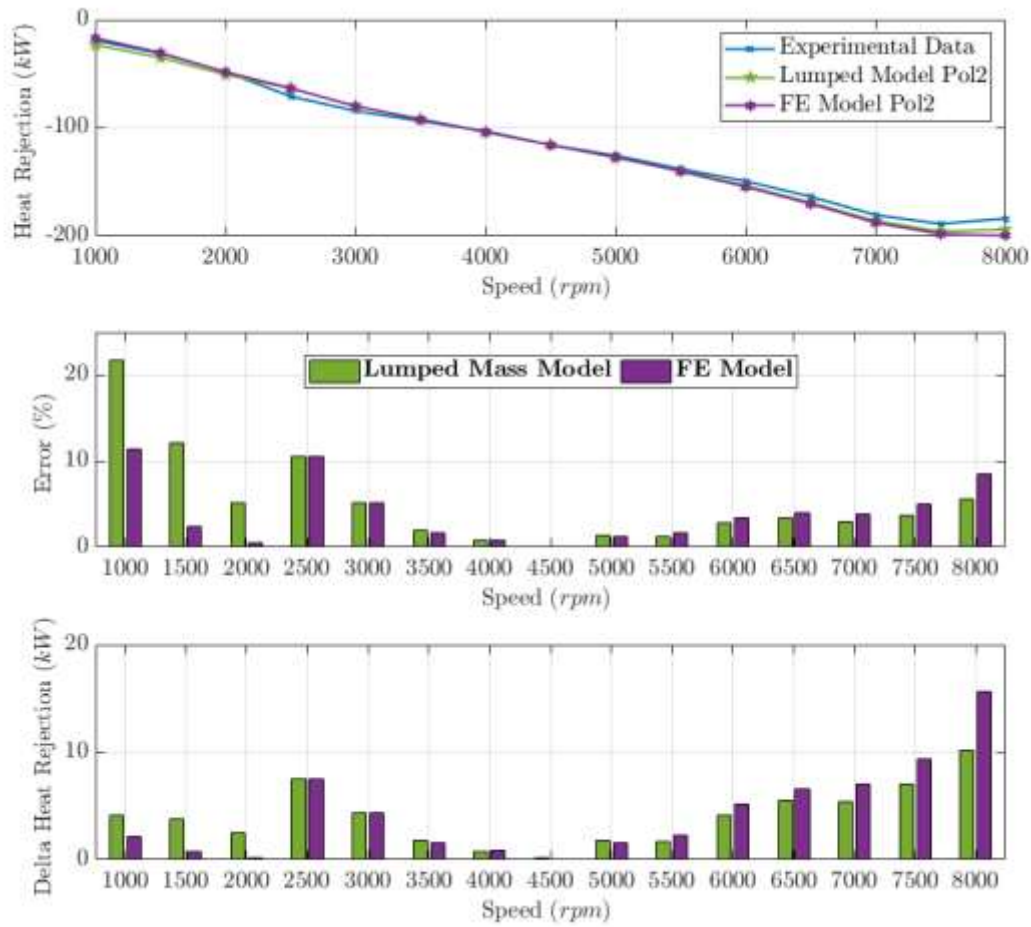
Figure 121: Coolant heat rejection, percentage error and delta heat rejection between Lumped Mass Model and FE Model.

5.4 Conclusion

In this chapter a direct comparison between two thermal modelling methodologies used in previous chapter is made. In the two thermal models the heat transfer multipliers calculated with a first and second order correlation, from Chapter 4, is imposed. The engine simulation results are compared with experimental data over an engine sweep, 1000 rpm to 8000 rpm at full load. The results are analysed and discussed in detail and the two models are assessed through a final comparison.

Engine block and head temperatures of both banks of the V6 engine are taken into consideration during the analysis and bar charts are used to highlight the error percentage between the models. The focus is shifted on the right bank of the engine and a more detailed analysis is conducted on both methodologies. It is observed that both models estimate the temperature as expected during the thermal calibration, with no consistent difference between the two fittings. However, the second order correlation shows slightly better performance in terms of error percentage in each cylinder temperature comparison. The lumped mass model is excelling at estimating the middle cylinder temperature, but this is due to the fact that the temperature is calculated considering two thermal nodes and averaging them as a result temperature. Meanwhile the FE model only considers one thermal node given the fact that the mesh of the model is more accurate than the lumped mass model. In the interbore area of the engine the model lumped model shows a better estimation temperature comparing to the FE model. This can be explained firstly because the lumped mass model has a simpler mesh and the temperature gradient calculated in this part of the engine is higher than the FE model. Secondly, because FE considers one thermal node as per thermocouple, it is more precise in terms of position and have a lower temperature gradient in the result, the temperature is underestimated. Thirdly the simplification made to the water jacket volume and consequently to the heat transfer multiplier do not help the solver to calculate the correct temperature.

For the head, the two models produce different results for the intake valve seat temperature estimation, with the finite element model underestimating the temperature and the lumped mass model overestimating it. Both models are far from the 5% error acceptance. For the exhaust valve seat, the lumped mass model can

predict the temperature, while the finite element model unpredicts it. As it is described in the calibration paragraph, for the lumped mass model the assumption of considering two thermal nodes to calculate the exhaust valve temperature is taken. For the FE model only one thermal node is considered.

However, for the exhaust valve bridge, both models predict the temperature within the error range.

Both models are considered validated given the error range and even though there are critical issues on some areas of the engine.

The lumped mass shows superior performance compared to the FE model in terms of block temperatures. However, considering that this is a first stage of a thermal methodology, the FE model has higher margin of modelling improvement both from a hydraulic perspective and a thermal calibration strategy. The FE model provides a more accurate representation of the overall temperature distribution over the engine block, particularly from the perspective of the head engine. The FE model achieves more satisfactory results in terms of estimating exhaust valve bridge temperature. This is a key factor for this work. Finally, an analysis of the coolant heat rejection is made showing the overall fidelity of the two simulation models. The results shown a higher difference in terms of coolant heat rejection at lower and higher engine speed condition. The biggest difference is at 8000 rpm where the lumped mass model overestimate by ~ 10 kW more than the experimental data, while the FE model at the same engine point is overestimating of ~15 kW relative to the experimental data. The methodology undertaken in this study do not consider this parameter in the validation process. This should be implemented in the future, but as the simulations model are performing, at this stage the two models can be also considered validated, because the error is less than 8% overall.

While the current study primarily focuses on validating temperature predictions within thermal models, an essential avenue for future work involves assessing the broader impact of these predictions on key engine performance metrics. This forward-looking analysis aims to provide a more comprehensive evaluation of the models' effectiveness in representing real-world engine behavior.

- Predictive Mode Analysis

Running the thermal models in a predictive mode allows for assessing their capabilities in predicting crucial engine performance parameters. This includes, but is not limited to, engine efficiency, power output, and emissions. By comparing model predictions with experimental data in a predictive mode, a deeper understanding of the models' accuracy in capturing overall engine performance can be achieved. In this context, further development of the FE model is expected to yield more significant benefits compared to the lumped mass model.

- Specific Parameters and Performance Metrics

Identifying and highlighting specific parameters or performance metrics critical to the application is essential for a detailed evaluation. For instance, fuel efficiency, thermal stress on components, and other relevant factors contribute significantly to the overall performance of the engine. Analyzing how well each model predicts these specific metrics provides insights into the models' applicability and areas for potential refinement. While both models exhibit an overall good fidelity of results, choosing between them for further development depends on considerations such as runtime, where the lumped mass model may emerge as a more efficient option.

- Application to different engine application

Considering the potential application of thermal models to power-dense V engines, utilized in heavy-duty applications (e.g., marine and industrial engines) and light-duty engines, is a crucial step in assessing the models' versatility. Understanding how well the models perform across a range of engine types and sizes will enhance their utility and generalizability. The FE model, with its capability to handle complex geometry, demonstrates great potential for future development. This becomes particularly relevant for heavy-duty applications, where computational cost during simulation, linked to the size of the geometry, is a significant factor.

- Reduction in Simulation Runtime and Cost

One of the anticipated advantages of developing a robust thermal modeling system is the potential reduction in simulation runtime and, consequently, cost during the development stage. Investigating the efficiency gains in terms of computational resources and time can provide valuable insights into the practical applicability of the models in an industrial context.

In conclusion, future work should extend beyond the validation of temperature predictions to encompass a detailed analysis of the impact on key engine performance metrics. This approach not only enhances the understanding of model accuracy but also contributes to the refinement and improvement of thermal modeling methodologies. The application potential for power-dense V engines across various domains underscores the significance of this research in advancing both efficiency and cost-effectiveness in the development process.

Chapter 6 - Conclusion and Outlook

6.1 Summary

This chapter reviews the work described in the previous chapters and summarises the key points arising from section 1.3.

This thesis presents the work undertaken to develop a robust and time-efficient 1D thermal model methodology for a V6 gasoline engine, which is subsequently validated against experimental data. It investigates different hydraulic and thermal calibration methodologies and exploits a final flexible and robust procedure for hydraulic and thermal calibration process. The current work also makes a direct comparison between experimental and simulation results to select the best modelling methodology.

6.2 Conclusions

In the ever-evolving landscape of vehicle development, this research introduces novel and transformative methodologies, leveraging advanced simulation tools to revolutionize engine development. The overarching novelty lies in the comprehensive approach towards digital modeling and optimization, addressing key challenges and pushing the boundaries of traditional methodologies.

This study introduces a novel integration of simulation tools within the V model for engineering development, presenting a holistic and interconnected approach. The comprehensive utilization of GT-Suite simulation software showcases a paradigm shift in how digital tools are harnessed for achieving significant milestones.

The research recognizes simulation tools as game-changers in vehicle engine research, providing a crucial avenue to explore fuel consumption, emissions, and ways to enhance engine efficiency and performance. There is a notable emphasis on the pivotal role of simulation in cost reduction, time minimization, and heightened certainty throughout the intricate process of engine development.

The study explores hydraulic and thermal approaches with versatile applicability, extending beyond traditional V gasoline engines to encompass hybrid vehicles, electric vehicles, hydrogen combustion engines, and mild hybrid systems. It makes a ground-breaking contribution to the 1D modeling phase, promising not only accuracy but also a substantial reduction in simulation runtime.

Recognition of the challenges posed by power-dense V engines, including those in heavy-duty applications like marine and industrial engines, and the proposal of methodologies that transcend traditional boundaries. There is an anticipation of a paradigm shift in simulation development, addressing computational cost challenges in heavy-duty applications.

The research introduces two distinct thermal models: the lumped mass thermal model and the finite element model, showcasing innovation and departure from conventional approaches. There are advancements in the calibration strategy, integration of thermocouples, and the application of the Design Optimizer, adding layers of sophistication to thermal modelling methodologies.

The study conducts meticulous comparative analysis between the lumped mass and finite element models, highlighting the strengths of each in predicting engine temperatures. Validation of both models within acceptable error ranges is performed, providing critical insights into their performance across different areas of the engine.

A forward-looking approach is emphasized, moving beyond temperature predictions towards a detailed analysis of the impact on key engine performance metrics. Future work focuses on predictive mode analysis, specific parameters and performance metrics, diverse engine applications, and a reduction in simulation runtime and cost.

The ultimate value of this research lies in the potential to save significant costs in new engine development programs, offering transformative efficiency gains and marking a pivotal step in automotive innovation.

The conclusions of this work are presented against the objective presented in Chapter 1. Each of the objectives are resolved below with the corresponding remarks.

1) Research the state of art for 1D thermal engine modelling (using a 1D commercial software – GT-Suite).

The literature review highlighted the importance of simulation softwares and consequently simulation models in addressing research and development challenges. They offered a multitude of approaches to tackle complex problems. The current work has analysed a specific research area which focuses on the use of mono dimensional simulation model using GT-Suite software to develop engine thermal models. The benefits of having a 1D simulation model for thermal management use are the ability to perform system analysis at all levels, the advantage in terms of simulation run time, compared to a 3D CFD models and finally the ability to build a robust, but at the same, time flexible simulation model.

2) Evaluate a range of different modelling approaches and associated calibration methodologies.

Based on the work carried out during the literature review phase, different modelling approaches have been investigated. A chronological approach has been used to describe how the different modelling techniques were used and implemented. For example from one of the first modelling approach used by Lauerta [93] , and Millo [94] to arrive to one of the latest works done by Graziano [95]. Most of the works reviewed are based on in line engine cylinders and a basic methodology in terms of hydraulic modelling and thermal modelling have been explained. Based on this, the research work has proposed to fill the detected research gaps and to answer three main research questions:

- How can the hydraulic 1D modelling methodology be further implemented and renew to achieve a minimum calibration work on V type engine ensuring a flow rate a pressure distribution?

- In the context of power dense V engines, what novel approach can be explored within the thermal 1D methodology to optimise the calibration process, utilising experimental engine metal temperature and dedicated heat transfer multipliers for the engine block and head, and how can this methodology be validated across different engine operating points?

The hydraulic modelling methodology has been performed using two different engine coolant water jacket geometries, but always referring to the same engine

family. Using the A-Sample three different methods have been explored and implemented. The methods are "Method One Volume", "Method Separate Volume 1", "Method Separate Volume 2". After considering the benefits and the limitation of each method, "Method Separate Volume 1" has been chosen. This is due to the fact that this modelling approach results to be the best in terms of pressure estimation along the coolant circuit. This indicates that the methodology holds significant potential for the subsequent modelling steps, involving the hydraulic and thermal calibration of the model.

3) Detail a robust approach to the hydraulic and thermal calibration process.

The hydraulic and thermal calibration is a key part of this work. As the hydraulic modelling technique has been chosen and implemented over two different cooling geometries, a calibration approach has been required to have a correct coolant flow rate over the two engine banks. This has been also a key part as that the thermal engine balance is critical for a V engine. The approach used has been described in Chapter three. For the A-Sample model ten orifices have been defined in the 1D model and have been tuned to achieve the best pressure match along the cooling circuit at a range of flow rate conditions. The same approach has been used for the C-Sample geometry. The only difference was in the C sample, the position of one of the orifices were different from the A-Sample (In the C-Sample an orifice is defined in the cylinder five coolant entrance), but this has been caused by the different water coolant geometry. The calibration methodology applied has given the expected results. Both models were validated, with an error of less than 5% compared to 3D CFD approaches adopted in the engine design phase.

Regarding the thermal approach two different methodologies have been investigated. Based on the literature review done, it has been possible to develop 1D engine thermal model using a lumped mass approach and a finite element approach. These two approaches have been able to be used thanks to a discretisation technique that can be carried out using GT-Suite. The method consists of converting and consequently discretising a 3D CAD volume to a 1D part. The engine thermal masses are then considered as lumped masses or as a finite element. This work has both implemented the methodologies based on what has already been done and renewed the approach. From a thermal calibration perspective, the approach used is completely new. The methodology used considers experimental data from an

engine thermal survey. These temperatures are directly utilised in the thermal model to impose a temperature target in certain part of the engine while a calibration factor of the HTC multiplier defined in the water jacket parts, which were discretised from the actual engine geometry, are used to adjust the heat transfer coefficient (estimated with the Colburn analogy) and it will be used to converge on these temperatures.

4) *Compare and identify the most promising methodologies.*

The final comparison and identification of the most promising methodology has been done using experimental data. The engine tests have been outside the University of Bath laboratories by a third party consultancy. A direct comparison has been performed between the two models where the lumped mass excels in terms of absolute error, with the finite element model outperforming at estimating exhaust valve bridge temperature. This aspect reaches an important point during the development of the thermal model because the head maximum metal temperature was an important parameter to be studied and a crucial priority for all engine performance development strategies.

5) *Select the best methodology.*

Finally, the best and most promising engine thermal methodology has been chosen. Both models were considered validated given the error range discussed in Chapter 4 -

The Lumped Mass model demonstrates superior performance than the FE model in terms of block temperatures. However, as this is a first stage of a thermal methodology the FE model has higher margin of modelling improvement both from a hydraulic perspective and a thermal calibration strategy. The overall temperature distribution over the engine block is more accurately represented from the FE model. The FE model has achieved outstanding results in terms of estimating exhaust valve bridge temperature than the Lumped mass model. This was a key factor for this work. Knowing the fact that the exhaust valve region of the head is the hottest point of the combustion chamber, having a thermal engine model capable to predict this temperature with an error of less than 5% of the absolute temperature value, will help to develop new thermal strategies as well as for calibration strategies and enabling further development for IC engines.

The aim of this work has been to investigate and validate a renew modelling methodology to be adopted by the OEMs and the research field in the thermal management simulation environment. This is driven by the need to have a more efficient simulation tool to study a more complex problem in the engine development phase. In this work different modelling methodologies have been investigated and a hydraulic and thermal methodology has been deployed to be used for different V engine applications. From the obtained understanding a deeper knowledge on how to develop powertrain thermal models can be used. These findings can be applied to a wide variety of engine geometries. More importantly with a newer version of the software more and more powertrain systems can be discretised both as lumped mass or finite element model and the thermal calibration strategies implemented once experimental thermal survey data are available.

Chapter 7 - Future Work

The work conducted could have an impact on several research development areas. The future of the new powertrain system development will always consider the thermal management systems as a key area to be developed and further investigated. ICE, hybrid and full electric powertrain systems will continue to push the boundary in terms of thermal efficiency and having a robust and flexible simulation model will help the technology moving forward. New simulation software with new features will be available in the future and yet roust modelling methodologies are required for calibrating and validating the simulation models. This work allows the use of the hydraulic and thermal methodologies for different thermal model approaches. The potential to further implementation of the hydraulic model lies in the complexity of the geometry. In this thesis the cylinder head water jacket has been considered as a single part, but the thermal calibration has shown that there is progress required in certain zones of the head. This will allow to implement and better match the intake valve seat and exhaust valve seat zones (for example in the FE model). A roughness study was not present in this work due to the confidentiality with third party. This factor also plays a role for both the hydraulic and the thermal calibration. It can be implemented as well considering transient simulation, as for example warm up phase simulations. Another step that could be done is having a proper sensitivity analysis to all the parts discretised from CAD to 1D environment and for every engine geometry discover which area of the engine need more modelling work.

The thermal model could be implemented both for the lumped mass and finite element models. The first one in terms of calibration strategy, which means using more dedicated heat transfer coefficient multipliers and defining those in the critical engine areas discovered in this work. For the finite element, the first step will be to implement the mesh discretisation. It will be possible to do a mesh study analysing the trade-off between a refine mesh against model fidelity. This process can be done also considering a 1D FRM engine performance model This will help calculate the temperature in the thermal nodes and will keep the simulation run time reasonable. Secondly more thermals nodes could be considered in the thermal calibration process, where they are used to impose and target the experimental temperatures.

A more precise definition of HTC multipliers can be applied. However, this it will be strictly related to the hydraulic modelling.

These implementation to the engine thermal model development are key to continue to push the research boundary in the engine development field. In the past few years electrification seemed to be the topic in the research field while the ICE engine where considered almost the past. With a new research topic: i.e. H2 engines, low temperature combustion LTC and lean burn engine. i.e. both technologies change gas side heat transfer and the latter aim to minimise heat rejection to coolant and as such a robust thermal modelling approach is needed to fully optimise these approaches and understand them in the "digital twin" age.

The hydraulic and the thermal modelling methodology is transferrable to future technologies associated with BEV and fuel cell vehicles such as battery pack development, fuel cell thermal management and electric machine cooling.

The future trajectory of this study extends beyond the validation of temperature predictions, delving into a more comprehensive evaluation of thermal models' influence on critical engine performance metrics. Key areas for future exploration encompass:

- Predictive Mode Analysis:

Running thermal models in predictive mode to assess their proficiency in predicting vital engine performance parameters. A comparative emphasis on the FE model's advantages over the lumped mass model in predictive applications.

- Specific Parameters and Performance Metrics:

Identification and prioritization of specific parameters crucial for engine performance. Evaluation of each model's predictive capacity for these metrics, with due consideration given to runtime efficiency for model selection.

- Application to Different Engine Types:

Exploration of the adaptability of thermal models across a spectrum of engine types and sizes. Special attention to power-dense V engines in heavy-duty and light-duty applications, with the capability of the FE model to handle complex geometries being a pivotal factor.

- Reduction in Simulation Runtime and Cost:

Investigation into the efficiency gains in terms of computational resources and time. Assessment of the practical applicability of models in an industrial context, with the overarching goal of streamlining development processes for enhanced efficiency and cost-effectiveness.

In conclusion, the envisioned future work aims to propel the understanding of thermal models' overarching impact on overall engine performance. This exploration is poised to guide the ongoing refinement and enhancement of thermal modeling methodologies, ultimately contributing to more efficient and cost-effective automotive development practices.

Appendix A
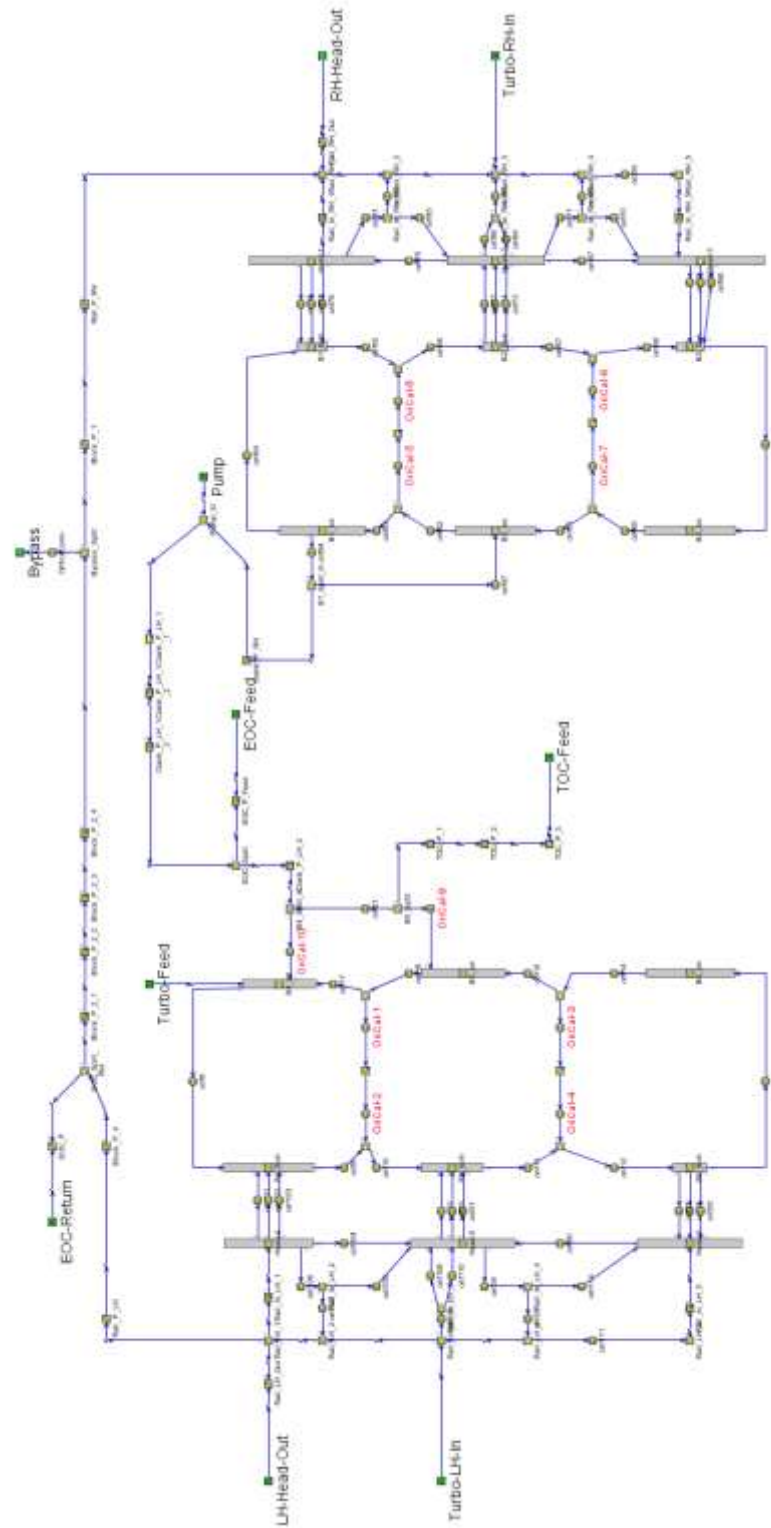
Figure 122: C Sample - Model H - 1D Hydraulic model discretised.

Figure 123C Sample - Model MH - Lumped mass 1D Thermal Model.
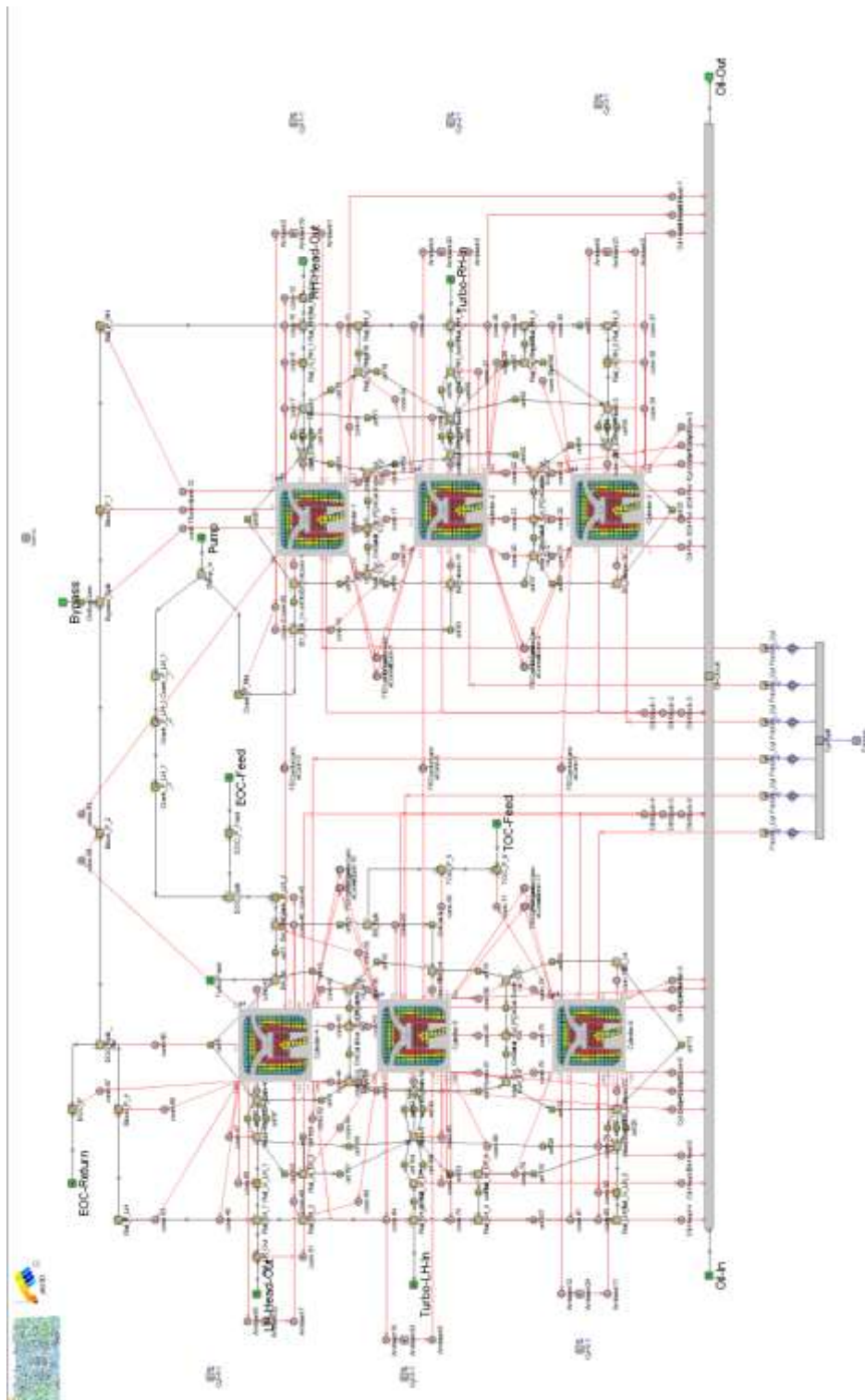
Figure 124:Model H Finite Element (FE) Engine thermal model

Appendix B

In the Table 11 are listed the sensors used in the engine thermal survey. The list was given by the engine manufacturer.

Table 11: Engine thermal survey sensor list.

Sensor location Component	Primary System	Fitting Supplied	Type of Sensor Required
Cylinder Block	Cylinder Block	1/8 BSP Pressure Ferule	Normal Pressure line (Clear)
Cylinder Block	Cylinder Block	1.5 metal temp	3mm K-Type
Cylinder Block	Cylinder Block	1/8 BSP Pressure Ferule	Normal Pressure line (Clear)
Cylinder Block	Cylinder Block	1.5 metal temp	3mm K-Type
Cam Cover	CCV	1/8 BSP Pressure Ferule	PVC Mid Temp (Black)
Cam Cover	CCV	1/8 BSP Pressure Ferule	PVC Mid Temp (Black)
Turbo	Exhaust	1.5 Surface Temp Thermocouple	1.5mm K-Type Surface Temp
Turbo	Exhaust	1.5 Surface Temp Thermocouple	1.5mm K-Type Surface Temp
Assy Oil / Water Pump	Cooling System	1/8 BSP Pressure Ferule	Normal Pressure line (Clear)
Assy Oil / Water Pump	Cooling System	3mm 1/8 BSP Temp	3mm K-Type
Coolant Feed Pipe	Cooling System	1/8 BSP Pressure Ferule	Normal Pressure line (Clear)
Coolant Feed Pipe	Cooling System	3mm 1/8 BSP Temp Temp	3mm K-Type
Cylinder Block	Cylinder Block	1.5 K-Type Metal Temp	1.5mm K-Type
Cylinder Block	Cylinder Block	1.5 K-Type Metal Temp	1.5mm K-Type
Cylinder Block	Cylinder Block	1.5 K-Type Metal Temp	1.5mm K-Type
Cylinder Block	Cylinder Block	1.5 K-Type Metal Temp	1.5mm K-Type
Cylinder Block	Cylinder Block	1.5 K-Type Metal Temp	1.5mm K-Type
Cylinder Block	Cylinder Block	1.5 K-Type Metal Temp	1.5mm K-Type
Cylinder Block	Cylinder Block	1.5 K-Type Metal Temp	1.5mm K-Type
Cylinder Block	Cylinder Block	1.5 K-Type Metal Temp	1.5mm K-Type
Cylinder Block	Cylinder Block	1.5 K-Type Metal Temp	1.5mm K-Type
Cylinder Block	Cylinder Block	1.5 K-Type Metal Temp	1.5mm K-Type

Cylinder Block	Cylinder Block	1.5 K-Type Metal Temp	1.5mm K-Type
Cylinder Block	Cylinder Block	1.5 K-Type Metal Temp	1.5mm K-Type
Cylinder Block	Cylinder Block	1.5 K-Type Metal Temp	1.5mm K-Type
Cylinder Block	Cylinder Block	1.5 K-Type Metal Temp	1.5mm K-Type
Cylinder Head	Cylinder Head	1.5 Surface Temp Thermocouple	1.5mm K-Type Surface Temp
Cylinder Head	Cylinder Head	1.5 Surface Temp Thermocouple	1.5mm K-Type Surface Temp
Exhaust Manifold	Exhaust	1.5 Surface Temp Thermocouple	1.5mm K-Type Surface Temp
Cylinder Head	Cylinder Head	1.5 K-Type Metal Temp	1.5mm K-Type
Cylinder Head	Cylinder Head	1.5 K-Type Metal Temp	1.5mm K-Type
Cylinder Head	Cylinder Head	1.5 K-Type Metal Temp	1.5mm K-Type
Cylinder Head	Cylinder Head	1.5 K-Type Metal Temp	1.5mm K-Type
Cylinder Head	Cylinder Head	1.5 K-Type Metal Temp	1.5mm K-Type
Cylinder Head	Cylinder Head	1.5 K-Type Metal Temp	1.5mm K-Type
Cylinder Head	Cylinder Head	1.5 K-Type Metal Temp	1.5mm K-Type
Cylinder Head	Cylinder Head	1.5 K-Type Metal Temp	1.5mm K-Type
Fuel Injectors	Fuel		
Cylinder Head	Cylinder Head	1.5 K-Type Adhesive	1.5mm K-Type
Cylinder Head	Cylinder Head	1.5 K-Type Adhesive	1.5mm K-Type
Cylinder Head	Cylinder Head	1.5 K-Type Adhesive	1.5mm K-Type
Cylinder Head	Cylinder Head	1.5 K-Type Adhesive	1.5mm K-Type
Cylinder Head	Cooling System	1/8 BSP Pressure Ferule	Normal Pressure line (Clear)
Cylinder Head	Cooling System	3mm 1/8 BSP Temp	3mm K-Type
Cylinder Head	Cooling System	1/8 BSP Pressure Ferule	Normal Pressure line (Clear)
Cylinder Head	Cooling System	3mm 1/8 BSP Temp	3mm K-Type
Cylinder Head	Cylinder Head	1.5 K-Type Metal Temp	1.5mm K-Type
Cylinder Head	Cylinder Head	1.5 K-Type Metal Temp	1.5mm K-Type
Heatshield	Other	1.5 Surface Temp Thermocouple	1.5mm K-Type Surface Temp
Heatshield	Other	1.5 Surface Temp Thermocouple	1.5mm K-Type Surface Temp
Intake manifold	Intake	3mm 1/8 BSP Temp	3mm K-Type
Test Bed - Cylinder Block O-Ring Plug	Lubrication	1/8 Hydraulic (Oil pressure)	Braided Hose (Hydraulic)

1/4" BSP	Lubrication	3mm Fixed TC in Gallery Plug	3mm K-Type
Intake manifold	Intake	1/8 BSP Pressure Ferule	Normal Pressure line (Clear)
Intake manifold	Intake	3mm 1/8 BSP Temp	3mm K-Type
Intake manifold	Intake	1/8 BSP Pressure Ferule	Normal Pressure line (Clear)
Intake manifold	Intake	3mm 1/8 BSP Temp	3mm K-Type
Oil Cooler	Cooling System	3mm 1/8 BSP Temp	PRT - temp
Oil Cooler	Cooling System	3mm 1/8 BSP Temp	PRT - temp
Lower crank case	Lubrication	3mm 1/8 BSP Temp	PRT - temp
Oil Cooler	Lubrication	3mm Fixed TC in Gallery Plug	PRT - temp
Heatshield	Other	1.5 Surface Temp Thermocouple	1.5mm K-Type Surface Temp
Heatshield	Other	1.5 Surface Temp Thermocouple	1.5mm K-Type Surface Temp
Oil Filter Housing	Lubrication	3mm 1/8 BSP Temp	3mm K-Type
Turbo	Exhaust	1/8 BSP Pressure Ferule	Pig Tail Pressure
Turbo	Exhaust	4.5mm 1/8 BSP	4.5mm K-Type Inconel
Turbo	Exhaust	1/8 BSP Pressure Ferule	Pig Tail Pressure
Turbo	Exhaust	4.5mm 1/8 BSP	4.5mm K-Type Inconel
Test Bed - Sump plug	Lubrication	3mm 1/8 BSP Temp	3mm K-Type
Test Bed - Sump plug	Lubrication	1/8 Hydraulic (Oil pressure)	Braided Hose (Hydraulic)
Test Bed	Cooling System		
Test Bed			
Turbo	Exhaust	1.5 Surface Temp Thermocouple	1.5mm K-Type Surface Temp
Turbo	Exhaust	1.5 Surface Temp Thermocouple	1.5mm K-Type Surface Temp
Turbo Coolant Drain	Cooling System	3mm 1/8 BSP Temp	3mm K-Type
Turbo Coolant Drain	Cooling System	1/8 BSP Pressure Ferule	Normal Pressure Line (Clear)
Turbo Coolant Drain	Cooling System	3mm 1/8 BSP Temp	3mm K-Type
Turbo Coolant Drain	Cooling System	1/8 BSP Pressure Ferule	Normal Pressure Line (Clear)

Turbo Coolant Feed	Cooling System	1/8 BSP Pressure Ferule	Normal Pressure Line (Clear)
Turbo Coolant Feed	Cooling System	3mm 1/8 BSP Temp	3mm K-Type
Turbo Drain	Cooling System	1.5 Surface Temp Thermocouple	1.5mm K-Type Surface Temp
Turbo Run-on Pump	Cooling System	1/8 BSP Pressure Ferule	Normal Pressure Line (Clear)
Turbo Run-on Pump	Cooling System	3mm 1/8 BSP Temp	3mm K-Type
Turbo	Exhaust	3mm 1/8 BSP Temp	3mm K-Type
Turbo	Exhaust	3mm 1/8 BSP Temp	3mm K-Type

Bibliography

[1]   "Cop26   explained."   [Online].   Available: https://webarchive.nationalarchives.gov.uk/ukgwa/20230401054904/https://ukcop 26.org/wp-content/uploads/2021/07/COP26-Explained.pdf.   [Accessed: 13-Jun-2023].

[2]   EPA, "Global Greenhouse Gas Emissions Data," 2021. [Online]. Available: https://www.epa.gov/ghgemissions/global-greenhouse-gas-emissions-data#Trends. [Accessed: 15-Nov-2021].

[3]   ICCT The International Council on Clean Transportation, "Europe," 2021. [Online]. Available: https://theicct.org/europe. [Accessed: 16-Nov-2021].

[4]   ICCT The International Council on Clean Transportation, "China," 2021. [Online]. Available: https://theicct.org/china. [Accessed: 16-Nov-2021].

[5]   ICCT The International Council on Clean Transportation, "India," 2021. [Online]. Available: https://theicct.org/india. [Accessed: 16-Nov-2021].

[6]   ICCT The International Council on Clean Transportation, "Latin America," 2021. [Online]. Available: https://theicct.org/latin-america. [Accessed: 16-Nov-2021].

[7]   I. T. I. C. on C. Transportation, "United States," 2021. [Online]. Available: https://theicct.org/united-states.

[8]   W. F. Lamb *et al.*, "A review of trends and drivers of greenhouse gas emissions by sector from 1990 to 2018," *Environ. Res. Lett.*, vol. 16, no. 7, 2021.

[9]   G. Grassi *et al.*, "Reconciling global-model estimates and country reporting of anthropogenic forest CO2 sinks," *Nat. Clim. Chang.*, vol. 8, no. 10, pp. 914–920, 2018.

[10]   S. Kirschke *et al.*, "Three decades of global methane sources and sinks," *Nat. Geosci.*, vol. 6, no. 10, pp. 813–823, 2013.

[11]   Michael Eves, David Kilpatrick, Paul Edwards, and Jonathan Berry, "SF6 Alternatives A Literature Review on SF6 Gas Alternatives for use on the Distribution Network," *West. Power Distrib. Innov.*, vol. 1, pp. 9–10, 2018.

[12]   M. Crippa *et al.*, "EDGAR v4 . 3 . 2 Global Atlas of the three major Greenhouse Gas Emissions for the period 1970-2012 . Supplementary Information," *Earth Syst. Sci. Data*, vol. 2010, pp. 1–20, 2012.

[13]   The European Parliament and the Council of the European Union, "Regulation (EU) 2019/631 of the European Parliament and of the Council of 17 April 2019 setting CO2 emission performance standards for new passenger cars and for new light commercial vehicles, and repealing Regulations (EC) No 443/2009 and (EU) No

510/201," *Off. J. Eur. Union*, vol. 62, no. L111, pp. 13–53, 2019.

[14]   European Parliament and Council of the European Union, "REGULATION (EC) No 715/2007 OF THE EUROPEAN PARLIAMENT AND OF THE COUNCIL of 20 June 2007 on type approval of motor vehicles with respect to emissions from light passenger and commercial vehicles (Euro 5 and Euro 6) and on access to vehicle repair and mai," *Off. J. Eur. Union*, vol. L171, no. December 2006, pp. 1–16, 2007.

[15]   Z. Liu, L. Li, and B. Deng, "Cold start characteristics at low temperatures based on the first firing cycle in an LPG engine," *Energy Convers. Manag.*, vol. 48, no. 2, pp. 395–404, 2007.

[16]   M. Gumus, "Reducing cold-start emission from internal combustion engines by means of thermal energy storage system," *Appl. Therm. Eng.*, vol. 29, no. 4, pp. 652–660, 2009.

[17]   C. C. Daniels and M. J. Braun, "The friction behavior of individual components of a spark-ignition engine during warm-up," *Tribol. Trans.*, vol. 49, no. 2, pp. 166–173, 2006.

[18]   X. Tauzia, A. Maiboom, H. Karaky, and P. Chesse, "Experimental analysis of the influence of coolant and oil temperature on combustion and emissions in an automotive diesel engine," *Int. J. Engine Res.*, vol. 20, no. 2, pp. 247–260, 2019.

[19]   F. Payri, P. Olmeda, J. Martin, and R. Carreño, "A New Tool to Perform Global Energy Balances in DI Diesel Engines," *SAE Int. J. Engines*, vol. 7, no. 1, pp. 43–59, 2014.

[20]   L. A. Smith, W. H. Preston, G. Dowd, O. Taylor, and K. M. Wilkinson, "Application of a first law heat balance method to a turbocharged automotive diesel engine," *SAE Tech. Pap.*, vol. 4970, 2009.

[21]   C. Donn, W. Zulehner, D. Ghebru, U. Spicher, and M. Honzen, "Experimental heat flux analysis of an automotive diesel engine in steady-state operation and during warm-up," *SAE Tech. Pap.*, 2011.

[22]   M. Bovo and J. Somhorst, "A High Resolution 3D Complete Engine Heat Balance Model," *SAE Tech. Pap.*, vol. 2015, 2015.

[23]   C. A. Romero, A. Torregrosa, P. Olmeda, and J. Martin, "Energy balance during the warm-up of a diesel engine," *SAE Tech. Pap.*, vol. 1, 2014.

[24]   F. Rabeau and S. Magand, "Modeling of a thermal management platform of an automotive D.I diesel engine to predict the impact of downsizing and hybridization during a cold start," *SAE Tech. Pap.*, vol. 1, 2014.

[25]   J. Chastain, J. Wagner, and J. Eberth, "Advanced engine cooling - Components, testing and observations," *IFAC Proc. Vol.*, vol. 43, no. 7, pp. 294–299, 2010.

[26] J. Ning and F. Yan, "Temperature Control of Electrically Heated Catalyst for Cold-start Emission Improvement," *IFAC-PapersOnLine*, vol. 49, no. 11, pp. 14–19, 2016.

[27] B. Minovski, J. Andrić, L. Löfdahl, and P. Gullberg, "A numerical investigation of thermal engine encapsulation concept for a passenger vehicle and its effect on fuel consumption," *Proc. Inst. Mech. Eng. Part D J. Automob. Eng.*, vol. 233, no. 3, pp. 557–571, 2019.

[28] J. Zhao, R. Fu, S. Wang, H. Xu, and Z. Yuan, "Fuel economy improvement of a turbocharged gasoline SI engine through combining cooled EGR and high compression ratio," *Energy*, vol. 239, p. 122353, 2022.

[29] R. Y. Dahham, H. Wei, and J. Pan, "Improving Thermal Efficiency of Internal Combustion Engines: Recent Progress and Remaining Challenges," *Energies*, vol. 15, no. 17, 2022.

[30] A. J. Torregrosa, P. Olmeda, J. Martín, and B. Degraeuwe, "Experiments on the influence of inlet charge and coolant temperature on performance and emissions of a DI Diesel engine," *Exp. Therm. Fluid Sci.*, 2006.

[31] A. Torregrosa, A. Broatch, P. Olmeda, and C. Romero, "Assessment of the influence of different cooling system configurations on engine warm-up, emissions and fuel consumption," *Int. J. Automot. Technol.*, vol. 9, no. 4, pp. 447–458, 2008.

[32] Y. Wang, Q. Gao, T. Zhang, G. Wang, Z. Jiang, and Y. Li, "Advances in integrated vehicle thermal management and numerical simulation," *Energies*, vol. 10, no. 10, 2017.

[33] T. Priede and D. Anderton, "Likely Advances in Mechanics, Cooling, Vibration and Noise of Automotive Engines.," *Proc. Inst. Mech. Eng. Part D Transp. Eng.*, vol. 198, no. 7, pp. 95–106, 1984.

[34] I. Parks, "Wall a 2," vol. 199, p. 212170, 1904.

[35] J.-P. Zammit, P. J. Shayler, and I. Pegg, "Thermal coupling and energy flows between coolant, engine structure and lubricating oil during engine warm up," in *Vehicle Thermal Management Systems Conference and Exhibition (VTMS10)*, Woodhead Publishing, 2011, pp. 177–188.

[36] A. A. Kenny, C. F. Bradshaw, and B. T. Creed, "The Engineering Resource For Advancing Mobility Electronic Thermostat System for Automotive Engines," 2016.

[37] X. Zou, J. A. Jordan, and M. Shillor, "A dynamic model for a thermostat," *J. Eng. Math.*, vol. 36, no. 4, pp. 291–310, 1999.

[38] E. Cortona and C. H. Onder, "Engine thermal management with electric cooling pump," *SAE Tech. Pap.*, no. 724, 2000.

[39] J. W. Whitefoot, "DETC2010-28457," pp. 1–8, 2010.

[40] H. Liu, M. Wen, H. Yang, Z. Yue, and M. Yao, "A Review of Thermal Management System and Control Strategy for Automotive Engines," *J. Energy Eng.*, vol. 147, no. 2, 2021.

[41] H. H. Pang and C. J. Brace, "Review of engine cooling technologies for modern engines," *Proc. Inst. Mech. Eng. Part D J. Automob. Eng.*, vol. 218, no. 11, pp. 1209–1215, 2004.

[42] J. R. Wagner, V. Srinivasan, D. M. Dawson, and E. E. Marotta, "Smart thermostat and coolant pump control for engine thermal management systems," *SAE Tech. Pap.*, no. 724, 2003.

[43] B. Yao, F. Yang, H. Zhang, E. Wang, and K. Yang, "Analyzing the performance of a dual loop organic rankine cycle system for waste heat recovery of a heavy-duty compressed natural gas engine," *Energies*, vol. 7, no. 11, pp. 7794–7815, 2014.

[44] D. Di Battista and R. Cipollone, "Experimental and numerical assessment of methods to reduce warm up time of engine lubricant oil," *Appl. Energy*, vol. 162, pp. 570–580, 2016.

[45] H. Cho, D. Jung, Z. S. Filipi, D. N. Assanis, J. Vanderslice, and W. Bryzik, "Application of controllable electric coolant pump for fuel economy and cooling performance improvement," *J. Eng. Gas Turbines Power*, vol. 129, no. 1, pp. 239–244, 2007.

[46] T. Wang and J. Wagner, "Advanced automotive thermal management - Nonlinear radiator fan matrix control," *Control Eng. Pract.*, vol. 41, pp. 113–123, 2015.

[47] T. Mitchell, M. Salah, J. Wagner, and D. Dawson, "Automotive thermostat valve configurations: Enhanced warm-up performance," *J. Dyn. Syst. Meas. Control. Trans. ASME*, vol. 131, no. 4, pp. 1–7, 2009.

[48] H. Coutitouse and V. T. M. S. A, "Cooling System Control in Automotive Engines," 2019.

[49] C. J. Brace, H. Burnham-Slipper, R. S. Wijetunge, N. D. Vaughan, K. Wright, and D. Blight, "Integrated cooling systems for passenger vehicles," *SAE Tech. Pap.*, no. 724, 2001.

[50] R. D. Chalgren, "Thermal comfort and engine warm-up optimization of a low-flow advanced thermal management system," *SAE Tech. Pap.*, no. 724, 2004.

[51] J. R. Wagner, M. C. Ghone, D. W. Dawson, and E. E. Marotta, "Coolant flow control strategies for automotive thermal management systems," *SAE Tech. Pap.*, no. 724, 2002.

[52] P. Janowski, P. J. Shayler, S. Robinson, and M. Goodman, "The effectiveness of heating parts of the powertrain to improve vehicle fuel economy during warm-up," *Veh. Therm. Manag. Syst. Conf. Exhib.*, pp. 211–221, Jan. 2011.

[53]   A. Osman, A. S. Sabrudin, M. A. I. Hussin, and Z. A. Bakri, "Design and simulations of an enhanced and cost effective engine split cooling concept," *SAE Tech. Pap.*, vol. 2, 2013.

[54]   C. Dardiotis, G. Martini, A. Marotta, and U. Manfredi, "Low-temperature cold-start gaseous emissions of late technology passenger cars," *Appl. Energy*, vol. 111, pp. 468–478, 2013.

[55]   F. Will and A. Boretti, "A New Method to Warm Up Lubricating Oil to Improve the Fuel Efficiency During Cold Start," *SAE Int. J. Engines*, vol. 4, no. 1, pp. 175–187, 2011.

[56]   I. Drives, "High Power and Efficiency," vol. 81, no. August, 2020.

[57]   B. J. Luptowski, O. Arici, J. H. Johnson, and G. G. Parker, "Development of the enhanced vehicle and engine cooling system simulation and application to active cooling control," *SAE Tech. Pap.*, vol. 2005, no. 724, 2005.

[58]   R. W. Page, W. Hnatczuk, and J. Kozierowski, "Thermal management for the 21st century - Improved thermal control & fuel economy in an Army Medium Tactical Vehicle," *SAE Tech. Pap.*, no. 724, 2005.

[59]   M. Chanfreau, B. Gessier, A. Farkh, and P. Y. Geels, "The need for an electrical water valve in a THErmal management intelligent system (THEMIS™)," *SAE Tech. Pap.*, no. 724, 2003.

[60]   R. D. Chalgren and D. J. Allen, "Light duty diesel advanced thermal management," *SAE Tech. Pap.*, no. 724, 2005.

[61]   J. Cho, K. Kim, K. Yang, I. Suh, and H. Kim, "The CAE Analysis of a Cylinder Head Water Jacket Design for Engine Cooling Optimization," *SAE Tech. Pap.*, vol. 2018-April, pp. 1–7, 2018.

[62]   J. F. Eberth, J. R. Wagner, B. a Afshar, and R. C. Foster, "Thermal Management System Architectures," no. 724, 2004.

[63]   R. D. Chalgren and T. Traczyk, "Advanced secondary cooling systems for light trucks," *SAE Tech. Pap.*, no. 724, 2005.

[64]   J. H. Chastain and J. R. Wagner, "Advanced thermal management for internal combustion engines - Valve design, component testing and block redesign," *SAE Tech. Pap.*, no. 724, 2006.

[65]   C. J. Brace, H. Burnham-Slipper, R. S. Wijetunge, N. D. Vaughan, K. Wright, and D. Blight, "Integrated cooling systems for passenger vehicles," *SAE Tech. Pap.*, no. 724, 2001.

[66]   J. P. Szybist *et al.*, "What fuel properties enable higher thermal efficiency in spark-ignited engines?," *Prog. Energy Combust. Sci.*, vol. 82, 2021.

[67]   N. Shkolnik and A. Shkolnik, "Rotary high efficiency hybrid cycle engine," *SAE*

Tech. Pap., 2008.

[68]	T. V. Johnson, "Review of diesel emissions and control," *SAE Tech. Pap.*, vol. 3, no. 1, pp. 16–29, 2010.

[69]	N. Lam, M. Tuner, P. Tunestal, A. Andersson, S. Lundgren, and B. Johansson, "Double Compression Expansion Engine Concepts: A Path to High Efficiency," *SAE Int. J. Engines*, vol. 8, no. 4, pp. 1562–1578, 2015.

[70]	T. Shinagawa, M. Kudo, W. Matsubara, and T. Kawai, "The New Toyota 1.2-Liter ESTEC Turbocharged Direct Injection Gasoline Engine," *SAE Tech. Pap.*, vol. 2015-April, no. April, 2015.

[71]	T. Yamada, S. Adachi, K. Nakata, T. Kurauchi, and I. Takagi, "Economy with superior thermal efficient combustion (ESTEC)," *SAE Tech. Pap.*, vol. 1, 2014.

[72]	D. Takahashi, K. Nakata, Y. Yoshihara, and T. Omura, "Combustion Development to Realize High Thermal Efficiency Engines," *SAE Int. J. Engines*, vol. 9, no. 3, pp. 1486–1493, 2016.

[73]	P. Lott, M. Casapu, J. D. Grunwaldt, and O. Deutschmann, "A review on exhaust gas after-treatment of lean-burn natural gas engines – From fundamentals to application," *Appl. Catal. B Environ.*, vol. 340, no. May 2023, p. 123241, 2024.

[74]	D. Maizak, T. Wilberforce, and A. G. Olabi, "DeNOx removal techniques for automotive applications – A review," *Environ. Adv.*, vol. 2, no. August, p. 100021, 2020.

[75]	D. Takahashi, K. Nakata, Y. Yoshihara, Y. Ohta, and H. Nishiura, "Combustion Development to Achieve Engine Thermal Efficiency of 40% for Hybrid Vehicles," *SAE Tech. Pap.*, vol. 2015-April, no. April, 2015.

[76]	E. S. Mohamed, "Development and analysis of a variable position thermostat for smart cooling system of a light duty diesel vehicles and engine emissions assessment during NEDC," *Appl. Therm. Eng.*, vol. 99, pp. 358–372, 2016.

[77]	D. J. Allen and M. P. Lasecki, "Thermal management evolution and controlled coolant flow," *SAE Tech. Pap.*, no. 724, 2001.

[78]	Federal Highway Administration, "Systems Engineering for Intelligent Transportation Systems," *Systems Engineering for Intelligent Transportation Systems*. [Online]. Available: https://ops.fhwa.dot.gov/publications/seitsguide/section3.htm. [Accessed: 13-Jun-2023].

[79]	G. Sujesh and S. Ramesh, "Modeling and control of diesel engines: A systematic review," *Alexandria Eng. J.*, vol. 57, no. 4, pp. 4033–4048, 2018.

[80]	J. Zheng, "Use of an Engine Cycle Simulation to Study a Biodiesel Fueled Engine," no. August, 2009.

[81] B. Menacer and M. Bouchetara, "Parametric study of the performance of a turbocharged compression ignition engine," *Simulation*, vol. 90, no. 12, pp. 1375–1384, 2014.

[82] F. Kitanoski, W. Puntigam, M. Kozek, and J. Hager, "An engine heat transfer model for comprehensive thermal simulations," *SAE Tech. Pap.*, vol. 2006, no. 724, 2006.

[83] U. Bryakina and G. Seider, "Prediction of Engine Warm-up and Fuel Economy utilizing GT ' s Customized FE Cylinder Structure Objects," in *European GT Conference 2016*, 2016.

[84] J. C. Wurzenberger, R. Heinzle, M. V. Deregnaucourt, and T. Katrasnik, "A comprehensive study on different system level engine simulation models," *SAE Tech. Pap.*, vol. 2, 2013.

[85] O. Arici, J. H. Johnson, and A. J. Kulkarni, "The vehicle engine cooling system simulation part 1 - Model development," *SAE Tech. Pap.*, no. 724, 1999.

[86] W. Nessim and F. Zhang, "Powertrain Warm-Up Improvement Using Thermal Management Systems," *Int. J. Sci. Technol. Res.*, vol. 1, no. 4, pp. 151–155, 2012.

[87] J. Dohmen, R. Barthel, and S. Klopstein, "Virtual development of cooling systems," *MTZ Worldw.*, vol. 67, no. 12, pp. 14–17, 2006.

[88] T. Banjac, J. C. Wurzenberger, and T. Katrašnik, "Assessment of engine thermal management through advanced system engineering modeling," *Adv. Eng. Softw.*, vol. 71, pp. 19–33, 2014.

[89] V. Kumar, S. A. Shendge, and S. Baskar, "Underhood thermal simulation of a small passenger vehicle with rear engine compartment to evaluate and enhance radiator performance," *SAE Tech. Pap.*, 2010.

[90] C. Croitoru, I. Nastase, F. Bode, A. Meslem, and A. Dogeanu, "Thermal comfort models for indoor spaces and vehicles - Current capabilities and future perspectives," *Renew. Sustain. Energy Rev.*, vol. 44, pp. 304–318, 2015.

[91] F. Pirotais, J. Bellettre, O. Le Corre, M. Tazerout, G. De Pelsemaeker, and G. Guyonvarch, "A diesel engine thermal transient simulation: Coupling between a combustion model and a thermal model," *SAE Tech. Pap.*, no. 724, 2003.

[92] B. Sangeorzan, E. Barber, and B. Hinds, "Development of a one-dimensional engine thermal management model to predict piston and oil temperatures," *SAE Tech. Pap.*, 2011.

[93] J. Lahuerta and S. Samuel, "Numerical simulation of warm-Up characteristics and thermal management of a GDI engine," *SAE Tech. Pap.*, vol. 2, 2013.

[94] F. Millo, S. Caputo, C. Cubito, A. Calamiello, D. Mercuri, and M. Rimondi, "Numerical Simulation of the Warm-Up of a Passenger Car Diesel Engine Equipped with an Advanced Cooling System," *SAE Tech. Pap.*, 2016.

[95] E. Graziano, L. Bruno, P. Corrado, S. Pierson, and G. Virelli, "Set-Up and Validation of an Integrated Engine Thermal Model in GT-SUITE for Heat Rejection Prediction," *SAE Tech. Pap. Ser.*, vol. 1, 2019.

[96] M. Bovo, "Complete Engine Thermal Model, a Comprehensive Approach," *SAE Int. J. Engines*, vol. 11, no. 2, pp. 3–11, 2018.

[97] "From Low to High Voltage Technology Automated Driving 2021," vol. 82, no. April, 2021.

[98] M. V. Alexander, "A modern approach to evaluation of ethylene glycol based coolants," *SAE Tech. Pap.*, 1988.

[99] J. Gao, G. Tian, A. Sorniotti, A. E. Karci, and R. Di Palo, "Review of thermal management of catalytic converters to decrease engine emissions during cold start and warm up," *Appl. Therm. Eng.*, vol. 147, no. October 2018, pp. 177–187, 2019.

[100] A. Choukroun and M. Chanfreau, "Automatic control of electronic actuators for an optimized engine cooling thermal management," *SAE Tech. Pap.*, no. 724, 2001.

[101] R. Burke *et al.*, "Systems approach to the improvement of engine warm-up behaviour," *Proc. Inst. Mech. Eng. Part D J. Automob. Eng.*, vol. 225, no. 2, pp. 190–205, 2011.

[102] O. Schatz, "Cold start improvement by use of latent heat stores," *SAE Tech. Pap.*, 1992.

[103] J. Kim, J. Oh, and H. Lee, "Review on battery thermal management system for electric vehicles," *Appl. Therm. Eng.*, vol. 149, no. September 2018, pp. 192–212, 2019.

[104] G. Xia, L. Cao, and G. Bi, "A review on battery thermal management in electric vehicle application," *J. Power Sources*, vol. 367, pp. 90–105, 2017.

[105] P. R. Tete, M. M. Gupta, and S. S. Joshi, "Developments in battery thermal management systems for electric vehicles: A technical review," *J. Energy Storage*, vol. 35, no. January, p. 102255, 2021.

[106] Y. Kuze, H. Kobayashi, H. Ichinose, and T. Otsuka, "Development of new generation hybrid system (THS II) - Development of Toyota Coolant Heat Storage System," *SAE Tech. Pap.*, vol. 2004, no. 724, 2004.

[107] G. E. Andrews, A. M. Ounzain, H. Li, M. Bell, J. Tate, and K. Ropkins, "The use of a water/lube oil heat exchanger and enhanced cooling water heating to increase water and lube oil heating rates in passenger cars for reduced fuel consumption and CO2 emissions during cold start," *SAE Tech. Pap.*, no. 1, 2007.

[108] E. Block, "GT-SUITE," 2017.

[109] F. Millo, G. di Lorenzo, E. Servetto, A. Capra, and M. Pettiti, "Analysis of the performance of a turbocharged s.i. engine under transient operating conditions by

means of fast running models," *SAE Int. J. Engines*, vol. 6, no. 2, pp. 968–978, 2013.

[110] B. A. Lerch, D. J. Keller, and R. World, *Thermocouple in a Materials Calibration and Accuracy Testing Laboratory*, no. April 2002. 2020.